An Examination of the Development of Rapid-onset Diabetes Induced by Elevated Exogenous Glucocorticoids and a High-fat Diet in Young Sprague-Dawley Rats

Jacqueline L. Beaudry

A DISSERTATION SUBMITTED TO THE FAULTY OF GRADUATE STUDIES IN PARTIAL FULFILMENT OF THE REQUIREMENTS FOR THE DEGREE OF

DOCTOR OF PHILOSOPHY

GRADUATE PROGRAM IN KINESIOLOGY AND HEALTH SCIENCE

YORK UNIVERSITY,

TORONTO, ONTARIO

September 2013

ABSTRACT

Acute increases in glucocorticoids (GCs) during a perceived stressful event are functionally important for many biological processes that include energy homeostasis. Perpetual hypothalamic-pituitary-adrenal (HPA) axis activity continually elevates GC secretion and may induce many metabolic complications, such as peripheral insulin resistance, ectopic fat accumulation, hyperglycemia, and dyslipidemia that can increase risks of developing type 2 diabetes mellitus (T2DM). The progression into T2DM remains complex and many controversies have yet to be resolved. In particular, the effect of GCs on pancreatic islet function remains relatively understudied. Therefore, we set out to develop a novel rodent model of T2DM in young male Sprague-Dawley rats. First, we demonstrated that 2 weeks of elevated GCs and HFD induced rapid-onset diabetes (ROD), which included the following symptoms: body weight loss, hepatic steatosis, increased glucose intolerance, insulin resistance, and ectopic fat accumulation. Next, we further examined the effects of ROD on pancreatic islet function and found that ROD animals had increased β-and α-cell mass, but impaired β-cell glucose responsiveness, resulting in hyperglycemia. Regular exercise restores alterations in HPA activity and helps to protect against GC-induced hyperglycemia. This led us to investigate if regular exercise in our ROD model would help to protect against T2DM development. We found that volitional exercise was sufficient to attenuate symptoms of ROD, however not all symptoms were successfully restored, i.e. normalized glucose control and peripheral insulin resistance. We next investigated if pharmacologic agents would be able to fully reverse ROD. We demonstrated that non-selective GC receptor (GRII) antagonist fully

normalized our ROD phenotype, whereas selective GRII antagonists only partially attenuated some of the ROD symptoms. Collectively, these studies take an integrative approach to T2DM development induced by GCs and HFD. We developed a model that mimics symptoms of T2DM and concluded that GCs and HFD synergistically, not independently act to induce severe insulin resistance that burdens islet adaptive capacity. Regular exercise and pharmacological interventions were sufficient to attenuate ROD development and these therapies may be useful techniques to individuals suffering from HPA axis hyperactivity and dyslipidemia.

ACKNOWLEDGMENTS

I would like to begin my acknowledgements of my PhD thesis dissertation to my supervisor, Dr. Michael Riddell. First of all, thank you very much for taking me on as your PhD student for four years and trusting me to develop a project underlining the lab's goals. I have learned so much during my time in the Riddell lab and at York University. Your constant encouragement, enthusiasm and appreciation for my work have carried me to my final years of my project. I may have the skin that looks like the "inside of a mushroom", but I can cannulate a rat and isolate islets better than anyone else! Hopefully, I will always live up to my nickname as the "Jack of all Trades"!

To the past and present "Riddellian's": Jon Campbell; thank you for introducing me to the Riddell lab techniques and being extremely patient with me while I learn all of your tricks. Hopefully, this will continue during our time in the Drucker lab together. Anna D'souza; You and me buddy! I loved every second working with you. You were my rock during the first two years of studying ROD. I could not have asked for a better lab partner. Ashley Peckett (Ashla); I think we were always destined to work together. Childhood gymnastic competitors to Riddell lab mates, fate is funny sometimes. I always admire your positivity and outlook on life. Thank you for being such a fantastical friend and lab mate. Yaniv Shpilberg; You always know how to say the darnst things. I will miss you for your humor and outlandish statements. Erwan Leclair; I will never think of France without thinking of you. That goes for a good bottle of wine, stinky cheese, iPhone whistle chime, fresh oysters, restaurant TV shows and nose bleeds! I am so happy that I met you and had the chance to work with you. Your unconventional and hilarious humour, positive attitude, unpredictability is far too unforgettable. I hope we remain life-long friends. Emily Dunford (Emla); You have been my rock for the past 2 years of working with ROD. I could not feel more comfortable leaving the project in your hands. You will do great. It was awesome working, running and hanging out with you. I hope we can stay friends for a long time even though you have a Dutch background. Trevor Teich; you are a natural in the lab. I am so happy you decided to stay on as a Master's student. You will do great wherever you end up. Good luck. Thank you for all of your hard work. Dessi Zaharieva; you have an incredible positive outlook to life and I hope that never goes away. You have always been enthusiastic about my project and are always willing to lend an ear and advice. Good luck with your future research career. You will be a star. To my family: Thank you for your tremendous encouragement in my academic career. I could not have gone as far as I did without your constant support. I am always amazed by your interest in my work and delighted to carry on conversations and debates about science.

To my husband: You have always supported me since day one of our relationship. You have an incredible serenity and virtue about you that no one can possibly match. You know exactly what to say to ground my thoughts and to encourage me when I need it the most. I am so proud and thankful to have you in my life. I cannot be happier.

TABLE OF CONTENTS

LIST OF TABLES/FIGURES

CHAPTER 5: GLUCOCORTICOIDS RECEPTOR II ANTAGONISTS AND RAPID-ONSET DIABETES IN SPRAGUE-DAWLEY RATS

CHAPTER 7: EXTENDED RESULTS

LIST OF ABREVIATIONS

11-DHC	-	11-deoxycorticosterone
11β-HSD1	-	11β-hydroxysteroid dehydrogenase1
AP-1	-	Activating protein-1
ACTH	-	Adrenocorticotrophin hormone
AUC	-	Area under the curve
AVP	-	Arginine vasopressin
ANOVA	-	Analysis of variance
CRH	-	Corticotrophin releasing hormone
CRH1	-	Corticotrophin releasing hormone receptor1
CBG	-	Cortisol binding globulin
ELISA	-	Enzyme-linked immunosorbent assay
EX	-	Exercise
ER	-	Endoplasmic reticulum
FFA	-	Free fatty acids
GCs	-	Glucocorticoids
GR and GRII	-	GC receptor II
GRE	-	GC-response element
G6P	-	Glucose-6-phosphate
GSIS	-	Glucose stimulated insulin secretion
GLUT1, 2, 4	-	Glucose transporter protein 1, 2 and 4
HFD	-	High-fat diet
HPA	-	Hypothalamic pituitary adrenal
I-κB	-	Inhibitor of nuclear factor
IRS1 and 2	-	Insulin receptor substrate 1 and 2
ITT	-	Insulin tolerance test
INS-1E	-	Insulin secreting cell line
IL-6	-	Interleukin-6
JNK	-	Jun NH2-terminal kinase
LCFA	-	Long-chain fatty acids
MC2R	-	Melanocortin 2 receptors (MC2R)
MR	-	Mineralocorticoid or type I receptor
NADPH	-	Nicotinamide adenine dinucleotide phosphate
NF-κB	-	Nuclear factor-κB
ORO	-	Oil red O
OGTT	-	Oral glucose tolerance test
PVN	-	Paraventricular nucleus
PR	-	Progesterone Receptor
POMC	-	Pro-opiomelanocortin
PKA	-	Protein kinase A
PKC	-	Protein kinase C
ROD	-	Rapid-onset Diabetes
RIA	-	Radio-immunoassay

SED	-	Sedentary
StAR	-	Steroidogenic acute regulatory
TG	-	Triglyceride
T1DM	-	Type 1 diabetes mellitus
T2DM	-	Type 2 diabetes mellitus
ZDF	-	Zucker diabetic fatty rats

LITERATURE REVIEW Chapter 1

1. Thesis Objectives and Hypothesis

Type 2 diabetes mellitus (T2DM) is a widely recognized disease that plagues ~ 300 million people worldwide (1). Interestingly, although T2DM is extensively studied, this multifaceted disease remains poorly understood. Various risk factors have been identified as contributing to the onset of T2DM, such as increased whole body insulin resistance, ectopic fat accumulation in insulin sensitive tissues, physical inactivity, poor nutrition, and genetics. Many of these factors exist in combination with other factors, but usually they are studied independently of one another. It is widely accepted that increased levels of "stress" deteriorate glucose homeostasis, which overwhelms pancreatic islet function. The literature is unclear about the role that "stress" plays in T2DM progression as it is unknown whether elevations in stress, secreted as glucocorticoids (GCs), have a direct role on T2DM development. Previous research suggests that acute elevation in GCs *in vivo* increases β-cell secretory capacity (2), but GC exposure *in vitro* results in β-cell dysfunction (3). Rodent models of diabetes are useful as they mimic symptoms and disease progression displayed in T2DM humans, but are usually limited by spontaneous gene mutations that are rare in the human population or require daily injections of pharmacological agents, which can artificially elevate stress levels. Thus, an adequate rodent model of T2DM is necessary to enhance our integrative approach into the effects of stress-induced diabetes.

Objectives

The main focus of this thesis was to develop a novel rodent model of T2DM induced by elevations in GCs and high-fat diet (HFD). There are many studies that investigate these risk factors independently, but rarely have they been examined concomitantly, as they exist in individuals with T2DM. Secondly, this thesis aimed to determine the involvement of the islet function on T2DM development caused by elevated GCs and HFD. Thirdly, the focus of this thesis was to determine if therapeutic approaches, such as regular exercise and GC receptor II (GRII) antagonists were sufficient to reduce risks of metabolic dysfunction with our rodent model of T2DM.

Hypothesis

Both acute GCs and HFD independently promote widespread whole-body insulin resistance, but typically do not result in T2DM onset, at least in the short-term, as β-cell compensation tends to occur. We hypothesized that in combination, acute elevations in GCs and HFD would rapidly promote T2DM development by overwhelming the pancreatic β-cell compensatory system, thus resulting in lower efficacy in islet glucose responsiveness. In contrast, we also predicted that regular exercise via voluntary wheel running or GRII antagonism via pharmacological intervention would attenuate the development of metabolic dysfunction, through preservation in β-cell function and protection against whole body insulin resistance.

The following is an extensive review of the literature, as this thesis takes an integrative approach to examine elevated levels of stress and T2DM development, and as such requires examination of various topics. It encompasses an explanation of healthy

pancreatic function, diabetes onset, GC metabolism and physiology, GCs and T2DM, exercise and GC metabolism, exercise and T2DM, non-selective and selective GC antagonists.

1.2. Pancreas Overview

1.2.1. The Pancreatic Islet

The pancreas is a vital endocrine organ that regulates energy homeostasis by the secretion of a variety of hormones. It consists of an array of endocrine cell types clustered into masses called the islets of Langerhans that make up tiny, but essential cells of the pancreas. The different cell types that exist within the islets are β, α, δ, F and ε-cells that secrete hormones such as insulin, glucagon, somatostatin, pancreatic polypeptide and ghrelin, respectively (4). The bulk of the islets (~ 70% of total islet volume) consist of the β-cells, responsible for managing glucose homeostasis through the secretion of the hormone insulin. The β-cells are typically located centrally within the islets of rodents and are surrounded by the other cell types, α-cells (~ 20%), δ-cells (~ 5-10%), F-cells (~ 5%) and ε-cells (~ < 1%) along the perimeter of the islet. In humans, however, all the different islet cell types are interspersed among the β-cells, but the majority of cells are aligned along the islet blood vessels in no particular sequence (5). This intricate structure suggests that microcirculation within the islet does not have an effect on paracrine dynamics in the human islet (6). The orientation of the β-cells is an integral part of the rat islet, as it allows blood flow to drain from the central portion of the islet outward; other islet cell types are exposed to high concentrations of insulin, which, in turn, can dramatically influence stimulation or inhibition on hormone secretion. Healthy and highly

functional islets, especially β-cells, are critical for insulin secretory capacity that assists glucose uptake into skeletal muscle and adipose tissue and inhibits hepatic glucose production from the liver, ultimately contributing to blood glucose clearance. In the case of abnormal or dysfunctional β-cells, the development of diabetes can occur (either T1DM or T2DM).

T1DM develops as an autoimmune disease that targets and down-regulates pancreatic insulin-producing β-cells, leaving individuals unable to synthesize their own insulin. The body's resistance to insulin defines T2DM, where individuals are able to produce large amounts of insulin, but remain insulin insensitive (reviewed in, (7)). However, if this condition remains untreated, individuals may become dependent upon exogenous insulin as β-cells become exhausted with trying to maintain euglycemia (8).

1.2.2. Insulin

Insulin secretion is a coordinated response from various stimulatory factors including nutrient stimuli, neural input, and varying levels of paracrine/endocrine islet-produced hormones. In healthy individuals, β-cells release enough insulin in the fasting and post prandial (~ 2 hours) state to maintain basal insulin concentrations (~ 0.4 ng/ml) (9). This small amount of insulin released into the portal circulation helps to limit excessive hepatic glucose production between meals. There are two phases of insulin secretion that follow a distinct pattern, post prandial of a mixed meal: the first phase of insulin secretion occurs between ~ 8–10 minutes followed by a second phase that occurs between ~ 30–45 minutes afterwards and can stay elevated for 120 minutes. These levels

of insulin can vary depending on the carbohydrate content of a meal and the insulin sensitivity of the individual (10). In non-diabetic individuals, after the ingestion of a meal (~ 90-120 minutes), insulin concentrations should be enough to return blood glucose levels back to basal levels (11). Therefore, β-cell function is considered to be "impaired", if blood glucose concentrations do not return to pre-meal basal levels and depending on the level of hyperglycemia may result in the clinical diagnosis of pre-diabetes or diabetes mellitus. Potential causes of impaired insulin secretion are β-cell dysfunction, reduced β-cell mass, or both. Pancreatic β-cell dysfunction may be considered a desensitization of normal β-cells to either glucose- or insulin-signaling or impaired glucose responsiveness (12). If an individual displays any abnormalities in their first or second phase of glucose stimulated insulin secretion, then this is usually a sign of early onset of T2DM (13). These characteristics of T2DM individuals will be further discussed in section 2.4.

Glucose-stimulated insulin secretion (GSIS) is promoted by the closure of ATP-senstive potassium (K_{ATP}) channels on the β-cell membrane, as a result of depolarization of the cell. Prior to the electrical closure of the K_{ATP} channels, glucose enters the β-cell through the Na^+-independent glucose transporter protein (GLUT2), which has a very high affinity for glucose in the plasma. Glucose entry into the β-cell increases the activity of glucokinase, which converts glucose into glucose-6-phosphate (G6P), which in turn, yields pyruvate, leading to the generation of ATP molecule from the mitochondria. The elevated ratio of ATP/ADP depolarizes the β-cell membrane potential and drives the K_{ATP} channels to close, allowing the entry of extracellular calcium (Ca^{2+}) via voltage-dependent Ca^{2+} channels, as well as from mobilization of cytosolic Ca^{2+}. Subsequently,

the rise in Ca^{2+} levels induces the activation of several pathways that increase GSIS, such as phosphorylation of protein kinase A (PKA) and C (PKC). These proteins help facilitate the fusion of insulin-containing granules to the β-cell plasma membrane for exocytosis of insulin into circulation. PKA is activated by the rise in cAMP levels from the influx of Ca^{2+} into the cell, and PKC is translocated to the plasma membrane as a result of the increase in $Ca2^{+}$ and diacylglycerol (DAG) concentrations. These Ca^{2+}-stimulated protein kinases are thought to regulate myosin light-chain kinase, which phosphorylates secretory granules and modulates their movement to the surface of the β-cell membrane that initiates the release of insulin (14). Refer to Figure 1.1. Image adopted from Beaudry and Riddell, 2012 (15).

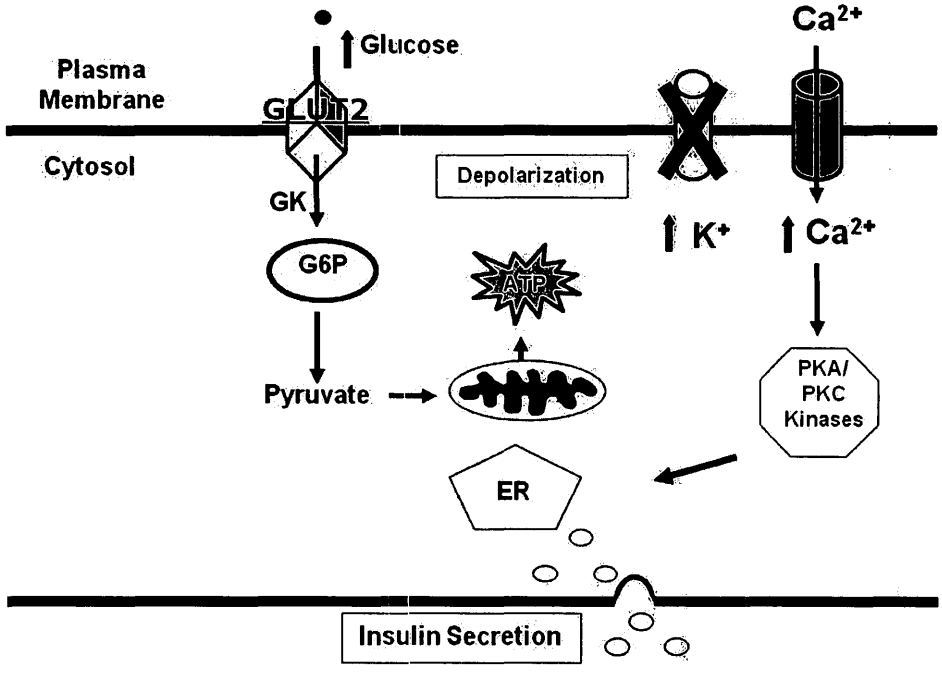

Figure 1.1. Glucose-stimulated insulin secretion. A rise in blood glucose levels stimulate GLUT2 proteins on the β-cell membrane to take up glucose into the cell. The GK enzyme acts to convert glucose into G6P that later breaks down into pyruvate that is utilized by the mitochondria to yield ATP. The increase in the ATP/ADP ratios depolarizes the plasma membrane and promotes the closure of the

K_{ATP} channels that drives Ca^{2+} into the cell through the Ca^{2+} voltage-dependent channels. The entry of Ca^{2+} into the cell increases the phosphorylation of PKA/PKC that helps to mobilize the insulin β-granules from the ER to exit the β-cell through exocytosis. Glucose transport 2, GLUT2; glucokinase, GK; glucose 6 phosphate; protein kinase A and C, PKA/PKC; endoplasmic reticulum, ER.

1.2.3. Glucagon

Another major hormone secreted by the pancreatic islets is glucagon, which signals the liver to release glucose into the circulation. Glucagon is responsible for the counter-regulation of blood glucose concentrations and is released during hypoglycemia. A fall in the plasma glucose levels will shut off the secretion of insulin in β-cells, and will stimulate glucagon and epinephrine release from the adrenal gland (5). Glucagon stimulates hepatic glucose output by stimulating glycogenolysis and gluconeogenesis, while concurrently reducing glycogenesis and glycolysis, thus helping to return blood glucose levels to a euglycemic level (~ 4-6 mM) (16). The exact mechanisms that stimulate glucagon secretion are still controversial in the literature and many hypotheses exist. It is not clear if circulating glucose levels directly influences α-cells or if glucagon secretion is stimulated by the autonomic nervous system and/or paracrine/endocrine products secreted by other islet cell types. Most literature supports the latter argument that the effects of paracrine/endocrine secretory products play a significant role in glucagon secretion (5, 17). In brief, glucagon is released downstream by the entrance of Ca^{2+} into the α-cell, similar to the mechanisms involved in insulin secretion (18). In the presence of low glucose, sensed by the GLUT1 protein, the α-cell is electrically active, unlike the β-cell in this condition, primarily because of the increase in ATP/ADP ratio. This process activates the closure of K_{ATP} channel that depolarizes the α-cell membrane

allowing for the transfer of the action potential to the voltage-dependent Na^+, Ca^{2+} and K^+ channels (17). Thus the Ca^{2+} channels open and permit the entry of Ca^{2+} into the α-cell, triggering the movement of the glucagon-containing secretory granules to the cell membrane for exocytosis. The increase in circulating plasma glucose immediately lowers the influx of Ca^{2+} in the α-cells and therefore decreases the release of glucagon stores (6). The ion channels in the α-cells mimic similar channels found in the β-cells; however, the Na^+ channels are thought to play a more prominent role in the secretion of glucagon in the α-cells (5). These mechanisms just described are a brief explanation as to how low glucose levels can stimulate the release of glucagon. Recently, investigators have argued that the stimulation of glucagon is more likely a result of other factors such as paracrine/endocrine products and autonomic output (19). In this case, factors such as insulin, Zn^{2+} and γ-aminobutyric acid (GABA), co-secreted with insulin, play major roles in inhibiting the release of glucagon secretion in euglycemic conditions. They cause α-cell membrane hyperpolarisation induced by further closure of K_{ATP} channels that leads to inactivation of Na^+ channels, thereby decreasing glucagon secretion (19). There is still much debate about the exact role and mechanisms of glucagon secretion in the healthy islet, as well as in the disease state.

1.2.4. Introduction to Insulin Resistance/T2DM Pathology

Insulin resistance develops when peripheral organs such as skeletal muscle, liver, adipose and pancreas lose their ability to respond to insulin. In particular, skeletal muscle loses the ability to translocate the glucose transporter 4 (GLUT4) to the surface membrane, which would normally act to allow the uptake of glucose into the myocyte,

resulting in higher levels of glucose in the circulation (20). The liver can also develop insulin resistance, which disables insulin action to suppress gluconeogenic mechanisms, and hepatic glucose production becomes elevated (21, 22). As a result, glucose is continually produced from the liver through gluconeogenesis (non-glucose sources), perpetuating the state of hyperglycemia. In adipose tissue, insulin resistance leads to suppressed glucose uptake and increased lipolysis, as well as the release of proinflammatory adipokines (23). In an attempt to return the systemic glucose concentrations back to euglycemia (4-6 mM), pancreatic β-cells increase their cellular mass and release of insulin (24). Therefore, as insulin resistance is left untreated, it is likely that β-cell compensation will fail and eventually hyperglycemia will prevail (8). There is still much debate in the literature whether hyperinsulinemia drives insulin resistance, or vice versa, however, it appears that hyperinsulinemia is often the result, as well as a driver, of insulin resistance (25).

Poor glucose control in diabetes is well known to promote secondary complications or comorbidities, including cardiovascular disease, retinopathy, nephropathy and neuropathy (26). Therefore, diabetes control is essential and there are several interventions that help to reduce risks of adverse effects, such as insulin, diet, and exercise management (27, 28). A cluster of risk factors is linked to diabetes development, such as insulin resistance, obesity, physical inactivity and increased stress; however, the exact mechanism for diabetes development remains unknown (reviewed in (15)).

1.2.5. Impairments in Islet Function and Progression into T2DM

Maintenance of β-cell mass is critical to preserve normal GSIS and glucose homeostasis. In healthy pancreatic β-cells, glucose tolerance is sustained by proper β-cell adaptation to surrounding substrate conditions that balances β-cell mass through controlled up-regulation of proliferation/neogenesis mechanisms and regulated β-cell death. Therefore, as there is a greater insulin demand in the body, β-cell turnover changes by increasing proliferation/neogenesis and decreasing β-cell death that up-regulate β-cell mass. This is termed compensation (24). An imbalance in β-cell compensation demonstrates impaired β-cell growth and responsiveness, resulting in more β-cell death than growth (29). Prolonged disturbance in β-cell regulation pathways may result in the onset of T2DM development, where individuals display decreased β-cell mass and dysfunction (30).

During the progression of diabetes development, there are several steps that gradually limit β-cell compensation and ultimately survival (refer to Figure 1.2., image adapted from (15)). These include healthy compensation to various short-term stimuli, but long-term exposure induces altered adaptation leading to β-cell dysfunction, eventual reduction in β-cell mass and/or possibly exhaustion (8, 31). In brief, β-cell compensation typically occurs gradually as an individual's need for insulin increases with age, inactivity and increased body fat content. In the incidence of further insulin requirement, the islets compensate by inducing β-cell hyperplasia and hypertrophy mechanisms that result in an increase in insulin release and plasma levels (8). Blood glucose levels remain relatively normal as compensation ensues, although β-cells become highly sensitive to

glucose levels resulting in an overall increase in GSIS and sometimes hyperinsulinemia (32). Over time, if individuals maintain inactive lifestyles or an excessive caloric intake, β-cell compensation is no longer able to attain euglycemia (33). At this point, individuals may be classified as 'pre-diabetic' and may exhibit impairments in GSIS, however retain some ability to respond and avoid hyperglycemia (34). These individuals may demonstrate impaired glucose tolerance, in response to an oral glucose challenge, as well as elevated fasting glucose levels (6.1-6.9 mM); however, they do not exhibit overt hyperglycemia (>7.0 mM). It is important to note that being pre-diabetic may still put an individual at risk of developing cardio metabolic diseases. Interestingly, obese-insulin resistant individuals may take years to develop hyperglycemia and can sustain their state for long periods of time, sometimes up to several years (35-37). Finally, as the pre-diabetic condition is left untreated, individuals start to deplete their β-cell population, through up-regulated pathways of β-cell apoptosis/death, and ultimately develop T2DM (8). It has been reported that individual β-cells may reduce their functionality by up to ~ 75% with the onset of T2DM (38). Furthermore, as T2DM progresses, individuals lose the ability to synthesize insulin altogether and are forced to rely on exogenous insulin to regulate glucose uptake. The mechanisms of β-cell dysfunction have not been fully uncovered, but a vast number of studies have shown a variety of factors that play a role in limiting adequate β-cell compensation. These factors include increased levels of free fatty acids, glucose (i.e. lipo- and gluco-toxic effects), obesity, oxidative stress, GCs, and physical inactivity (39). An excellent model to study β-cell dynamics in the development of obese T2DM is the ultization of the classic model, the obese Zucker diabetic fatty

(ZDF) rat. Previous studies have shown that these animals demonstrate spontaneous hyperglycemia due to insufficient amount of β-cell mass and compensation (40) (ZDF will be discussed further in section 1.4.1). Unfortunately, β-cell dynamics in individuals with T2DM have yet to be fully elucidated, but similar to the ZDF rats, individuals with T2DM demonstrate reduced β-cell mass when compared to obese non-diabetic subjects (30, 41). However, the reduction in β-cell mass is suggested to be a consequence of, and not a reason for, T2DM, but further investigations are required to draw conclusions (42).

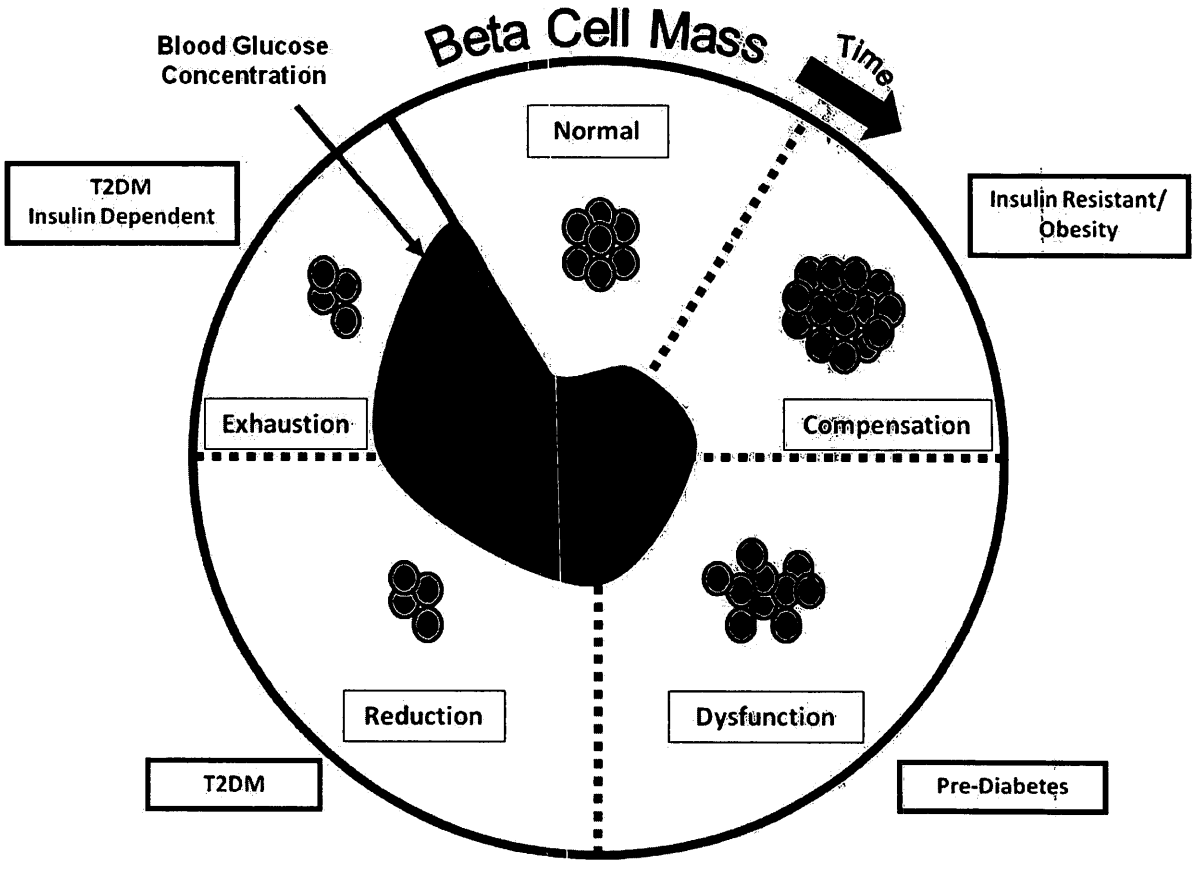

Figure 1.2. Development of T2DM. Pancreatic β-cells regulate blood glucose levels by increasing insulin synthesis and secretion, termed compensation. If an individual develops insulin resistance or becomes obese, β-cell populations may compensate by

increasing in size and mass that increases levels of insulin to maintain euglycemia. If β-cell compensation is continued for long periods of time then it could fail leaving depleted β-cell populations, termed pre-diabetes. If this condition remains untreated then individuals may progress to an even further reduction in β-cell populations that are insufficient to maintain euglycemia and hyperglycemia ensues leaving an individual with T2DM. Eventually if T2DM is not reversed then β-cells become exhausted and an individual may become insulin dependent.

Many studies have investigated β-cell dynamics and diabetes development, whereas very few studies have examined α-cell function in diabetes progression. As diabetes develops, there are major complications in the release of glucagon from the α-cells, as shown in rodent and cell-line studies. This is termed, "glucose blindness", where α-cells are unable to detect low levels of glucose in the plasma (17). This area of research is poorly understood, but it is thought that α-cell dysfunction is secondary to β-cell destruction with diabetes onset (17). Some research that has highlighted β-and α-cell populations in diabetes has suggested that in cases of T1DM, α-cells make up ~ 75% of the islet, but no differences in mass were found when compared to control subjects (43). Moreover, individuals with T2DM exhibit α-cell hyperplasia, and since α-cells comprise a greater proportion of the islet, leading to greater α-cell mass (6). Together, these results demonstrate that there are major differences between β- and α-cell regulation, compensation and progression with the onset of diabetes, and the type of diabetes development. More studies need to be carried out to further the understanding of these mechanisms underlying the pathogenesis of diabetes.

1.2.6. Hyperlipidemia, Obesity and T2DM development

Many risk factors contribute to the onset of obesity including genetic and environmental factors, i.e. increased social stress and poor dietary habits. It is unlikely that there is one factor alone that may induce obesity and more likely that a combination of factors combine, such as food consumption and decreased physical activity (44). A common model in rodents used to study obesity or increased levels of lipids is diet-induced obesity (DIO). In these studies, a diet typically high in saturated fat is used to induce obesity in otherwise healthy rodents, such as Wistar (45), Sprague-Dawley rats (46) or C57BL/6J mice (47-49). It is important to keep in mind that not all high-fat diets (HFD) administered in experimental models of obesity are similar. In general, a HFD consists of an increased caloric range between 30-60% of calories from fat compared to a standard laboratory chow diet (50), where the source of fat usually comes from animal lard. It is likely that animals sustained on a HFD for less than 2 weeks will develop early signs of obesity and insulin resistance (51), and animal strains more resistant to DIO take typically longer periods (> 8 weeks in Sprague Dawley rats) to show signs of metabolic dysfunction (52). These studies are applicable in today's society as there has been a dramatic epidemic of obesity, where more than 60% of people with T2DM in the United States are categorized as being overweight (53). Moreover, as obesity is the most common cause of insulin resistance in humans, it is the rate of obesity that is driving the parallel to the increased incidence of T2DM (54). It is important to note that rodent studies of DIO may not exactly relate to human obesity, as there appears to be a complexity of other factors that may induce weight gain, including increased

psychological and emotional stress (55). Taken together, obesity-induced insulin resistance factors do not necessarily act separately, but rather synergistically with other factors such as increased levels of stress to induce metabolic abnormalities and, potentially, T2DM.

1.3. Metabolic Effects of Stress and Glucocorticoids

1.3.1. General Overview of Stress

Scientifically the term, 'stressor' is difficult to define, partly because of the complexity of the stress response and partly because of individual differences in what people perceive as being stressful. Therefore, a general definition of 'stress' is "when homeostasis is threatened or perceived to be" (56). The stress response initiated by intrinsic or extrinsic factors involves sophisticated and integrated biological reaction mechanisms that occur at the molecular, cellular, and physiological levels. The primary mediators of the stress response are detected and achieved through activation of the hypothalamic pituitary adrenal (HPA) axis that act on peripheral tissues such as the liver, muscle and adipose tissue to mobilize energy substrates (56). The amount, predictability and perceived control of the stressor determine whether or not an organism is able to re-establish homeostasis (57). Thus, if equilibrium is not recovered and the individual remains in a state of chronic stress, then the risk of developing various diseases is greatly heightened. In rodent models of stress, research incorporates a number of areas including: exercise, physical restraint, electric shock or near drowning, exposure to extreme cold and an introduction of a socially dominant member of the same species (58). The stress

response, in humans, is more likely to increase to psychological rather than physical adverse events, which include emotional, social, or professional factors. In addition, the onset of a stressor becomes even more multifaceted as it may include hardship developed in a number of social and emotional situations and is difficult to simulate in a laboratory environment. The stress response during psychological stress may be more damaging than the stressor itself, as it may accumulate overtime if the presence of the stressor is not removed and it becomes viewed as a chronic type of stress. Chronic stress is associated with a number of metabolic disturbances including cardiovascular disease, insulin resistance and central obesity (59-62); however, physical activity, a stressor in and of itself, provides beneficial adaptations rather than deleterious effects to the body in rodents (63), as well as in humans (64). Despite differences in the causations of psychological and physical stress, both responses activate the HPA axis, but it is the adaptive ability of the stress response system to re-establish homeostasis that determines the degree of damage of the stressor.

1.3.2. The Hypothalamic-Pituitary-Adrenal (HPA) Axis

Typical acute activation of the HPA axis is present in a diurnal, pulsatile pattern (65) that in humans is decreased in early evening hours (~ 6-10 pm) and increased in early morning hours (~ 6-10 am) (66). This activation is also present in rodents, but because of their nocturnal nature they display increased activity in the early evening hours and decreased activity in the early morning hours (67). The HPA axis is centralized in the brain and the hypothalamus and can be activated by many different neural pathways through various internal and external stimuli. These signals converge at the

parvocellular neurons located in the dorsomedial region of the paraventricular nucleus (PVN) to stimulate the release of corticotrophin releasing hormone (CRH) and arginine vasopressin (AVP) into the median eminence (68). Both of these hormones travel through the hypophyseal portal circulation to corticotrophs located in the anterior pituitary where they stimulate the secretion of adrenocorticotrophin hormone (ACTH) and its precursor pro-opiomelanocortin (POMC) (69). About half of the parvocellular neurons contain AVP (70), which indirectly increases ACTH synthesis and release in response to prolonged stress (71). AVP on its own does not stimulate POMC gene transcription, but distinctly promotes the stimulatory effect of CRH on the activation of ACTH secretion (72). AVP increases the effect of CRH on ACTH secretion by binding to the V1b receptors (73), a process that increases the phosphorylation of PKC, ultimately increasing the release of intracellular stores of Ca^{2+} (72). CRH stimulation of ACTH secretion is up-regulated by CRH binding to the CRH1 receptor (74). This receptor is classified as a G-protein coupled receptor, which activates through adenylate cyclase to increase intracellular cAMP levels subsequently activating PKA, increasing the influx of extracellular Ca^{2+} and resulting in the release of ACTH from the anterior pituitary gland (74). Once in the circulation ACTH binds to the melanocortin 2 receptors (MC2R) located in the zona fasciculata (75) of the adrenal cortex that stimulates the synthesis and release of glucocorticoids (GCs) through the PKA pathway leading to steroidogenesis (76).

GCs are secreted into the systemic circulation and are taken up into every tissue in the body where GC receptors (GRs) are expressed. They play key roles in several

metabolic pathways, regulating salt and water metabolism, blood pressure, immune function, and energy homeostasis such as glucose metabolism (77). These functions allow for sophisticated synchronization between brain and body that manages situations of stress, recovery and adaptation. GRs are expressed ubiquitously throughout the body in virtually every organ, but most widely expressed in neural tissue that provides negative feedback of the HPA axis (78). There are two closely related types of receptors that GCs can bind to: the mineralocorticoid or type I receptor (MR) and GC or type II receptors (GR) that initiate GC actions and suppress HPA axis activity (79, 80). The GR is expressed with highest density in the parvocellular PVN and in the pituitary corticotrophs, while the MR is localized in the limbic neurons (81). There is a considerable amount of co-expression of the GRs and MRs within the hippocampus and the dentate gyrus. The MR binds to GCs with a 10-fold greater affinity than the GR, and is highly occupied at basal levels of HPA activity (59). It is thought that the role of the MR is mostly to maintain basal HPA activity, and the GR is responsible for terminating the HPA activity during stress and the circadian peak of GC secretion (59). GC negative feedback on the HPA activity is primarily mediated through inhibition at the level of the hypothalamus, anterior pituitary, and the hippocampus, which subsequently inhibits the synthesis of CRH, AVP (82) and ACTH (72). These feedback mechanisms can occur within minutes of the rise in GC concentrations in the circulation and can act through both fast and delayed feedback. These types of feedback mechanisms act through either non-genomic or genomic mechanisms, respectively (83). Ultimately, the reinstatement of basal HPA axis activation is highly dependent upon the complete removal of the stressor.

1.3.3. Glucocorticoids (GCs)

Active forms of GCs are secreted by the adrenal gland either as cortisol or corticosterone, in humans and rodents, respectively. They reach virtually every tissue in the body via the circulation, a process which gears the brain and body to cope with various survival mechanisms such as stress, recovery and adaptation (81). Steroidogenesis is a biological process regulated by the gene expression of steroidogenic acute regulatory (StAR) protein that initiates the increase in cholesterol delivery to the inner mitochondrial membrane and is the rate-limiting step in GC synthesis and production (84). The enzyme 17α-hydroxylase catalyzes the synthesis of cholesterol into cortisol (in humans) in the area of the zona fasciculata located in the adrenal cortex. Another region of the adrenal gland, called the zona glomerulosa, does not contain the enzyme 17α-hydroxylase and as a result cannot synthesize GCs. Instead, this region is responsible for the synthesis and release of mineralocorticoids such as aldosterone, which plays a central role in water/electrolyte balance and blood pressure regulation. This pathway of GC synthesis is not the same in rodents as they do not process 17α-hydroxylase enzyme and are unable to move cholesterol in the mitochondria to make GCs. Therefore, rodents do not produce cortisol, but instead produce GCs such as corticosterone and the inactive GC, 11-deoxycorticosterone (11-DHC) (85). Inactive GCs are also released into the circulation from the adrenal gland, such as cortisone and 11-DHC in humans and rodents, respectively. It has been reported that the circulating active to inactive ratios range from as high as 8:1 (active to inactive ratio) (86), to as low as 3:1 (87); however, the physiological relevance is not fully understood. This reported

difference in active versus inactive ratios is likely due to the enzyme, 11β-hydroxysteroid dehydrogenase (11β-HSD1) that acts to convert GCs from their inactive to active form. This enzyme will be discussed in further detail in section 1.3.5.

Cortisol and corticosterone are hydrophobic hormones that are not able to circulate in the body without assistance of a carrier protein. Albumin is a water-soluble globular protein that binds ~ 15% of the body's cortisol during basal circadian circulation, while ~ 80% of the cortisol circulates with the assistance of the cortisol binding globulin (CBG) and ~ 5% is considered free cortisol (88). CBG is released from hepatocytes and circulates in the bloodstream with a concentration of 32-50 pg/ml (89). In instances of high stress where cortisol levels reach ~ 400-500 nmol/L, CBG becomes saturated and this development raises the levels of free cortisol significantly to levels higher than 20% in the circulation (90). The role of the CBG in the body is traditionally viewed as being a carrier protein; however, it may help buffer a large flush of free cortisol into the tissues during a stressful event or as a reserve for the body's store of cortisol in cases of inhibited or reduced cortisol in the circulation (89). There are other stimuli that are able to manipulate the amount of CBG in the circulation, ultimately altering the amount that enters the tissue. For example, patients with post-traumatic stress disorder, which traditionally exhibit low cortisol levels, exhibit elevations in CBG levels (91). Moreover, a stress response that activates cortisol, as well as interleukin-6 (IL-6) directly hinders the CBG gene transcription up-regulation, thereby indirectly increasing free cortisol levels and GC activity within the tissue (92). In humans, exogenous IL-6 has been shown to decrease CBG by ~ 50% as have illnesses such as sepsis and burns (90,

93). Very few studies have addressed the measurement of CBG in various stimuli such as exercise (94) and obesity (95), and no studies have investigated the levels in T2DM patients. An acute bout of exercise results in an up-regulation of CBG, from highly trained athletes to sedentary individuals (94). Interestingly, whole-body massive weight loss, as well as conditions such as obesity results in a decrease in CBG levels and increase in free cortisol (96). It has been suggested that CBG plays a role in people's adaptation to stressful environmental conditions (95). More research in this area of work would be beneficial to further understanding of GC physiology and may provide insight into various roles that GCs play in exercise and disease models.

1.3.4. Glucocorticoid Receptor (GR)

Cortisol is only considered to be biologically active when it is free and not bound to any carrier protein (97). Free cortisol or corticosterone is capable of entering the tissues, thus only a small portion of active GCs are able to enter into the cells, which helps to protect against GC excess in the tissues. On the other hand, inactive GCs (cortisone and 11-DHC) are very capable of circulating in the system without the assistance of a carrier protein and, because of this characteristic, can readily enter the cell. Upon crossing the tissue membrane or being converted from the inactive state by 11β-HSD1, active GCs bind to the GR and elicit their functions. The GR exists in the cytoplasm of the cell without a ligand bound as a large multi-protein complex made up of polypeptides, two molecules of hsp90, and many other proteins (98). Once the GCs occupy the binding sites on the GR, they dissociate from the hsp90 proteins, protein complex and undergo a change in the conformation. The GR complex translocates to the

nucleus where it homodimerizes or heterodimerizes with another GR complex. Depending on the type of dimerization it will bind to the GC-response element (GRE) found in the promoter region of GC-induced target genes and cause either activation or repression of gene transcription (81). Moreover, gene expression is not always manipulated by the binding of GR to the GRE, but, in fact, it can interact with other transcription factors and activate other proteins such as activating protein-1 (AP-1) and nuclear factor-κB (NF-κB) (98).

The GR is a member of the nuclear receptor family and contains a complex structure composed of various independent binding sites. It contains the following domains: amino-terminal regulatory, DNA-binding, hinge region, ligand-binding, and carboxyl-terminal domains (99). The whole body knockout model of GR in mice results in respiratory failure and eventual death of the animal at birth, thus demonstrating the critical role that the GR plays on the entity of biologic function (100). The GR gene exists in multiple splice variants on exon 9 that produce GRα, GRβ and MR (101). Ligand binding where it translocates to the nucleus and forms two homodimers between two GRα proteins activates the GRα. On the other hand, GRβ is unable to bind the ligand; suggestive of its shortened length compared to GRα, it does not participate in gene regulation or GC responsiveness (102). Moreover, GRβ resides in the nucleus and is thought to inhibit GRα activity. Therefore, it is classified as a dominant negative regulator of GC-induced gene expression that binds to the GRα, creating an inactive heterodimer (101, 103). As a result of the nature of these isoforms, it is suggested that they manipulate the role of GC within the tissues, possibly playing a more predominate

role of GRβ in various disease states such as those thought to be GC resistant (102). Moreover, to add to the complexity of GC regulation there are recent reports suggesting that as many as 7 GRα isoforms reported, and that each of them has its own set of gene regulation (99).

The activated GR complex (ligand bound) is responsible for the up-regulation of various anti-inflammatory proteins in the nucleus as well as the inhibition of the expression of proinflammatory proteins in the cytosol (prohibits movements of transcription factors from the cytosol into the nucleus). The former mechanism of action is referred to as transactivation, while the latter is transrepression (104). The binding of the GR complex to the positive GRE areas initiates the up-regulation of gene transcription of various anti-inflammatory proteins such as IL-10, annexin-a1 and inhibitor of nuclear factor (I-κB). This process, transactivation, is known to be the regulator of adverse effects of GCs. In contrast, the process known as transrepression is also regulated by the GR complex, where it inhibits the transcription of proinflammatory genes such as IL-6, NF-κB and AP-1(104). This pathway is the most targeted by anti-GC action agents that act through anti-inflammatory and immunosuppressive mechanisms.

1.3.5. The pre-receptor enzyme 11β-HSD1

Tissue exposure of GCs is manipulated through the number of GCs in the circulation reaching the tissues, but also is controlled by the pre-receptor enzyme 11β-HSD1 that is a low-affinity nicotinamide adenine dinucleotide phosphate (NADPH)-dependent enzyme, which acts to convert inactive GCs into active GCs. This enzyme is

expressed in most tissues such as those in the liver, adipose tissue, central nervous system, immune cells, skeletal and smooth muscles that arbitrate actions via GR (105). An isoenzyme similar to 11β-HSD1 is the high-affinity NADPH-dependent dehydrogenase, 11β-HSD2 which is predominately found in MR target tissues such as those in the kidney, colon, placenta, sweat and salivary glands (105). 11β-HSD2 is unique as it catalyzes the reverse mechanism of 11β-HSD1, whereby it converts cortisol to cortisone, in humans. The significance of the 11β-HSD1 regulation is interesting as it is known to increase the concentration of active GCs in the tissue by ~ 2-fold in transgenic mice (106). Also, higher 11β-HSD1 activity within the tissues has been associated with abnormal GC activity in the adipose tissue of obese individuals which leads to larger amounts of GCs within the tissues, promoting adverse effects of GCs (107). In addition, a mouse model knockout of 11β-HSD1 showed improved glycemic control and reduced body and visceral fat mass gain, concomitantly with chronic high-fat feeding (108). Together these investigations into this enzyme and its activity have isolated a role for its abnormal activity in relation to obesity and T2DM development. Further explanation of the role of 11β-HSD1 on pancreas specific abnormalities will be discussed in section 1.4.2.5. of this literature review.

1.3.6. Peripheral GC action

The peripheral actions of GCs are exerted in virtually every tissue as almost all tissues express GR. The tissue-specific responses are dependent upon the availability of the hormone, activity of 11β-HSD1 and the density of the GR (109). Acute stress helps to mobilize fuels from storage to be utilized in working tissues. In the adipocytes, greater

increases in GCs have been shown to cause greater lipolytic effects, which increase the release of fatty acids (110). In the liver, GCs up-regulate the increase in hepatic glucose production from non-glucose sources by influencing the transcription of rate-limiting enzymes such as phosphoenolpyruvate carboxykinase and glucose-6-phosphate (111). Skeletal muscle also helps to liberate fuels in times of acute stress by decreasing protein synthesis and increasing proteolysis. This process helps to increase the amino acid pool for the liver to drive gluconeogenesis (112). Therefore, acute stress is beneficial to an organism in times when fuel substrates are low, but prolonged activation of HPA axis and these pathways demonstrates perpetual hypercatabolism resulting in adverse effects.

1.3.7. Stress and Food Intake

The physiology of feeding behaviour and HPA axis has been a topic of study for many years as they are highly associated with one another. Elevations in GCs are shown to rise postprandially in humans (113, 114), as well as in rats (115). Many correlations exist between the activation of the HPA axis and food intake. The feeding centres in the brain are located in the PVN of the hypothalamus, which is the same location where the neurons synthesize and secrete CRH. Adrenalectomy in the rat results in hypophagia, as lower GCs decrease feeding behaviour regulation, and the administration of corticosterone reverses this effect (116, 117). In constrast, humans who typically practice "dietary restraint" (sic), such as those who are constantly watching their weight or are very conscious of their eating behaviours, show to have an increase in GC levels as this behaviour results in chronic stress (118). In addition, individuals who are non-dieters show an increase in stress with the absence of food (119). Stress-induced eating is likely

to initiate after a stressor or with the incidence of being presented with highly desirable or palatable foods (118). Chronically high levels of perceived stress are related to an increase in feeding (120) specifically for more palatable foods such as those with high fat and sugar content, whereas people who are in a state of contentment will be more likely eat healthy foods such as dried fruit (reviewed in, (121)). Interestingly, people who are able to perceive their own increased level of stress are more likely to change their regular eating habits. It is estimated that ~ 40% of people will increase their feeding behaviour in a highly stressed state and ~ 40% of people will do the opposite and decrease their eating behaviour. The other ~ 20% will not change their habits (121, 122). Moreover, it is suggested that those who are more likely to be overweight will generally increase food intake in the stressed state whereas those who are underweight are more likely to eat less (123). The relationship between weight gainers and losers may be related to levels of circulating insulin, as it is an anabolic hormone, thus increasing energy stores. Therefore, those people who have a higher body mass index generally have an increase in insulin levels, which may be indicative of their increased storage capacity (121, 124). Importantly, acute physical and emotional stress in laboratory environments is up-regulated with food intake and shifts desires towards foods with higher fat and sugar content (125) even if the subjects are not hungry or do not have a homeostatic drive for more calories (118). Although in conditions of chronic stress rats will decrease their total food intake, given the choice they will choose more palatable foods (126). This response has been suggested to help "dampen" the stress response under conditions of chronic stress (126). It is important to note that as a result of chronic or sustained stress, animals

will decrease food intake eventually causing a reduction in body weight (127). Moreover, the removal of the stressor from chronically stressed animals does not appear to help regain the weight lost (128). Therefore, it appears that chronic elevations in GCs play a major role in food intake and body mass regulation that could induce permanent or long-lasting detrimental effects to whole-body physiology.

1.3.8. GC-Induced Ectopic Fat Deposition

Adipose tissue is particularly essential in the body that helps mobilize energy stores when fuel substrates are needed and stores excess energy in basal conditions. Lipids are stored in the adipose tissue as triglycerides (TGs) and upon mobilization they are broken down by lipases, which results in molecules of fatty acids and glycerol (110). GCs play a role in regulating energy flux within the adipose tissue and can influence adipose tissue morphology. GCs are classically defined as being catabolic as they induce lipolysis and liberation of fatty acids; however, GCs act differently in the adipose tissue when given exogenously or in a chronically elevated state. A clear link now exists between increased levels of GCs and ectopic adiposity. A meta-analysis conducted showed that increased perceived stress in adolescence and abdominal obesity were highly correlated and demonstrates the relationship between increased GCs and fat accumulation (129). Moreover, other studies investigating the effects of environmental, social, and psychosocial stress have been linked to increases in the incidence of obesity (130). GCs may cause adipocytes to hypertrophy, as a result, increase storage or GCs may induce hyperplasia, which promotes more adipocytes (131). Excess GCs, as found in individuals with Cushing's syndrome (132) and rodents given exogenous GCs (106, 133), result in

both enlarged and more adipocytes, thus demonstrating the link between GCs and ectopic fat.

1.3.9. Cushing's syndrome

Cushing's syndrome results in abnormal elevation in GCs that induce detrimental physiological effects over the body. It is suggested that the most common cause of Cushing's syndrome is the administration of pharmacologic doses of oral or topical steroids (134). Other ways patients can develop Cushing's syndrome is through an ACTH–secreting pituitary tumor, ectopic (non-pituitary) ACTH production, or an adrenal tumor (135). A commonality with these different origins is that there is loss of the diurnal secretion of GCs and negative feedback on the HPA axis, thereby leading to a constant elevation in circulating GCs. Cushing's syndrome is hard to detect because sometimes the symptoms can take years to develop, and the vast metabolic and physiologic dysfunctions are complex. Hypercortisolism can lead to numerous abnormalities such as an increase in central obesity, muscle atrophy and weakness, bone loss, depression, glucose intolerance, hypertension, insulin resistance and adrenal suppression possibly leading to adrenal insufficiency (135). Cushing's syndrome exists in ~ 3% of obese individuals possibly leading to poor glycemic control (136). Moreover, patients with Cushing's syndrome who develop central obesity have an increased risk (60-80%) of developing glucose intolerance and perhaps diabetes if the disease persists without intervention (137, 138). Several therapeutic options can help to control hyperglycemia (GR antagonists, discussed in section 1.5) in Cushing's syndrome patients; however, most patients rely on insulin to reduce glucose levels (135). Hyperglycemia usually prevails after the onset of

hypercortisolemia and therefore, glucose control might be easier to treat once elevated levels of cortisol have been lowered (63). Although the exact prevalence of Cushing's syndrome in individuals with T2DM has been hard to identify as many symptoms of these two diseases overlap, it is suggested that ~ 25% of those using steroids could potentially develop T2DM (138). If surgery is unsuccessful, there are several interventions that Cushing's syndrome patients can pursue to help lower hypercortisolemia, including diet, exercise and pharmacological agents such as GC antagonists. Interestingly, very few studies have been conducted in all of these areas on Cushing's syndrome patients and therefore more studies would provide further insight into the disease prevalence and intervention. Further discussion will follow in section 1.5.7.

1.4. Stress and T2DM

1.4.1. GCs and Insulin Resistance/T2DM

Many factors have been identified with the onset of T2DM such as increased whole-body insulin resistance as a result of elevated ectopic fat (139) and pancreatic β-cell dysfunction due to lipid and glucose toxicity (140, 141). One aspect that these symptoms have in common is that they can be induced with increased levels of GC exposure (142, 143). Interestingly, elevated GCs have been shown to precede hyperglycemia in humans (135) and in rodents (63, 144), and are related to the severity of diabetes. Moreover, as previously mentioned the use of topical, inhalant, and cream steroids is greatly associated with an increased incidence of glucose intolerance/insulin

resistance and possibly diabetes development (145). In addition, Hoes et al., 2011 (146) reported that they discovered that 11% of their subjects with arthritis had undiagnosed cases of T2DM and 35% had impaired glucose metabolism. The elevation of GCs have been linked to T2DM development for many years (147), but to this date the exact mechanisms by which short- and long-term GC excess influence β-cell function remain inconclusive.

There are many rodent models of T2DM that researchers choose to study the development of diabetes and its link to elevated GCs. One in particular is the ZDF rat model that exhibits a mutation in the leptin receptor gene and spontaneously becomes hyperinsulinemic ~ 4-7 weeks of age, then becomes hyperglycemic by ~ 7-12 weeks (148, 149) and displays many other similar characteristics of obese T2DM individuals. Research shows that the increase in GC levels precedes symptoms of diabetes, as ZDF rats develop hypercortisolemia at ~ 3 weeks into experimental protocol (63, 144, 150). These ZDF model studies provide strong evidence that there is an association between the elevation of GCs and the onset of diabetes. Therefore, it is important to identify the direct and indirect effects of GCs on islet/β-cell function as this may provide a link to T2DM onset or at least β-cell dysfunction.

1.4.2. GCs and Islet Function

Some studies have examined the effects of GC exposure and islet function, but the exact mechanisms of action remain unclear, as some studies suggest that GCs promote and others suggest that GCs inhibit β-cell function. It does appear that results may be

related to duration, dose and how GCs are administered *in vivo* or *in vitro.* Therefore, the following paragraphs have been divided into the appropriate headings to provide the clearest explanation of the literature.

1.4.2.1. Acute GC treatment and *In vivo* β-cell Function

Peripheral insulin resistance is a major concern with GC therapy, but studies suggest that it may be dependent on the duration and the dose (151, 152). In rodent studies, acute *in vivo* administration (< 5 days) of dexamethasone, a synthetic GC agonist, induced many morphological and physiological alterations to Wistar rat islets such as increased β-cell compensation/adaptation mechanisms through an increase in β-cell mass, size and proliferation (153). Moreover, another study demonstrated that raising doses of dexamethasone increased levels of cyclin D and phosphorylation of insulin receptor substrate 2 (IRS2), indicative of augmented islet proliferation and compensatory mechanisms (154). Dexamethasone treatment also induced hyperinsulinemia and increased basal, glucose and arginine-stimulated islet insulin secretion, which was also found to be dependent upon varying, doses of GCs (0.1-1.0 mg/kg) (152) and duration of doses in lean C57BL/6J mice islets (155). In another study, high doses of dexamethasone (1 mg/kg) were shown to increase GSIS, indicating that dexamethasone increased Ca^{2+} influx after glucose uptake (2). PKCα levels were found to be up-regulated in islets of the dexamethasone-treated rats as well as an increase in docking of secretory granules to the β-cell membrane, indicating that dexamethasone induces hyperinsulinemia by increased PKCα activation, insulin exocytosis and peripheral insulin resistance (2).

There is still much debate as to the exact mechanisms for the diabetogenic actions of acute elevations in GCs in humans, but some recent studies suggest that it deteriorates islet function. Two days of GC administration (prednisolone, 75 mg) in humans, results in a blunted first-phase glucose- and arginine-stimulated c-peptide secretion (156) and diminished islet glucose sensitivity, but no changes in fasting insulin levels. Moreover, in the same study (156), similar results were found in individuals using chronic GCs for less than 14 days, evidence which paralleled other studies (157, 158). These results are important, as there are very few studies in the literature that have examined these links between acute GC administration and β-cell dysfunction, in humans. Moreover, the differences between acute administration of GCs in rats and humans are unclear, as it appears that in rats, GCs induce increased islet compensation while in humans they cause β-cell dysfunction or glucose insensitivity. Moreover, rodents that overexpress islet specific GR demonstrate a reduction of insulin secretion and β-cell function (159, 160), which further supports the hypothesis that GC excess may play a direct role on islet dysfunction and T2DM development.

1.4.2.2. Acute GC treatment and *In vitro* β-cell Function

Although there have been various studies conducted on *in vitro* GC administration in rodent islets, there is still much debate over what GCs do to islet function, and the varying effects observed may be related to dose and duration of GC exposure. As dexamethasone exposure (1-6 hours) and concentration (1-100 nmol/L) were increased in a serial fashion, β-cell function was increasingly impaired, as evident by a lowering of insulin synthesis (161). Similar results were also reported in isolated healthy mouse islets

as higher levels of dexamethasone and longer incubation periods resulted in lower insulin secretory capacity impairing the efficacy of Ca^{2+} on the secretory process (3). The effect of 4 hours of dexamethasone treatment in the insulin secreting cell line (INS-1E) demonstrated that abnormal Na^{+}/K^{+} ATPase activity in β-cells caused β-cell membrane hyperpolarization (162). This treatment increased voltage-gated K^{+} channel activity, lowering appropriate Ca^{2+} influx into the cell and consequently decreasing insulin secretion (163). Another study indicated that INS-1E cells subjected to 20 hours of prednisolone showed impairments in insulin biosynthesis, GSIS, and increases in apoptotic markers (164). This study found that prednisolone treatment induced irregular amount of ER stress through unfolded protein response elements, which caused β-cell dysfunction in the INS-1E cells. A supraphysiological level of corticosterone (10-500 ng/ml) for 3 days also results in abnormal islet function in isolated β-cells from Wistar rats (aged 8-12 weeks) (165). This study also found that corticosterone-exposed β-cells had a blunted first-phase Ca^{2+} response to increased concentrations of glucose (8.3 mM). This study confirmed that the blunted response of the β-cell was mediated through the GR as RU486 treatment, a non-selective GRII antagonist normalized β-cell Ca^{2+} influx and insulin response to glucose challenge. Together these findings suggest that acute GC treatment *in vivo* in humans and *in vitro* in rodents is mediated through the GR that cause major β-cell dysfunction and possibly T2DM onset.

1.4.2.3. Prolonged GC treatment and β-cell Function

In contrast to acute GC treatment, evidence suggests that prolonged GC treatment (> 5 days) increases GSIS via β-cell expansion in healthy rodents, thereby limiting

diabetes development. In a study that administered dexamethasone to Wistar rats for 24 days reported that less than 20% of the animals became diabetic (166). Interestingly, hyperglycemic rats induced by dexamethasone had significantly lower GSIS suggesting failure of β-cell compensation, while rats that remained healthy (normal glycemic) demonstrated elevated β-cell compensation through increased *ex vivo* arginine-stimulated insulin secretion. Moreover, GCs (2 mg/kg, for 12 days) administered to healthy male Sprague-Dawley rats induced hyperglycemia and hyperinsulinemia, as a result of increased peripheral insulin resistance (167). Further analysis of the islets *ex vivo* revealed that the β-cells adaptively increased glucose responsiveness, but not efficacy of glucose to stimulate insulin secretion (167).

Moreover, unlike long-term GC treatment in healthy rats the Zucker (*fa/fa*) rats treated with dexamethasone for longer than 10 days reduced GSIS (166). These results suggest that GC excess, similar to the example of islet specific GR transgenic mice (159, 160), compromises appropriate islet responses to increased peripheral insulin resistance (168). Therefore, it may be concluded that in animal models that already have increased levels of GCs and metabolic dysfunction, such as the ZDF rat, the addition of more GCs (via dexamethasone injections) overwhelms the islet compensatory system, thereby resulting in lower GSIS.

Chronic exogenous GC therapy in humans (> 1 year) is common for a many inflammatory conditions such as rheumatoid arthritis, cancers and dermatitis. In these instances, even in healthy individuals given a low- (7.5 mg) and high-dose (30 mg) of prednisolone for 2 weeks, insulin secretion can become impaired along with hepatic

glucose production (146, 156). It is extremely important that physicians prescribing even low-doses of GCs to be aware of the detrimental implications that can take place with GC therapy (146). Recently, a study investigated the incidence of elevated GCs associated with hyperglycemia and T2DM in children and found 80% of patients admitted to the paediatric unit had blood glucose levels > 200 mg/dl (169). In addition, mortality was also correlated to increased blood glucose levels > 200 mg/dl which was associated with increased GC levels. Unfortunately, the issue that chronic GC treatment induces diabetogenic effects in patients with inflammatory or autoimmune conditions continues to be under-monitored.

In general, acute GCs promote β-cell compensation *in vivo* in otherwise healthy rodents, but alter glucose sensing mechanisms *in vitro,* as the islet is unable to compensate appropriately. Prolonged GC treatment in humans is a concern for longer-term users and especially in children; however, GC treatment may be most detrimental to those who exhibit a compromised metabolic system and GCs in excess may induce β-cell dysfunction.

1.4.2.4. GCs and α-cell Function

There are limited studies on effects of acute and prolonged GC treatment on α-cell function and glucagon secretion. Dexamethasone treatment increases fasting plasma glucagon concentrations in insulin resistant first degree relatives of patients with T2DM (170) as well as in rodents (154). Moreover, it is reported that early onset diabetes is associated with α-cell dysfunction as glucagon is secreted at abnormally high levels during oral glucose challenge (171) and α-cell mass increases linearly with a rise in

peripheral insulin resistance (172). Although the mechanisms of GC-induced α-cell function and glucagon secretion are virtually unknown, they may result as a secondary defect of GC-induced β-cell dysfunction.

1.4.2.5. 11β-HSD1 Activity and Islet Function

Elevated 11β-HSD1 is found in pancreatic islets of obese/diabetic rodents (173) as well as in islets from ZDF rats (174). It is thought that the increase in GC action in the islet caused by elevated 11β-HSD1 activity suppresses insulin secretion (155, 173), thereby promoting diabetes development. In lean healthy mice increased islet 11β-HSD1 activity was associated with increased GSIS, thus demonstrating a link between GC activation and regulation of genes involved in insulin secretion (155). Recently, however, the use of a β-cell specific 11β-HSD1-overexpression model suggests that elevations in this enzyme actually improve insulin release mechanisms and protects against HFD-induced diabetes (175). These results are supported by previous work, showing that islets cultivated with the inactive GC (11-dehydrocorticosterone) result in a rapid doubling in 11β-HSD1 protein (176). Therefore, the increase in 11β-HSD1 protein may help the β-cell to compensate during increased levels of insulin resistance. A threshold may exist where increased levels of GCs override the system and induce β-cell decompensation, but these studies remain under reported.

1.4.3. Lipids and Islet Function

Elevations in free fatty acids (FFAs) are usually found in obese, insulin resistant or diabetic individuals and more importantly in those who suffer from hypercortisolemia

(135). Acute accumulation of FFAs in the circulation has been shown to increase β-cell mass as a defense mechanism against insulin resistance that promotes β-cell compensation. Lipotoxicity within the β-cell induced by increases in FFA levels has long been known to result in impairments in β-cell function *in vivo* and *in vitro* (177). Prolonged elevations in FFAs have been shown to decrease β-cell insulin secretion (178, 179), in addition to reducing the expression of the insulin gene thereby inducing insulin biosynthesis (180). In contrast, administration of HFD or lipid infusions in rodent models has not consistently demonstrated impairments of β-cell function *in vivo* and it is suggested that this may be the result of varying degrees of insulin sensitivity among individual subjects (140).

FFAs are normally taken up into the β-cell by proteins along the mitochondria membrane and utilized for β-oxidation. FFAs enter into the β-cell via the plasma membrane or they are mobilized from TG stores found within the β-cells. They are broken down into long-chain fatty acids (LCFA) and transported into the mitochondria. Simultaneously, glucose is also taken up into the β-cell and utilized by glycolytic mechanisms that yield pyruvate. This substrate is helpful towards FFAs usage in the β-cell as pyruvate is also utilized by the mitochondria in combination with FFAs for β-oxidation. This process increases the amount of citrate produced by the mitochondria and as β-oxidation continues to cycle there is an accumulation of citrate in the cytosol. Citrate can be broken down into acetyl-CoA and then into malonyl-CoA that blocks activity of carnitine palmitoyltransferase I and subsequently inhibits LCFA uptake into the mitochondria (181, 182). LCFAs accumulate in the cytosol along with by-products such

as ceramides that are damaging to the β-cell (183). Although LCFAs in excess do not have an effect on insulin secretion, they have been shown to inhibit insulin gene expression (180). This impairment in β-cell function creates stress on the mitochondria and greatly contributes to overall β-cell dysfunction. Studies show that only palmitate and oleate FFAs are known to decrease insulin secretion, and further, palmitate is the only FFA known that induces a reduction in insulin gene expression factors (180) and causes lipid peroxidation products which are known to cause impaired insulin secretion. In addition to the rise in lipid intermediates such as ceramides, within β-cells, increases in FFAs have also been shown to directly contribute to an activation of c-Jun NH2-terminal kinase (JNKs) (184, 185). Up-regulation of the JNK is associated with the impairment of insulin signaling pathways by phosphorylating serine residues of IRS2 and decreasing downstream effects of GSIS (185). This is not the only mechanism of β-cell dysfunction induced by elevations in FFAs, as oxidative stress also plays a role in FFA-induced β-cell impairments (186, 187). It is known that pancreatic β-cells have low antioxidant defenses (188) and these features increase islet vulnerability to reactive oxygen species that decrease function (189). Moreover, increased FFAs have been linked to endoplasmic reticulum stress and unfolded protein response that promotes β-cell apoptosis (190). As shown, FFAs may disrupt several processes in β-cells, which impair GSIS and insulin biosynthesis. Therefore, in addition to detrimental effects of GCs, lipids also induce harmful conditions that can destroy healthy β-cell function and compensation.

1.4.4. Combined effects of GCs and HFD treatment on Islet Function

There are very few studies that have investigated the combined effects of GCs and HFD on β-cell function, but some have shown that both factors induce impairments to normal β-cell function. For example, Holness et al., 2005 (191) examined the combined effects of repeated dexamethasone injections (100 μg/kg of body weight) for 5 days and HFD in Wistar rats for 4 weeks. These treatments resulted in extreme glucose intolerance after acute intravenous glucose challenge despite major β-cell compensation, evidenced by hyperinsulinemia. This study suggested that the observed results were in part because of impaired first and delayed second-phase insulin response. In addition, *ex vivo* experiments confirmed those islets from dexamethasone-HFD rats had an impaired first-phase insulin response, but had an overall higher GSIS than those animals that were treated with a HFD alone. Gremlich et al., 1997 (192) also showed similar effects in isolated male Sprague Dawley rat islets, where GLUT2 and subsequent insulin release was impaired with fatty acid (palmitate) administration into the islet media. These results were even more apparent when islets were subjected to dexamethasone as GLUT2 protein content decreased by 65%, thus lowering insulin secretion. These data suggest that HFD in addition to GC treatment impairs *in vivo* and *ex vivo* glucose sensitivity.

1.5. GCs and Exercise

1.5.1. Exercise Protocols; Forced vs. Volitional

Forced training in rodents is a good laboratory method that provides precise control over the amount, intensity and duration of exercise being performed. It also can

provide beneficial effects such as lower body weight gain and increased skeletal muscle citrate synthesis activity indicative of mitochondrial biogenesis (193). There are 3 main categories that forced training methods for rodents can be divided into: 1) treadmill running, induced by foot shocks at the base of the treadmill (194) or bursts of air, 2) forced swimming, often with weighted attachments (144) and 3) ladder climbing, usually encouraged with electrical shock (195). Although forced exercise training has its advantages, it also invokes fear in order to encourage animals to exercise (electrical shock, bursts of air, or drowning). In addition, forced exercise training is usually conducted during the daytime when animals are usually sleeping and GC levels are at their lowest (196). Therefore, forced exercise training can exhibit various alterations in the body that are similar to chronic stress and not due to exercise training alone, such as adrenal hypertrophy, decreased CBG protein concentration in the plasma and ultimately artificially raised plasma GCs (193). Therefore, it is hard to differentiate the outcomes of exercise or increased stress levels especially when monitoring HPA axis activity.

Voluntary wheel running is also a beneficial exercise regime that involves attaching a running wheel to a standard rodent cage and allowing animals to exercise on their own. This exercise will typically commence during the evening hours and it is preferrable to forced trained exercise protocols because it allows the effects of exercise to be studied without psychological/circadian disturbances to the HPA axis (197). Most laboratory housed animals such as mice, rats, squirrels, hamsters and even rabbits will voluntarily run on a running wheel apparatus (63, 198-201). Voluntary exercise can be quantified by tallying the number of wheel revolutions completed by the animal;

however, it is difficult to control the amount of running each animal is doing and the intensity of the exercise. It is interesting because there are noticeable differences between rats and their various running behaviours, some will run > 10 km per evening and some will run < 2 km. These observations are consistent within certain animals, as some will always run more than others. It is very unlikely an animal that does not typically run > 10 km a night will suddenly start to run much longer distances than it has in the past. However, all rodents are likely to run more if they are food deprived. Interestingly, the quantity of exercise in voluntary running depends on the species of animal (201) and, age of the animal, as younger animals typically exercise more than older ones (202). Typically, hamsters will reach maximal activity almost immediately after being put into running wheels, while rats will need an inhabitation period and this will take them ~ 4 weeks to reach their maximum running distances (203). Moreover, in contrast to forced exercise training, rodents exposed to voluntary running will press a bar for wheel access. This behaviour indicates that rodents are motivated to exercise and giving them wheel access is viewed as a reward (204). Interestingly, a recent study by Cook et al., 2013 (205) suggests that forced treadmill exercise is a worse training model than voluntary exercise in a rodent model of colitis. They found that forced training greatly increased incidence of gut inflammation and induced higher mortality rates than voluntary wheel running which showed to be protective against colitis onset. In regard to these and previously mentioned findings, voluntary wheel running may be a better regulator of HPA function while forced training exercise may exacerbate HPA activity inducing excess GCs.

1.5.2. Acute vs. Chronic Exercise and HPA activation

Acute exercise is often neglected as a major physiologic stressor, but, in fact, it does stimulate the HPA axis resulting in an increase in GCs, that can remain elevated for several hours into recovery (~ 2 hours) (206). However, the activation of the HPA axis appears to be reflective of the intensity and duration of the exercise. For example, light to moderate intensity exercise does not increase relative activation of the HPA axis, but as exercise intensity progressively increases, as does GC release and secretion (207). Surprisingly, as exercise intensity reaches higher levels, GC circulation is reduced (207). This is thought to result as a protective mechanism to prevent the complete depletion of energy stores and possibly limit GC excess (207). The mobilization of various energy stores is important during exercise so that organs and tissues have a proper supply of fuel. GCs induce fuel yielding mechanisms in the body during exercise as a mechanism to prevent hypoglycemia. This is evident in a study of adrenalectomized rats that underwent 4 hours of swimming to show that they had less of a decrease in liver and muscle glycogen stores when compared to healthy rats. Moreover, the adrenalectomized rats displayed an episode of hypoglycemia following exercise (208). There appears to be a different relationship with the effect of acute exercise and adipose tissue regulation, as adrenalectomized rats do not have alterations in lipolytic rates after exercise (209). The mechanisms of acute exercise on peripheral tissue exposure to GCs are not known. Moreover, in endurance-trained men the effect of acute exercise lowered monocyte GC sensitivity suggesting adaptations to exercise training in the HPA axis (210), but more studies are needed to be conducted to confirm these results.

As acute exercise elevates GCs in the circulation and sometimes hours after exercise (210), it would be reasonable to believe that regular exercise training might extend episodes of endogenous hypercortisolemia. This is not the case with exercise training, where exercise leads to positive adaptations and encourages improved insulin sensitivity in peripheral tissues (211). Therefore, it is hypothesized that chronic exercise leads to various adaptive mechanisms that decrease both peripheral sensitivity to GCs and activity of the HPA axis, which prevents adverse effects of hypercortisolemia (212). Over the years there has been a lot of focus on the effect of forced exercise training and the regulation of the HPA axis. There is much diversity over these findings reported in the literature on exercise training and HPA activity as some studies find a decrease (207, 213-215) whereas some find increases (216) in HPA activity. Interestingly, some suggest that different stressors may result in either activation or adaptation to the stressor (193, 214). As previously mentioned, forced exercise training creates variability in the data as it is difficult to decipher if the activation of the HPA axis is due to the forced nature of the exercise or if it related to the exercise itself.

In brief, < 4 weeks of volitional wheel running induces an increase in HPA axis activity (197), but with sustained training HPA axis activation lowers back to basal levels prior to wheel axis in rodents (217-220). The effect of regular exercise and HPA axis activation appears to be regulated at the level of the hypothalamus as exercise training has been shown to decrease mRNA and protein levels of CRH in mice (217). Moreover, HPA activation appears to have less of an impact on peripheral tissues with exercise training. For example, elite trained men showed decreased sensitivity to exogenous GCs

in their blood monocytes following exercise (210). This was also found in trained rats that had lower GR expression in renal and myocardial tissues (221). Another study in hamsters showed that 4 weeks of volitional running induced lower hepatic and skeletal muscle expression of 11β-HSD1 as well as lower GR expression (200); interestingly, there were increases in 11β-HSD1 expression in the adipose tissue. Together it is evident that there are clear differences in acute versus chronic exercise training in rodents and in human studies, however, in general acute exercise stimulates HPA axis and prolonged exercise training induces variations in HPA activity, but both protect individuals against insulin resistance and insensitivity.

1.5.3. Exercise and Islet Function

Prolonged exercise training promotes decreases in insulin secretion regardless of the exercise protocol in both rodents and humans. For example, long-term swim training (8-12 weeks) in rats lowers GSIS in isolated islets (222), while increasing islet insulin storage (223). Similar results were found with voluntary wheel running (36 days) in rats (224), as well as treadmill trained rats (8 weeks) (225, 226), where insulin release measured directly from a single β-cell was also significantly lower after the training (225). These effects of exercise and islet function are similar to findings in human studies (227-229). It is important to note that measurements of insulin secretion are indirect measurements of islet function, as it is not possible to measure GSIS from healthy human subjects at this point in time. Moreover, exercise training promotes β-cell survival, growth, and restoration that may contribute to healthier populations of islets in rodents, (i.e. balance in oxidative species) that may limit unnecessary β-cell compensation (230-

232). Moreover, resistance training (4 days) in rats increases arginine-stimulated insulin release, but not GSIS (233) and short-term exercise stimulated more GSIS in exercise trained rats compared to sedentary rats (223). These findings may be a result of acute exercise training rather than the type of exercise, but it is known that exercise training decreases GSIS in rodents and humans, possibly due to improved insulin action in the peripheral tissues. See Figure 1.3. for summary of acute elevations in GCs and exercise on β-cell function. Image adapted from Beaudry and Riddell, 2013.

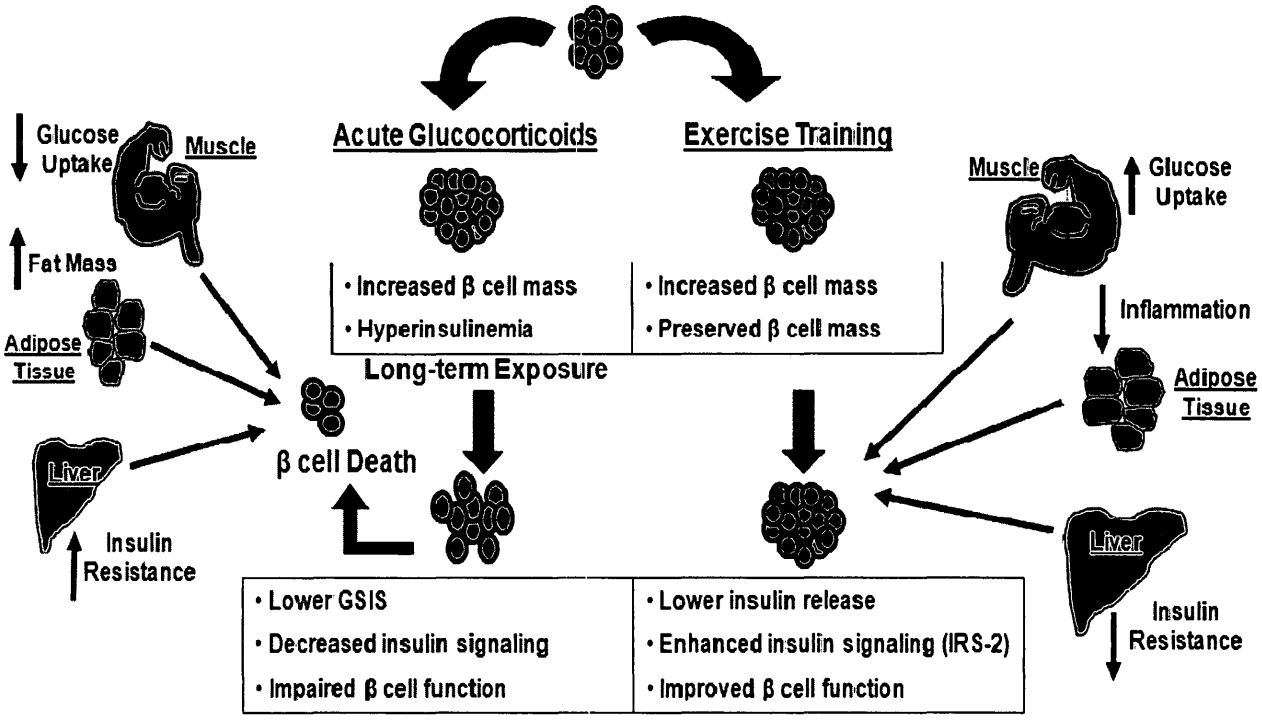

Figure 1.3. Acute elevations in GCs and exercise training on β-cell function. Acute elevations in GCs promotes insulin resistance that indirectly increases β-cell mass and hyperinsulinemia. On the other hand, if GCs remain elevated then this may induce severe insulin resistance and lead to β-cell dysfunction and eventually β-cell death. Acute exercise training maintain β-cell mass, but preserves β-cell function. Longer periods of exercise training tend to promote lower insulin secretion in response to lower peripheral insulin resistance and increased insulin sensitivity.

1.5.4. Exercise and HFD/Obesity/Insulin resistance

Exercise is a known HPA stressor as it works to mobilize fuels for energy, but it also helps individuals improve insulin action in the peripheral tissues (211). The benefits of exercise are thought to limit tissue sensitivity to stress or GC excess. Therefore, the absence of exercise is likely to promote metabolic dysfunction and emotional unrest. Evidently, a way to avoid early onset of metabolic dysfunction and prevent GC insensitivity, is to perform regular exercise (234). Diets that are high in fat induce increased incidence of insulin resistance and can lead to early onset T2DM (235). Moreover, HFD induces β-cell mass expansion and proliferation as the islets attempt to compensate with increased insulin secretion to help normalize glucose levels in blood (236) and with constant consumption of a HFD can lead to T2DM as β-cells decompensate (237). Thus, 12 weeks of exercise training in 90% pancreatectomized rats on HFD improved levels of β-mass through increased levels of proliferation and neogenesis similar to the levels of controls, thereby demonstrating that exercise has a positive effect on β-cell function even in a compromised state (238).

Cytokines are released due to increases in inflammatory markers from the adipose tissue such as tumor necrosis factor α and IL-6 (239) that are exceedingly high in obese and insulin resistant individuals (240). These inflammatory markers are thought to drive insulin resistance (54), which potentially could override the system and exhaust β-cell function (23). However, regular exercise has been shown to improve inflammatory regulation and GC sensitivity in obese rats (241), while forced exercise increases inflammation and exacerbates the abnormal obese condition. In humans, moderate

intensity exercise (~ 1200 kcal per week at 40-55% VO_2max) in overweight sedentary adults for 8 months improved islet insulin secretion more than vigorous exercise (~ 2000 kcal per week at 65-80% VO_2max) (242). The moderate intensity group had a better improvement in insulin secretion, as there were no alterations in their first phase insulin response. The higher intensity group augmented their insulin sensitivity, but had greater decline in their compensatory first-phase insulin secretion. However, the exact mechanisms behind exercise intensities are not clear, but there are differences in the adaptation to the type of exercise performed. These differences may result with more vigorous exercise intensities as they tend to promote elevated GC action that could disrupt normal β-cell function.

1.5.5. Exercise and ZDF rat

It is important to study various forms of exercise and stress on the body as diseases may respond differently depending on the type and intensity of the exercise. For instance, it may be more important to study a more intense exercise in individuals with T2DM that already have depleted β-cell populations, as it may stimulate β-cell growth and function. To investigate the effect of exercise on β-cell function in a T2DM population researchers typically utilize the ZDF rat model. In particular, 5 weeks of swim training in ZDF rats demonstrated improved glycemic control as they exhibited lower glucose and higher insulin concentrations compared to sedentary ZDF rats. In a follow-up study in ZDF rats, swim training showed to decrease circulating GCs and increase β-cell proliferation, mass and islet volume (144); as a result, the exercised ZDF rats compared to sedentary controls showed elevated insulin levels in the basal state and greater

improvements in glycemic control. These results were attributed to higher expression of GLUT2, PKB, and lower ubiquitinated protein aggregates within islets compared to sedentary controls suggesting that forced exercise stimulates GSIS, decreases cellular stress and prevents β-cell depletion. Similar results were found in ZDF rats that were exercise trained with 6 weeks in voluntary running wheels (150). Regular exercise preserved insulin mRNA transcription levels and reversed hyperglycemia. Isolated islets responded normally to glucose and fatty acids; however, there were no differences in glucose and fatty acid cycling in active compared to inactive ZDF rats. Therefore, this study demonstrates that the defect in ZDF animals is simply due to the loss of normal lipid regulation at the β-cell level. Unfortunately, voluntary exercise was unable to fully reverse this effect in ZDF rats but it was suggested that β-cell dysfunction can be linked to ER stress which may be induced by accumulation of toxic lipid by-products such as ceramides in the ZDF rat (150). Moreover, treadmill exercise in ZDF rats improved β-cell morphology and prevented diabetes development attributed to improved AMPK activation, thought to increase Ca^{2+} influx simulating insulin secretion (243).

In addition to improvements in β-cell function, exercised ZDF rats have lower circulating GCs compared to inactive controls, after 5 weeks of forced training (63, 144, 213), which is reported to be even lower after 3 weeks of voluntary running (63, 150). It may be plausible that lower GC activation might contribute to better β-cell function in the exercised ZDF rats, but no studies have investigated the effect of exercise in the ZDF rat and GC activity in the β-cell. Thus, it can be concluded from these studies that non-volitional and volitional exercise help to prevent early onset of T2DM in the ZDF rats

perhaps by improving β-cell compensation, reducing islet oxidative stress and in part lowering basal HPA axis activity.

1.5.6. Exercise and T2DM

It has been established that diet and exercise are important factors that help to prevent insulin resistance, and early onset T2DM in humans (244, 245). Endurance exercise and training improves glucocorticoid sensitivity in humans (246), and regular daily exercise decreases the risk of developing T2DM in rodents (63, 200, 219, 220) and in humans (247-249). Moreover, acute exercise, which is often overlooked by prolonged training periods, has been shown to induce effective health benefits, as 1 week of exercise was able to restore normal glucose tolerance in T2DM individuals (250-252). One of the first studies to investigate endurance training in T2DM was Krotkiewski et al., 1985 (253) and they confirmed that 3 months of an individualized exercise training program enhanced insulin secretory response to exogenous glucose and arginine challenge. The elevation in insulin secretory capacity was thought to occur as a result of augmented β-cell mass; however, the direct measurement of β-cell mass is not probable in living humans at this moment in time. Exercise intervention is important to help improve β-cell compensation as Dela et al., 2004 (254) showed that after 4 weeks of exercise individuals classified as 'moderate' insulin secretors were able to improve their insulin response to a glucose-arginine test by evidence of higher c-peptide concentrations compared to 'low' insulin secretors. A recent study showed that aerobic and resistance training improved metabolic parameters and insulin sensitivity, but no change occurred in β-cell function; this may have resulted due to changes found with truncal fat (255).

Indeed, exercise is an important modulator of β-cell function, but it also helps to promote insulin action in the peripheral tissues of T2DM individuals. For example, exercise improves glucose intolerance as it increases GLUT4 translocation in skeletal muscle that helps to contribute to glucose clearance and is protective against T2DM development (28, 256). Moreover, voluntary wheel running prevented the rise in oxidative stress and inflammatory markers such as hepatic expression of JNK and serine IRS1 in diabetic rats (257), that are typically found elevated in diabetic individuals (258). Therefore, exercise may help to limit circulating inflammatory markers thought to drive early onset T2DM, potentially preserving β-cell function.

However, not all exercise training programs are beneficial for T2DM. Burns et al., 2007 (259) showed that early-onset obese T2DM individuals were less likely to exhibit to clinical benefits of exercise training. This study shows that there are still unresolved issues in regard to the mechanism involved with T2DM and exercise training. In addition, it also shows that exercise therapy in T2DM patients is multifaceted and an individualized program may be an appropriate method to treat these individuals.

1.5.7. Exercise and Cushing's syndrome

Currently there are no studies that have directly investigated the role of any exercise regime in Cushing's syndrome patients, but there are exercise therapy recommendations for patients after surgery has been completed. It is advised that patients slowly start to introduce exercise into their daily routines and gradually increase the exercise intensity as they feel it is appropriate. However, there is no literature that supports these claims and exercise prescribed as a therapy is only based on evidence that

exercise lowers HPA axis activation (64, 260). One case study, which follows a young boy during his treatment of Cushing's syndrome (261) reports that the individual maintained a healthy normal life following 15 years after surgery due to a regimented diet and exercise program (261), but there are no specifics about the exercise therapy indicated in the study and there is no way of knowing the exact amount, duration or intensity of exercise that was performed.

Some studies have investigated the effects of forced exercise on chronic dexamethasone injections in rodents (262-264). Aerobic exercise training was effective at improving blood prolife as well as cardiometabolic alterations such as hyperglycemia, glucose intolerance, dyslipidemia, liver steatosis, muscular atrophy and improved blood profile (262). Additionally, swim training improved insulin sensitivity (264) in dexamethasone injected rats suggesting that exercise training can override the negative feedback of the HPA axis activation induced by dexamethasone. Moreover, 8 weeks of treadmill training improved dexamethasone-induced hyperinsulinemia, muscular glycogen loss and muscle atrophy in male Wistar rats (263). There are no studies reported that investigate the effects of voluntary wheel running on hypercortisolemia.

1.6. GR Antagonism

1.6.1. GR antagonism therapy

There are associated pathologies, as previously mentioned, in individuals with hypercortisolemia (Cushing's syndrome) such as cardiometabolic abnormalities, obesity, insulin resistance, impaired glucose control and the early onset of T2DM (265). As a

result of these links between excess GCs and metabolic dysfunction, it has become quite urgent in the pharmacological field to develop a novel therapeutic agent that will reduce the effects of chronically elevated GCs, especially since a number of individuals with T2DM are now being identified as having Cushing's syndrome or elevated GCs (266). To date, several GC inhibitors, such as the non-selective GRII receptor antagonist, Mifepristone (11β-[P-(dimethylamino)phenyl]-17β-hydroxy-17-(1-propynl)estra-4,9-dien-3-one) or RU486, several selective GRII antagonists, none of which has been approved to be used in human subjects, and lastly, 11β-HSD1 inhibitors, that act to help regulate local, tissue and specific GC exposure; however, they are not safe for pharmacological distribution. In the following sections the non-selective and selective GRII antagonists will be further discussed.

1.6.2. Non-selective GR antagonists

GRII are found ubiquitously throughout the body tissues, and active GCs are allowed to bind freely as a ligand. Once the GRII is occupied by a ligand, the complex translocates to the nucleus where it acts as a transcription factor to activate or repress the expression of genes necessary for a variety of cellular events. GR antagonism results in the competitive blockage of the GC ligand binding to the GR complex, which hinders the receptor from releasing the associated hsp90 proteins, and prevents nuclear translocation. Some of the complexes still reach the nucleus, but the transcriptional activity is rapidly weakened (98). RU486 code is named after its inventor, Roussell-Uclaf, and is a known as a non-selective GRII antagonist that inhibits the GRII. It is considered to be non-selective as it also inhibits the androgen and progesterone receptor (PR) (267), but has no

affinity for the MR. It has recently gained FDA approval as the pharmacological agent, Korlym™, 2012, for the specific treatment of patients with hypercortisolemia or those suffering from Cushing's syndrome (268, 269).

RU486 administration has demonstrated great improvements on metabolic abnormalities and dysfunctions induced through hypercortisolemia. For example, RU486 improves glycemic control, body weight gain, and insulin sensitivity in rodents given HFD for 4 weeks (48). In addition, RU486 treatment actually results in clear activation of the HPA axis, but without clinical abnormalities (270) and normal weight gain in healthy men (271). RU486 has been reported to be given to a variety of patients with Cushing's syndrome (272), where it improves metabolic symptoms of T2DM and glucose intolerance such as lower glycated hemoglobin, fasting glucose, blood pressure, insulin resistance, and waist circumference (272). It is considered an ideal pharmacological agent, as it is absorbed quickly, exists for a long time in the circulation (half-life up to 48 hours), and has a greater binding affinity to GRII than other GC agonists such as dexamethasone (3 to 4 times) and cortisol itself (18 times) in humans (273-275).

RU486 appears to be the ideal agent for individuals with hypercortisolemia, but it is nowhere near perfection. It requires consistent patient monitoring as it can result in many debilitating side effects such as elevated circulating GCs, endometrial hyperplasia, hypokalemia (overstimulation of the MR) and aborted pregnancy, due to its occupancy with the PR (267, 276). The potent inhibition of the GRII is a potential problem with RU486 treatment as it interrupts GC negative feedback to the HPA axis. Indirectly these properties can lead to increased concentrations of circulating GCs (reviewed in (267)),

potentially leading to adrenal insufficiency. In addition, one dose of RU486 (600 mg) will bind to the PR and blocks its action, resulting in endometrial wall thickening, which causes early termination of a pregnancy (276). Evidently this side effect remains to be one of the greatest ethical issues with the use of RU486 and the only solution is constant patient monitoring and cycling on and off RU486 treatment to try and reduce high GC levels.

1.6.3. Selective GR antagonists

Currently, there is a race to replace RU486 with more specific selective antagonists for the GRII (277), ideally with no affinity for the PR, MR, ER and AR. To date, there are no antagonists of this nature that have been tested in humans and very few studies have been conducted in rodent models (48, 278, 279). Of these studies in rodents, selective GRII antagonists have been shown to play a role in the attenuation of detrimental GR-dependent pathways in the brain (compound C108297) (278), whole-body steady state glucose metabolism (48), deleterious effects of electroconvulsive shock-induced retrograde amnesia (280) and body mass gain (279). Moreover, the selective GRII antagonists such as C112716 and C113083 have been reported to reverse mass gain induced by olanzapine, aserotonin inhibitor, administered for anti-psychotic effects (279). No studies have been published that show the effects of selective antagonists on models of hyperglycemia or diabetes. However, previous studies published present anticipatory effects of selective GRII antagonists; but sometimes these compounds do not act as ideal antagonists. For example, C108297 does not completely reverse adverse GC effects in the brain. Previous research shows that this antagonist may

actually work partly as a partial agonist, as per *in vitro* assay results thus counteracting the GRII antagonist effects (278, 281). Although selective GRII antagonists have some major advantages over non-selective GRII antagonists, they still have a long way to go to reach the ideal anti-hypercortisolemic pharmacological agent. To date there are no selective GRII antagonists that have been approved for human clinical trials and RU486 so far is best agent accessible to patients to help to eliminate adverse effects of excess GCs in humans.

Objectives

The central aim of this thesis was to investigate the role of elevated GCs and HFD on T2DM development in young health male Sprague-Dawley rats and the effect of these conditions on pancreatic islet adaptations. In addition, the aim of this thesis was to examine the role of therapeutic options, such as regular exercise and the administration of GC receptor II (GRII) antagonists in our rodent model of T2DM.

Hypothesis

We hypothesized that elevations in GCs and HFD would promote T2DM development by impairing islet adaptation in otherwise young healthy male Sprague-Dawley rats. We also hypothesized that regular wheel running exercise would reduce the development of T2DM in our rodent model and the administration of GRII antagonists would attenuate, if not reverse T2DM development by improving β-cell function and whole body insulin resistance.

MANUSCRIPT-#1 Chapter 2

Short-term Elevations in GCs and HFD in the Male Sprague-Dawley Rat

Rationale for Manuscript #1

It is obvious that T2DM encompasses a significant portion of the world's population and the prevalence is only projected to rise if no effective therapy is soon developed (53). An efficient way to study the progression or onset of T2DM is to utilize rodent models that share similar pathogenesis to that of T2DM humans. However, it is difficult to obtain adequate results and majority of the time the disease progression varies between rodent and humans. There are many rodent models of pre-diabetes and T2DM, such as partial pancreatectomy, long-term high-fat diet, and ZDF rodent models, to name a few (282). The ZDF rodent is one of the most widely utilized and accepted model of T2DM as it shares similar phenotypes with T2DM patients. A link between elevations in GCs and T2DM has been established in humans, however concrete mechanisms of T2DM onset have yet to be determined (145, 266). Similarly, ZDF rats develop hypercortisolemia prior to symptoms of T2DM, such as insulin resistance, hyperglycemia/hyperinsulinemia, and β-cell dysfunction. Unfortunately the ZDF model is limited as rats develop diabetes due to leptin receptor gene deficiency, unlike many humans who develop T2DM (283). Moreover, it is doubtful that T2DM is induced solely by elevations in GCs, and more likely to develop in combination with increased FAs and ectopic lipid accumulation (63), which very few studies have accomplished. Therefore,

the goal of this study was to develop a relatively inexpensive rodent model of T2DM induced by GCs and HFD that possessed similar characteristics as humans with T2DM.

Author Contributions

Conceived and designed the experiments: Y.S., J.L.B., A.D., J.E.C. and M.C.R. Performed the experiments: Y.S., J.L.B. and A.D. Analyzed the data: Y.S., J.L.B., A.D. and A.P. Wrote the manuscript: Y.S. and J.L.B. Edited the paper: M.C.R.

J.L.B. performed oral glucose tolerance test, insulin tolerance test, and preparation of islet histology, plasma analyses of insulin, corticosterone, NEFAs, leptin, triglycerides and mRNA data for this manuscript.

J.L.B. contributed to Figure 1, 2, 3 and 4 and table 1 and 2.

This manuscript was published in the journal of *Disease Models and Mechanisms*, 2012, Sep;5(5):671-80. DOI:10.1242/dmm.008912

A Rodent Model of Rapid-onset Diabetes Induced by Glucocorticoids and High-fat Feeding

Running title: A Rodent Model of Glucocorticoid-Induced Diabetes

Yaniv Shpilberg[1,*]
Jacqueline L. Beaudry[1,*]
Anna D'souza[1]
Jonathan E. Campbell[1]
Ashley Peckett[1]
Michael C. Riddell[1,ǂ]

[1]School of Kinesiology and Health Science, Faculty of Science and Engineering,
York University,
4700 Keele Street, Toronto, ON, Canada, M3J 1P3
[*] These authors contributed equally to this work
[ǂ] Author for correspondence

Please address correspondence to Dr. Michael C. Riddell,
School of Kinesiology and Health Science, 4700 Keele Street,
Toronto, ON, Canada, M3J 1P3
Telephone: (416) 736-2100 ext. 40493
Email: mriddell@yorku.ca

Key Words: Type 2 diabetes mellitus, Corticosterone, High-fat diet, Glucose intolerance, insulin resistance, ectopic fat, liver steatosis, pancreatic islet, 11-βhydroxysteroid dehydrogenase type 1

Abstract

Glucocorticoids (GCs) are potent pharmacological agents used to treat a number of immune conditions. GCs are also naturally occurring steroid hormones (e.g. cortisol, corticosterone) produced in response to stressful conditions that are thought to increase the preference for calorie dense 'comfort' foods. If chronically elevated, GCs can contribute to the development of type 2 diabetes mellitus (T2DM), although the mechanisms for the diabetogenic effects are not entirely clear. The present study proposes a new rodent model to investigate the combined metabolic effects of elevated GCs and high-fat feeding on ectopic fat deposition and diabetes development. Male Sprague-Dawley rats (aged 7-8 weeks) received exogenous corticosterone or wax (placebo) pellets, implanted subcutaneously, and were fed either a standard chow diet (SD) or a 60% high-fat diet (HFD) for 16 days. Animals given corticosterone and a HFD (cort-HFD) had lower body weight and smaller relative glycolytic muscle mass, but increased relative epididymal mass, compared with controls (placebo-SD). Cort-HFD rats exhibited severe hepatic steatosis and increased muscle lipid deposition compared with placebo-SD animals. Moreover, cort-HFD animals were found to exhibit severe fasting hyperglycemia (60% increase), hyperinsulinemia (80% increase), insulin resistance (60% increase) and impaired β-cell response to oral glucose load (20% decrease) compared with placebo-SD animals. Thus, a metabolic syndrome or T2DM phenotype can be rapidly induced in young Sprague-Dawley rats by using exogenous GCs if a HFD is consumed. This finding might be valuable in examining the physiological and molecular mechanisms of GC-induced metabolic disease.

Introduction

Presently, there are a number of available rodent models used to represent both the pre-diabetic or insulin-resistant disease (284, 285) and hyperglycemic conditions associated with the development of type 2 diabetes mellitus (T2DM) (282). These animal models are important because they allow for examination of the disease state at the tissue and cellular level, and thus might help to develop new treatments and therapies for patients. Ideally, a good rodent model of T2DM should represent a similar metabolic profile and pathogenesis to humans with pre-diabetes or T2DM. However, few models fully capture all characteristics of the disease pathophysiology (ectopic fat deposition, insulin resistance and hyperglycemia), and sometimes the models used do not reflect what typically occurs in humans, perhaps because genetic models or chemical agents are used to induce hyperglycemia, rather than attempting to examine the established risk factors for diabetes (286). For example, the Zucker diabetic fatty (ZDF) rat, first established in the early 1980s (287), is one of the most commonly used models of T2DM because it develops severe insulin resistance, β-cell compensation then decompensation, and eventually overt hyperglycemia by ~ 8–10 weeks of age (40). Although ZDF rats are leaner than the original Zucker fatty rat strain, the former express higher basal glucose and insulin levels and excessive ectopic fat deposition because of leptin receptor deficiency, which causes hyperphagia and altered substrate metabolism (287). One major limitation of the ZDF model is that it does not mimic the vast majority of humans who develop T2DM with an intact leptin receptor gene (283), not to mention that it is a costly and genetically spontaneous model that is not easily manipulated. Indeed, non-genetic

lifestyle-induced models of T2DM are scarce because most rodent species are relatively resistant to prolonged periods of high-fat feeding and/or physical inactivity and might not develop the hyperglycemic phenotype desired by the researcher (282).

Considerable evidence from human studies (58, 266) and various rodent models (22, 288, 289) suggest that elevations in glucocorticoids (GCs) are tightly linked with diabetes development, either at the circulating or cellular level. At the cellular level, the pre-receptor enzyme 11-β-hydroxysteroid dehydrogenase type 1 (11-βHSD-1) and the glucocorticoid receptor (GR), act to modulate intracellular GC action, which can dramatically influence tissue function (liver, muscle, adipose tissue and brain) to promote metabolic syndrome (290). The activity of 11-βHSD-1 has also been closely followed in those with diabetes and is suspected to be involved in the pathogenesis of the disease (291). Interestingly, elevations in GCs alter food intake, energy expenditure and ectopic fat deposition, and promote widespread whole body insulin resistance (110). In particular, elevation of GC levels in rodents (121), or even increases in stress levels in humans (292), promotes the consumption of energy dense 'comfort' foods. These associations between GCs and altered metabolism suggest a possible role of these stress hormones in the etiology of T2DM development. Indeed, exogenous GCs are potent diabetogenic agents that, when prescribed for the treatment of many acute and/or chronic conditions, increase whole body insulin resistance and plasma glucose levels and cause muscle proteolysis, all features of T2DM development. In one study, a striking tenfold increased risk of diabetes development was calculated for patients receiving hydrocortisone at a dose of ~ 120 mg/day (293).

Generally, it is believed that the transition from an insulin resistant or pre-diabetic state into overt T2DM occurs when the secretory capacity of the pancreatic β-cells is no longer able to maintain euglycemia to combat insulin resistance. It is plausible that the chronic up-regulation of GCs could act directly on pancreatic islets, inducing insulin resistance (151). However, it is also possible that increased circulating free fatty acid levels and excessive ectopic lipid deposition, which clearly induce whole body insulin resistance, in addition to elevations in GCs themselves, are the combined driving forces behind disease development (55, 63, 294).

Surprisingly, very little research has been done on the collective effect of GCs and high-fat feeding, although each stressor on its own can result in insulin resistance (284, 295). The purpose of this present study is to develop a cost-effective, GC- and high-fat-fed-induced rodent model of diabetes mellitus. We believe that this model of rapid-onset diabetes (ROD) mimics many of the symptoms observed in patients with T2DM (285), as well as provides evidence that elevated GCs induce diabetes advancement if susceptible individuals do not consume a balanced diet.

Methods

Ethics statement

All experiments were approved by the York University Animal Care Committee in accordance with the Canadian Council for Animal Care guidelines.

Animals

Forty young (~ age 7–8 weeks; initial weight 200–250 g) male Sprague-Dawley rats were purchased from Charles River Laboratories (Montreal, QC, Canada). Only male rats were selected for this study because female rats have differences in reproductive hormones throughout their ovulatory cycle that could affect glucose metabolism (296). All animals had a 7 day habituation period to a 12-hour light-dark cycle (lights on at 08:00 hours and lights off at 20:00 hours) in a temperature (22–23°C) and humidity (50–60%)-controlled room. The animals (body mass 200–250 g) were then randomly assigned to one of four groups: placebo-treated and fed a rodent standard diet (placebo-SD); placebo-treated and fed a high-fat diet (placebo-HFD); corticosterone-treated and fed a standard diet (cort-SD) and corticosterone-treated and fed a high-fat diet (cort-HFD) (n=8–10 per group; all individually housed). A timeline of the treatment protocol is presented in Fig. 4.

Surgical procedures and design

Following habituation, all placebo-treated animals had 4×100 mg wax pellets (~0.2 cm in diameter each) implanted subcutaneously between their scapulae under aseptic conditions (termed day 0), whereas glucocorticoid-treated animals had 4×100 mg of corticosterone (C2505, Sigma-Aldrich, Oakville, Ontario, Canada) pellets surgically implanted in an identical surgical procedure (see below). Pilot data from our laboratory found that a 200 mg corticosterone implant failed to significantly increase peak corticosterone levels over a 2 week period (see supplementary material Fig. S1). In

addition, these rats did not develop fasting hyperglycemia when given with a HFD. Pellets were created by similar protocols to those published by Meyer et al. (297). Briefly, this involves the subcutaneous implantation of solid corticosterone pellets formed from the molten hormone and weighing ~100 mg. Purified corticosterone was carefully melted in a small stainless steel spoon over a low gas flame and then poured into a 6 mm diameter hole drilled in a paraffin block. After the pellet cooled and solidified, it was removed from the wax with the aid of a scalpel and trimmed to the correct weight. Rats were anesthetized at 5% isoflurane and maintained at 2.5% isoflurane for the remainder of the surgery while steroid pellets were implanted in the nape of the neck. After the skin in the area had been shaved and treated with an ethanol-alcohol solution (Betadine, Purdue Products, Stamford, CT), a small incision was made, and the underlying fascia was spread and separated with a hemostat and inserted into the opening. The pellet was placed under the skin at least 2 cm caudal to the incision, which was then closed with 9-mm wound clips (VWR, Mississauga, ON, Canada). Rats then recovered in individually housed sterilized, standard rodent cages. Following recovery from surgery, SD-fed animals were given rodent SD (14% fat, 54% carbohydrate, 32% protein and 3.02 calories/g) ad libitum, whereas HFD-fed animals were provided with a 60% HFD (60% fat, 21% carbohydrate, 18% protein and 5.1 calories/g) ad libitum (Cat# TD. 06414, Harlan Laboratories, Madison, WI). The composition of the fat in the HFD was as follows: saturated: 37%; monounsaturated: 47%; polyunsaturated: 16%. Food intake and body weight were measured every other day.

Plasma analyses

Whole blood was collected via the tail-nick procedure and placed in EDTA microvette tubes (~50 µl) at 20:00 hours on day 6 and 14 and at 08:00 hours on day 7 and 15 to determine 'peak' and 'trough' corticosterone levels, as previously described (Campbell et al., 2010), and insulin and leptin levels. Immediately following blood collection, plasma samples were separated from whole blood by centrifugation (90 seconds at 13,000 g) and frozen at −20°C until further analysis. Commercially available kits were used to measure insulin (INSKR020, Crystal Chem, Downers Grove, IL), corticosterone (07-120102, MP Biomedicals, Solon, OH), non-esterified free fatty acids (HR Series NEFA-HR, Wako Chemicals, Richmond, VA), triglycerides (TR0100, Sigma-Aldrich, Oakville, ON, Canada) and leptin (RADPK-81K, Milliplex rat adipokine kit, Millipore, Etobicoke, ON, Canada) at select time points (see below) from blood collected via tail-nick or from trunk blood collected at the end of the experimental period (i.e. decapitation).

Oral glucose tolerance test

On day 12, following an overnight fast, body mass was determined and blood glucose level assessed via tail-nick and a hand-held glucometer (Contour blood glucose meter, Bayer, Toronto, ON, Canada). In addition, ~40 µl of plasma was collected via tail-nick for basal insulin measurements (see above). Following this, an oral gavage of 50% glucose (1.5 g/kg body weight) was performed on each animal (time 0), followed by blood collection for insulin and glucose every 30 minutes. At 120 minutes after oral

glucose gavage, animals were returned to their regular housing conditions and respective diets. HOMA-IR values were calculated according to the formula: [insulin (μ units/ml) × glucose (mmol/l)]/22.5. HOMA-β values were calculated according to the formula: [insulin (μ units/ml) × 20]/[glucose (mmol/l) – 3.5]. Values represent fasting glucose and insulin levels (298).

Intraperitoneal insulin tolerance test

On day 15, all animals were fasted overnight with body weights and blood glucose recorded, as stated above. The following morning (day 16), the animals were injected intraperitoneally (IP) with 0.75 units insulin/kg body weight (time 0). Blood glucose levels were measured at 5, 10, 20 and 30 minutes post IP injection. At the end of the 30 minutes, animals were killed via decapitation and trunk blood was collected and separated into plasma as described above. Gastrocnemius, soleus, plantaris and epitrochlearis muscles, left and right adrenals, inguinal subcutaneous and epididymal adipose depots, and liver were removed, weighed and flash frozen in liquid nitrogen. Insulin resistance was measured as the AUC for the glucose concentrations during the insulin tolerance test. All tissues were stored in −80°C until further analysis.

Tissue processing

Pancreas was excised from animals, weighed and cut into ten randomized pieces. Each piece was washed in saline and then placed into 10% buffered formalin for 48 hours. After the incubation period, pancreas pieces were placed into 70% ethanol and prepared for paraffin embedded sectioning. Pancreas pieces were sectioned into 5-μm

thick sections and mounted onto microscope slides, stained with eosin and counterstained with hemotoxylin. Representative islets from each animal treatment group were identified at 20 × magnification and analyzed for islet areas using the slide scanner software (Aperio Scanscope CS, Vista, CA, scanned at the Advanced Optical Microscopy Facility, University Health Network, Princess Margaret Hospital, Toronto, ON, Canada).

Frozen liver and muscle tissue from each animal were snap frozen, cryosectioned (10-μm thick) and stained with Oil Red O for neutral lipid content as previously described (299) . Briefly, muscle and liver sections were fixed in 3.7% formaldehyde at room temperature. During this time, Oil Red O solution consisting of 0.5 g Oil Red O powder (Sigma-Aldrich, Canada) and 100 ml of 60% triethyl phosphate (Sigma-Aldrich, Canada) was combined and filtered. Following fixation in paraformaldehyde, slides were then immersed in filtered Oil Red O solution for 30 minutes. Immediately after, slides underwent three washes with ddH2O, were allowed to air dry for 10 minutes and were then sealed with Permount (Sigma-Aldrich, Canada). Images were acquired at 10× magnification using a Nikon Eclipse 90i microscope (Nikon, Canada) and Q-Imaging MicroPublisher 3.3 RTV camera with Q-capture software.

mRNA expression

Epididymal and subcutaneous fat pad total RNA was isolated using the Trizol reagent (Invitrogen, Carlsbad, CA) and Eppendorf spin columns were used to concentrate RNA. Total RNA concentrations were quantified by ultraviolet spectrophotometry at 260 nm, and RNA purity was verified by the 260- to 280-nm ratio (Nanodrop ND-1000;

Fisher Scientific, Wilmington, DE). Total RNA was diluted to 1 μg/μl using RNA-free water and the first-strand of cDNA was synthesized with DNase I (Invitrogen) and reverse transcribed to cDNA using SuperScript II RNase H-RT (Invitrogen). Duplicate samples of 5 μl of mRNA were quantified using a Bio-Rad MyIQ single color real-time PCR detection system using SYBR green (Bio-Rad, Mississauga, ON, Canada). Each reaction contained 12.5 μl SYBR green mix, 1 μl of each forward and reverse primer (5 μM), and 5.5 μl RNase-free H2O. The PCR protocol conditions consisted of an initial denaturation for 3 minutes at 95°C, followed by 30 cycles at 95°C for 15 seconds, annealing at 60°C for 45 seconds and extending at 72°C for 30 seconds. Analysis was conducted using the 2^^ method. All samples were normalized to the expression level of the housekeeping gene β-actin, which did not significantly change among experimental treatments. Primer sets were as follows: 11-βHSD-1 Forward: 5′-GGGAGGCCATGTGGTATTGAC-3′, Reverse: 5′-CGAGTTCAAGGCAGCGACAC-3′. Glucocorticoid Receptor (GR) Forward: 5′-CCAAAACTCACTCGGATGCA-3′, Reverse: 5′-AGGTGCTTTGGTCTGTGGGATA-3′. Beta Actin Forward: 5′-TGTGGCATCCATGAAACTAC-3′, Reverse: 5′-CTCAGGAGGAGCAATGATCT-3′.

Statistical analyses

For all experiments, the appropriate one-or two-way ANOVA was performed as required to identify significant differences between treatment groups using Statistica 6.0 software (StatSoft, Tulsa, OK), with significance found when $P<0.05$. If significant differences were found by a one- or two-way ANOVA, then the Tukey's honestly significant difference post-hoc test was performed. Data are presented as mean ± s.e.m.

Results

Corticosterone treatment results in attenuated body mass gains despite hyperphagia, but increases relative central adipose mass and muscle atrophy

At day 11 of treatment, all corticosterone-treated rats exhibited attenuation in body mass growth and less gross caloric intake compared with placebo-treated rats (Table 1). Caloric intake (expressed relative to whole animal body mass) was ~twofold higher in animals given corticosterone and a high-fat diet (cort-HFD), compared with all other treatment groups (Table 1). Cort-HFD rats had more than a twofold greater relative epididymal fat pad mass when compared with controls [placebo-treated rats fed a standard chow diet (placebo-SD); 9.81±1.65 versus 4.56±0.54 g/kg body mass, $P<0.05$, main effect of diet, $P<0.01$]. Epididymal fat pad mass was not significantly elevated in either cort-SD- or placebo-HFD-treated rats when compared with placebo-SD-treated rats (5.82±0.28 versus 5.27±0.57 g/kg, $P=0.06$). Mesenteric fat mass was also visibly more abundant in cort-HFD-treated rats than the other three groups (observational results). Corticosterone treatment resulted in reduced relative adrenal mass (extended results) and decreased thymus mass, as expected (observational results). Cort-HFD rats, in particular, had increased liver and pancreatic mass (all $P<0.05$). Absolute muscle mass was lower in all corticosterone-treated animals (extended results), although relative mass of the soleus and plantaris was unchanged. Cort-HFD rats had lower relative epitrochlearis muscle mass compared with the placebo-SD group (Table 1; $P<0.01$).

Cort-HFD results in hyperglycemia, hyperinsulinemia, insulin resistance and reduced insulin tolerance

Cort-HFD animals demonstrated dramatically elevated fasted blood glucose levels (i.e. fasting hyperglycemia) compared with all other groups (14.0±1.9 mmol/l in cort-HFD compared with 4.2±0.2 mmol/l in the placebo-SD group; $P<0.05$; Fig. 1A). Neither the cort-SD nor placebo-HFD groups demonstrated fasting hyperglycemia. Moreover, following an oral glucose gavage on day 13, only cort-HFD animals had sustained hyperglycemia throughout the 120 minutes of the glucose tolerance test ($P<0.05$; Fig. 1A). By contrast, the cort-SD group had mildly elevated blood glucose levels, compared with placebo-SD, but only at 30 and 60 minutes post oral glucose gavage ($P<0.05$; Fig. 1A). The placebo-HFD group failed to demonstrate elevated glucose levels at any time during the glucose tolerance test, as expected based on the short timeframe of treatment. Fasted insulin level in the cort-HFD group was elevated ~threefold compared with all other groups ($P<0.05$; Fig. 1B). No differences in fasting insulin concentrations were found among the cort-SD, placebo-SD and placebo-HFD groups.

The homeostasis model assessment for insulin resistance (HOMA-IR) was used to determine insulin resistance on the basis of fasted insulin and glucose levels. The cort-SD group had a twofold higher HOMA-IR than the placebo-SD group, whereas the cort-HFD group had a 15-fold increase compared with placebo-SD animals ($P<0.05$; Fig. 1C). The HOMA-β index, commonly used as an index of β-cell function, showed cort-SD animals to have an ~twofold increase in β-cell function relative to the placebo-SD group, whereas

the cort-HFD group demonstrated reduced HOMA-β levels relative to all other groups ($P<0.05$ compared with the cort-SD group). Moreover, cort-HFD animals had a 20% decrease in HOMA-IR levels and no differences were found in placebo-HFD compared with placebo-SD animals ($P<0.05$; Fig. 1D).

An insulin tolerance test was also carried out in all treatment groups on day 15 to further characterize whole body insulin sensitivity. As expected, cort-HFD animals had higher plasma glucose levels prior to and after the insulin injection, compared with all other treatment groups ($P<0.05$; Fig. 1E). The cort-HFD group also demonstrated a 2.5-fold higher glucose area under the curve (AUC) following insulin injection, illustrating impaired insulin sensitivity ($P<0.05$; Fig. 1F). There were no differences found in glucose response to insulin injection among the other three groups.

Cort-HFD treatment impairs normal corticosterone circadian rhythm, as well as increasing fasting insulin, leptin and triglycerides levels

All treatment groups demonstrated a normal circadian rhythm of corticosterone secretion prior to pellet surgery, as measured by trough and peak corticosterone levels measured in the early evening (20:00 hours) and in the morning (08:00 hours) (Table 2). However, 7 days after pellet implantation, cort-SD- and cort-HFD-treated animals both had significantly elevated corticosterone levels at the 08:00 hour measurement only ($P<0.05$; Table 2). On day 10, the cort-HFD group demonstrated more than a 17-fold rise in fasting plasma insulin, a >fivefold elevation in plasma leptin levels and >threefold

elevation in plasma triglyceride levels compared with placebo-SD animals ($P<0.05$; Table 2).

Corticosterone treatment causes islet hyperplasia and increases ectopic fat deposition, effects that were further exacerbated with high-fat feeding

To demonstrate altered islet morphology, pancreas sections were collected and stained with hemotoxylin and eosin. As shown, there were no observed differences between placebo-SD and placebo-HFD islet area (Fig. 2A). However, corticosterone treatment increased islet area, with the greatest increase observed in the cort-HFD group (Fig. 2A). In addition to elevations in visceral adiposity, Oil red O staining of liver and tibialis anterior muscle sections revealed increased ectopic lipid accumulation in both corticosterone-treated groups, effects that were exacerbated with the HFD (Fig. 2B and C). HFD feeding alone caused a much less pronounced effect on ectopic lipid deposition.

Cort-HFD significantly augments adipose tissue 11-βHSD-1 expression, whereas cort-SD treatment increases GC receptor expression

Cellular GC activity and the genomic effects of GCs within tissues are largely determined by the presence of active and inactive hormone in the circulation as well as the cellular expression of the pre-receptor enzyme 11-βHSD-1 and GR. As previously mentioned, 11-βHSD-1 acts in various target tissues to convert inactive GCs (11-dehydrocorticosterone) into their active form (corticosterone) (290). To determine the effects of corticosterone and HFD treatment on cellular mediators of GC action, we performed real-time PCR (RT-PCR) to analyze mRNA expression of GR and 11-βHSD-1

in visceral (epididymal fat pads) and subcutaneous adipose tissue because we hypothesized that corticosterone treatment would increase the expression of 11-βHSD-1 in visceral tissue but also exacerbate its effects with high-fat feeding. In epididymal fat depots, corticosterone treatment significantly increased 11-βHSD-1 mRNA expression, regardless of diet type. By contrast, GR expression was only elevated in cort-SD compared with placebo-SD animals ($P<0.05$; Fig. 3A and B). In subcutaneous adipose depots, 11-βHSD-1 mRNA expression was elevated twofold in both corticosterone-treated groups; however, this increase was greatly augmented by the HFD ($P<0.05$; Fig. 3C). Compared with the placebo-SD group, GR mRNA expression tended to be elevated in the cort-SD group and was significantly reduced in the placebo-HFD group ($P<0.05$; Fig. 3D).

Discussion

T2DM is a complex disease and the mechanisms for its development are probably varied. However, it is generally held that whole body insulin resistance is related to increased ectopic lipid accumulation in insulin-sensitive tissues (177) and that β-cell dysfunction occurs via lipid and glucose toxicity of the islets (140, 141) . One possible mediator of T2DM development is an elevation in circulating and/or tissue levels of GCs (142, 143). Indeed, exogenous GC treatment dramatically increases the odds ratio of developing T2DM in humans (145). The goal of the present study was to develop a new non-genetic model of GC-induced diabetes that is cost effective and rapidly inducible. The main finding of this study is that the simple combination of exogenous GCs with a HFD rapidly induces excessive ectopic fat deposition, hyperinsulinemia and/or insulin

resistance, and severe hyperglycemia in young Sprague-Dawley rats, effectively mimicking GC-induced diabetes mellitus.

Strengths and limitations of the corticosterone- and HFD-induced diabetic model

Rodent models of metabolic syndrome or diabetes should largely reflect the biochemical profile and pathogenesis that occurs clinically in humans with pre-diabetes or T2DM. The rodent model presented here, what we term as the 'rapid onset of diabetes' (ROD) model, clearly exaggerates the fundamental physiological parameters that are typically observed in individuals with T2DM who might have chronically elevated GC levels and who may consume an energy dense 'westernized' HFD. Here, we clearly demonstrate that the combination of elevated GCs and a HFD in otherwise healthy Sprague-Dawley rats induces a diabetic phenotype including glucose intolerance, insulin resistance, hyperglycemia and hyperinsulinemia as early as 1 week post intervention and produces a blood biochemical profile that is strikingly similar to T2DM individuals. Interestingly, HOMA-IR and HOMA-β scores indicate extremely elevated levels of insulin resistance and β-cell dysfunction in this model, despite major increases in β-cell compensation, as measured by increased islet areas in the cort-HFD group. It is important to note that neither corticosterone alone nor HFD alone promoted hyperinsulinemia or hyperglycemia in this short timeframe of study, thereby suggesting that these two treatments (i.e. GCs and HFD) have a synergistic effect on diabetes development. Moreover, cort-HFD animals were found to have increased levels of hepatic and muscle fat accumulation (Fig. 2B, C), which was not observed when corticosterone or a HFD was tested alone. Importantly, prolonged corticosterone treatment alone, in similarly aged

Sprague-Dawley rats over a period of 6–8 weeks, failed to promote any observable increases in fasting glucose or impaired glucose tolerance (our unpublished observations). Taken together, the exposure to elevated GCs, in combination with a HFD, rapidly induces an obvious T2DM phenotype in young Sprague-Dawley rats, which are otherwise very resistant to the development of hyperglycemia.

One limitation of this model is that the procedure does require some surgical expertise, general anesthesia and possibly an increased risk for infection because of immune system suppression. An alternative to this procedure would be to provide these animals corticosterone in their drinking water, as has been previously established in a murine model of metabolic syndrome (295). However, the surgical implantation of corticosterone provides a more steady state drug exposure that more effectively abolishes the diurnal GC rhythm, compared with providing it in the drinking water, because animal water consumption tends to be primarily in the early evening (295).

We acknowledge that our model does affect the immune system and the endogenous hypothalamic-pituitary-adrenal (HPA) axis, because ROD animals display decreases in thymus and adrenal weights. However, these results have been shown in various other models of corticosterone administration, i.e. spiking rodent drinking water with high amounts of corticosterone (295). We also realize that immune suppression is not characteristic of the diabetic phenotype (type 1 or type 2), nor is the endogenous HPA axis down-regulated, unless diabetic individuals are on exogenous GCs.

The physiological relevance of the amount of corticosterone that was administered to the animals in our study also warrants discussion. Because the corticosteroid-treated animals in this study received ~20 mg/day/kg body weight (~6.25 mg/day in rats that weighed ~0.3 kg), we estimate that our treatment might be fivefold higher in corticosterone dose (assuming that there was no loss in drug potency with the procedure used to manufacture the pellets) than in humans treated with exogenous GCs that are known to increase the risk of diabetes development (300) . It was decided that, for the purpose of this study, we wished to treat the animals with the 'most tolerable dose' of corticosterone as a proof of principle to rapidly induce hyperglycemia and hyperinsulinemia.

Prevalence of GC-induced diabetes in humans

The prevalence of GC-induced diabetes in clinical populations, or in individuals exposed to chronic stress, is not clear. According to Lansang and Hustak (145), GC-induced hyperglycemia might be quite common. In humans with rheumatoid arthritis who are receiving corticosteroid therapy, ~ 10% develop diabetes in the first 2 years of drug commencement (300). In a case control report, the incidence of initiating an oral hypoglycemic agent or exogenous insulin (i.e. indicative of diabetes development) increased dramatically with GC treatment and was positively correlated with the amount of drug that the patients were receiving. More specifically, a striking tenfold increased risk (i.e. 10.34 odds ratio compared with no treatment) was calculated for patients receiving a hydrocortisone-equivalent dose of =120 mg/day (293). Moreover, studies of a

single intravenous dexamethasone injection of just 10 mg, which is equivalent to ~260 mg of hydrocortisone (145), causes sustained hyperglycemia within ~4 hours in healthy humans (301, 302). Taken together, it is clear that exogenous GCs in modest to high doses promote hyperglycemia in otherwise healthy humans.

Effects of corticosterone treatment on food intake, body mass and body composition

Elevations in GC levels have widely been cited as promoting hyperphagia, particularly the increased consumption of energy dense 'comfort' foods (292, 303). Despite increased food intake, at least expressed relative to body mass, the corticosterone-treated animals in this study clearly demonstrate significantly lower body weight (Table 1). Although the mechanism for attenuated growth is unclear, GCs are well known to reduce overall body mass and body length, probably by promoting muscle proteolysis and by lowering the growth hormone (GH)–IGF-1 axis in young growing mammals (110). Indeed, Dong et al. demonstrated that attenuation in body weight gain with elevations in GCs is associated with a reduction in overall protein synthesis but not with reduced energy intake (304). More specifically, GCs are thought to reduce skeletal muscle protein synthesis and elevate proteolysis specifically in muscles containing a high proportion of fast twitch type II fibers (305). In support of this, the cort-HFD-treated animals in this study showed a significant reduction in epitrochlearis (primarily composed of type II fibers) but not in soleus (primarily type I) muscle mass, suggesting that this treatment attenuates growth primarily in glycolytic muscle fibers. The observed muscle atrophy coincides with evidence from individuals with T2DM who experience

reduced muscle strength and atrophy particularly when glycemic control is poor (306-308).

As expected, we found that body mass gain was dramatically attenuated with corticosterone treatment but, surprisingly, a HFD did not increase body mass in corticosterone-treated animals. It is well established that the development of T2DM from a state of pre-diabetes is often associated with reductions in body mass, perhaps because a large number of calories are lost to glycosuria. In contrast to our observations that increased corticosterone exposure attenuates body mass gains in rodents, Karatsoreos et al. (295) showed that C57/BL6 mice exposed to high amounts of corticosterone (100 μg/ml) in their drinking water for 4 weeks had elevated body mass gains, despite initial reductions in mass, compared with placebo treatment (295). However, C57/BL6 mice are genetically engineered to rapidly develop insulin resistance when they are metabolically challenged (309, 310) and the study by Karatsoreos et al. (295) used mature mice that were well past their adolescent growth phase when the GC-induced inhibition of the GH–IGF-1 axis would have less influence on body mass gains. It is also crucial to note that, although the C57/BL6 mice that were provided corticosterone in their drinking water did develop insulin resistance, they did not develop hyperglycemia (i.e. T2DM). Thus, the body mass gain in that study might have been more dramatic than what was observed in our study because the cort-HFD animals would have had substantial caloric loss due to glycosuria.

One of the hallmarks of the development of metabolic syndrome and T2DM is the elevation in ectopic lipid accumulation in non-subcutaneous adipose stores (increased

central adiposity, muscle and liver lipid accumulation). In this new ROD model, we observed dramatic increases in ectopic lipid deposition with corticosterone treatment, particularly in those animals fed a HFD (Table 1). Corticosterone is known to stimulate an increase in fat accumulation within central adipose stores because of an increased number of adipocytes as well as via adipose cell hypertrophy (110, 311). Increased visceral adiposity is characterized as an important factor in the development of T2DM in human subjects (312, 313). Similarly, cort-HFD-treated rats did have increases in visceral adiposity, which might have played a role in the progression of their insulin resistance. Indeed, intracellular lipid accumulations in endocrine pancreas, liver and skeletal muscle cells have all been previously shown to contribute to the pathogenesis of impaired insulin secretion and insulin resistance (304, 314). In support of the notion that ectopic fat accumulation promoted the diabetes phenotype, ROD animals exhibited significant increases in ectopic fat deposition in the liver and muscle compared with all other animals (Fig. 2), which coincided with their deteriorated insulin sensitivity. Numerous studies have demonstrated the link between ectopic fat deposition and insulin resistance in persons with overt T2DM (315, 316). Future studies are needed, however, to determine whether the increase in lipid end products associated with increased ectopic fat deposition is a driving force behind the development of T2DM in this rodent model, as has been proposed in humans with excessive liver and muscle lipid deposition (317).

Glucose tolerance and insulin sensitivity

Compared with all other treatment groups, cort-HFD rats demonstrated deteriorating glycemic control and severe insulin resistance, as measured by both oral

glucose and insulin tolerance tests (Fig. 1). Cort-HFD animals exhibited a threefold elevation in plasma glucose concentration and a 17-fold increase in insulin level compared with placebo-SD animals. Moreover, following oral gavage of glucose, cort-HFD animals had sustained elevations in glucose and insulin concentrations, thereby demonstrating similar characteristics to individuals with T2DM (318, 319). Measurement of HOMA-IR revealed almost a 70-fold increase in whole body insulin resistance in cort-HFD rats compared with the placebo-SD and placebo-HFD groups. Moreover, higher HOMA-β index values in cort-SD animals indicate a higher pancreatic β-cell function compared with placebo-treated animals. Importantly, however, the HOMA-β value was significantly lower in cort-HFD-treated animals compared with cort-SD animals despite the finding that cort-HFD animals had larger islet areas than all other groups (Fig. 1). These results suggest that the combination of elevated corticosterone with a HFD might initially increase β-cell compensation, possibly as a result of elevated insulin resistance, but that these β-cells have insufficient capacity to secrete enough insulin to normalize glycemia in response to oral glucose stimulation. In other words, although cort-HFD animals have increased islet areas and elevated insulin concentrations (in both the basal and stimulated states) compared with all other groups, these animals remain extremely glucose intolerant because of insufficient insulin signaling within various insulin target tissues.

Intracellular GC activation and other plasma markers of insulin resistance or T2DM

Our ROD model exhibits hyperglucocorticoidemia, exaggerated GC tissue reactivation and increased diabetes-related blood markers, all of which are present in humans and rodents with overt T2DM. Indeed, our cort-HFD animals show elevations in plasma GC levels beyond those observed with corticosterone treatment alone (Table 2), thereby suggesting that a HFD might exaggerate hyperglucocorticoidemia. Importantly, hyperglucocorticoidemia is frequently observed in both humans and rodent models of diabetes (63, 288, 320, 321). It has been previously proposed that heightened levels of plasma GCs in animals exhibiting metabolic syndrome might be a result of increased 11-βHSD-1 activity in liver, muscle and adipose tissue (322). From our data, we can conclude that our corticosterone-treated animals have an increase in 11-βHSD-1 activity within adipose tissue (Fig. 3). This finding is more exaggerated in corticosterone-treated animals given a HFD, which might help to explain the higher circulating levels of corticosterone.

Finally, it is important to note that the ROD model has other metabolic similarities to diabetes development, including hyperleptinemia and hyperlipidemia. Leptin is secreted by the adipocytes in response to increased adiposity and is thought to play a role in the development of peripheral insulin resistance and perhaps in the progression of T2DM, although the role of this adipokine in disease development is controversial (323). We confirm here that elevation in plasma leptin levels occurs in corticosterone-treated animals and that these increases are dramatically enhanced by a

HFD (Table 2). Moreover, ROD animals experience hypertriglyceridemia similar to rodent models of and individuals with T2DM (287, 324), perhaps due to increased fat intake and/or dramatic increases in insulin resistance caused by corticosterone and high-fat feeding. Further research is required, however, to establish the mechanisms of hyperglycemia development in this model (e.g. defective hepatic and muscle insulin signaling, glucose turnover and/or β-cell function).

Conclusion

In conclusion, the present study demonstrates a new cost effective rapidly inducible rodent model of GC-induced T2DM, which has a similar anthropometric, biochemical and pathogenic profile as patients with severe insulin resistance or metabolic disease. This ROD model can be considered a new important tool for determining the complex multi-organ and multi-tissue connections between elevated GC levels and the development of metabolic syndrome and T2DM.

Table 1. Body composition and caloric intake of placebo- and corticosterone-treated rats.

	Placebo-SD	Placebo-HFD	Cort-SD	Cort-HFD	Main Effect of Cort	Main Effect of Diet	Interaction
Gross body mass (g)	358.86±5.57	350.84±4.52	265.87±7.40#	226.12±9.05#	**p<0.001**	**p<0.01**	**p<0.05**
Caloric Intake (kcal/kg body mass * day)	0.28±0.01	0.42±0.01#	0.33±0.01#	0.61±0.02#	**p<0.001**	**p<0.001**	**p<0.001**
Left Adrenal mass (g/kg body mass)	0.10±0.01	0.10±0.01	0.03±0.01	0.05±0.06	**p<0.001**	———	———
Epitrochlearis mass (g/kg body mass)	0.14±0.01	0.15±0.01	0.18±0.01	0.09±0.02#	———	**p<0.01**	**p<0.01**
Soleus mass (g/kg body mass)	0.42±0.01	0.40±0.02	0.42±0.02	0.49±0.06	———	———	———
Epididymal fat pad mass (g/kg body mass)	4.56±0.54	5.82±0.28	5.27±0.57	9.81±1.65#	**p<0.05**	**p<0.01**	**P=0.06**
Liver mass (g/kg body mass)	39.90±1.44	36.16±1.21	58.35±3.83†	68.62±3.20†	**p<0.001**	———	**p<0.05**
Pancreas mass (g/kg body mass)	2.48±0.13	2.61±0.08	3.92±0.46	3.40±0.52	**p<0.01**	———	———

Note: * indicates significance from Placebo-SD ($p<0.05$). The † indicates significance from the respective placebo group ($p<0.05$). The # indicates significance versus all other treatment groups ($p<0.05$) All values are means ± SEM, n=7-10.

Table 2. Plasma composition of corticosterone (ng/ml), fasted insulin (ng/ml), leptin (pg/ml), triglycerides (mM) and non-esterified fatty acids (NEFAs) (mM) in Placebo-SD, cort-SD, Placebo-HFD and cort-HFD animal groups.

	Placebo-SD	Placebo-HFD	Cort-SD	Cort-HFD	Main Effect of Cort	Main Effect of Diet	Interaction
Peak corticosterone (ng/ml)	270.3±51.3	303.2±140.7	295.2±74.4	585.6±126.9	——	——	——
Trough corticosterone (ng/ml)	45.6±12.8	19.8±3.8	310.0±60.3#	595.9±122.0#	**p<0.001**	——	**p<0.05**
Insulin (ng/ml)	0.27±0.05	0.50±0.32	0.63±0.29	4.65±0.36#	**p<0.001**	**p<0.001**	**p<0.001**
Leptin (ng/ml)	1.20±0.19	3.08±0.55	4.59±0.72	6.23±0.42	**p<0.001**	**p<0.001**	——
Triglycerides (mM)	0.13±0.01	0.19±0.02	0.24±0.04	0.40±0.13	**p<0.05**	**p<0.05**	——
NEFAs (mM)	0.92±0.01	0.79±0.16	0.62±0.05	0.62±0.06	——	——	——

Note: The * indicates statistical significance from Placebo group ($p<0.05$). The # indicates significance versus all other treatment groups ($p<0.05$). All values are ±SEM. N=5-6 per group.

Figure Captions

Figure. 1. Corticosterone treatment increases glucose intolerance and insulin sensitivity. (A) Glucose concentrations (mmol/l) were measured every 30 minutes post oral glucose load (1.5 g/kg). (B) Insulin concentrations (ng/ml) during the oral glucose tolerance test (OGTT). (C) HOMA-IR, as calculated by the formula: [insulin (μU/ml) × glucose (mmol/l)]/22.5. (D) HOMA-β, as calculated by the formula: [20 × insulin (μ units/l)]/[glucose (mmol/l) – 3.5]. This calculation indicates the functional response of the pancreatic β-cells to a bolus of glucose. A higher HOMA-β value suggests a greater response of the βcells to glucose, indicating higher β-cell function. (E) Glucose concentrations during the insulin tolerance test. (F) Insulin resistance, as measured by the AUC for glucose levels following the insulin tolerance test. All values are means ± s.e.m., n=5–6. *, Statistical significance from all other treatment groups, $P<0.05$. #, significance from cort-SD, $P<0.05$, using a two-way ANOVA. †, cort-SD significantly different from placebo-SD, $P<0.05$.

Figure. 2. Histochemistry staining analysis. (A) Pancreatic islet hemotoxylin and eosin staining, indicating pancreas islet areas. (B) Liver Oil Red O staining, indicating liver total lipid content. (C) Tibialis anterior Oil Red O staining, indicating muscle total lipid content in placebo-SD, cort-SD, placebo-HFD and cort-HFD animals (20× magnifications).

Figure. 3. Tissue determination of corticosterone action in adipose tissue. (A) Relative 11-βHSD-1 and (B) GR mRNA expression in epididymal fat deposits. (C) 11-βHSD-1 and (D) GR mRNA expression in subcutaneous fat deposits in placebo-SD, cort-SD, placebo-HFD and cort-HFD rats. All protein was standardized to β-actin expression. n=3–5. *, $P<0.05$ from placebo-SD; #, significance from cort-SD. All values are ± s.e.m.

Figure. 4. Treatment protocol timeline. Animals were given 7 days of habituation before pellet surgeries were performed (day 0). Also on this same day, plasma corticosterone levels as well as blood glucose levels were sampled (i.e. basal measurements). On day 7, corticosterone and blood glucose measurements were repeated and animals were fasted overnight on the night of day 11. Animals were then given an oral glucose tolerance test (OGTT) on day 12 and were subsequently allowed a 2-day wash-out period before another plasma corticosterone and blood glucose sample was taken (evening of day 14). Animals were then fasted on the night of day 15 and finally subjected to an insulin tolerance test (ITT) on day 16.

Figure 1.

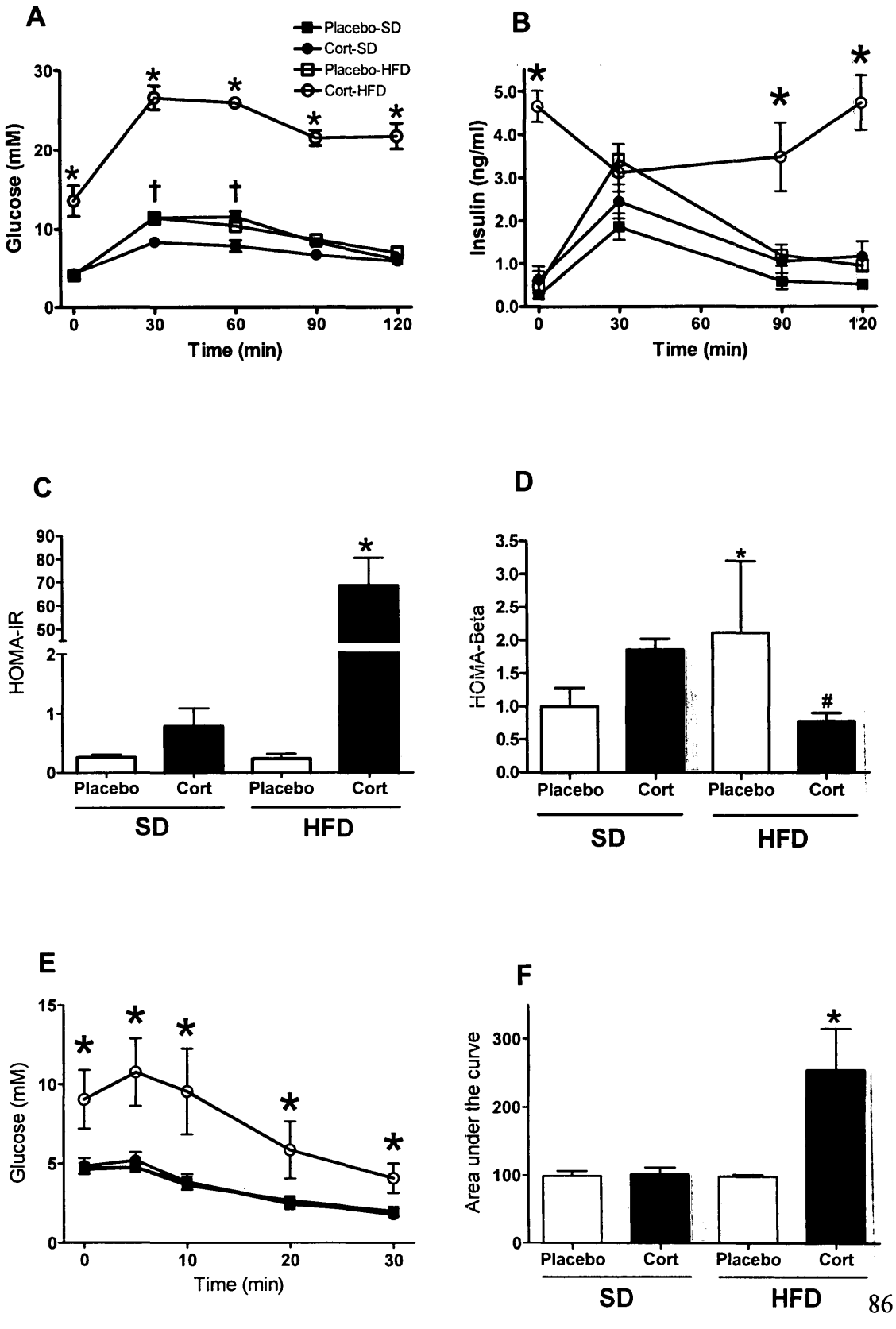
A
Placebo-SD
Cort-SD
Placebo-HFD
Cort-HFD
Glucose (mM)
Time (min)
B
Insulin (ng/ml)
Time (min)
C
HOMA-IR
Placebo
Cort
Placebo
Cort
SD
HFD
D
HOMA-Beta
Placebo
Cort
Placebo
Cort
SD
HFD
E
Glucose (mM)
Time (min)
F
Area under the curve
Placebo
Cort
Placebo
Cort
SD
HFD

Figure 2.

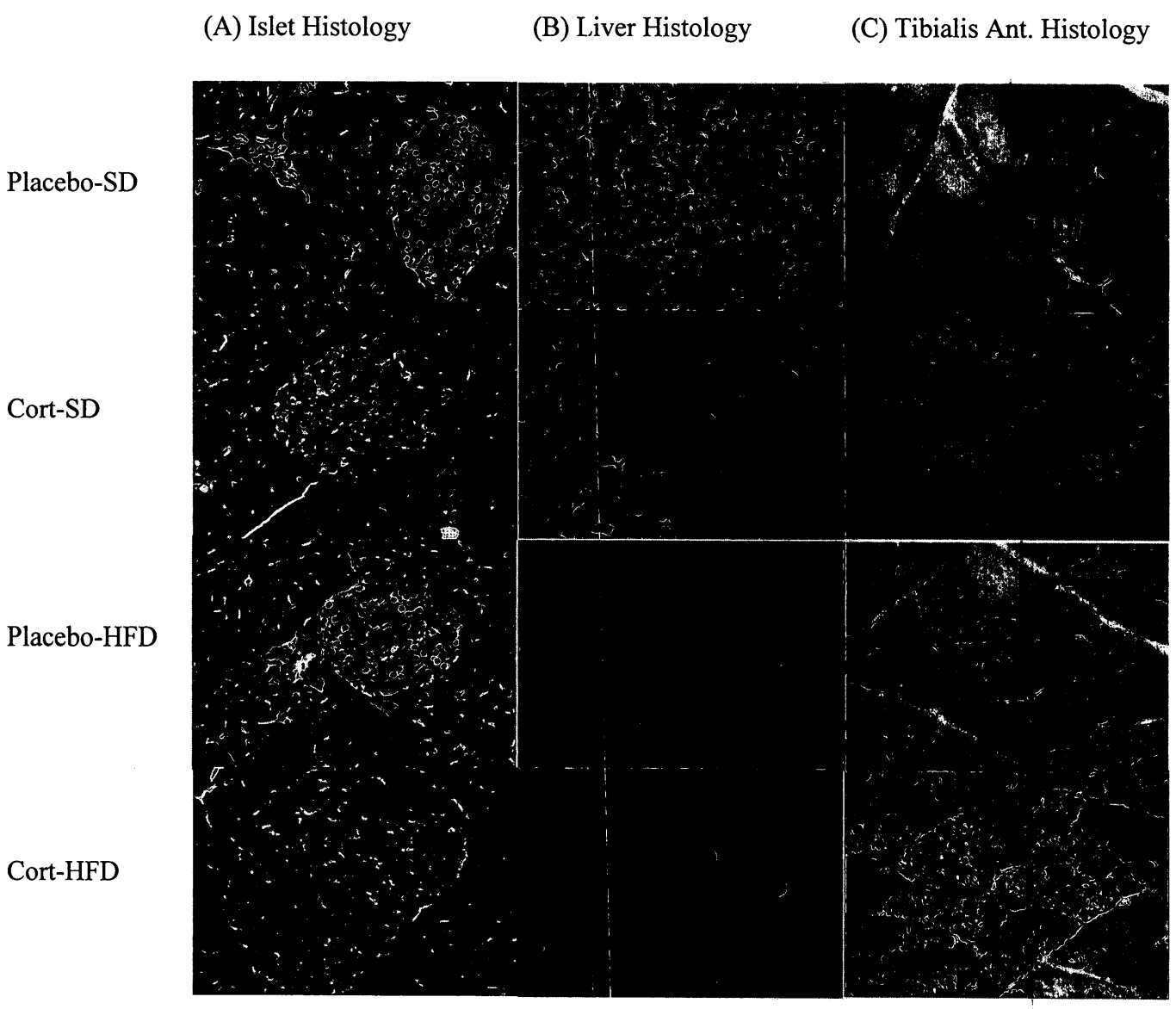
(A) Islet Histology
(B) Liver Histology
(C) Tibialis Ant. Histology
Placebo-SD
Cort-SD
Placebo-HFD
Cort-HFD

Figure 3.

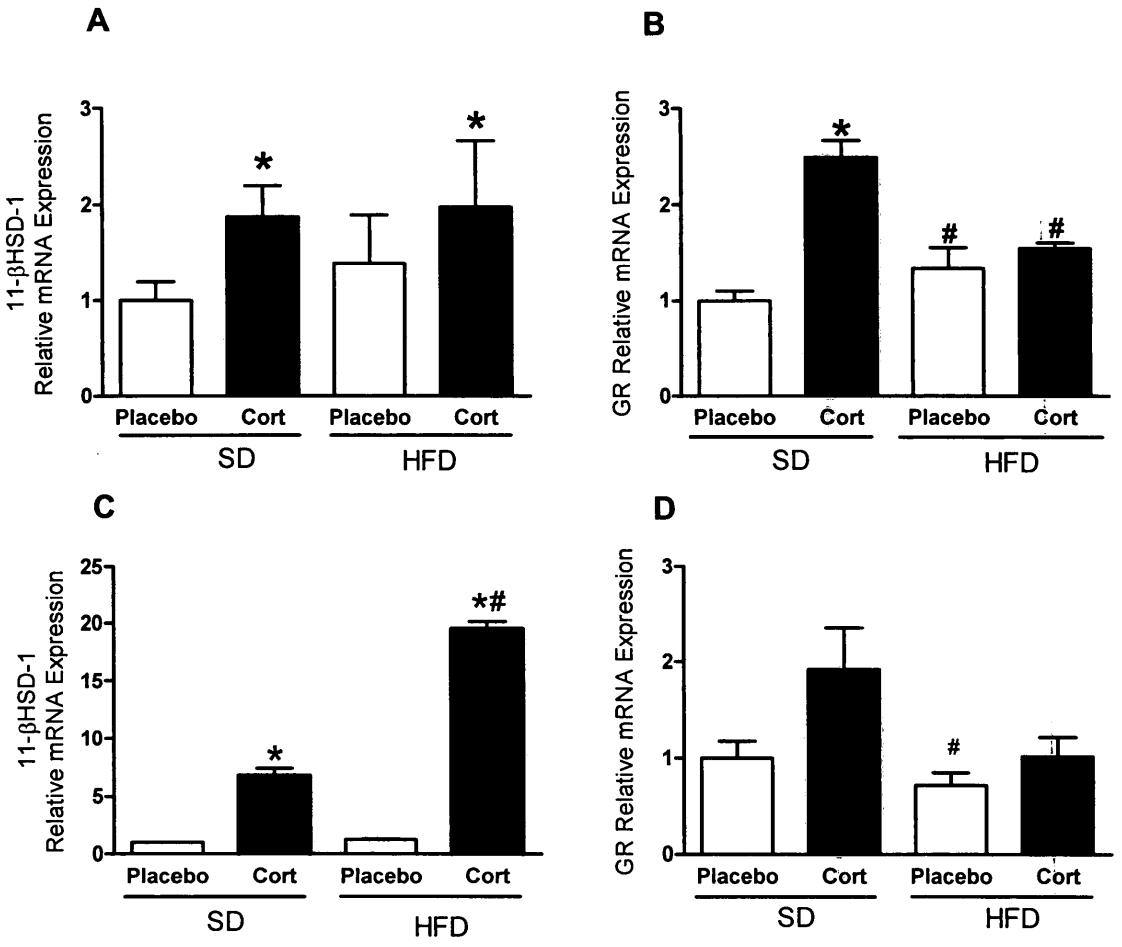
A
11-βHSD-1
Relative mRNA Expression
3
2
1
0
*
*
Placebo
Cort
Placebo
Cort
SD
HFD
B
GR Relative mRNA Expression
3
2
1
0
*
#
#
Placebo
Cort
Placebo
Cort
SD
HFD
C
11-βHSD-1
Relative mRNA Expression
25
20
15
10
5
0
*
*#
Placebo
Cort
Placebo
Cort
SD
HFD
D
GR Relative mRNA Expression
3
2
1
0
#
Placebo
Cort
Placebo
Cort
SD
HFD

Figure 4.

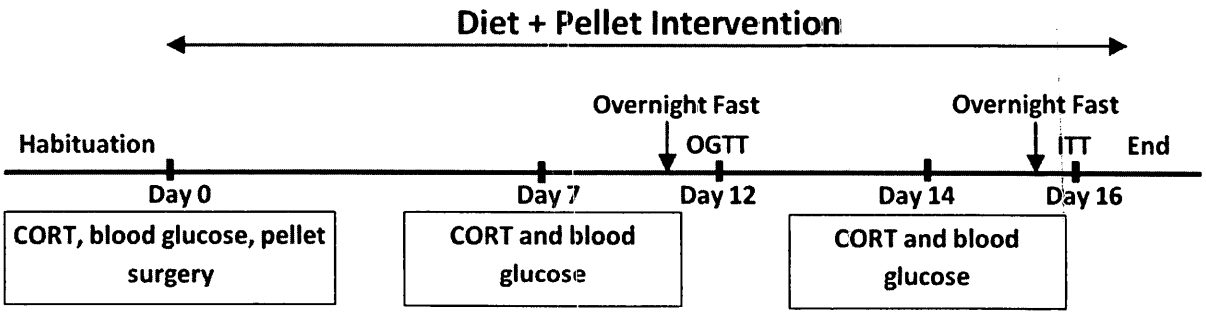
Diet + Pellet Intervention
Overnight Fast
Overnight Fast
Habituation
OGTT
ITT
End
Day 0
Day 7
Day 12
Day 14
Day 16
CORT, blood glucose, pellet surgery
CORT and blood glucose
CORT and blood glucose

MANUSCRIPT-#2 Chapter 3

The Effects of GCs and HFD on Islet Adaptations in the Sprague-Dawley Rat

Rationale for Manuscript #2

Manuscript #1 demonstrated that elevated GCs, by implantation of corticosterone pellets and a HFD (60% total calories from fat) induced a rapid-onset T2DM phenotype in otherwise healthy young male Sprague-Dawley rats. Our treatment showed that 2 weeks of treatment induced fasting hyperglycemia, hyperinsulinemia, severe peripheral insulin resistance, increased visceral adiposity, hepatic steatosis, and muscle lipid deposition. This study described the effects on whole body physiology with elevations in GCs and HFD that evidently overwhelmed pancreatic β-cell compensation capacity leaving animals overtly diabetic. Chronic elevations in GCs are known to destroy glucose homeostasis, but the literature is undecided as to the role that short-term increases in GCs play on islet function. Some studies suggest that acute GC treatment *in vivo* increases insulin resistance, β-cell mass, and secretion thereby up-regulating islet compensation mechanisms in rodents (2, 154). Whereas other studies suggest that *in vitro* administration of GCs deteriorates β-cell function and decreases insulin secretion (3, 161). In addition, lipid accumulation has been shown to directly impair islet function thereby decreasing insulin secretion (177, 180). Therefore, as increased GCs and lipid concentrations have both been linked to islet dysfunction, the goal of our second manuscript was designed to enhance our understanding of *in vivo* and *ex vivo* islet adaptations to elevations of GCs and HFD by use of our ROD model in young rats.

Author Contributions

Conceived and designed the experiments: J.L.B., A.D. and M.C.R. Performed the experiments: J.L.B., A.D. and T.T. Analyzed the data: J.L.B., A.D., T.T. Wrote the manuscript: J.L.B. Edited the paper: A.D., T.T., R.T. and M.C.R.

J.L.B. performed all animal surgeries, oral glucose tolerance test, insulin tolerance test, preparation of islet histology, quantification of β-and α-cell mass, size and number, plasma analyses of glucose, insulin, corticosterone, glucagon, NEFAs, PKC- α and 11β-HSD1 protein analysis, pancreatic islet isolations, acute ex vivo experiments with isolated islets and all statistical analyses data for this manuscript.

J.L.B. contributed to Figure 1, 2, 3, 4, 5, 6, 7, 8 and table 1 and 2.

This manuscript was published in the journal of *Endocrinology*, 2013, Jun 13. [Epub ahead of print]. DOI:10.1210/en.2012-2114

Exogenous Glucocorticoids and High-fat Diet cause Severe Hyperglycemia and Hyperinsulinemia and Limit Islet Glucose Responsiveness in Young Male Sprague-Dawley Rats

Running title: Islet Responses to GCs and High-Fat Diet

Jacqueline L. Beaudry[1]
Anna D'Souza[1]
Trevor Teich[1]
Robert Tsushima[2]
Michael C. Riddell[*1]

[1]School of Kinesiology and Health Science, Faculty of Health, Muscle Health Research Center and Physical Activity and Chronic Disease Unit, York University, 4700 Keele St., Toronto, ON, Canada, M3J 1P3
[2]Department of Biology, York University, 4700 Keele St., Toronto, ON, Canada, M3J 1P3
[*]Author for correspondence

Please address correspondence to Dr. Michael C. Riddell,
School of Kinesiology and Health Science, Faculty of Health, Muscle Health Research Center and Physical Activity and Chronic Disease Unit, York University 4700 Keele Street,
Toronto, ON, Canada, M3J 1P3
Telephone: (416) 736-2100 ext. 40493
Fax: 416-736-5774
Email: mriddell@yorku.ca

Key Words: Exogenous glucocorticoid therapy, High-fat feeding, Insulin resistance, Islet adaptations, Type 2 diabetes mellitus

Abstract

Corticosterone (CORT) and other glucocorticoids cause peripheral insulin resistance and compensatory increases in β-cell mass. A prolonged high-fat diet (HFD) induces insulin resistance and impairs β-cell insulin secretion. This study examined islet adaptive capacity in rats treated with CORT and a HFD. Male Sprague-Dawley rats (age ~ 6 weeks) were given exogenous CORT (400 mg/rat) or wax (placebo) implants and placed on a HFD (60% calories from fat) or standard diet (SD) for 2 weeks (N=10 per group). CORT-HFD rats developed fasting hyperglycemia (>11 mM) and hyperinsulinemia (~ 5-fold higher than controls) and were 15-fold more insulin resistant than placebo-SD rats by the end of ~2 weeks (Homeostatic Model Assessment for Insulin Resistance [HOMA-IR] levels, 15.08±1.64 vs. 1.0±0.12, $P<0.05$). Pancreatic β-cell function, as measured by HOMA-β, was lower in the CORT-HFD group as compared to the CORT-SD group (1.64±0.22 vs. 3.72±0.64, $P<0.001$) as well as acute insulin response (0.25±0.22 vs. 1.68±0.41, $P<0.05$). Moreover, β- and α-cell mass were 2.6- and 1.6-fold higher, respectively, in CORT-HFD animals compared to controls (both $P<0.05$). CORT treatment increased p-protein kinase Cα content in SD but in not HFD-fed rats, suggesting that a HFD may lower insulin secretory capacity via impaired glucose sensing. Isolated islets from CORT-HFD animals secreted more insulin in both low and high glucose conditions; however, total insulin content was relatively depleted after glucose challenge. Thus, CORT and HFD, synergistically not independently, act to promote severe insulin resistance, which overwhelms islet adaptive capacity, thereby resulting in overt hyperglycemia.

Introduction

Exogenous glucocorticoids (GCs) can have acute beneficial outcomes for the treatment of some inflammatory conditions (325), however they are associated with widespread metabolic effects that have the potential to deteriorate glucose homeostasis. Acutely, GCs lower skeletal muscle glucose transport (151) and increase hepatic glucose production (326). Chronically, GCs promote increases in visceral adiposity and excess ectopic lipid deposition (110). Not surprisingly, therefore, prolonged GC treatment is associated with an elevated risk for the development of type 2 diabetes (T2DM) in humans, although the exact prevalence of GC-induced diabetes in humans is unknown (145). Synthetic GC treatment, such as those given prednisolone treatment, for 2 days (327), 2 weeks (156), as well as 3 months (146), demonstrates impaired first-phase insulin response and action. Thus, GCs can indirectly pose major stress on pancreatic islet function by dramatically increasing insulin secretory demand (15). Whether GCs cause any direct effects on islet function remains unclear; however, some evidence suggests both enhanced (153, 155) and impaired (161, 166) insulin secretion depending on the duration of exposure and experimental models used (3, 162, 165, 166). Short-term GC treatment (1–6 h) to isolated islets from lean rodents has been shown to blunt the first-phase and delay the second-phase insulin response thereby reducing the islet insulin response to glucose challenge (3, 161). However, long-term GC exposure (~2 wk of dexamethasone treatment in rats) is associated with increased insulin release with glucose challenge *in vitro* (167). Together, these results display the vast conflicting observations with respect to GC exposure and islet function.

In addition to peripheral insulin resistance, GC therapy induces elevations in free fatty acids (FFAs) along with increased food consumption and the preference for energy-dense foods (110). Elevations in lipids have long been known to induce β-cell dysfunction *in vivo* and *in vitro*—a phenomenon known as lipotoxicity (177) whereby chronically high levels of FFAs lead to a decrease in insulin secretion along with lower insulin gene expression (180). However, *in vivo* rodent models of high-fat diet (HFD) have not consistently demonstrated impairments of β-cell function (140).

Although GCs and FFAs are often elevated with obesity, pre-diabetes, and diabetes, rarely have the independent and synergistic effects of these environments been studied in combination on islet function. Recently, we developed a rodent model of GC-induced diabetes in young male Sprague-Dawley rats, showing that a diabetic phenotype can be rapidly induced when animals are exposed to elevations in exogenous corticosterone (CORT), the active GC in rodents, and a HFD (328). The aim of this study was to examine the *in vivo* and *ex vivo* islet adaptations that result from this model of diabetes and test the hypothesis that elevated GC exposure in combination with a HFD exceeds the adaptive capacity of the islets to maintain glucose homeostasis. We demonstrate here that short-term (~ 2 wk) administration of CORT and a HFD results in hyperglycemia despite increases in β-cell mass, largely because of severe whole-body insulin resistance and impaired islet glucose sensitivity.

Methods

Ethics statement

All experiments were approved by the York University Animal Care Committee in accordance with the Canadian Council for Animal Care guidelines.

Animal characteristics, surgical procedures, and design

Male Sprague-Dawley rats (225–250 g, 6 wk post weaned; Charles River Laboratories, St. Constant, Quebec, Canada) were divided into 4 treatment groups (N=10 per group). Each rat

received subcutaneous implantation of either CORT pellets (4 x 100 mg; C2505; Sigma, Oakville, Canada) or wax pellets, as previously described (328), so that 4 groups existed: wax pellet treatment fed a standard diet (placebo-SD; controls); CORT pellet treatment fed a standard chow diet (CORT-SD); wax pellet treatment fed a HFD (placebo-HFD); and CORT pellet treatment fed a high-fat diet (CORT-HFD). All animals were individually housed (lights on 12 h: lights off 12-h cycle) after 1 week of acclimatization and given their respective diets immediately following surgery. CORT was sampled on the evening of the sixth day after pellet implantation via tail nick from each rat at 2000 h and again 12 h later (0800 h). These samples were later analyzed for CORT levels using a RIA kit (MP Biomedical, Solon, Ohio). Blood glucose values were also measured on day 6 (fed state) via a handheld blood glucose meter (Bayer, Contour,

New York).

Diet specifications

Standard diet (SD) (Purina Lab diet, 5012, St Louis, Missouri) or a HFD (TD.06414; Harlan Laboratories, Madison, Wisconsin) was provided *ad libitum* following recovery from pellet implant surgeries. The HFD consisted of 5.1 kcal/g and the SD consisted of 3.4 kcal/g. Total fat content (60% of total calories) of the HFD was composed of 37% saturated fats, 47% monounsaturated fats, and 16% polyunsaturated fats.

Plasma analyses

Animals were administered an oral glucose tolerance test (OGTT; 1.5 g/kg body mass) on day 12 and an insulin tolerance test (ITT) on day 16 by i.p. insulin injection, as previously described (328). Capillary blood glucose concentration was measured by a handheld glucometer and blood samples from tail nick were collected in EDTA-coated microvette tubes, and plasma was subsequently analyzed for insulin (INSKR020; Crystal Chem, Downers Grove, Illinois) and FFA levels (NEFA kit, HR Series NEFA-HR; Wako Chemicals, Richmond, Virginia). Glucose and insulin area under the curve (AUC) were measured by each individual's fasting glucose and insulin levels. For technical and experimental reasons, the day of termination ranged from 2 to 5 days after the ITT to allow for subsequent islet isolation studies and trunk blood was collected for hormone analysis. Homeostatic Model Assessment for Insulin Resistance (HOMA-IR) was calculated based on the following equation: Glucose (mM) X Insulin (μ units x L)/22.5. Homeostatic Model Assessment for β-cells (HOMA-β) was calculated based on the

following equation: 20 X Insulin (μ units x L)/ Glucose (mM) 3.5, according to Kiraly et al (144).

Assessment of islet morphology

Immunohistochemistry

The entire pancreas was extracted upon euthanization and immersed in 10% buffered Formalin or 4% paraformaldehyde (Sigma) for up to 48 hours. Tissues were washed in 70% ethanol, embedded in paraffin, and later serial sectioned onto slides. A random selection of slides from each group was dewaxed in xylene, dehydrated in ethanol, and washed in PBS. Antigen unmasking/epitope retrieval was performed by high-pressurized heat in a 10 mM solution of sodium citrate buffer, pH 6.0. Slides were incubated in a protein blocking solution (Signet) and then probed for insulin (1:500, guinea pig; Dako, Burlington, Ontario, Canada) and glucagon (1:200, rabbit, Cell Signaling, no. 2760, Boston, Massachusetts; New England Biolabs, Whitby, Ontario, Canada) and proliferating cell nuclear antigen (PCNA) (1:4000, mouse; Cell Signaling no. 2586). After an overnight incubation at 4°C, slides were immunostained with a secondary antibody of biotinylated goat antiguinea pig (Vector LabsBA1000, Burlington, Ontario, Canada at 1:500 dilutions), antirabbit (Vector LabsBA7000at 1:500 dilutions), and antimouse (Vector Labs BA9200 at 1:500 dilutions) for insulin, glucagon, and PCNA, respectively. A labeling reagent (Ultrastreptavidin horseradish peroxidase, Convance Signet SIG-32242-95, Princeton,New Jersey) and diaminobenzadine (Sigma) were applied to slides until brown staining was visible. Slides were counterstained in

hematoxylin (Sigma, Canada). Representative slides of insulin and glucagon were used for measurements of β- and α-cell mass, islet areas, β-cell number, and β- and α-cell size. Terminal transferase-mediated dUTP-digoxigenin nick end-labeling (TUNEL) staining protocols were performed by the University Health Network group at Toronto General Hospital.

Quantification of β-cell mass, islet area, α-cell size, and number of β-cells per islet

Estimated β-cell mass per animal was measured as the product of the total cross-sectional area of insulin-positive stained β-cells divided by total tissue area and multiplied by mass of the isolated pancreas (mg) at euthanization. On average, 1000 to 1500 islets were analyzed per group at 20 x magnification. Tissue areas were objectively quantified, using a positive pixel count algorithm, representing the insulin-positive areas with slide scanner software (Aperio Scanscope CS, Vista, California). The sum of the positive and strong positive pixel areas for each pancreas section was chosen as the best representation of positive insulin stained areas.

All islets were individually circled around the positively insulin-stained cells and were regarded as the total insulin-positive stained areas using a positive pixel count algorithm as previously described. The number of islets per squared millimetre was determined by adding the number of counted islets per slide and then dividing by the total tissue stained area. Islet areas (μm^2) were found by adding together the total islet areas and dividing by the total number of islets per slide. To quantify the size of the individual β-cells per islet area, all distinct nuclei surrounded by insulin-positive stained areas were

counted as a β-cell within each islet. Then the insulin-stained area on each slide (sum of β-cell area, μm^2) was divided by the total number of β-cells counted on each slide to determine β-cell size. This analysis also allowed calculation of the number of β-cells per average islet by taking total islet areas and dividing by previously determined β-cell size. All of these methods were modified protocols from previously published reports by Kiraly et al (144) and Bates et al (329). Measurements of PCNA quantification, α-cell mass, area, size, and number of α-cell were quantified in a manner similar to insulin-positive staining.

Islet isolations and Western analysis

Another set of identically treated animals (5–6 per group) were killed 18 to 21 days after the start of treatment to examine *ex vivo* islet function and a similar protocol was used with modifications (330, 331). Collagenase solution (20 mL; 4.6 mg per 10 mL of RPMI 1640 without glucose and glutathione [Wisent], 10 mM HEPES, 1% penicillin-streptomycin, glucose [50% dextrose]) was used to digest the pancreas for 20 minutes in a 37°C water bath with periodic agitation. RPMI buffer with 7% fetal bovine serum (FBS) was added to the digested pancreas and then shaken vigorously. Vials were centrifuged for 4 minutes at 1600 g at 4°C. The supernatant was discarded and RPMI with 7% FBS was added and gently shaken to dissolve the pellet. The new mixture was filtered through a mesh fabric (500 μm^2 pore size) into a new conical tube. This new mixture was centrifuged for 4 minutes at 1200 g at 4°C. The remaining pellet was suspended in Histopaque-1077 (H8889; Sigma, Canada) and topped off with a layer of RPMI without FBS. The mixture was centrifuged 25 minutes at 2700 g at 4°C. The

mixture was poured into a new conical tube and Kreb's buffer (125mMNaCl, 4.7mMKCl, 1.2 mM, 5 mMNaHCO3, 2.5mMCaCl2, 2.4mMMgSO4, 10mM HEPES, 0.5% BSA, pH 7.4). The mixture was centrifuged 4 minutes at 1400 g at 4°C. The remaining pellet was dissolved in Kreb's buffer and islets were selected and cultured in filtered RPMI buffer overnight (24 h) at 37°C, 5% CO_2 unless islets were used for western analysis at which point they were collected and stored at 80°C until further analysis. Fifty micrograms of protein were run on SDS-PAGE and proteins were transferred to a polyvinyldifluoride membrane and blocked in 10% powered milk and Tris-buffered saline with Tween20 for 2 hours. Primary antibodies were protein kinase C (PKC; 5578, Cell Signaling at 1:500 dilution), phosphorylated-PKCα (sc-12356; Santa Cruz at 1:1000 dilution), 11β-hydroxysteroid dehydrogenase type 1 (11-HSD1, ab39364; Abcam at 1:500 dilution) and β-actin (ab6276; Abcam at 1:20 000 dilution) were probed overnight at 4°C until the following morning when secondary antibodies were added to membranes of either biotinylated antimouse or antirabbit (at 1:10 000 dilution) were incubated for 1 hour at room temperature and then washed and imaged. Membranes that were probed with p-PKC antibody were then stripped, blocked, and reprobed with PKC antibody overnight and incubated in secondary antibodies for 1 hour, washed, and then imaged. Images were detected on a Kodak *In vivo* FX Pro imager and molecular imaging software (Carestream Image MI SE, version S.0.2.3.0, Rochester, New York) was used to quantify protein content.

Glucose-stimulated insulin secretion (GSIS) and insulin content measurements

Islets were separated into a 12-well culture plate (6–10 islets/well in 3 batches) and given a pre-incubation period for 30 minutes in Kreb's buffer 0.1 mM glucose 0.1% BSA dissolved in Kreb's buffer. Media were flushed and islets were given fresh Kreb's buffer with 2.8 mM glucose 0.1% BSA for 1 hour at 37°C, 5% CO_2. Media were changed to Kreb's buffer with 16.7 mM glucose 0.1% BSA for 1 hour at 37°C, 5% CO_2. Immediately following each incubation period, media collected were spun at 5000 rpm at 4°C for 10 minutes and frozen at 20°C for further analysis. Islets were placed in 1mL cold lysis buffer (acid-ethanol solution), sonicated (15 s), and centrifuged at 14 500 rpm at 4°C for 10 minutes. Supernatant was collected and stored at 20°C until further analysis of insulin content. Insulin was measured using an RIA kit (Millipore, Billerica, Massachusetts).

Statistical analyses

All data are represented as mean ± SE, with a criterion of $P<0.05$ and $P<0.001$, and were assessed using one-way and two-way ANOVAs as means of statistical significance except for determination of pellet mass differences between CORT treatment groups and acute insulin response (AIR) between placebo-SD and CORT-HFD where an unpaired Student's t test was used. Individual differences were evaluated using Tukey's HSD post hoc test (Statistica 6.0 software), with adjustments made for multiple comparisons. In each figure different letters denote statistical significance between groups. All fold differences are expressed as relative to the placebo-SD group.

Results

Exogenous CORT increases plasma CORT and abolishes diurnal rhythm

After 2 weeks of pellet implantation (at the time of euthanization), there were no significant differences found in the pellet mass excised from CORT-SD and CORT-HFD animals (Table 1), thereby suggesting that CORT absorption was not influenced by dietary treatment. CORT levels were higher at peak (2000 h) than at trough (0800 h) in placebo-treated animals 2 weeks after pellet implantation (Table 1). In contrast, CORT-treated animals had elevated basal CORT values that were indistinguishable from peak concentrations. Left and right adrenals were ~ 50% smaller in CORT-treated animals compared to the two placebo groups, confirming that the exogenous CORT promoted feedback inhibition of ACTH release ($P<0.05$, Table 1). CORT treatment decreases lean mass, increases adipose tissue mass, and promotes hyperglycemia. All groups were similar in body mass prior to treatment (day 0). Six days following CORT implantations, CORT treated animals were smaller in mass compared to placebo-treated animals ($P<0.05$, Table 2). Relative food intake was increased in CORT-HFD animals compared to placebo-HFD at day 6 ($P<0.05$, Table 2). HFD resulted in greater epididymal fat pad mass compared to placebo-SD animals, with the greatest increase observed in the CORT-HFD group ($P<0.05$, Table 2). Both CORT-treated groups had elevated fed blood glucose levels relative to the placebo groups on day 6 (main effect of treatment, $P<0.05$). Non-esterified fatty acids were elevated in all treatment groups compared to placebo-SD, but were highest in the CORT-HFD group ($P<0.05$, Table 2).

Severe glucose intolerance and hyperinsulinemia were induced with CORT-HFD treatment

Fasting blood glucose levels were the highest in CORT-HFD animals, whereas all other treatment groups had similar fasting glucose levels ($P<0.05$, Figure 1A). Glucose AUC during an OGTT was also highest in CORT-HFD animals compared to all other groups ($P<0.05$; Figure 1A'). Fasting insulin levels were highest in CORT-HFD animals compared to all other treatment groups ($P<0.05$; Figure 1B). Insulin AUC was higher in CORT-SD than in the controls and CORT-HFD animals ($P<0.05$; Figure 1B'). AIR is thought to be an early defect in the course of diabetes development and this response can be estimated as the change in insulin levels during the first 15 minutes following oral glucose gavage in rats (191). CORT-HFD animals demonstrated lower AIR compared to CORT-SD and placebo-SD and placebo-HFD groups ($P<0.05$, Figure 1C). Figure 1D demonstrates the relationship between fasting glycemia and insulin levels in each of the treatment groups, indicating that higher glucose concentrations were associated with increased insulin levels ($r^2=0.42$, $P<0.05$). This regression is based on all groups plotted on the same graph; independently the linear regressions are as follows: placebo-SD, $r^2=0.005$, CORT-SD, $r^2=0.003$, placebo-HFD, $r^2=0.04$, and CORT-HFD, $r^2=0.02$ (not statistically significant, independently). HOMA-IR index indicated that CORT-HFD animals were ~ 15-fold more insulin resistant than placebo-SD and ~ 4-fold more insulin resistant than CORT-SD rats (Figure 2A; $P<0.05$). HOMA-β, a measure of β-cell function, was elevated in the CORT-SD group by 3.5-fold compared to the placebo-SD group (Figure 2B, $P<0.05$). In contrast, the CORT-HFD group had a 2-fold lower

HOMA-β compared to the CORT-SD, suggesting the addition of a HFD reduced β-cell function. Following an i.p. insulin injection to assess insulin sensitivity, the CORT-HFD group continued to have elevated blood glucose levels compared to all other groups ($P<0.05$, Figure 2C). CORT-HFD animal's maintained 2-fold higher glucose AUC levels than all other treatment groups (Figure 2C').

CORT and HFD induce islet hyperplasia and hypertrophy

Islet morphology was investigated by insulin, glucagon, TUNEL, and PCNA-positive staining (Figure 3, A–P). Compared to placebo-SD rats, both HFD- and CORT-treated rats had a lower degree of apoptosis as measured by TUNEL staining (placebo-SD, 0.16 ± 0.18; CORT-SD, 0.064 ± 0.08; placebo-HFD, 0.1 ± 0.1; CORT-HFD, 0.03 ± 0.03 divide values by 103; (Figure 3, I–L). PCNA, a marker of cell replication and islet proliferation (332) , was up-regulated in all CORT-treated animals relative to placebo groups, thus demonstrating increased cell proliferation (placebo-SD, 100.0 ±9.1; CORT-SD, 288.5 ± 9.8; placebo-HFD, 74.6 ± 21.5; CORT-HFD, 337 ± 116.2; Figure 3, M–P). Insulin-positive staining measured as β-cell mass revealed a 2.6-fold greater mass in the CORT-HFD group compared to placebo-SD controls (Figure 4A; $P<0.05$), whereas CORT-SD treatment resulted in a 1.8-fold increase in β-cell mass. To determine if increased β-cell mass was a reflection of changes in islet morphology, the number of islets per squared millimeter of analyzed tissue was measured and found to increase with CORT-HFD treatment compared to all treatment groups (Figure 4B; $P<0.05$). CORT treatment resulted in larger islet area with a greater number of smaller β-cells as compared to placebo controls (Figure 4, C, D, and F; $P<0.001$). Islets were also grouped

into various size groupings to demonstrate the differences in islet size distributions (Figure 4E). CORT treatment resulted in ~ 20% fewer islets in the smallest size group (<5000 μm^2) and ~ 15% more islets in the largest size group (15 000 + μm^2) compared to placebo-treated animals, regardless of diet. Plasma glucagon levels were elevated in CORT-HFD animals compared to placebo-SD ($P<0.05$; Figure 5A). In addition, the CORT-HFD group had the largest α-cell mass and size (μm^2) compared to all other treatment groups (Figure 5, B and C; $P<0.05$), indicating α-cell hypertrophy.

CORT treatment increases β-cell secretory capacity

It has been previously reported that PKCα plays an essential role in the insulin secretory process and its dysfunction may contribute to hyperglycemia in GC-treated rodents (2). Protein content of total PKCα normalized to β-actin was more highly expressed in islets treated with CORT regardless of diet (Figure 6A; $P<0.05$), suggesting that CORT treatment increases total PKCα expression, perhaps as a result of increased β-cell proliferation. Protein content for p-PKCα normalized to β-actin was up-regulated in the islets derived from CORT-SD, but not in CORT-HFD, rats compared to the islets from the placebo-SD rats (Figure 6B; $P<0.05$).

CORT treatment increases islet 11β-hydroxysteroid dehydrogenase type 1 (11β-HSD1) expression

The activity of tissue-specific 11β-HSD1 manipulates the level of active CORT in various organs in the body (290). Moreover, this enzyme has been shown to decrease GSIS in pancreatic murine and human islets (333) , potentially contributing to diabetes

development (176). Therefore, we assessed the protein content of 11β-HSD1 to determine a functional relationship between insulin secretion and active GC regeneration in the islets. The protein content of 11β-HSD1 was up-regulated in the islets from CORT-treated animals compared to placebo treated groups, regardless of diet (Figure 7; $P<0.05$).

CORT-HFD isolated islets exhibit enhanced insulin responses to glucose

To determine *ex vivo* β-cell function, islets were isolated from all treatment groups, stabilized in culture, and then subjected to low and high concentrations of glucose (2.8 and 16.7 mM). CORT-HFD islets released more insulin than the islets from all other groups in both glucose conditions (Figure 8A; $P<0.05$), although the fold change in insulin secretion from the low-glucose to the high-glucose media was lowest in the placebo-HFD and CORT-HFD islets (Figure 8A'). Total insulin content was measured after the islets were exposed to high levels of glucose in all treatment groups. CORT-HFD islets expressed the lowest levels of insulin content compared to all other treatment groups (Figure 8B; $P<0.05$), possibly indicating a greater depletion of insulin in response to high glucose in the media.

Discussion

Exogenous GCs cause insulin resistance and may promote diabetes development (334). A HFD in conjunction with exogenous GCs may increase diabetes risk, although few studies have investigated the amalgamation of these treatments. In this study, we show that the combination of CORT and a HFD results in severe insulin resistance with β-cell proliferation that promotes fasting hyperinsulinemia, but this adaptation is

insufficient to maintain glucose homeostasis, particularly in response to an oral glucose challenge. We also show that, at least in the short term, β-cell apoptosis is not increased with CORT and a HFD, but impairment in β-cell glucose sensing *in vivo*, likely as a result of chronic hyperglycemia and profound insulin resistance that overwhelms insulin secretory capacity. Although a number of previous studies have investigated the physiological adaptations to HFD (reviewed in Ref. (140)) and exogenous CORT treatment alone (2, 153, 161, 166, 335, 336), we are aware of only one other study that has combined the two to examine potential synergistic effects on islet function and diabetes development (191). In that investigation, dexamethasone (~ 100 μg kg^{-1} body weight day^{-1}; 5 d) and a HFD acted synergistically to induce glucose intolerance by impairing GSIS *in vivo*, similar to our findings (Figure 1). Moreover, short-term GC treatment (1–6 h) to isolated islets from lean rodents has been shown to blunt the first-phase and delay the second phase insulin response (3, 161). In contrast to these *in vivo* and *ex vivo* findings, previous studies conducted in various rodent models have demonstrated that prolonged GC exposure (equal to or longer than 5 d) increases GSIS (151, 153, 167, 191). Interestingly, and similar to our observations, GCs administered to healthy men cause impairments in several β-cell insulin secretory pathways and has been shown to inhibit the normal insulin response (156). Moreover, first-degree relatives of patients with T2DM who are treated with corticosteroids develop severe insulin resistance and may develop impaired glucose tolerance, depending on their islet function (170). Thus we conclude that in our model there is detriment to β-cell function by placing

severe demands on insulin requirements in a fasted state and a blunted capacity to respond to glucose challenge.

As expected, based on our previous study (328), we found that exogenous GCs promote hyperinsulinemia, in both the fasted and the fed state (OGTT) (Figure 1A and Table 2), but that the addition of a HFD markedly increases glucose intolerance and prevents the appropriate insulin response to a glucose challenge (Figure 1,A'and B'). In a previously mentioned study (191) , dexamethasone and a HFD precipitated glucose intolerance in rats by impairing the negative feedback loop between insulin sensitivity and secretion. Similarly, our study demonstrates the rapid onset of overt diabetes that occurs within 1 to 2 weeks and with no evidence of β-cell mass decompensation but with obvious impairments in insulin responsiveness to oral glucose challenge (Figure 1B'). Indeed, CORT-HFD animals demonstrate impaired first-phase insulin response during glucose challenge as measured by the acute insulin response (Figure 1C), suggestive of impaired glucose sensitivity *in vivo*. On the other hand, it is unlikely 2 weeks of CORT-HFD treatment resulted in complete destruction of β-cell insulin secretion and more likely that the rise in hyperglycemia/hyperinsulinemia was driven by increased peripheral insulin resistance.

Separately, both elevated CORT and a HFD increase peripheral and islet insulin resistance (140, 152), reduce insulin-mediated glucose disposal, and lower muscle glycogen synthesis (337, 338). We found a modest association between fasted glucose and insulin levels (r^2=0.42, Figure 1D), thereby suggesting that severe hepatic insulin resistance induces fasting hyperglycemia in CORT-HFD animals, as documented

previously (339). Indeed, this model of short-term CORT treatment induced a ~ 5-fold increase in HOMA-IR compared to controls and the addition of a HFD exacerbated insulin resistance by ~ 15-fold compared to controls (Figure 2A). Therefore, the combination of the two treatments appears to be the driving force for elevated fasting glucose and insulin levels. To determine if CORT and HFD treatment affect β-cell function, a HOMA-β index was used. CORT-SD treated animals had improved β-cell function compared to all other treatment groups but the addition of HFD decreased β-cell function relative to CORT-SD animals, such that values were similar to what was observed in the placebo-treated groups (Figure 2B). One interpretation is that CORT-HFD treated rats had normal β-cell function, but were in an environment of severe insulin resistance that requires enhanced function. In addition to impairments in hepatic insulin sensitivity and possibly β-cell function, our model demonstrates decreases in skeletal muscle insulin-mediated glucose uptake, as evidenced by poor glucose responsiveness to exogenous insulin challenge (Figure 2C and C'). Together, these results show that elevations in CORT and HFD induce severe peripheral insulin resistance, reflected by direct and indirect effects on the liver, skeletal muscle, and β-cell function, which represents characteristics similar to those with Cushing's syndrome or with GC-induced diabetes (151, 170).

A HFD given to rodents has been shown to up-regulate islet mass due to an increase in compensatory β- and α-cell mass (49). However, prolonged elevation in FFAs results in β-cell death (340) and can cause the accumulation of ceramides that impair insulin processing (i.e., irregular folding of the insulin peptide) (180) and transcription

(185). However, we found no evidence that HFD and CORT caused increased β-cell death, at least in the short term (Figure 3, I–L), but that this treatment significantly increases islet areas through increased β- and α-cell mass (Figure 3, A–H). PCNA staining was significantly up-regulated in the CORT-treated animals, suggestive that proliferation was increased in response to the insulin resistance (Figure 3, M–P). However, despite the fact that there is clear evidence of islet adaptation to CORT-HFD treatment, these islets are still unable to maintain euglycemia, even in the fasted state.

Very few studies have examined the effects of HFD and/or short-term CORT treatment on glucagon secretion. Interestingly, fasting plasma glucagon increases after dexamethasone treatment in insulin-resistant first-degree relatives of patients with T2DM (170). We demonstrate here that circulating plasma glucagon levels are increased with CORT and HFD (Figure 5A), along with increases in α-cell mass (Figure 5, B and C), which likely further exacerbates hyperglycemia. We found that α-cell mass is up-regulated in CORT-HFD-treated rats primarily as a result of increased α-cell hypertrophy, as there was no change found in α-cell number, but the treatment induced increased α-cell size. Early stages of diabetes are associated with α-cell dysfunction as glucagon is secreted at abnormally high levels during an oral glucose challenge (171) and α-cell mass increases linearly with a rise in peripheral insulin resistance (172). Although the mechanisms for increased α-cell mass with CORT treatment are unknown, it may be an additional diabetogenic feature of the combination of exogenous CORT and HFD treatment.

There are several crucial elements involved in the insulin secretory system (341), such as PKC, which is an important regulatory enzyme involved in insulin secretion by activating the movement of β-cell insulin granules for exocytosis (342-345). GC administration in rats, results in an up-regulation of the PKC activation pathway, induced by increased Ca^{+2} release from intracellular stores, thereby leading to increased insulin secretion (2). Similar to previous findings by Rafacho et al (2), we demonstrate here that GCs in combination with a SD increases both total PKC expression and islet p-PKCα content (Figure 6). However, unique to our study, we show that the addition of HFD with CORT administration decreases islet p-PKCα content compared to CORT-SD animals. As previously described (346), chronic high glucose impairs normal PKC phosphorylation, thought to induce islet desensitization, thereby limiting insulin secretion. Furthermore, a study in the GK rat, which spontaneously develops impaired β–cell function, suggests impairments in PKC activation (347). Thus, we speculate that at least a part of the impaired insulin response in the AIR of CORT-HFD animals may result because of reduced PKC activation, partly due to sustained hyperglycemia, although it should be noted that PKC regulation is not the only potential mechanism involved in insulin secretion and therefore other key regulatory proteins may be at play.

Elevated tissue GC excess, driven by increased levels of the intracellular GC regenerating enzyme 11β-HSD1 in adipose tissue, liver, and skeletal muscle, is implicated in the development of insulin resistance (108). Elevated 11β-HSD1 activity and/or expression is also found in pancreatic islets of obese/diabetic rodents (173) as well as lean mice treated with GCs (155), but the functional consequence of this increase is

unclear. It is proposed that the increase in GC reactivation caused by elevated 11β-HSD1 activity suppress insulin secretion (173), thereby promoting diabetes development. Recently, however, the use of a β-cell specific 11β-HSD1 over expression model suggests that elevations in this pre-receptor enzyme actually improves insulin release mechanisms and protects against HFD-induced diabetes (175). In this study, we found that CORT treatment increases 11β-HSD1 protein content in islets, independent of diet (Figure 7). These results are supported by previous work, showing that islets cultivated in the inactive GC (11-dehydrocorticosterone) results in a rapid doubling in 11β-HSD1 protein (176) and provides further evidence that elevations in this enzyme may be a compensatory mechanism supporting insulin hypersecretion (155, 175).

Elevated fatty acid exposure (48 h) leads to the reduction of GSIS *in vitro* (348); however, *in vivo* GSIS reports are relatively inconsistent and may be due to variations on insulin sensitivity within individual islets (140) . Short-term CORT treatment has been shown to enhance insulin release *in vivo* (2) by up-regulating IRS-2 signaling pathway (154, 349) . We exposed isolated islets to low- (2.8 mM) and high-glucose (16.7 mM) concentrations and found that islets derived from CORT-HFD animals had greater GSIS compared to all other groups (Figure 8A). This may be explained, however, by the greater β-cell mass in the CORT-treated animals. Moreover, CORT-HFD islets that were subjected to high glucose exposure *ex vivo* demonstrated lower total insulin storage compared to all other groups (Figure 8B) and this was likely due to increased insulin secretion during the glucose challenge. In addition, it should be noted that although CORT-HFD islets have higher insulin secretion in high glucose media, their relative fold

increase over that observed in the low glucose media is less than that observed in SD groups (Figure 8A'). These findings on isolated islets suggest that, although CORT-HFD-treated animals are able to secrete high amounts of insulin in response to glucose *in vivo*, that *ex vivo* they do suggest some forms of islet desensitization to changes in glucose concentrations.

Conclusions

In summary, short-term exposure to CORT and a HFD play a synergistic role in the development of insulin resistance, β-cell mass compensation, and relative fasting hyperinsulinemia. However, *in vivo*, insulin responsiveness is blunted following oral glucose load in CORT-HFD treated animals despite the increase in β-cell mass. These disturbances are associated with increases in circulating glucagon levels and islet 11β-HSD1 protein expression. In contrast, *ex vivo*, islets derived from CORT-HFD animals exhibit an up-regulated absolute insulin response, although the fold change from low-glucose exposure is lower. Taken together, these results demonstrate that the combination of exogenous CORT treatment in conjunction with a HFD induces severe hyperinsulinemia/hyperglycemia as a result of whole-body insulin resistance, hyperglucagonemia, and an inappropriate responsiveness of β-cells to glucose challenge.

Table 1. Plasma corticosterone levels (ng/ml), adrenal gland mass (mg/BW) and pellet weights (mg) after 2 weeks of treatment.

	Placebo-SD		CORT-SD		Placebo-HFD		CORT-HFD	
Pellet Mass Loss[1]	N/A		76.42 ± 3.1		N/A		67.52 ± 3.9	
	AM	**PM**	**AM**	**PM**	**AM**	**PM**	**AM**	**PM**
Corticosterone	219±33	496±44**	637±54*	659±40*	208±44	606±53**	703±71*	784±43*
	Left	**Right**	**Left**	**Right**	**Left**	**Right**	**Left**	**Right**
Adrenal mass	0.09±0.005	0.09±0.004	0.04±0.007#	0.03±0.01#	0.1±0.01	0.1±0.012	0.04±0.003#	0.04±0.004#

[1]Value shown is the estimated amount of CORT dissolved over 2 weeks.

Note: * indicates statistical significance from placebo-SD (controls) during corresponding time points that corticosterone levels were measured ($p<0.05$). ** indicates statistical significance between AM and PM corresponding corticosterone levels within each treatment group ($p<0.05$). # indicates statistical significance of corresponding left and right adrenals from controls. BW=Body Weight. All values are mean ± SE.

Table 2. Animal body mass (g), average food consumption (kcal/g of BW)[1], epididymal fat pad mass (g/BW), pancreas (g/BW), fed blood glucose (mM), non-esterified fatty acids (NEFAs, mM) at day 0 and day 6 after pellet implantation in controls (placebo-SD), CORT-SD, placebo-HFD and CORT-HFD rats.

	Placebo-SD		CORT-SD		Placebo-HFD		CORT-HFD	
Day	**0**	**6**	**0**	**6**	**0**	**6**	**0**	**6**
Body Mass	314±4.12	362±4.18	316±4.55	270±7.65*,#	313±2.82	366±2.82	310±3.74	271±7.62*,#
Food Consumed[1]	N/A	0.42±0.0	N/A	0.52±0.03*	N/A	0.35±0.01*	N/A	0.46±0.02*,#
Epididymal fat pad mass	N/A	8.5±0.45	N/A	12.67±1.12*	N/A	13.96±1.76*	N/A	22.45±1.76*,$,#
Pancreas mass	N/A	3.15±0.37	N/A	4.15±0.45	N/A	3.27±0.34	N/A	3.59±0.55
Fed blood glucose	5.7±0.6	5.6±0.5	5.9±0.2	15.7±2.6*,#	5.8±0.3	6.0±0.1	5.8±0.2	19.2±1.7*,#
NEFA levels	N/A	0.84±0.19	N/A	2.07±0.21*	N/A	1.45±0.35*	N/A	3.33±0.25*,S,#

Note: The * indicates significance from placebo-SD (controls) on the same day ($p<0.05$). The $ indicates significance between CORT-SD and CORT-HFD. The # indicates significance from placebo-HFD. BW=Body Weight. [1]Average food consumption measurements were taken every two days and the data represented in the table is that of a 24 hour period. All values are mean ± SE.

Figure Captions

Fig. 1. Blood glucose levels (mM) (A) and plasma insulin levels (ng/mL) (B) after an oral glucose gavage. Glucose AUC (A=) and insulin AUC (B=) during an OGTT expressed in arbitrary units. N=7–10 for each group. AIR between basal and 15 minutes relative to placebo-SD (C) and fasting insulin (ng/ml) vs fasting blood glucose (mM) were analyzed by linear regression (r2=0.42) (D). N= 5–7 for each group. In all bar graphs, bars that do not share the same letters are statistically significant from each other ($P<0.05$; a t test was used to measure significance between placebo-SD and CORT-HFD in C). All values are means ± SE.

Fig. 2. Measurements of insulin resistance, β-cell function, and insulin sensitivity. HOMA-IR index indicates whole-body insulin resistance (A) and HOMA-β index indicates β-cell function (D). Insulin sensitivity during an ip administered insulin tolerance test. Glucose (mM) levels after insulin injection (C) and glucose AUC (C=). N=9–10 for each group. In all graphs, bars that do not share the same letters are statistically significant from each other ($P<0.05$). All values are means ± SE. Note that the closed triangles in C are obscured by the closed squares.

Fig. 3. Images of islet morphology indicating insulin (A–D), glucagon (E–H), TUNEL (I–L), and PCNA (M–P) positive staining. Arrows indicate apoptotic cells that are TUNEL positive. All images are 20 x magnification.

Fig. 4. Insulin-positive staining indicates β-cell mass (A), number of islets per pancreas area (mm^2) (B), islet area (μm^2) (C), number of β-cells per islet (D), percentage of islets per size grouping (μm^2) (E), and β-cell size (μm^2) (F). N= 6–7 per group. In all graphs, bars that do not share the same letters are statistically significant from each other (graph A–C and E, $P<0.05$, graph D and F, $P<0.001$). *, statistical significance where $P<0.05$. #, statistical significance where $P<0.001$ (E). All values are means ± SE.

Fig. 5. Fed plasma glucagon levels (A). Glucagon-positive staining indicates α-cell mass (B), α-cell size (μm^2) (C). N=6 per group. In all graphs, bars that do not share the same letters are statistically significant from each other ($P<0.05$, graph A, $P<0.001$). All values are means ± SE.

Fig. 6. Relative total PKCα content in isolated islets (A). Relative p-PKCα content in isolated islets (B). N=4–5 per group. All protein content was normalized to β-actin content. In all graphs, bars that do not share the same letters are statistically significant from each other ($P<0.05$). All values are means ± SE.

Fig. 7. Relative 11β-HSD1 protein content in isolated islets. All protein content was normalized to β-actin content. N=4–6 per group. Bars that do not share the same letters are statistically significant from each other ($P<0.05$). All values are means ± SE.

Fig. 8. Isolated islet GSIS, in 2.8 and 16.7 mM glucose (ng/mL/islet/h) (A). Fold change in insulin secretion from 2.8 mM (A'). Total insulin content (ng/ml) corrected by number of islets from each treatment group (B). N=5–6 per group. In all graphs, bars that do not share the same letters are statistically significant from each other ($P<0.05$). All values are means ± SE.

Fig.1.

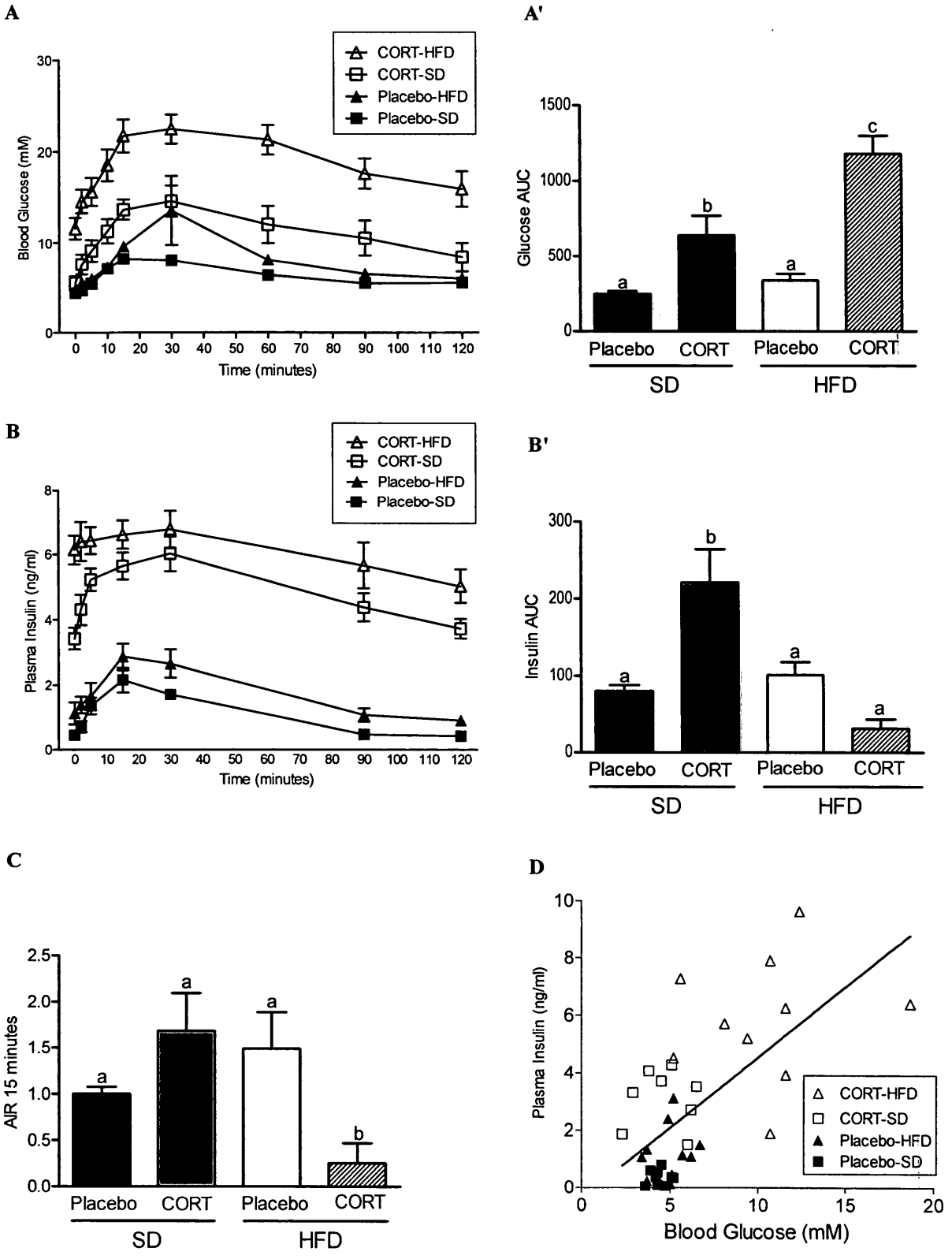
A
CORT-HFD
CORT-SD
Placebo-HFD
Placebo-SD
Blood Glucose (mM)
Time (minutes)
A'
Glucose AUC
Placebo
CORT
Placebo
CORT
SD
HFD
B
Plasma Insulin (ng/ml)
Time (minutes)
B'
Insulin AUC
C
AIR 15 minutes
D
Plasma Insulin (ng/ml)
Blood Glucose (mM)

Fig.2.

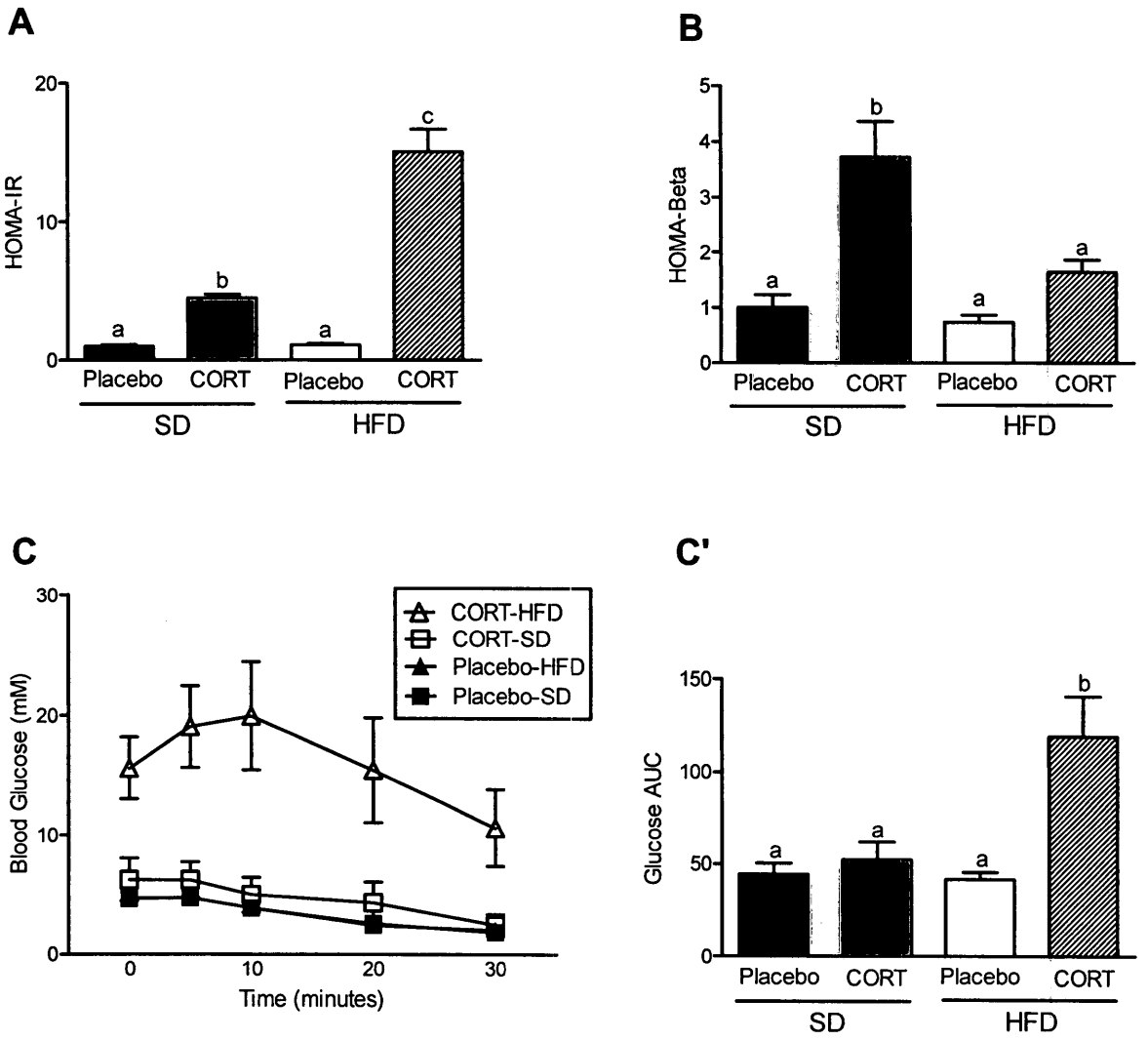
A
HOMA-IR
20
10
0
a
b
a
c
Placebo
CORT
Placebo
CORT
SD
HFD
B
HOMA-Beta
5
4
3
2
1
0
a
b
a
a
Placebo
CORT
Placebo
CORT
SD
HFD
C
Blood Glucose (mM)
30
20
10
0
CORT-HFD
CORT-SD
Placebo-HFD
Placebo-SD
0
10
20
30
Time (minutes)
C'
Glucose AUC
150
100
50
0
a
a
a
b
Placebo
CORT
Placebo
CORT
SD
HFD

Fig.3.

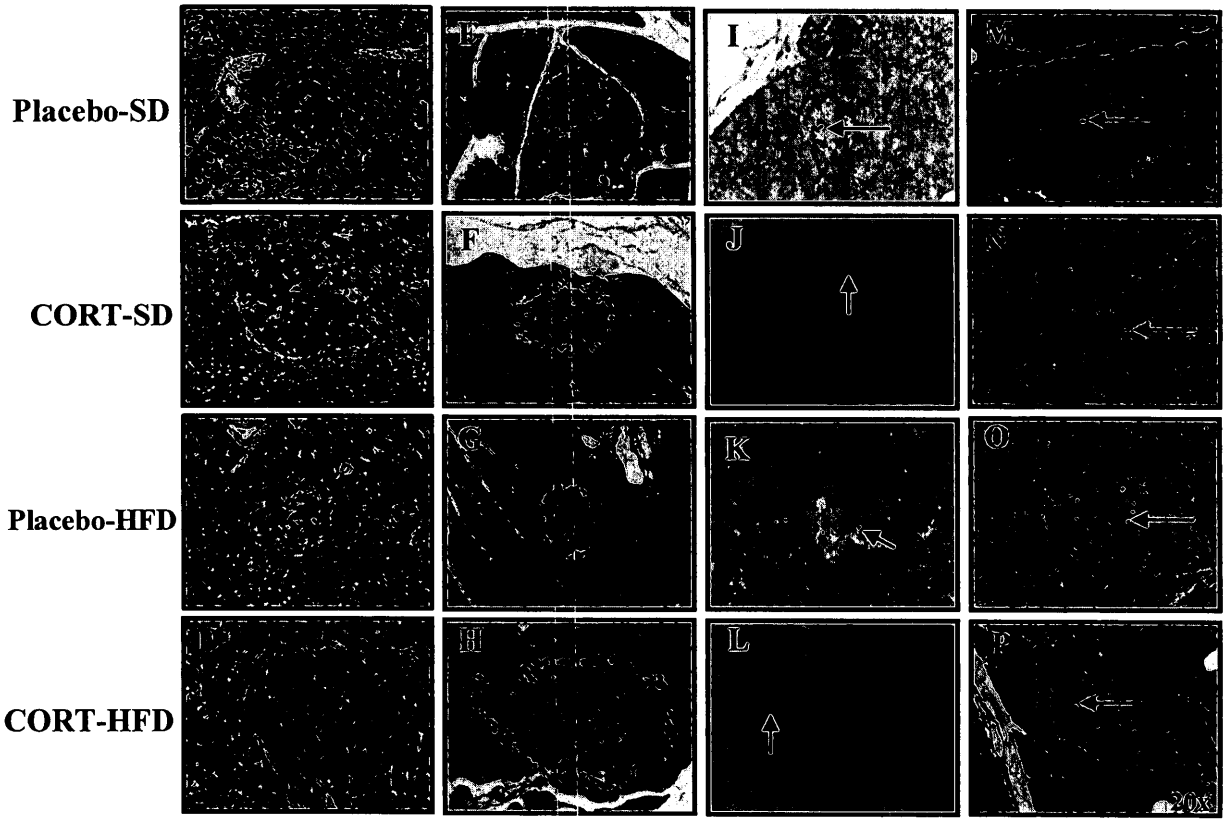
Insulin
Glucagon
TUNEL
PCNA
Placebo-SD
CORT-SD
Placebo-HFD
CORT-HFD
E
I
M
F
J
N
G
K
O
H
L
P
20x

Fig.4.

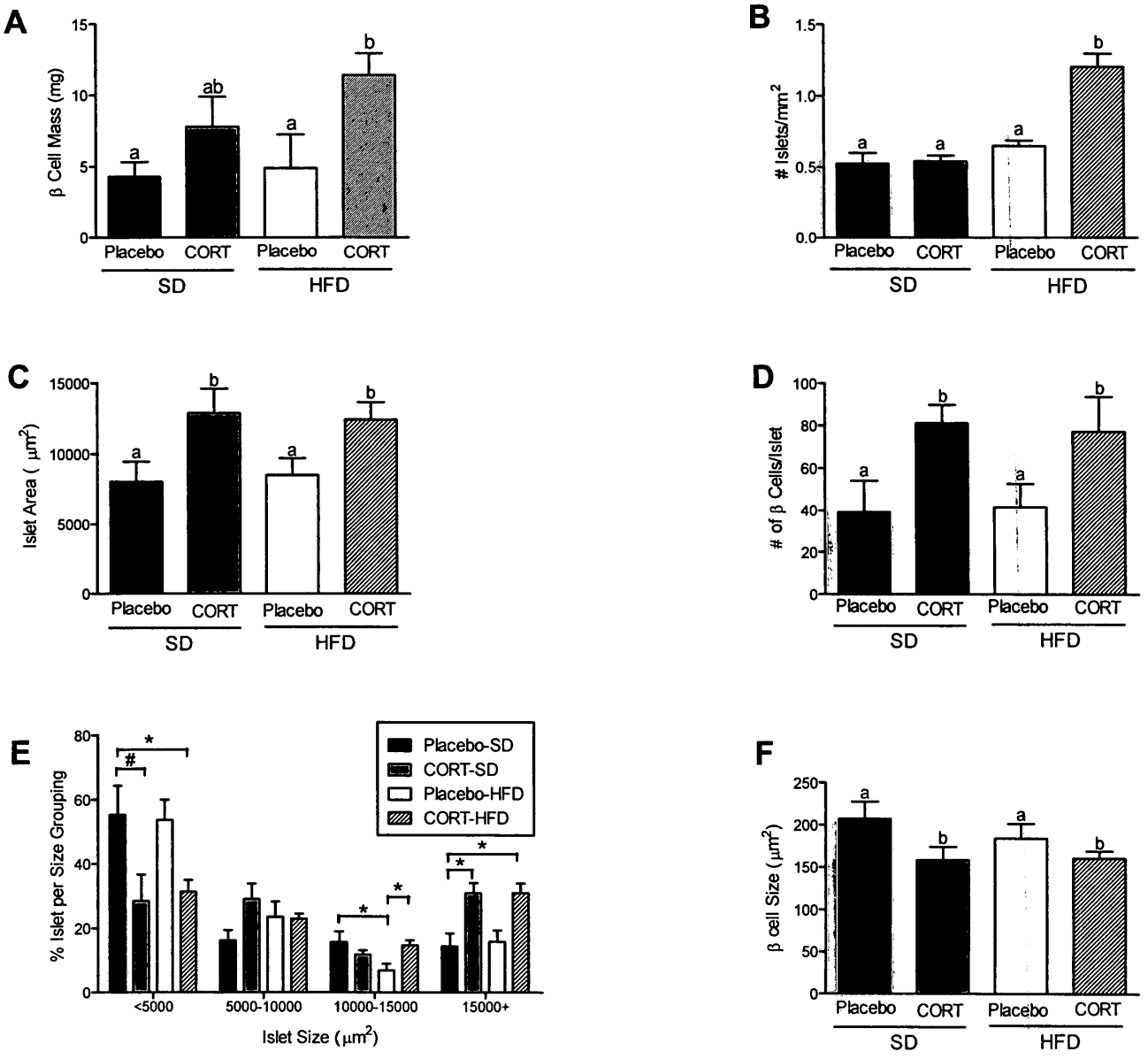
A
β Cell Mass (mg)
15
10
5
0
a
ab
a
b
Placebo
CORT
Placebo
CORT
SD
HFD
B
Islets/mm2
1.5
1.0
0.5
0.0
a
a
a
b
Placebo
CORT
Placebo
CORT
SD
HFD
C
Islet Area (μm2)
15000
10000
5000
0
a
b
a
b
Placebo
CORT
Placebo
CORT
SD
HFD
D
# of β Cells/Islet
100
80
60
40
20
0
a
b
a
b
Placebo
CORT
Placebo
CORT
SD
HFD
E
% Islet per Size Grouping
80
60
40
20
0
*
#
*
*
*
*
*
Placebo-SD
CORT-SD
Placebo-HFD
CORT-HFD
<5000
5000-10000
10000-15000
15000+
Islet Size (μm2)
F
β cell Size (μm2)
250
200
150
100
50
0
a
b
a
b
Placebo
CORT
Placebo
CORT
SD
HFD

Fig.5.

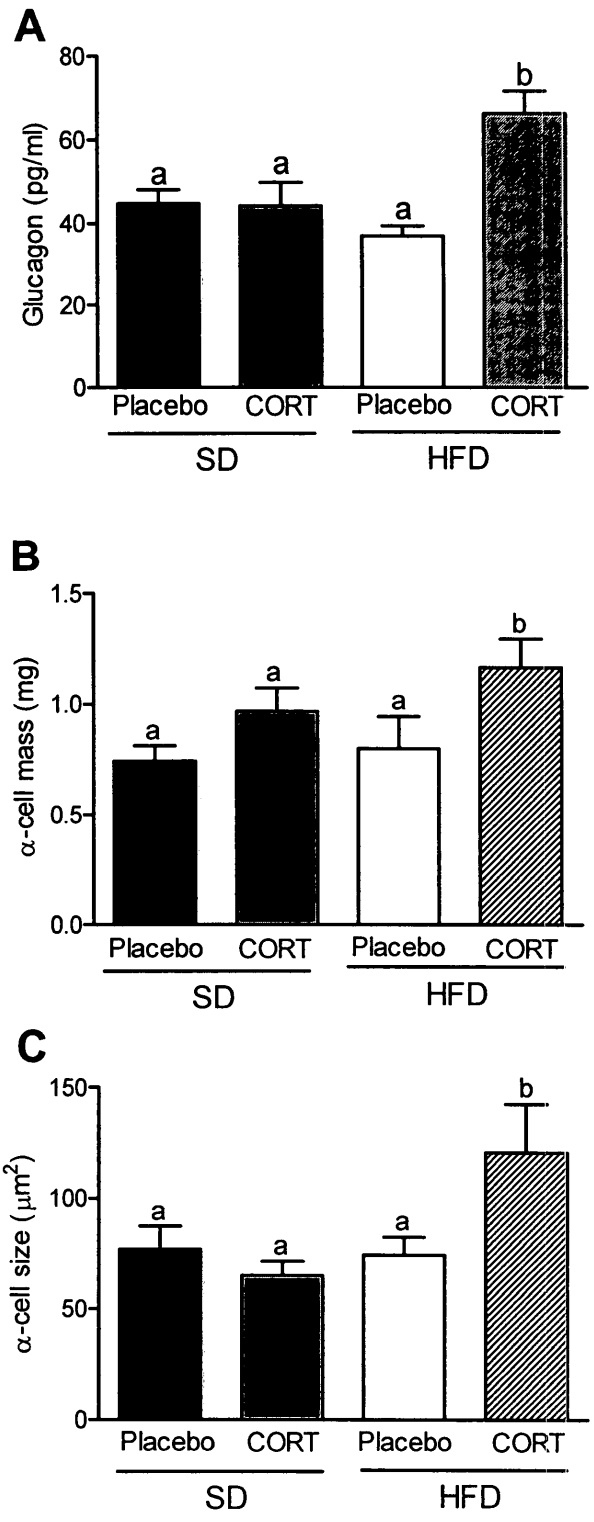
A
Glucagon (pg/ml)
80
60
40
20
0
a
a
a
b
Placebo
CORT
Placebo
CORT
SD
HFD
B
α-cell mass (mg)
1.5
1.0
0.5
0.0
a
a
a
b
Placebo
CORT
Placebo
CORT
SD
HFD
C
α-cell size (μm²)
150
100
50
0
a
a
a
b
Placebo
CORT
Placebo
CORT
SD
HFD

Fig.6.

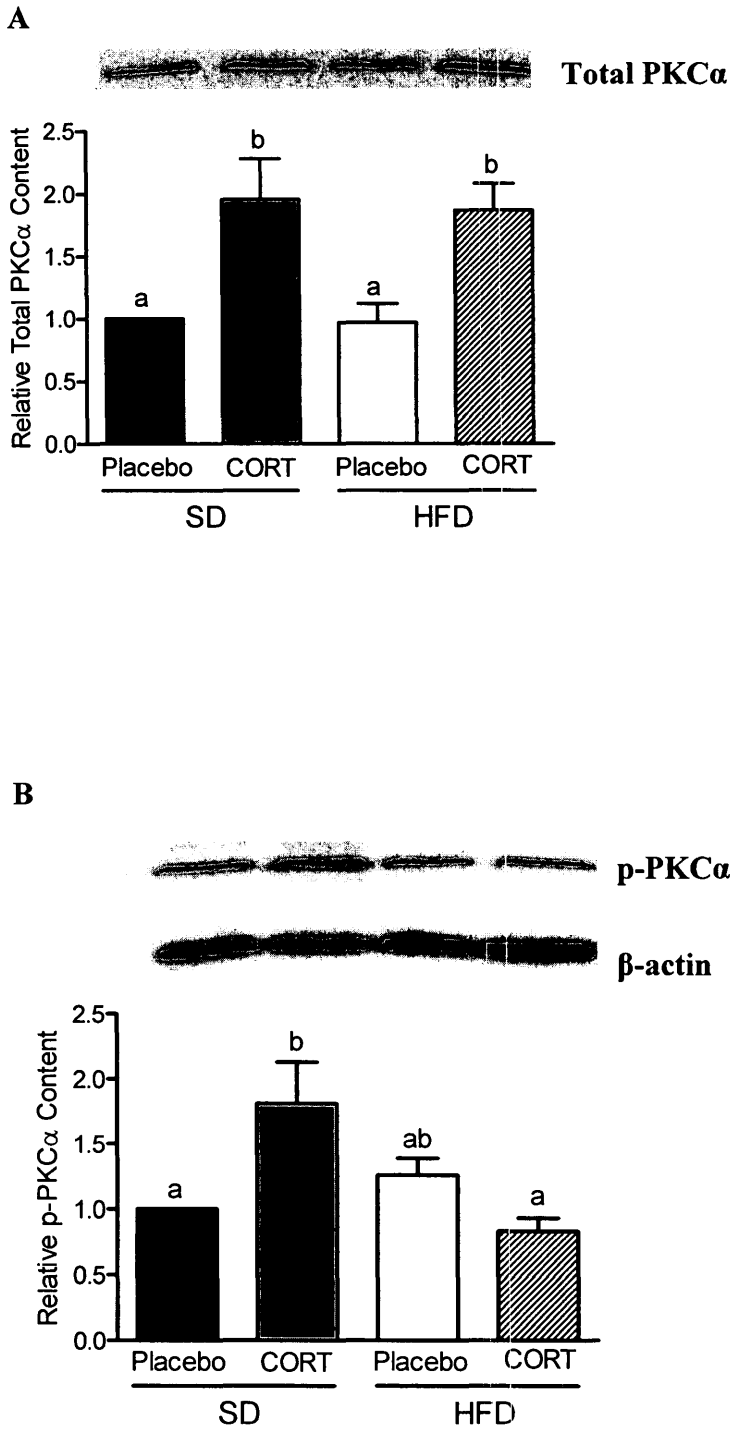
A
Total PKCα
Relative Total PKCα Content
2.5
2.0
1.5
1.0
0.5
0.0
a
b
a
b
Placebo
CORT
Placebo
CORT
SD
HFD
B
p-PKCα
β-actin
Relative p-PKCα Content
2.5
2.0
1.5
1.0
0.5
0.0
a
b
ab
a
Placebo
CORT
Placebo
CORT
SD
HFD

Fig. 7.

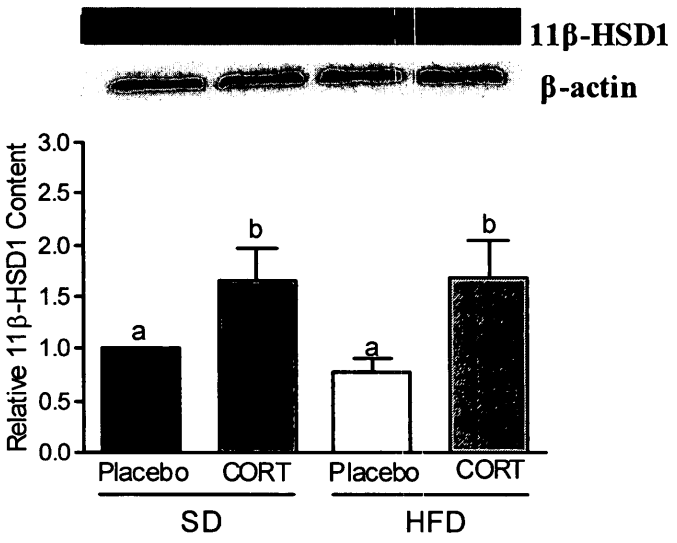
11β-HSD1
β-actin
Relative 11β-HSD1 Content
3.0
2.5
2.0
1.5
1.0
0.5
0.0
a
b
a
b
Placebo
CORT
Placebo
CORT
SD
HFD

Fig. 8.

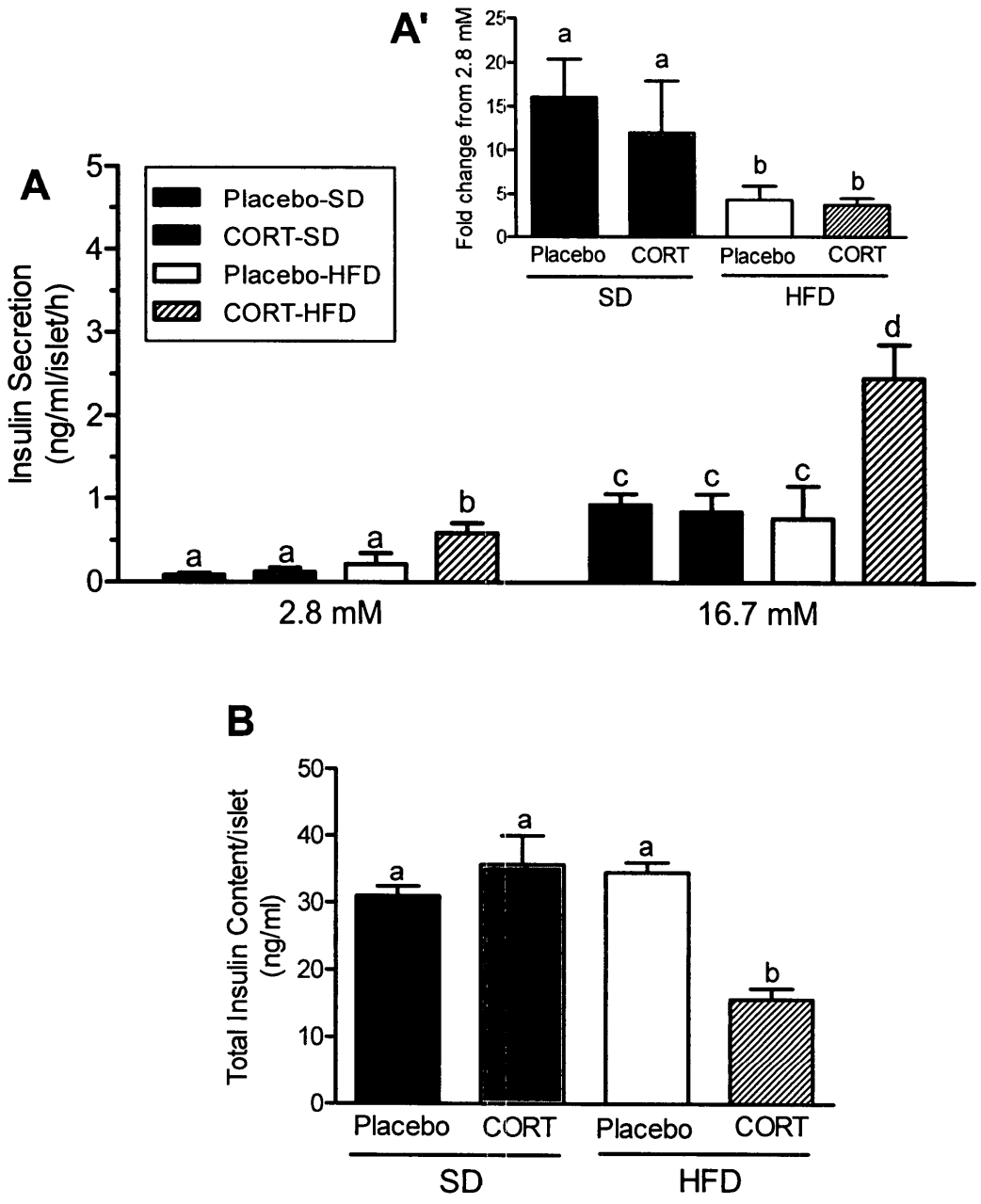
A
A'
B
Placebo-SD
CORT-SD
Placebo-HFD
CORT-HFD
Insulin Secretion (ng/ml/islet/h)
Fold change from 2.8 mM
Total Insulin Content/islet (ng/ml)
2.8 mM
16.7 mM
Placebo
CORT
SD
HFD

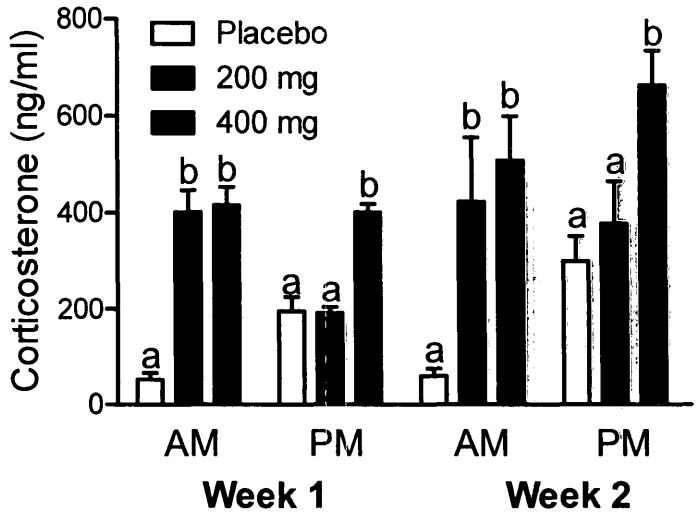

Figure1. Supplemental figure for manuscript #1 demonstrating diurnal corticosterone levels in rats treated with wax (placebo) or corticosterone (200 or 400 mg) pellet implants for a 14 day period (pilot data). Plasma corticosterone concentrations were measured at peak (8 PM) and trough (8 AM) in placebo-treated (wax), and in 200 mg corticosterone-treated or 400 mg corticosterone-treated rats. 400 mg of corticosterone presented sustained abolishment of diurnal corticosterone pattern compared to 200 mg of corticosterone treatment. Therefore, this amount of corticosterone was selected as a means of ROD development. N=3 for each group. Values are means ± SE.

MANUSCRIPT-#3 Chapter 4

Regular Exercise and Rapid-onset Diabetes Development in the Sprague-Dawley Rat

Rationale for Manuscript #3

Both manuscript #1 and #2 highlighted the detrimental effects of elevated GCs concomitantly with HFD on whole-body physiology and islet adaptive capacity. Previously our laboratory has demonstrated that long-term regular exercise via voluntary wheel running restores alterations in HPA activation (220). Regular exercise has long been known to improve glucose tolerance and islet glucose sensitivity in healthy humans. Moreover, exercise has been shown to improve hyperglycemia/hyperinsulinemia and β-cell dysfunction in ZDF rats by lowering hypercortisolemia (63, 144, 150). Regular exercise can reverse T2DM-like symptoms (255), however little is known about the effect of voluntary exercise on chronically elevated GCs concurrently with high-fat feeding. To date, there are very few studies investigating the effect of exercise and GC-induced T2DM. One study suggests that 8 weeks of exercise training via treadmill running attenuated dexamethasone-induced hyperglycemia, insulin resistance and muscular glycogen depletion (263). Therefore, our goal for manuscript #3 was to study the effects of volitional exercise on GC and HFD-induced diabetes. We hypothesized that voluntary wheel running (4 weeks) would improve glucose intolerance, whole-body insulin resistance, impaired islet glucose responsiveness in our model of ROD.

Author Contributions

Conceived and designed the experiments: J.L.B., E.C.D. and M.C.R. Performed the experiments: J.L.B., E.C.D. and A.J.P. Analyzed the data: J.L.B., E.C.D., A.J.P. and M.C.R. Wrote the paper: J.L.B. Edited the manuscript: E.C.D. and M.C.R.

J.L.B. performed all animal surgeries, recording of running distances, food intake, animal mass, oral glucose tolerance test, insulin tolerance test, plasma analyses of glucose, insulin, corticosterone, NEFAs, quantification of HOMA-IR and beta, pancreatic islet isolations, acute ex vivo experiments with isolated islets and all statistical analyses data for this manuscript.

J.L.B prepared and designed Table 1 and 2 and Figure 1, 2, 4, 5, 6 and 7.

Acknowledgements

We thank Dessi Zaharieva for helping with preliminary data collection and experimental design for this project and Trevor Teich for helping to edit the manuscript.

This manuscript will be submitted to the *Journal of Applied Physiology*.

Voluntary Wheel Running Attenuates Hyperglycemia, Visceral Adiposity and Impaired Islet Responsiveness Induced by Exogenous Glucocorticoids and a High-fat Diet

Running title: Exercise improves glycemia and islet sensitivity induced by glucocorticoids and high-fat diet

Jacqueline L. Beaudry[1]
Emily C. Dunford[1]
Ashley J. Peckett[1]
Michael C. Riddell[*1]

[1]School of Kinesiology and Health Science, Faculty of Health, Muscle Health Research Center and Physical Activity and Chronic Disease Unit, York University, 4700 Keele St., Toronto, ON, Canada, M3J 1P3
[*]Author for correspondence

Please address correspondence to Dr. Michael C. Riddell,
School of Kinesiology and Health Science, Faculty of Health, Muscle Health Research Center and Physical Activity and Chronic Disease Unit, York University 4700 Keele Street,
Toronto, ON, Canada, M3J 1P3
Telephone: (416) 736-2100 ext. 40493
Fax: 416-736-5774
Email: mriddell@yorku.ca

Key Words: Glucocorticoids, type 2 diabetes mellitus, high-fat diet, voluntary wheel running, glucose intolerance, insulin sensitivity, visceral obesity, insulin secretion

Abstract

We have established a rapid-onset diabetic rodent model, induced by elevations in the stress hormone corticosterone (CORT) and a high-fat diet (HFD). Together, these treatments induce severe impaired insulin action and islet glucose responsiveness. Regular exercise alleviates insulin insensitivity and restores β-cell function. We examined the effect of voluntary exercise (EX) on diabetes development in CORT and HFD treated male Sprague-Dawley rats (~ 6 weeks old). Animals were acclimatized to running wheels for 2 weeks, then given either wax (placebo) or CORT pellets, a HFD and split into 4 groups; placebo-SED or -EX and CORT-SED or -EX. After an additional 2 weeks of running combined with treatment, CORT-EX animals had reduced visceral adiposity, improved muscle composition and oxidative capacity compared to CORT-SED animals ($p<0.05$). CORT-EX animals had improved fasting glucose (14.3±1.6 vs. 18.8±0.9 mM) and acute insulin response to glucose challenge (~ 2-fold) compared to CORT-SED animals ($p<0.05$). CORT-EX animals had improved β-cell function (~ 2.5-fold) and peripheral insulin sensitivity compared to CORT-SED animals ($p<0.05$). Glucose challenge administered to islets *ex vivo* showed that CORT-EX islets lower insulin secretion to levels almost comparable to placebo-SED islets. We conclude that EX improves overall body composition (but not body mass) and metabolic profile of animals administered CORT and HFD by reducing glucose intolerance, insulin insensitivity, impaired islet responsiveness and improving muscle oxidative capacity. These results suggest that the detrimental effects of elevations in GCs and circulating fatty acids may be lessened with regular exercise, even in situations of hypercortisolemia.

Introduction

The stress response triggers the hypothalamic-pituitary-adrenal (HPA) axis resulting in the downstream secretion of glucocorticoids (GCs). This signal helps to mobilize fuel substrates needed to meet the metabolic demands of the body. In the short-term, activation of GCs is ideal in situations of physical activity however, prolonged stimulation of the HPA axis can present major physiological consequences to the body. Chronic elevation in GCs, as seen in patients with Cushing's syndrome, can induce many metabolic disturbances such as increased visceral adiposity (110), peripheral insulin resistance (135), non-alcoholic fatty liver disease (339), and impaired islet function (350), all of which are major risk factors that augment the possibility of the development of type 2 diabetes (T2DM) (145). Rodent (63, 144) and human (145, 351, 352) studies of T2DM also demonstrate elevated HPA axis activity suggesting links between raised GC concentrations and disease progression.

Rodent models of T2DM such as the ZDF rat, which spontaneously develops hyperglycemia/hyperinsulinemia at ~ 12 weeks of age, help to study links between HPA axis activity and diabetes development. Our previous research shows that elevations in HPA axis activity precedes symptoms of diabetes, as ZDF rats develop hypercortisolemia at ~ 3 weeks into the experimental protocol (63, 144) while hyperglycemia and glucose intolerance is not evident ~ week 7. These ZDF model studies provide strong evidence that there is an association with the initial elevation of GCs and the onset of diabetes.

It is important to note that not all activators of HPA axis can promote adverse metabolic effects. Physical activity, by definition, is considered a physiological 'stressor'

that can disrupt the homeostatic balance of energy dynamics within the body (353). If exercise is not performed regularly, physical inactivity can be a major contributor to the development of many cardio-metabolic diseases, especially T2DM (28, 247-249, 354). Endurance exercise is an excellent stimulator of the HPA axis in rodents (197, 219, 220, 355) and in humans (64, 356, 357) and this subsequent GC secretion is relatable to exercise intensity (358). However, volitional exercise such as wheel running in healthy rodents does not continually increase HPA activity as GCs return to basal levels just weeks after initiation (200, 220, 355). In addition, lower GCs are found in ZDF rats within 5 weeks of non-volitional swimming exercise (63, 144, 213) and as early as 3 weeks with voluntary wheel running (63, 150) compared to inactive controls. These studies in ZDF rats and exercise also show many positive effects on diabetes prevention that demonstrate how exercise can restore glycemic control, preserve β-cell mass (144), improve β-cell dysfunction and increase islet insulin stores (150). Although exercise in its various forms can reverse T2DM-like symptoms in part by lowering circulating GCs, little is known about the effect of voluntary exercise on a model of chronically elevated GCs, such as Cushing's syndrome. In fact, there are no studies to date specifically investigating any type of exercise and Cushing's syndrome. These studies are imperative as it is unclear whether exercise improves insulin sensitivity and glucose homeostasis by lowering circulating GCs as is seen with volitional or non-volitional exercise in ZDF rats. Or rather if exercise works independently of circulating GCs to improve muscle insulin action and pancreatic islet function.

Recently, our laboratory has developed an animal model of rapid-onset diabetes induced through elevated levels of corticosterone, (CORT, active GC in rodents) and a high fat diet (60% calories from fat) (HFD) (328, 350). We have established that elevations in CORT and a HFD result in severe hyperglycemia and hyperglucagonemia, despite hyperinsulinemia and increased β-cell mass, largely due to extreme whole-body insulin insensitivity and impaired islet glucose responsiveness. Voluntary exercise is known to normalize glucose tolerance and islet glucose sensitivity (15) through up-regulated mechanisms of skeletal muscle glucose uptake, i.e. GLUT4 translocation (28, 151, 359), oxidative capacity (360) and pancreatic islet function (150). Therefore, we hypothesize that voluntary exercise will alleviate hyperglycemia, insulin resistance and preserve β-cell function in our model of elevated GCs and HFD. The aim of our study is to investigate the role of volitional exercise on 1) whole-body glucose homeostasis, 2) islet responsiveness and glucose sensitivity, 3) adaptive peripheral tissue function, i.e. islet insulin secretion and skeletal muscle oxidative capacity, in our model of elevated levels of CORT and HFD.

Methods

Animals: Approximately 40 male Sprague-Dawley rats (Charles River Laboratories, initial mass of 225-250 g, six weeks post-weaned) were individually housed (lights on 12 h: lights off 12 h cycle) after one week of acclimatization to room temperature (22-23°C) and humidity (50-60%) controlled facilities. Animals were divided into four experimental groups that consisted of two sets of sedentary (SED) and two sets of exercise-trained (EX) animals.

Experimental Design: After the acclimation period each exercising animal was placed into a standard rodent cage and given 24 h access to a standard running wheel (Harvard Apparatus). Each wheel was equipped with a magnet and sensor that was wired to an electronic counter. Wheel revolutions were counted each time the magnet passed the sensor and the numbers on the counters were recorded and reset to zero daily. The wheel revolutions were multiplied by the wheel circumference (106 cm) to accurately calculate the running distance of each animal (previously reported in (220)). SED animals were housed in similarly sized cages as EX animals but without access to a running wheel. During the two weeks of wheel introduction, animals were given standard rodent chow (Purina) and water *ad libitum*.

Pellet Surgeries: Upon surgery day (day 14), each rat received a subcutaneous implantation of either corticosterone (CORT) pellets (4 x 100 mg; Sigma, Burlington, Ontario, Canada, Cat# C2505) or wax (placebo) pellets, as previously described (328). Immediately following surgery all rats were placed into sterile cages without running wheels for 24 h to recover and were given *ad libitum* access to a high-fat diet (HFD). This diet consisted of 60% of the total calories from fat and 5.1 kcal per gram (D12492, Research diets); this diet was maintained to the end of the experimental protocol and all animals received the same diet. The final four experimental groups consisted of two sets of EX animals; one group received wax pellets (placebo-EX) and the other group received CORT pellets (CORT-EX) and two sets of SED animals; one group received wax pellets (placebo-SED) and the other group received CORT pellets (CORT-SED). This study was carried out in accordance with the recommendations of the Canadian

Council for Animal Care guidelines and was approved by the York University Animal Care Committee.

CORT sampling: On day 21 at approximately 0800 h blood samples were collected from each animal via saphenous vein for CORT concentration measurements. A small area of hair on the lateral upper hindlimb was removed with an electric razor and wiped with a thin layer of petroleum jelly. Once the saphenous vein was located, a sterile 25-gauge needle was used to puncture the vein and whole blood was collected in lithium-heparin coated microvette capillary tubes (Sarstedt, Montreal, Québec, Canada, Cat# 16.443.100) and centrifuged at 12,000 rpm for 5 minutes, transferred into polyethylene tubes and stored at -80°C until further analysis of CORT concentrations using a radioimmunoassay kit (MP Biomedical, Solon, OH, USA). Fed blood glucose concentrations (mM) were measured on day 21 using a single drop of blood (2 µl) with a handheld glucometer (Bayer Contour, Rochester, NY, USA), after blood was collected for CORT measurements. This sampling was repeated on day 28 so that CORT concentrations could be assessed two weeks after pellets were implanted.

Oral glucose and intraperitoneal insulin tolerance test: As previously described in (328) animals were fasted overnight (16 h) and were administered an oral glucose tolerance test (OGTT, 1.5 g/kg body mass) on day 26. Each animal's basal blood glucose (fasting, time 0) was measured via saphenous vein using a glucometer and collected for later analysis of plasma insulin concentrations via ELISA 96-well kit (Crystal Chem, Downers Grove, IL, USA, Cat# 90060). Blood glucose was also measured and recorded for time 5, 15, 30, 60, 90 and 120 minutes post oral gavage. Blood was collected to

measure plasma insulin for time 15, 30, 60 and 120 minutes post oral gavage. An insulin tolerance test (ITT) was performed on day 30 after an overnight fast by intraperitoneal insulin injection, (previously reported in (328)). For these tests, blood glucose concentrations were measured with a glucometer at time 0, 5, 10, 20 and 30 minutes post insulin injection. Non-esterified fatty acids (NEFAs) concentrations were measured from fasted plasma collections (NEFA kit, HR Series NEFA-HR, Wako Chemicals, Richmond, VA, USA). Glucose and insulin area under the curve (AUC) was measured relative to the lowest fasting glucose and insulin levels of a placebo-SED animal. The acute insulin response (AIR) was determined between the difference in basal plasma insulin (fasting insulin levels) and 15 minutes following the oral glucose gavage (previously reported in (191, 350). This measurement represents the secretion of insulin in response to an exogenous glucose load. Homeostatic Model Assessment for β-cells (HOMA-β) as previously reported in (328, 350) was calculated based on the following equation: 20 x Insulin (μ units·L)/Glucose (mM)-3.5 (361).

Glucose stimulated insulin secretion (GSIS) experiments: All animals were killed by decapitation on days 31-35 of the experimental protocol and islet isolations were carried out as previously reported methods (350) that were originally modified from (330, 331). Collagenase pancreas digestion was followed by Histopaque-1077 (H8889, Sigma, Canada) pellet suspension followed by re-suspension in KREB's buffer (125 mM NaCl, 4.7 mM KCl, 1.2 mM, 5 mM $NaHCO_3$, 2.5 mM $CaCl_2$, 2.4 mM $MgSO_4$, 10 mM Hepes, 0.5% BSA, pH-7.4). Islets were hand selected and cultured in filtered RPMI buffer (Wisent) overnight (24 h) at 37°C, 5% CO_2. Islets were separated into a 12-well culture

plate (6-10 islets/well in 3 batches) and given a 30 minute pre-incubation period as previously described (350) . Islets were given fresh KREB's buffer with 2.8 mM glucose + 0.1% BSA for 1 hour at 37°C, 5% CO_2. Media was changed to KREB's buffer with 16.7 mM glucose + 0.1% BSA for 1 hour at 37°C, 5% CO_2. Immediately following each incubation period, media was collected, centrifuged and stored at -20°C for further analysis. At the termination of experiments, islets were placed in 1 ml cold lysis buffer (acid-ethanol solution), sonicated (15 s), and centrifuged at 14, 500 rpm at 4 °C for 10 minutes. Supernatant was collected and stored at -20°C until further analysis of insulin content. All insulin secretion data was normalized to total insulin content. Insulin was measured using radioimmunoassay kit (Millipore, Billerica, MA, USA).

Histology: Liver and skeletal muscle tissue from euthanized animals were frozen in liquid nitrogen, cryosectioned (10 μm thick) and stained with Oil Red O (ORO) for neutral lipid content as previously described (299). Liver sections were fixed with 3.7% formaldehyde for 1 h at room temperature while an ORO solution composed of 0.5 g ORO powder (Sigma-Aldrich, Canada) and 100ml of 60% triethyl phosphate (Sigma-Aldrich, Canada) was mixed and filtered. Following fixation in 3.7% formaldehyde, slides were immersed in filtered ORO solution for 30 minutes at room temperature. Slides immediately underwent five washes with ddH2O, were allowed to dry for 10 minutes and were sealed with Permount (Sigma-Aldrich, Canada). Liver images were acquired at 20 x magnification using a Nikon Eclipse 90i microscope (Nikon, Canada) and Q-imaging MicroPublisher 3.3 RTV camera with Q-capture Software. To identify skeletal muscle fiber type a metachromatic myosin ATPase stain was performed on cross

sections of the tibialis anterior muscle using a modified protocol (362) . Sections were pre-incubated in an acidic buffer (pH = 4.25) to differentially inhibit myosin ATPases within the different fiber types. In this protocol, type I fibers appear dark blue, type IIa appear very light blue and type IIb and IIx are not apparent from each other and are thus classified as IIb/x. These fibers appear bluish-purple. A representative image of the tibialis anterior for each group was acquired for analysis. Succinate dehydrogenase (SDH) activity was then assessed using histochemical analysis and expressed in relative optical density to placebo-SED (47). The same muscle regions of the tibialis anterior that were used for fiber typing were used for SDH activity determination. Serial sections were used to directly compare levels of SDH in each fiber, to each fiber type. SDH activity was assessed with Adobe Photoshop CS6, converted to greyscale and reported as the average optical density (60 fibers were counted per muscle section). The greyscale is evaluated on a range of completely black (0) to white (255). All images were acquired with a Nikon Eclipse 90i microscope and Q-Imaging MicroPublisher with Q-Capture software.

Statistical Analysis: All data are represented as means ± SE, with a criterion of $p<0.05$ and $p<0.001$ and were assessed using two-way ANOVAs as a means of statistical significance. Individual differences were calculated using Tukey's post-hoc test unless stated in figure captions as using Duncan's post-hoc test (Statistica 6.0 software). Bars that do not share the same letters are statistical significance from one another.

Results

Body mass. All animals had similar body mass prior to pellet surgery (day 14, ~ 350 g). Both placebo-treated groups gained mass after pellet surgery from day 14 to 24 (Fig. 2A). However, on experimental termination day (day 31-35) placebo-SED animals tended to weigh more than placebo-EX animals (472.7±14.4 vs. 438.7±31.5 g). Similar to previously reported findings, CORT groups lost body mass after pellet surgery compared to placebo animals (328, 339, 350) ($p<0.01$, Fig. 2A). No differences were found in relative body mass between CORT-EX and -SED animals on day 24; however, CORT-EX animals had heavier absolute body mass than CORT-SED animals at the termination of treatment (333.5±16.2 vs. 265.9±13.0 g, $p<0.05$).

Running Distances. On average CORT-treated runners ran longer distances than placebo runners (6541.7±467 vs. 3308.4±260 m, $p<0.05$, Fig. 2B). No differences were found between running distances prior to pellet surgeries and after 10 days of treatment (day 14 vs. day 24) within either placebo or CORT-treated groups ($p>0.05$). Running distances on each treatment day were plotted relative to running distances prior to surgery and no differences were found in either placebo or CORT-treated groups (Fig. 2C). This indicates that running distances prior to pellet surgery were not altered by pellet treatment, suggesting neither treatment had a significant effect on the animals' ability or desire to run, regardless of the individual being a short distance runner or a long distance runner.

Food intake and body composition. Relative food intake tended to be slightly higher in placebo-EX animals than placebo-SED although no significant differences were found ($p>0.05$, Table 1). Also no differences in relative food intake were found between CORT-SED and -EX animals but there was a main effect of pellet treatment across groups as CORT-treated animals had higher relative food intake than placebo-treated animals ($p<0.05$). Visceral adiposity as measured by relative epididymal fat depots was lower in CORT-EX compared to CORT-SED group ($p<0.05$, Table 1). There were no differences found between placebo-SED and -EX groups in visceral adiposity. Relative liver mass was up-regulated with CORT treatment compared to placebo-treated animals ($p<0.05$) but no differences were found with the addition of exercise in placebo or CORT-treated animals (Table 1). Relative gastrocnemius mass was lower with CORT-SED treatment compared to placebo-treated animals ($p<0.05$) and tended to be higher with CORT-EX treatment. No differences were found with relative tibialis anterior mass between any treatment groups. Relative soleus mass, a measurement of red oxidative muscle mass was higher in CORT-SED animals compared to CORT-EX animals and placebo-SED animals ($p<0.05$, Table 1). Relative epitrochlearis mass, a measurement of white glycolytic muscle mass was significantly lower in CORT-SED animals compared to placebo-SED animals. The exercise intervention greatly increased relative epitrochlearis mass in CORT-EX animals compared to CORT-SED animals ($p<0.01$, Table 1).

ORO and SDH staining. ORO staining of liver sections was used to quantify fat accumulation in all treatment groups. CORT-treated animals had increased red staining

compared to placebo-treated animals, indicating more lipid accumulation in the liver. There were no differences in liver fat accumulation between CORT-SED and –EX groups as well between placebo-SED and –EX groups. To determine any effects of training after 4 weeks of voluntary wheel running, the tibialis anterior of each animal was stained for SDH activity (Fig. 3E-H). SDH is an oxidative complex bound to the inner mitochondrial membrane of skeletal muscle cells and is responsible for oxidizing succinate to fumarate in the citric acid cycle (363). Strong SDH staining correlates with increased mitochondria and higher muscle fiber oxidative potential. Placebo- and CORT-EX muscle types had elevated oxidative capacity compared to placebo- and CORT-SED muscle ($p<0.001$, Fig. 3I). In type I and IIa muscle sections CORT-SED had lower oxidative capacity than all treatment groups ($p<0.05$, Fig. 3I). In type IIb/x muscle CORT-SED tended to have lower oxidative capacity than placebo-SED animals.

Plasma CORT, fasting NEFAs, glucose and insulin concentrations. CORT levels measured at 0800 h on day 21 were highest in CORT-SED and -EX groups compared to placebo-SED and -EX groups ($p<0.05$, Table 2). Placebo-SED animals had the lowest CORT levels compared to all other animal groups ($p<0.05$). CORT levels measured at 0800 h on day 28 were also highest in CORT-treated animal groups compared to placebo-SED but not significant from each other (CORT-SED vs. CORT-EX). On day 28, CORT levels in placebo-EX animals were higher than placebo-SED animals, similar to CORT-SED and lower than CORT-EX ($p<0.05$, Table 2). Fasted NEFA levels were highest in CORT-treated animals compared to placebo animals ($p<0.05$, Table 2). CORT-EX animals tended to have lower fasting NEFAs than CORT-SED animals and placebo-SED

animals tended to have higher fasting NEFAs than placebo-EX animals. Fasting blood glucose levels prior to oral glucose challenge were ~ 4-fold higher in CORT-SED animals than placebo-SED ($p<0.05$). CORT-EX animals had lower fasting blood glucose levels compared to CORT-SED although concentrations were still higher when compared to placebo-treated groups ($p<0.05$, Table 2). CORT-SED animals had ~ 5.4-fold increase in fasting plasma insulin levels compared to placebo-SED. CORT-EX animals had ~ 8-fold increase in fasting plasma insulin levels compared to placebo-EX animals ($p<0.05$, Table 2). CORT-EX animals tended to have higher fasting plasma insulin levels than CORT-SED animals but values were not statistically significant ($p>0.05$).

Oral glucose tolerance challenge. CORT-SED animals had markedly elevated blood glucose levels before and during the oral glucose tolerance challenge compared to all treatment groups ($p<0.05$, Fig. 4A). Voluntary wheel running in CORT animals reduced glucose intolerance compared to SED animals ($p<0.05$) however, CORT-EX animals still expressed higher glucose intolerance than the placebo groups ($p<0.001$, Fig. 4A'). Plasma insulin concentrations were highest in CORT-EX animals before and during the oral glucose tolerance challenge compared to all treatment groups ($p<0.001$, Fig. 4B). CORT-SED animals also had increased levels of plasma insulin during the oral glucose challenge that remained above the placebo-treated animals but were lower than the CORT-EX animals ($p<0.01$, Fig. 4B'). AIR was measured to determine the islet sensitivity to exogenous glucose (Fig. 4C). CORT-SED animals had the lowest AIR to glucose, indicating impaired islet responsiveness ($p<0.05$). Voluntary wheel running in both placebo- and CORT-treated groups greatly increased AIR by ~ 2-fold above

placebo-SED animals ($p<0.05$). To determine the influence of basal blood glucose levels on plasma insulin concentrations in each treatment group both parameters were plotted (Fig. 4D). The r^2 with all groups included was 0.47 and there was a significant linear regression ($p<0.0001$) meaning that higher fasted blood glucose concentrations were correlated with higher insulin levels. CORT-EX and CORT-SED animals had the highest glucose and insulin levels. Blood glucose and plasma insulin values in the placebo animals did not deviate from each other and clustered around 3.5-5.5 mM of glucose and less than 4 ng/ml of insulin.

In vivo β-cell function. HOMA-β was used to calculate basal β-cell function where higher HOMA-β scores indicate greater β-cell function. Voluntary wheel running improved β-cell function in CORT animals by ~ 2.5-fold compared to CORT-SED groups ($p<0.05$, Fig. 5A). It also increased β-cell function in placebo-EX animals compared to placebo-SED animals ($p<0.05$). No differences in HOMA-β levels were found between CORT-SED and placebo-SED groups ($p>0.05$). An insulin tolerance test was conducted to measure insulin sensitivity primarily in the skeletal muscle (Fig. 5B). CORT-SED animals had the highest glucose AUC levels compared to all treatment groups ($p<0.001$, Fig. 5B'). Voluntary wheel running reduced glucose AUC in CORT-EX animals indicating improved peripheral insulin sensitivity ($p<0.05$) presumably mediated through improved glucose uptake in the skeletal muscle.

Running distance vs. blood glucose, plasma insulin and CORT. To determine if fasting blood glucose, plasma insulin and CORT had an effect on running distance, each value from each EX animal group was plotted and a linear regression was used to

measure significance (Fig. 6). No significant correlations were found between placebo- and CORT-EX groups and their running distances versus fasting blood glucose (r^2=0.083, p>0.05), plasma insulin (r^2=0.023, p>0.05), and plasma CORT (r^2=0.003, p>0.05).

Ex vivo GSIS. Islets were harvested from each animal upon euthanization (Day 31-35) and challenged with low (2.8) and high (16.7) glucose (mM) media. In low glucose media, CORT-SED islets had higher relative GSIS than placebo-SED and -EX groups (p<0.05, Fig. 7). CORT-EX tended to have higher relative GSIS levels in low glucose media compared to placebo-SED and -EX groups. High glucose media significantly increased relative GSIS concentrations in all treatment groups compared to low glucose media. CORT-SED had the highest relative GSIS compared to placebo-SED and -EX all other treatment groups, whereas CORT-EX had higher relative GSIS than placebo-SED and –EX, but lower GSIS than CORT-SED.

Discussion

Voluntary wheel running initially activates the HPA axis while prolonged wheel access reduces GC elevation in healthy rodents. It is not known whether chronic voluntary exercise has the ability to reduce the detrimental effects of elevated GCs in rodents. For the first time, we demonstrate in our model of elevated GCs and HFD that voluntary exercise (~ 4 weeks) is able to alleviate symptoms of diabetes such as increased visceral adiposity, glucose intolerance, insulin insensitivity, and impaired islet glucose responsiveness. We validate these findings by showing that CORT-EX animals have lower glucose AUC, better acute insulin responsiveness, higher HOMA-β scores and

improved insulin sensitivity than CORT-SED animals. These novel findings suggest that even in situations of chronically elevated GCs, regular exercise is able to promote healthier metabolic function. To date no studies have been published on the role of voluntary exercise and exogenous elevations in GCs. These results suggest that individual's suffering from hypercortisolemia, i.e. Cushing's syndrome, may benefit from regular exercise to help alleviate hyperglycemia, excess fat accumulation, decreased muscle oxidative capacity and impairments in islet function.

Generally, GCs decrease body mass, although it appears to be dependent upon animal model/type, dosing and duration of treatment (153, 295, 364-367). In this study and in previously published works (328, 350), we demonstrate that treatment with CORT induces (~ 50%) a reduction in body mass compared to placebo-treated animals, regardless of diet treatment and increased food intake. Traditionally, voluntary wheel running in healthy animals demonstrates lower body mass gain (197, 220, 367, 367) as well as in obesity compromised rodent models (368, 369). However, in our study voluntary exercise did not prevent body mass loss in CORT-treated animals as both CORT-SED and –EX-treated groups had similar body masses throughout 10 days of treatment (Fig. 2A). These findings are similar to other studies in rats that show no differences in body mass loss with elevations in GCs and exercise, regardless of training regime, i.e. voluntary versus trained (263, 367, 367, 370). Some studies suggest that lower body mass shown in GC-induced models is a result of reduced food intake (263). However, we find that CORT-treated animals, regardless of being SED or EX, consume more Calories than the placebo-treated animals (~ 1.5-fold change, Table 1). These

results are similar to previous findings suggesting that chronic GC treatment strongly influences eating behavior centres in the brain, especially increasing preferences for foods with high-fat content, that override the anorexigenic effects of insulin (124). Therefore, regardless of food consumption CORT treatment significantly decreases body mass and voluntary exercise does not correct this adaptation.

Cushing's syndrome results in a variety of clinical symptoms that include: hypertension, low bone mass, hyperglycemia, depression, and muscle atrophy as well as abdominal obesity, which can lead to further complications (135, 371). GCs help to regulate adipose tissue by promoting mechanisms of differentiation and distribution but in excess GCs can induce severe fat accumulation through hypertrophy and hyperplasia in the adipocytes (110). In our model of elevated GCs and HFD, there is an excessive accumulation of visceral fat that is ~ 1.5-fold higher in CORT-SED than placebo-treated animals (Table 1), which parallels other previous work (133, 328, 371, 372). Exercise is known to help reduce body mass gain, specifically fat mass gain (373-375) even in instances of HFD (375, 376). In the present study, we demonstrate that voluntary wheel running is sufficient to attenuate visceral fat accumulation in animals treated with CORT and HFD. These results are similar to previous published work (377); however our study findings are novel as voluntary exercise exhibited changes in visceral adiposity even with elevations in CORT and the addition of HFD.

GCs induce body mass loss, which is usually accompanied by muscle atrophy (365). GCs specifically target type IIb fibers in the skeletal muscle; however, to date the mechanisms remain unknown (378). GCs also induce negative protein balance through

increased protein degradation and decreased protein synthesis (379), both potentially leading to an overall decrease in muscle contractility. In our present study, we demonstrate that CORT and HFD lead to lower epitrochlearis and gastrocnemius muscle mass. In contrast to other studies that have found dexamethasone-induced muscle loss with treadmill or uphill exercise (263, 370) we show that voluntary exercise was able to reverse muscle mass loss in gastrocnemius and further increase epitrochlearis muscle mass above placebo-SED animals. We suggest differences found in muscle mass are due to the nature of the exercise protocols. Treadmill exercise, although an excellent exercise stimulus is only performed in rats for 1 hour a day at ~ 20m/min (370) whereas voluntary wheel running is accessible to the animals 24 h a day and some animals are able to run distances >10 km. As such, it is likely that voluntary exercise is a more potent stimulator of preserving muscle mass than treadmill or uphill exercise in situations of hypercortisolemia. In addition, the soleus muscle did not decrease with CORT-SED treatment but instead increased in mass compared to the other treatment groups, a finding unique to our study. This mass increase has been a continued observation in our model and the mechanisms remain unknown. We suggest that since GCs primarily target white muscle tissue the soleus muscle could be preserved as it consists mostly of red muscle tissue.

GCs advance muscle atrophy by targeting fast-twitch, glycolytic muscles (380) and consequentially causing reduced muscle oxidative capacity (381). Here, we also find lower muscular oxidative capacity with CORT-SED treatment in type I and II fibers compared to placebo-SED fibers (Fig. 3I). We hypothesized that voluntary exercise

would increase muscle oxidative capacity as voluntary exercise for 10 weeks stimulates increased muscle oxidative capacity in Wistar-Kyoto rats with the metabolic syndrome (360). Similarly, we find that voluntary exercise promotes improved muscle oxidative capacity in all fiber types of the placebo-EX animals. Moreover, CORT-EX animals have similar oxidative capacity to the placebo-EX animals demonstrating that the lower oxidative capacity observed with CORT-SED is reversed with voluntary exercise. Therefore, we conclude that voluntary exercise is an adequate stimulus to improve skeletal muscle oxidative capacity even in situations of elevated GCs and HFD.

Animal models of T2DM, such as ZDF rats, have elevated levels of CORT prior to the onset of impaired glucose metabolism and abnormal glycemic control (63, 213). Exercise training and adaptations to psychological stress reduce elevations in GCs and lowers the risk of T2DM development in ZDF rats (144, 382). In this study and previously published work (328, 350) we show that elevated GCs induce severe glucose intolerance, hyperinsulinemia, impaired AIR, insulin resistance and β-cell function. Here, we show that (~ 4 weeks) daily voluntary wheel running was a sufficient amount of exercise to attenuate glucose intolerance and improve insulin response to exogenous glucose challenge (Fig. 4). Similar results have been found in exercise-trained humans where exercise improved glucose intolerance and insulin sensitivity just 10 days after being sedentary (247); exercise training also improved glucose intolerance induced from 10 days of dexamethasone treatment (263). In comparison to other published work on dexamethasone and treadmill exercise (263), we found that CORT-EX animals had elevated fasted and stimulated insulin levels during the glucose challenge compared to all

other treatment groups (Fig. 4B). These results are similar to those of Kiraly et al., 2008 (144), who showed increased fasting insulin at 11 weeks of a swim training intervention in ZDF rats compared to sedentary and lean controls as well as elevated β-cell mass, through increased cell proliferation (hypertrophy and hyperplasia) (144). Elevated plasma insulin levels were also found in exercised ZDF rats post glucose challenge compared to inactive controls (150). We show that voluntary exercise in both the placebo- and CORT-treated animals' results in a rise in AIR compared to both placebo- and CORT-SED animals (Fig. 4C). It is possible that elevated β-cell mass in both EX groups may contribute to elevated insulin response; however it was not measured in this study. We also show here that there is a correlation between fasted insulin and glucose levels when data is plotted together (Fig. 4D), indicating that higher glucose levels were associated with higher fasting insulin levels. However, CORT-EX animals have higher fasted insulin levels than CORT-SED animals, possibly indicating that CORT-EX animals have elevated islet compensation for higher glucose levels and therefore, may explain, in part, why these animals have attenuated glucose intolerance. Taken together, these data suggests that voluntary exercise results in more circulating insulin, but also in a more profound insulin response to exogenous glucose that is otherwise blunted with physical inactivity.

We have shown that CORT-SED treatment impairs the β-cell response to elevations in glucose (350). In the present study we show that β-cell function improves with exercise training in both placebo- and CORT-treated animals compared to their respective SED groups (Fig. 5A). These results are similar to ZDF rats (144) but no

studies have shown these effects in models of sustained elevation in exogenous GCs concomitantly with a HFD. Insulin sensitivity was severely abrogated in CORT-SED animals compared to placebo animals however voluntary exercise attenuated this response (Fig. 5B and B'). Exercise training improves insulin sensitivity in humans through the up-regulation of insulin action in the skeletal muscle (383). Voluntary exercise did lower insulin insensitivity in CORT-treated animals; however it did not normalize insulin sensitivity to that of the controls. Perhaps a longer exercise intervention would have promoted better exercise-induced insulin action at the level of the skeletal muscle.

Endurance training regardless of exercise protocol (swimming, voluntary, treadmill) results in reduced insulin release in isolated healthy rodent islets (222, 224, 226, 230, 384) and more specifically in the β-cell itself (225). Our findings suggest similar results, where placebo-EX animals tended to have lower GSIS (Fig. 7) compared to placebo-SED islets. As previously mentioned exercise training improves β-cell mass, through proliferation and increased β-cell neogenesis (144). In addition, voluntary wheel running (6 weeks) shows improvements in GSIS in ZDF rat islets as well as prevents complete depletion of insulin stores within the islet (150). Our study is the first to show that with voluntary exercise lowers relative GSIS in CORT-treated animals, although did not normalize to levels of placebo-SD or -EX. Our results were different to those found in active ZDF rats, in that GSIS was elevated in high glucose and palmitate media compared to inactive ZDF rat islets (150). These results differ as ZDF animals may have larger compensatory β-cell mass causing higher insulin levels. These differences could be the

result of different disease models and we conclude that abnormally elevated GSIS is attenuated with exercise training, as insulin requirement may be lower than CORT-SED islets.

Recently, we have shown that elevated short-term CORT in conjunction with a HFD induces severe hyperglycemia, hyperinsulinemia, along with impaired insulin response and glucose sensitivity despite increases in β-cell mass. In the present study, we were able to demonstrate that voluntary wheel running, concurrently with CORT and a HFD was sufficient to lower visceral adiposity, glucose intolerance, improve insulin response, muscle composition and oxidative capacity as well as increase β-cell function. These results are interesting and novel as it is not clear in the literature whether exercise is able to attenuate symptoms of T2DM independent of lower GC sensitivity. Our study shows that voluntary exercise attenuates symptoms of T2DM induced by elevated CORT and HFD and provides evidence that exercise can influence tissues independently from hypercortisolemia. Exercise intervention may be an ideal form of rehabilitation in individuals with hypercortisolemia or Cushing's syndrome as these individuals suffer from hyperglycemia, insulin insensitivity, muscular atrophy and increased central obesity. Therefore, they may benefit from the positive effects of regular exercise that help to control or attenuate symptoms, which could put them at a higher risk for diabetes development.

Table 1. Food intake and body composition.

	Placebo		CORT	
	SED	EX	SED	EX
Food intake	0.25±0.02[a]	0.30±0.02[a]	0.45±0.01[b]	0.44±0.02[b]
Epididymal Fat	17.0±1.0[a]	17.0±1.6[ac]	26.9±1.1[b]	21.8±1.4[c]
Liver	37.4±1.6[a]	37.7±1.6[a]	69.7±2.4[b]	69.3±6.8[b]
Gastrocnemius	4.7±0.2[ac]	5.4±0.5[a]	3.7±0.1[b]	4.2±0.2[bc]
Tibialis Anterior	1.5±0.04[a]	1.6±0.20[a]	1.35±0.05[a]	1.50±0.1[a]
Soleus	0.40±0.01[a]	0.45±0.1[ab]	0.52±0.03[b]	0.43±0.02[a]
Epitrochlearis	0.14±0.01[a]	0.17±0.02[abc]	0.11±0.01[b]	0.20±0.03[c]

Note: Values are means ± SE in kcal/g of BM/day for food intake and g/kg for tissue mass. Different letters beside each value indicate the mean was statistically significant from other groups that do not share the same letter. All analysis was carried out by a two-way ANOVA with a Tukey's post-hoc, where $p<0.05$. n=7-12.

Table 2. CORT, fasted NEFAs, glucose and insulin concentrations.

	Placebo		CORT	
	SED	EX	SED	EX
Day 21 CORT	66.0±17.1[a]	271.3±42.9[b]	566.2±65.6[c]	548.2±45.0[c]
Day 28 CORT	70.6±12.3[a]	375.0±44.7[b]	468.6±38.3[bc]	504.9±38.7[c]
Fasted NEFAs	0.45±0.1[a]	0.39±0.9[a]	1.0±0.1[b]	0.85±0.1[b]
Fasted Glucose	4.9±0.3[a]	5.1±0.2[a]	18.8±0.9[b]	14.3±1.6[c]
Fasted Insulin	1.24±0.3[a]	1.1±0.5[a]	6.8±0.6[b]	8.9±1.2[b]

All values are means ± SE in ng/ml for CORT and insulin. Values are in mM for glucose and NEFAs. Different letters beside each value indicate the mean was statistically significant from other groups that do not share the same letter. All analysis was carried out by a two-way ANOVA with a Tukey's post-hoc, where $p<0.05$. n=7-12.

Figure Captions

Fig.1. Schematic of experimental design. On day 0, all animals were individually housed and divided into one of four groups; placebo-EX, CORT-EX, placebo-SED and CORT-SED (EX, exercise and SED, sedentary). At this time, all EX animals were introduced to running wheels in their cages and allowed 2 weeks to acclimate to the experimental conditions. On day 14 either wax or CORT pellets were subcutaneously implanted into the animals according to the assigned experimental group and all animals were given a HFD (60%) *ad libitum*. Seven days after pellet surgeries (~ 0800 h) blood samples were taken to measure plasma CORT and blood glucose levels. On day 25 animals were fasted overnight (~ 16 h) and the following day (26) were administered an oral glucose tolerance test. On day 28 (~ 0800 h) blood samples were taken again to measure plasma CORT and blood glucose levels. On the evening of day 29, animals were fasted and on day 30 animals were administered an insulin tolerance test. All animals were euthanized between days 31-35 of the experimental protocol.

Fig.2. Body mass relative to pre-surgery body mass during pellet treatment (10 days) (A) and average daily running distances during pellet treatment (B) and average daily running distances relative to pre-surgery running distances (C). CORT-treated animals experienced ~ 10-15% body loss throughout the pellet treatment period while placebo-treated animals continuously gained mass ($p<0.05$). CORT-EX animals ran longer distances per day than placebo-EX animals ($p<0.05$) however CORT-EX animals ran more prior to surgery. No differences were found between CORT-EX and placebo-EX groups in running distances relative to pre-surgery running distances. Therefore, pellet implants had no impact on running distances. n=7-12. All values are means ± SE.

Fig.3. Measurement of liver lipid accumulation and muscle oxidative capacity was completed through ORO (A-D) and SDH staining (E-H). SDH activity was measured as the mean optical density relative to the placebo-SED group, for each fiber type: I, IIa, and IIb/x (I). CORT treatment increased liver lipid accumulation. Muscle oxidative capacity was increased in all placebo- and CORT-EX muscle types compared to placebo- and CORT-SED muscle. In type I and IIa muscle sections CORT-SED had lower oxidative capacity than placebo-SED animals. n=3-5 per group. In bar graphs, letters that are not the same are statistically significant from each other ($p<0.05$) using a two-way ANOVA with Duncan's post hoc test. All values are means ± SE.

Fig.4. Measurement of glucose tolerance (A and A'), insulin secretion (B and B') and insulin response (C and D). Blood glucose levels were greatly elevated with CORT-SED treatment compared to placebo treatment ($p<0.001$) but voluntary wheel running decreased glucose intolerance in CORT-treated animals ($p<0.05$). Plasma insulin levels post an oral glucose challenge were elevated with CORT treatment compared to placebo-treated animals and exacerbated with the addition of wheel running ($p<0.01$). n=7-12 for all above graphs. Acute insulin response (AIR) between basal and 15 minutes post exogenous glucose challenge was elevated with EX ($p<0.05$) and reduced with SED-treated animals ($p<0.05$). n=6-12. Higher fasting plasma insulin concentrations was

correlated with higher fasting blood glucose concentrations in both CORT-EX and SED groups (r^2=0.47, $p<0.0001$). n=6-12. In all bar graphs, letters that are not the same are statistically significant from each other using a two-way ANOVA with Tukey's (A' and B') and Duncan's (C) post hoc tests. All values are means ± SE except in D, where values are individual.

Fig.5. Measurement of β-cell function (A) and insulin sensitivity (B and B'). HOMA-β, an indicator of β-cell function, was increased with voluntary wheel running in placebo and CORT-treated animal groups ($p<0.05$). Insulin sensitivity measured by the response to an insulin bolus was improved with voluntary wheel running in CORT-treated animals ($p<0.05$). n=7-12. In all bar graphs, letters that are not the same are statistically significant from each other using a two-way ANOVA with Duncan's (A) and Tukey's (B and B') post hoc tests. All values are means ± SE.

Fig.6. Running distances versus fasted blood glucose (A), plasma insulin (B) and plasma CORT (C). No significant correlations were found in any groups with running distances and measured plasma parameters ($p>0.05$). n=7 for placebo-EX and 12 for CORT-EX. Linear regressions were performed to determine significance ((r^2=.083 (A), r^2=0.023 (B) and r^2=0.0003 (C)). All values are plotted as individual values.

Fig.7. Isolated islet glucose stimulated insulin secretion (GSIS), in low (2.8) and high (16.7) glucose (mM) media (% of total insulin content). CORT-SED treated group had higher insulin secretion in low and high glucose media compared to placebo-treated groups ($p<0.05$). Voluntary exercise normalized GSIS in CORT-treated animals ($p<0.05$). n=3-7 per group. The * indicates statistical significance from CORT-SED and the # indicates statistical significance from CORT-EX ($p<0.05$) using two-way ANOVA with Duncan's post hoc test. All values are means ± SE.

Figure 1.

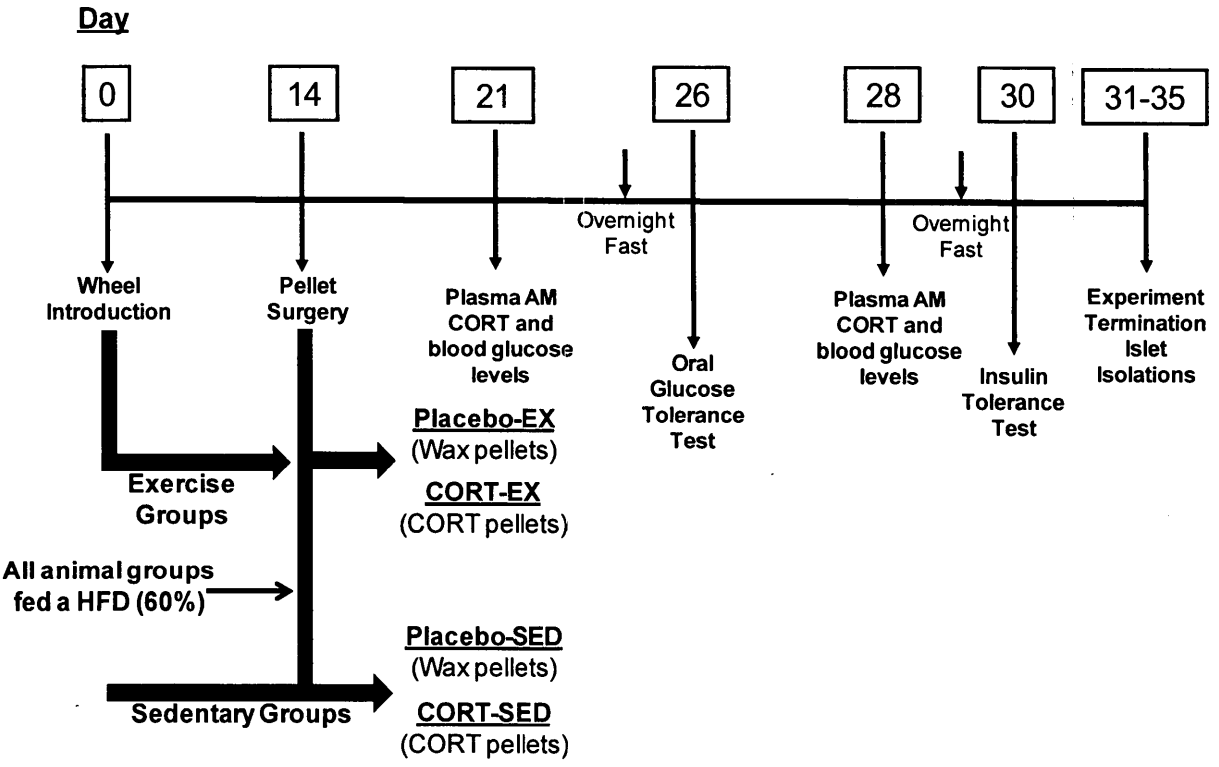
Day
0
14
21
26
28
30
31-35
Overnight Fast
Overnight Fast
Wheel Introduction
Pellet Surgery
Plasma AM CORT and blood glucose levels
Oral Glucose Tolerance Test
Plasma AM CORT and blood glucose levels
Insulin Tolerance Test
Experiment Termination Islet Isolations
Placebo-EX
(Wax pellets)
CORT-EX
(CORT pellets)
Exercise Groups
All animal groups fed a HFD (60%)
Placebo-SED
(Wax pellets)
CORT-SED
(CORT pellets)
Sedentary Groups

Figure 2.

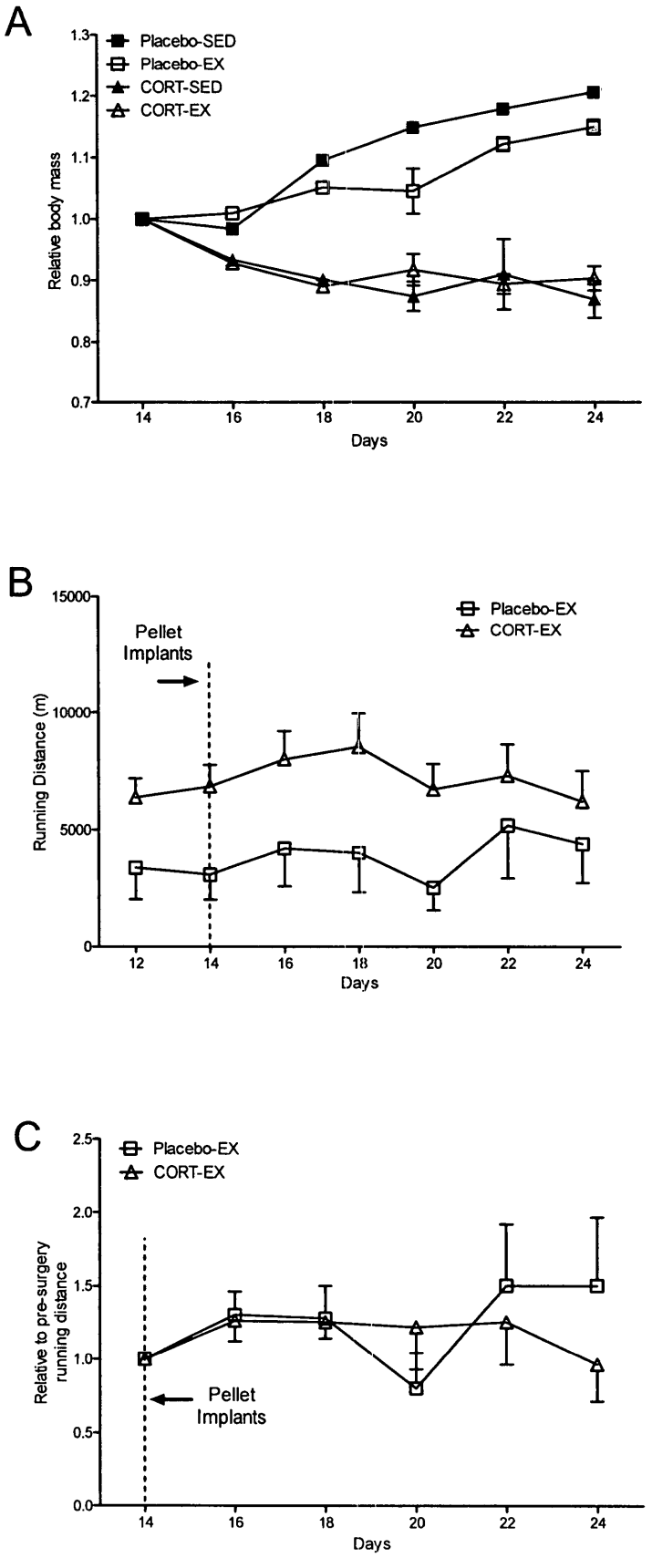
A
Placebo-SED
Placebo-EX
CORT-SED
CORT-EX
Relative body mass
1.3
1.2
1.1
1.0
0.9
0.8
0.7
14
16
18
20
22
24
Days
B
Placebo-EX
CORT-EX
Pellet Implants
Running Distance (m)
15000
10000
5000
0
12
14
16
18
20
22
24
Days
C
Placebo-EX
CORT-EX
Relative to pre-surgery running distance
2.5
2.0
1.5
1.0
0.5
0.0
Pellet Implants
14
16
18
20
22
24
Days

Figure 3.

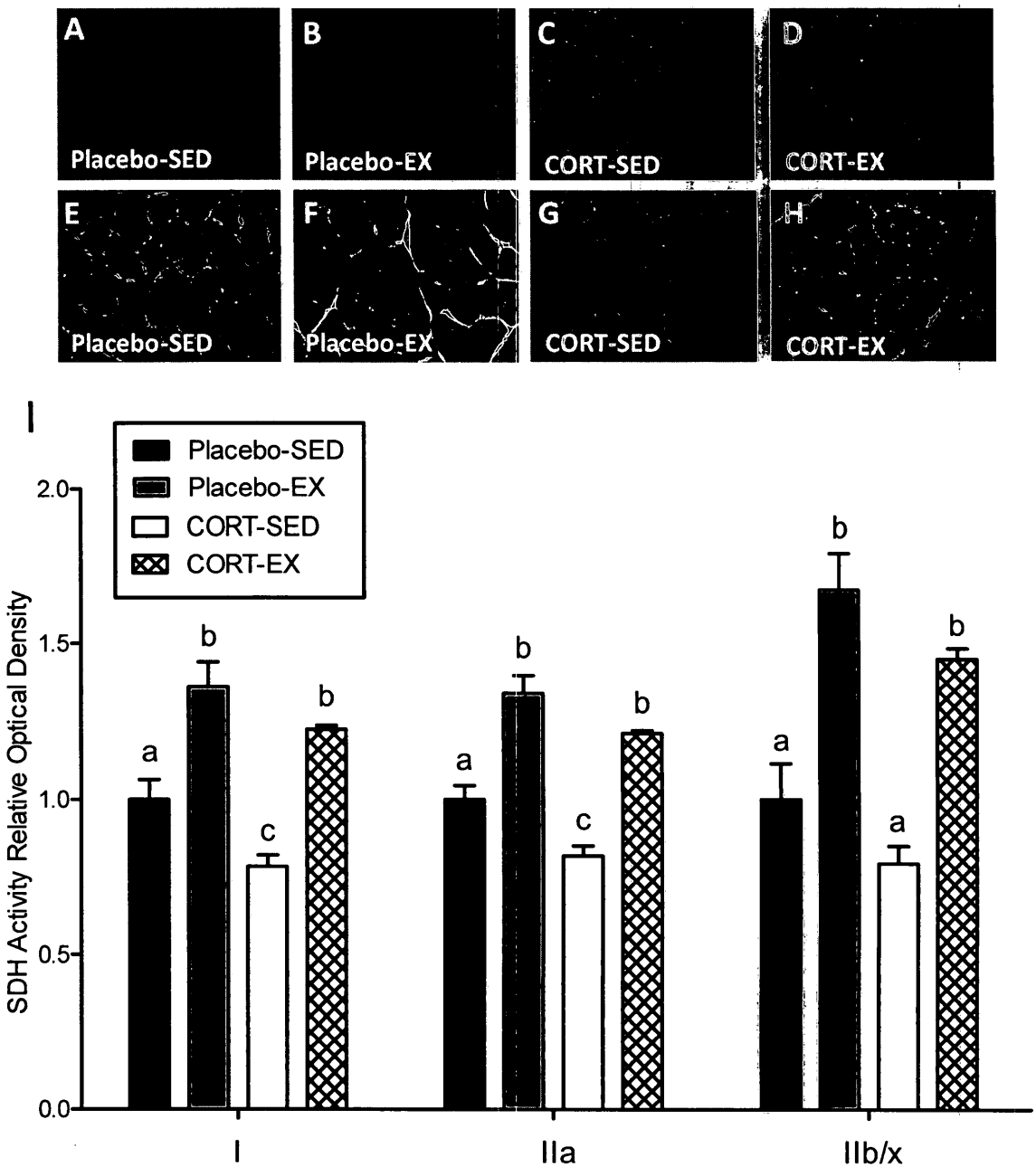
A
Placebo-SED
B
Placebo-EX
C
CORT-SED
D
CORT-EX
E
Placebo-SED
F
Placebo-EX
G
CORT-SED
H
CORT-EX
Placebo-SED
Placebo-EX
CORT-SED
CORT-EX
SDH Activity Relative Optical Density
2.0
1.5
1.0
0.5
0.0
a
b
c
b
a
b
c
b
a
b
a
b
I
IIa
IIb/x

Figure 4.

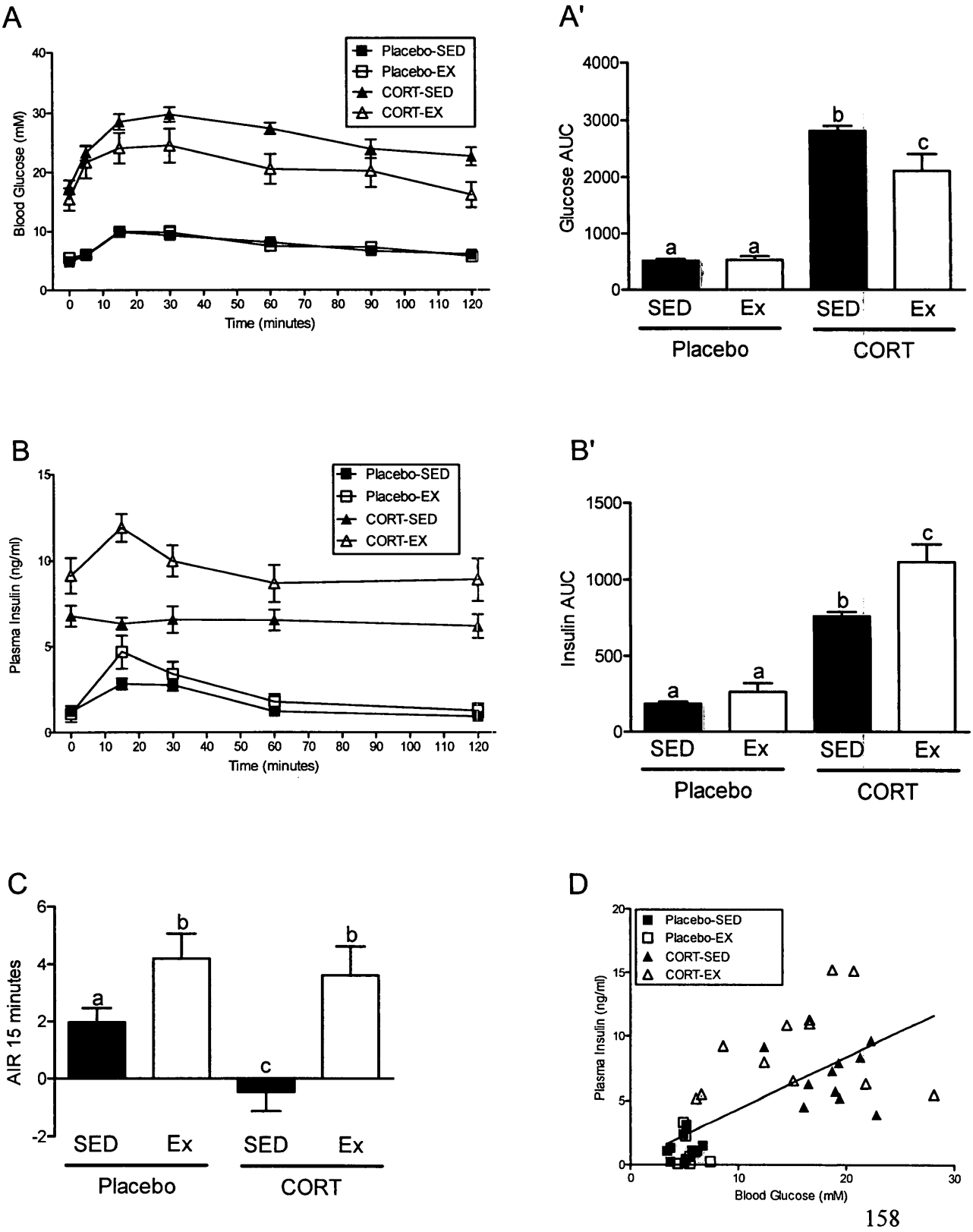
A
Placebo-SED
Placebo-EX
CORT-SED
CORT-EX
Blood Glucose (mM)
Time (minutes)
A'
Glucose AUC
SED
Ex
SED
Ex
Placebo
CORT
B
Plasma Insulin (ng/ml)
Time (minutes)
B'
Insulin AUC
C
AIR 15 minutes
D
Plasma Insulin (ng/ml)
Blood Glucose (mM)

Figure 5.

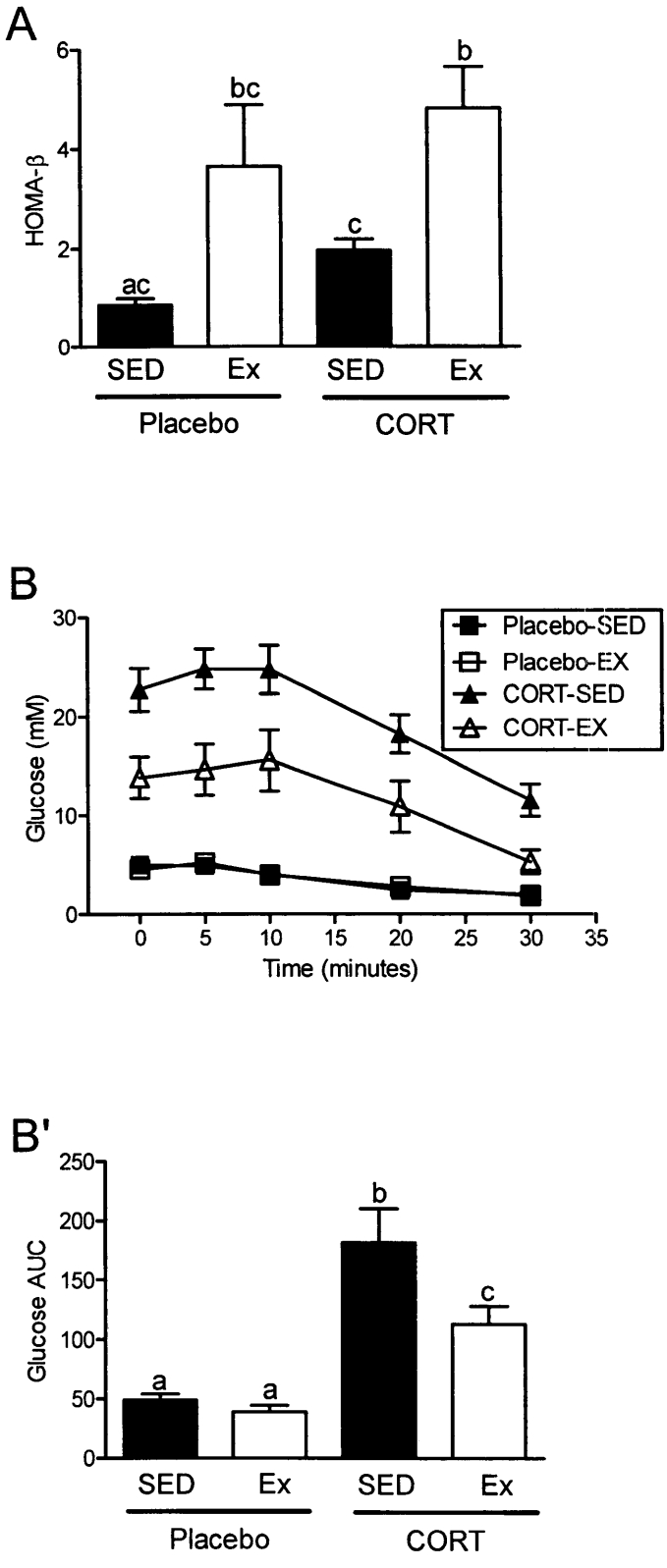
A
HOMA-β
6
4
2
0
ac
bc
c
b
SED
Ex
SED
Ex
Placebo
CORT
B
Glucose (mM)
30
20
10
0
Placebo-SED
Placebo-EX
CORT-SED
CORT-EX
0
5
10
15
20
25
30
35
Time (minutes)
B'
Glucose AUC
250
200
150
100
50
0
a
a
b
c
SED
Ex
SED
Ex
Placebo
CORT

Figure 6.

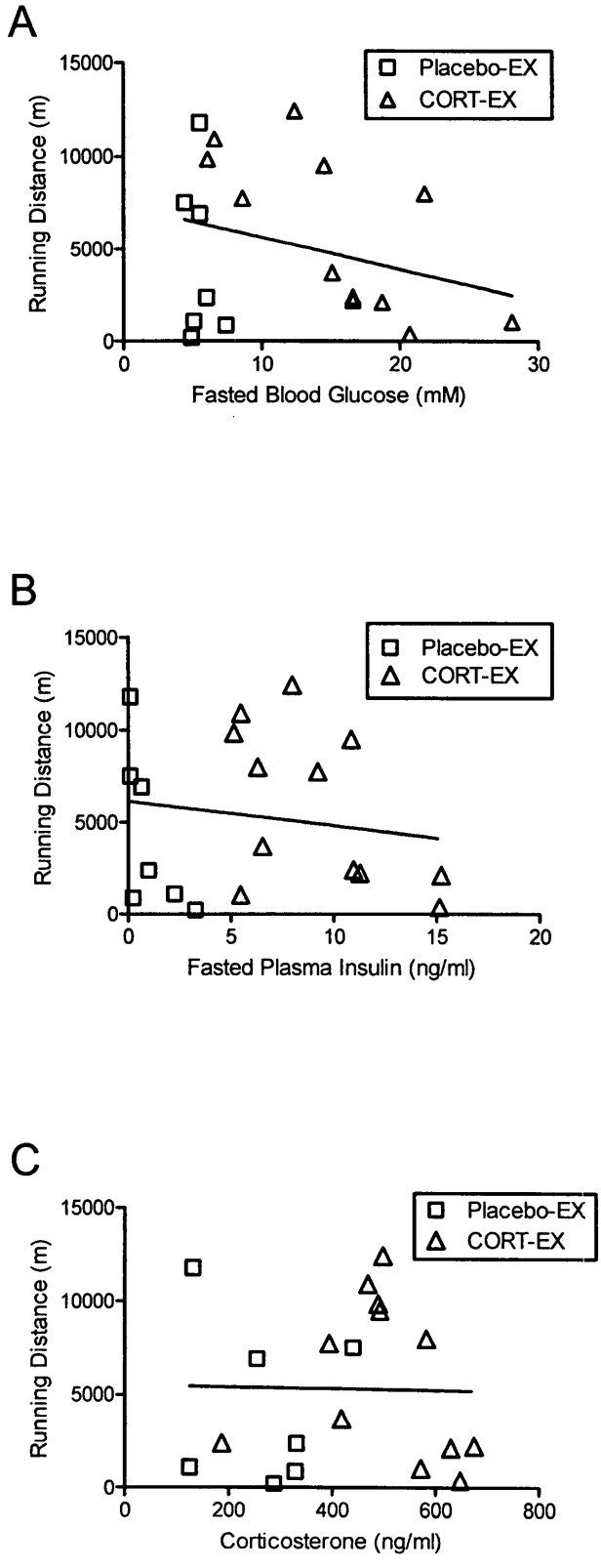
A
Placebo-EX
CORT-EX
Running Distance (m)
15000
10000
5000
0
0
10
20
30
Fasted Blood Glucose (mM)
B
Placebo-EX
CORT-EX
Running Distance (m)
15000
10000
5000
0
0
5
10
15
20
Fasted Plasma Insulin (ng/ml)
C
Placebo-EX
CORT-EX
Running Distance (m)
15000
10000
5000
0
0
200
400
600
800
Corticosterone (ng/ml)

Figure 7.

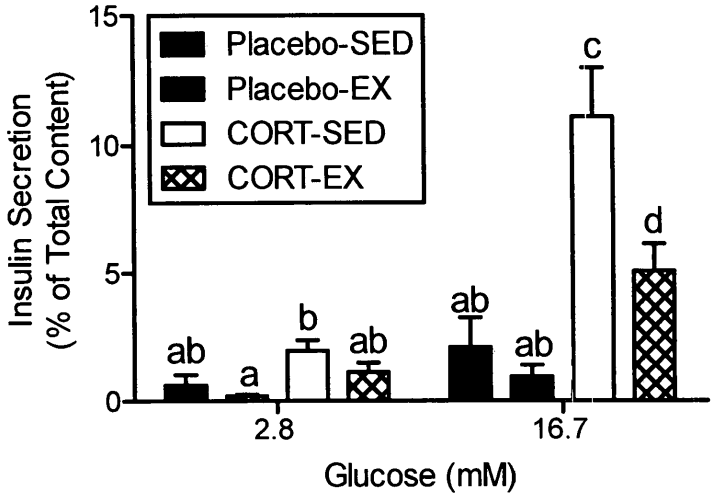
Placebo-SED
Placebo-EX
CORT-SED
CORT-EX
Insulin Secretion
(% of Total Content)
15
10
5
0
ab
a
b
ab
ab
ab
c
d
2.8
16.7
Glucose (mM)

MANUSCRIPT-#4 Chapter 5

Glucocorticoid Receptor II Antagonists and Rapid-onset Diabetes in Sprague-Dawley Rats

Rationale for Manuscript #4

Manuscript #3 demonstrated that voluntary wheel running was sufficient to attenuate symptoms of ROD, such as increased visceral adiposity, hyperglycemia, hindered muscle oxidative capacity, impaired insulin response to exogenous glucose challenge, and β-cell glucose insensitivity. However, not all symptoms of ROD were successfully restored with voluntary wheel running, i.e. normalized glucose control and peripheral insulin resistance. Therefore we were interested to determine if pharmacologic agents would be able to fully reverse the detrimental effects of ROD. Mifepristone (RU486) is a known non-selective GRII antagonist that inhibits the GRII, but not exclusively as it also inhibits the androgen and progesterone receptor (267). It is known to reverse symptoms of T2DM in individuals suffering from hypercortisolemia or with Cushing's syndrome, but due to its occupancy with other nuclear receptors it can produce some on undesirable side effects (276). Recently there are several selective GRII compounds being tested to replace the use of RU486, as they are thought to eliminate unwanted side effects. Therefore, the goal of manuscript #4 was to study the effects of selective GRII antagonists, such as C113176 and C108297, and non-selective antagonists, such as RU486 on ROD development.

Author Contributions

Conceived and designed the experiments: J.L.B., E.C.D., H.H. and M.C.R. Performed the experiments: J.L.B., E.C.D., D.Z. and T.T. Analyzed the data: J.L.B., E.C.D., D.Z., T.T., H.H., J.B. and M.C.R. Contributed reagents/materials/analysis tools: H.H., J.B. and M.C.R. Wrote the paper: J.L.B. Edited the manuscript: E.C.D., D.Z., T.T., H.H., J.B., and M.C.R.

J.L.B. performed all animal surgeries, daily gavaging of animals, food intake, animal mass, oral glucose tolerance test, insulin tolerance test, plasma analyses of glucose, insulin, corticosterone, NEFAs, quantification of HOMA-IR and beta, pancreatic islet isolations, acute *ex vivo* experiments with isolated islets and all statistical analyses data for this manuscript.

J.L.B prepared and designed Table 1, 2, 3 and Figure 1, 2, 3, 6.

This manuscript was submitted to *PLoS One* on September 17th, 2013. Submission # s-13-49757.

Effects of Selective and Non-Selective Glucocorticoid Receptor II Antagonists on Rapid-onset Diabetes in Young Rats

Running title: Glucocorticoid antagonists on rapid-onset diabetes

Jacqueline L. Beaudry[1]
Emily C. Dunford[1]
Dessi Zaharieva[1]
Trevor Teich[1]
Hazel Hunt[2]
Joseph K. Belanoff[2]
Michael C. Riddell[*1]

[1]School of Kinesiology and Health Science, Faculty of Health, Muscle Health Research Center and Physical Activity and Chronic Disease Unit, York University, 4700 Keele St., Toronto, ON, Canada, M3J 1P3
[2]Corcept Therapeutics, Menlo Park CA 94025
[*]Author for correspondence

Please address correspondence to Dr. Michael C. Riddell,
School of Kinesiology and Health Science, Faculty of Health, Muscle Health Research Center and Physical Activity and Chronic Disease Unit, York University 4700 Keele Street,
Toronto, ON, Canada, M3J 1P3
Telephone: (416) 736-2100 ext. 40493
Fax: 416-736-5774
Email: mriddell@yorku.ca

Key Words: Glucocorticoids, type 2 diabetes mellitus, high-fat diet, glucocorticoid antagonists, RU486, glucose intolerance, and insulin sensitivity

Abstract

Chronically elevated glucocorticoids (GCs) promote visceral fat mass accumulation, severe insulin resistance, hyperglycemia, skeletal muscle proteolysis and degradation to bone. Antagonism of the glucocorticoid receptor II (GRII) using Mifepristone (RU486) has been used to minimize these undesirable effects but at the expense of also blocking the progesterone receptor. A number of new selective GRII antagonists have recently been developed, but limited testing has been completed in animal models of hyperglucocorticoidemia. Therefore, two selective GRII antagonists (C113176 and C108297) were tested to determine their effects in a rodent model of GC-induced rapid-onset diabetes (ROD). Male Sprague-Dawley rats (~ six weeks of age) were placed on a high-fat diet (60%), given pellets containing corticosterone (CORT) or wax (control) and divided into five treatment groups. Each group was treated with either an antagonist or vehicle for 14 days after surgery: CORT pellets (400 mg/rat) + antagonists (80 mg/kg/day); CORT pellets + drug vehicle; and wax pellets (control) + drug vehicle. After 10 days of CORT treatment, body mass gain was increased with RU486 (by ~ 20% from baseline) and maintained with C113176 administration, whereas rats given C108297 had similar body mass loss (~ 15%) to ROD animals. Fasting glycemia was elevated in the ROD animals (>20 mM), normalized completely in animals treated with RU486 (6.2±0.1 mM, $p<0.05$) and improved somewhat in animals treated with C108297 and C113176 (14.0±1.6 and 8.8±1.6 mM, $p<0.05$ respectively). Glucose intolerance was normalized with RU486 and attenuated with C113176 and C108297, whereas acute insulin response was only improved with RU486 and C113176 treatment.

Also, peripheral insulin resistance was attenuated with C113176 treatment along with improved β-cell function while C108297 antagonism only provided modest changes. In summary, C113176 was an effective agent that minimized some GC-induced detrimental metabolic effects and may provide an alternative to the non-selective GRII antagonist RU486.

Introduction

Glucocorticoids (GCs) are naturally occurring steroid-derived hormones that are essential for healthy whole-body metabolism and adaptation to stressful environments. The hypothalamic-pituitary-adrenal (HPA) axis is the main regulator of GC secretion (cortisol in humans and corticosterone in rodents), operating normally in a diurnal rhythm and in response to stressors to increase GC release (385). GCs bind to receptors including GRII that are found ubiquitously throughout the body. The mineralocorticoid receptor (MR) also binds GCs. As GCs have ten times the affinity for MR compared to GRII, MR activity is most relevant in basal, non-stressful conditions. Expression of MR is low in most tissues except for in the hippocampus, kidneys, adipose tissue and heart (386). Once the GRII is occupied by a ligand, the complex translocates to the nucleus where it acts as a transcription factor to activate or repress the expression of genes necessary for cell proliferation, inflammation, immune development, reproduction (325) and energy homeostasis (77, 337).

Acute elevations in GCs are important for many biological functions, however, chronically high levels of GCs, such as those observed in patients suffering from Cushing's syndrome (135), result in unwanted metabolic disturbances such as reduced

growth (387), increased whole body insulin resistance (388), elevated fasting glucose levels (389) and possibly increased risk for type 2 diabetes mellitus (T2DM) development (138, 145, 146). Currently there are a large number of rodent (22, 288, 289) and human (58, 266) studies suggesting that the rise in circulating and/or cellular levels of GCs are connected with diabetes onset. At the cellular level, the pre-receptor enzyme, 11β-hydroxysteroid dehydrogenase type 1 (11β-HSD1) is responsible for conversion of inactive GCs into active GCs. This activity increases GC concentrations leading to the progression of tissue specific metabolic dysfunction (290) and, if left untreated, T2DM development (291). GRII antagonists have become an area of interest as they may eliminate unwanted metabolic effects of elevated GCs.

Mifepristone (RU486) is a non-selective GRII antagonist that competitively blocks the GRII, the progesterone receptor (PR), but not the MR (267). This receptor antagonist has recently gained FDA approval (Korlym™, 2012) for the treatment of patients with hypercortisolemia or Cushing's syndrome with established hyperglycemia, since it has been shown clinically to improve glucose tolerance in these patients (268, 269, 272). However, RU486 treatment requires consistent patient monitoring as it can result in various side effects such as endometrial hypertrophy, hypokalemia, and aborted pregnancy (267, 276). Currently, more specific antagonists selective for the GRII are being developed in the hope of eliminating the progesterone blocking properties of RU486 administration. A few studies of selective GRII antagonists have been conducted in rodent models (48, 278, 279). In these studies, selective GRII antagonists have been shown to play a role in the attenuation of detrimental GRII-dependent pathways in the

brain (278), whole-body steady state glucose metabolism (48), and body mass gain (279). However, no studies in this field have been conducted to investigate the role of selective GRII antagonists in a model of elevated GCs indicative of Cushing's syndrome and diabetes development.

Recently, we have developed a rodent model of rapid-onset diabetes (ROD) that involves the administration of increased levels of GCs by a slow release corticosterone pellet in combination with a high-fat diet (HFD) in young male Sprague-Dawley rats (328, 350). We are interested in the effects of GRII antagonists on ROD and hypothesized that this therapeutic treatment will help to prevent ROD development. In this present study, we tested two selective GRII antagonists, C113176 and C108297, in comparison to the non-selective GRII antagonist, RU486, in our established rodent model of ROD. We show that a new selective GRII antagonist, C113176, has beneficial effects in our model of ROD, attenuating the pathophysiological outcomes, including perturbed body mass, impaired glucose tolerance, reduced insulin release by pancreatic β-cells and insulin resistance.

Materials and Methods

This study was carried out in accordance with the recommendations of the Canadian Council for Animal Care guidelines and was approved by the York University Animal Care Committee (Protocol # 2010-15(R2)). All surgical procedures were performed under isoflurane anesthesia, and all efforts were made to minimize animal suffering.

Rodent Treatment and Experimental Design

Three sets of 20 male Sprague Dawley rats (Charles River Laboratories, 225-250 g, six weeks post-weaned) were individually housed (lights on 12 h: lights off 12 h cycle) after one week of acclimatization to the rodent facilities. Upon surgery day (day 0), each rat received a subcutaneous implantation of either corticosterone (CORT) pellets (4 x 100 mg; Sigma, Canada, Cat # C2505) or wax (control) pellets, as previously described (328). Immediately following surgery all rats were given *ad libitum* access to a high-fat diet (HFD), 60% of the total calories from fat and 5.1 kcal per gram of pellet (D12492, Research diets); this diet was maintained to the end of the experimental protocol. Rats recovered in sterile cages for two days and were then separated into five groups while being maintained on a HFD and were assigned either vehicle or GRII antagonist treatment (RU486, C113176 and C108297) at a dose of 80 mg/kg/day. The antagonist dose was chosen based on doses used in earlier studies (48). The following treatment groups were created; wax+ vehicle gavage controls (controls), CORT+vehicle (ROD), CORT+RU486 (RU486), CORT+C108297 (C108297), CORT+C113176 (C113176). All antagonists were first dissolved in DMSO which was further dissolved in a vehicle consisting of 0.5% HPMC + 0.1% Tween 80 by approximately 30 seconds of sonication. ROD animals who were given only vehicle received 10% DMSO + vehicle instead of an antagonist compound. Antagonists and vehicles were administered with a syringe and oral gavage tube (Instech, Plymouth, PA USA, Cat # FTP-18-75) twice daily, approximately 10 hours apart. Body mass and food intake were measured and recorded

daily for each rodent using an electronic scale (Mettler Toledo, Canada) and any changes in the rodents' health were noted and monitored.

Blood Sampling

Plasma CORT levels were sampled on the morning of the 7th and 14th day after pellet implantation at approximately 0800 h, using the animal's saphenous vein. Blood samples were collected in lithium-heparin coated microvette capillary tubes (Sarstedt, Des Grandes Prairies, Montreal, Québec, Canada, Cat # 16.443.100) and centrifuged at 12,000 rpm for 5 minutes so that the plasma could be collected into polyethylene tubes and stored at -80°C until further analysis. These samples were later analyzed for CORT levels using a radioimmunoassay kit (MP Biomedical, OH, USA).

Fed blood glucose concentrations were measured on day seven using a handheld glucometer (Bayer, Contour, NY, USA). On day 11, animals were fasted overnight (16 hours) and on day 12, animals were administered an oral glucose tolerance test (OGTT, 1.5 g/kg body mass). An insulin tolerance test (ITT) was administered on day 16 after an overnight fast by intraperitoneal (i.p.) insulin injection, (previously reported in (328, 350)). For these tests, all blood glucose concentrations were also measured with a handheld glucometer and blood samples drawn from saphenous vein were collected in microvette tubes (Sarstedt). The animals' plasma was subsequently analyzed for insulin (Crystal Chem, IL, USA, Cat # 90060) using the high-range assay method and for non-esterified fatty acids (NEFA) levels (HR Series NEFA-HR, Wako Chemicals). Glucose area under the curve (AUC) was measured relative to the fasting glucose levels of the

control animals, and insulin AUC was measured relative to each individual's fasting insulin levels. The acute insulin response (AIR) was determined by the difference between basal (fasting) insulin levels and insulin levels 15 minutes following the oral glucose gavage (previously reported in (191, 350)). This measurement represents the ability of the pancreatic β-cells to respond to exogenous glucose load.

Homeostatic Model Assessment for Insulin Resistance (HOMA-IR) was calculated as previously reported in (328) and is based on the following equation: Glucose (mM) x Insulin (μ units·L)/22.5 (361). This calculation represents basal glucose and insulin action on peripheral tissues, and primarily reflects the relationship between hepatic glucose output and insulin secretion (390). Homeostatic Model Assessment for β-cells (HOMA-β) was calculated based on the following equation: 20 x Insulin (μ units·L)/Glucose (mM)-3.5 (361). This measurement represents basal pancreatic β-cell function in response to basal glucose levels.

For technical and experimental reasons, the day of termination ranged from 2-5 days after the ITT to allow for subsequent tissue collection. Trunk blood was collected for further analysis. Tissues collected from animals euthanized via decapitation were as follows: liver, heart, epididymal fat pads, and skeletal muscles such as epitrochlearis, soleus, gastrocnemius and tibialis anterior.

Histology

Liver and skeletal muscle tissue from euthanized animals were snap frozen, cryosectioned (10 μm thick) and stained with Oil Red O for neutral lipid content as previously described (299). Muscle and liver sections were fixed with 3.7% formaldehyde for 1 h at room temperature while an Oil Red O solution composed of 0.5 g Oil Red O powder (Sigma-Aldrich, Canada) and 100ml of 60% triethyl phosphate (Sigma-Aldrich, Canada) was mixed and filtered. Following fixation in 3.7% formaldehyde, slides were immersed in filtered Oil Red O solution for 30 minutes at room temperature. Slides immediately underwent five washes with ddH2O, were allowed to dry for 10 minutes and were sealed with Permount (Sigma-Aldrich, Canada). Skeletal muscle and liver images were acquired at 10 x and 20 x magnifications respectively using a Nikon Eclipse 90i microscope (Nikon, Canada) and Q-imaging MicroPublisher 3.3 RTV camera with Q-capture Software. Intensity of Oil Red O staining of IMCL droplets on serial sections of the tibialis anterior was assessed with Adobe Photoshop CS6, converted to greyscale and reported as the average optical density (60 fibers were counted per muscle section). The greyscale is evaluated on a range of 0 (completely black) to 255 (completely white).

Western Blotting

Western blot analysis was carried out according to previously published work (350, 391). In brief, 50 micrograms of protein lysate from epididymal fat protein was run on a 12% SDS-page gel and proteins were transferred to a PVDF membrane (Bio-Rad, Canada). Membranes were blocked in 10% powdered milk and Tris-buffered saline with

Tween 20 at room temperature for 1 hour. Membranes were then incubated overnight at 4°C with polycolonal rabbit anti-11β-HSD1 (1:1000, Cat#10004303, Cayman Chemical Company, Ann Arbor, MI) and monoclonal mouse anti-α-tubulin (1:40000, Cat#ab7291, Abcam, Toronto, ON). The following morning the membranes were washed with TBST and incubated with goat anti-mouse (1:10000, Cat#ab6789, Abcam) and goat anti-rabbit (1:10000, Cat#ab6721, Abcam) secondary antibodies for 1 hour at room temperature. Membranes were then washed and imaged. Images were detected on a Kodak In vivo FX Pro imager and molecular imaging software (Carestream Image MI SE, version S.0.2.3.0, Rochester, New York) was used to quantify protein content.

Glucose stimulated insulin secretion (GSIS)

Islet isolations and ex vivo glucose challenges were carried out as previously reported (350). Collagenase pancreas digestion was followed by Histopaque-1077 (H8889, Sigma, Canada) pellet suspension followed by re-suspension in KREB's buffer. Islets were handpicked and cultured in filtered RPMI buffer (Wisent) overnight (24 h) at 37°C, 5% CO_2. Islets were separated into a 12-well culture plate (6-10 islets/well in 3 batches) and given a 30 minute pre-incubation period as previously described (350). Islets were given fresh KREB's buffer with 2.8 mM glucose + 0.1% BSA for 1 hour at 37°C, 5% CO_2. Media was changed to KREB's buffer with 16.7 mM glucose + 0.1% BSA for 1 hour at 37°C, 5% CO_2. Immediately following each incubation period, media was collected, centrifuged and stored at -20°C for further analysis. Insulin was measured using a radioimmunoassay kit (Millipore, Billerica, MA, USA).

Statistical Analysis

All data are represented as a mean ± SE, with a criterion of $p<0.05$ and were assessed using one-way ANOVAs as a means of statistical significance. All individual differences were evaluated using Tukey's post-hoc test unless otherwise stated as a student's t-test (Statistica 6.0 software and Prism Graph Pad version 5.1). Results from post-hoc analyses were denoted on each figure bar using letters. If bars do not share the same letters then mean values were statistically significant between treatment groups. If bars share the same letter then mean values were found to not be statistically significant from each other.

Results

Body mass

GC antagonist treatment commenced on day 2 of pellet treatment and body mass was measured every day relative to day 0 (pre-surgery) for 10 days. Animals weighed ~ 300-325 g prior to pellet surgery (Figure 1 shows the fold changes in mass over the 10 day period). ROD treatment resulted in ~ 15% body mass loss relative to pre-surgery mass and ~ 50% body mass difference compared to control animals 10 days after CORT treatment. In comparison, RU486 treatment increased body mass gain relative to ROD treated animals by day 4. Body mass continued to rise during the treatment period and ultimately resulted in ~ 20% mass gain over the 10 day period. Probably because of the initial mass lost from day 0 to 2, RU486 treatment did not fully reverse body mass loss in CORT treated animals when compared to controls (final mass on day 10: 352.7±5.9 g, vs.

397.6±6.1 g, in the RU486 treated animals and control animals respectively, $p<0.05$, Figure 1B). C113176 treatment recovered body mass to pre-surgery levels by day 8 (mass on day 10, 317.6±3.8 g), whereas C108297 treatment resulted in an overall mass loss of ~ 15% (mass on day 10, 259.3±4.4 g), similar to the ROD animals (mass on day 10, 266.5±3.1 g, Figure 1B).

Corticosterone and food intake

Normally, circulating CORT concentrations follow a diurnal pattern in rodents and fluctuate from high levels in early evening hours (i.e. peak, ~ 2000 h) to low levels in early morning hours (i.e. basal, ~ 0800 h). In this study, blood was sampled on day 7 and on day 14 at ~ 0800 h to determine basal CORT levels. Control animals had normal basal CORT levels on day 7 and day 14, values that were about 3-4-fold lower than all other treatment groups that received CORT pellets ($p<0.05$, Table 1). CORT pellet groups treated with ROD, RU486, C113176 and C108297 all had similar basal CORT levels at day 7 and 14 ($p>0.05$, i.e. not significant, Table 1).

Food intake was measured on day 10 of pellet treatment. ROD treated animals had an increase in absolute food intake compared to controls ($p>0.05$, Table 1). RU486 treated animals had the highest absolute food intake compared to all other groups ($p<0.05$, Table 1). Animals that were treated with C113176 or C108297 had similar absolute food intake to control animals (Table 1). Daily total kilocalorie intake relative to body mass was elevated in all CORT treated animals compared to controls ($p<0.05$) however, relative food intake was highest in ROD animals compared to all groups

($p<0.05$). Relative food intake was similar between RU486, C113176 and C108297 groups. Therefore, antagonist treatment lowered relative food intake compared to ROD animals but did not normalize food intake compared to the controls.

Hormone and blood analyses

Fed blood glucose concentrations were elevated in ROD animals compared to controls ($p<0.05$, Table 2). RU486 normalized fed blood glucose levels whereas C113176 and C108297 treated animals had similar levels compared to ROD treated animals (Table 2). All animals were fasted on the night of day 11 for ~ 16 h. Fasting blood glucose concentrations, measured the following day, were highest in ROD animals by ~ 4-fold compared to controls ($p<0.05$, Table 2). RU486 treatment normalized fasted glucose levels compared to controls, while C113176 treatment resulted in improved but not complete normalization of fasting blood glucose concentrations (Table 2). C108297 treated animals had significantly lower fasting blood glucose levels compared to ROD animals, however they had fasting blood glucose levels that were also higher than controls and RU486 treated rats ($p<0.05$, Table 2). ROD, RU486, C113176 and C108297 treated rats had higher fasting insulin concentrations compared to controls ($p<0.05$, Table 2). However, RU486 treatment resulted in lower fasting insulin levels compared to ROD animals, or rats treated with C113176 or C108297 ($p<0.05$). Insulin AUC was measured during the OGTT to determine *in vivo* insulin response to exogenous glucose. ROD, C113176 and C108297 treated animals had a similar AUC compared to control animals ($p>0.05$, Table 2). Interestingly, RU486 treatment resulted in a ~ 3-fold increase in insulin AUC compared to controls, and promoted the highest increase in insulin AUC

($p<0.05$, Table 2). Fasting NEFAs were measured on day 12, as high levels of free fatty acids are associated with an increased risk of diabetes (392). ROD, C113176 and C108297 treated rats demonstrated ~ 2-fold increase in fasting NEFAs compared to controls ($p<0.05$, Table 2). In contrast, RU486 normalized fasting NEFA concentrations to levels found in control animals.

Glucose tolerance and insulin response

An OGTT was performed on all animals on day 12 after an overnight fast to determine glucose tolerance and insulin response to exogenous glucose challenge (Figure 2A). The ROD group had the highest glucose concentrations throughout the OGTT challenge (Figure 2A) with a glucose AUC ~ 6-fold higher than controls ($p<0.05$, Figure 2B). RU486 treatment normalized glucose tolerance, with results similar to those observed in the control group. C113176 treatment resulted in an improvement in glucose tolerance compared to the results in the ROD group but values in the animals treated with C113176 were still ~ 2-fold higher than those observed in the animals in the control group ($p<0.05$, Figure 2B). Treatment with C108297 improved glucose tolerance compared to the ROD treated group, but glucose AUC was still ~ 4-fold higher than in control animals. Acute insulin response (AIR) was measured to determine insulin response at 15 minutes post oral glucose gavage. ROD animals had reduced AIR compared to all other groups ($p<0.05$, Figure 2C). RU486 treatment resulted in ~ 3-fold increase in AIR compared to the values in the control group ($p<0.05$), and C113176 treatment resulted in similar AIR levels to those observed with RU486 treatment, with higher AIR compared to animals in the control group (Figure 2C). Animals treated with

C108297 showed no differences compared to control animals or ROD treated animals ($p>0.05$).

Insulin sensitivity, insulin resistance and β-cell function

To determine peripheral insulin sensitivity primarily through skeletal muscle insulin action, an insulin tolerance test (ITT) was performed on all treatment groups. The ROD group had the highest fasting glucose concentrations and remained hyperglycemic (> 12 mM) 30 minutes post insulin bolus. RU486 treatment resulted in fully normalized insulin sensitivity, with glucose levels responding to insulin administration similarly to that observed in control animals. C113176 and C108297 treated animals had improvements in fasting glucose (~ 12 mM) and insulin sensitivity compared to ROD animals (Figure 3A), but treated animals did not have fully normalized insulin sensitivity. To determine insulin resistance as measured by liver insulin action, the HOMA-IR index was used. ROD animals were ~ 40-fold and ~ 30-fold more insulin resistant than control animals and RU486 treated groups ($p<0.05$, Figure 3B). RU486 treated animals were more insulin resistant than control animals (by~ 2-fold). However they were less insulin resistant than the ROD and the selective GRII antagonist treated groups. C113176 and C108297 treated animals showed attenuated increases in insulin resistance when compared to ROD animals., However these treatment groups remained more insulin resistant than control animals and RU486 treated animals ($p<0.05$, Figure 3B). The HOMA-β index was used to determine β-cell function; higher values indicate elevated β-cell response to basal glucose concentrations. No differences were found between ROD animals and control treated animals. Both RU486 and C113176 treatments improved β-

cell function by ~ 5-fold compared to all other groups ($p<0.05$, Figure 3C). C108297 treatment did not significantly impact the HOMA-β index.

Body Composition

Relative visceral fat mass was represented by the measured amount of isolated epididymal fat pad mass divided by body mass. All treatment groups had increased relative visceral fat mass compared to the control group ($p<0.05$, Table 3). No differences in fat mass were found between the groups treated with the antagonists. Liver mass was also increased in all treatment groups compared to controls ($p<0.05$) except for animals treated with RU486, in which liver mass was normalized (Table 3). Heart mass was increased with ROD and C108297 treatment and normalized with RU486 treatment. Animals treated with C113176 showed slight improvements compared to control animals ($p<0.05$, Table 3). It is known that CORT treatment specifically impairs white muscle growth (378). As expected, ROD animals had lower epitrochlearis mass compared to all other treatment groups ($p<0.05$). All groups that were administered an antagonist did not show changes in muscle mass relative to the animals in the control group (Table 3). The soleus muscle primarily consists of red, slow twitch muscle fibers and has been previously shown to increase with ROD treatment (328), although the mechanisms for this change remain unknown. ROD animals demonstrated an increase in soleus muscle mass ($p<0.05$, Table 3) whereas RU486 treated animals only had a slight trend towards an increase in soleus muscle mass compared to control animals ($p>0.05$, Table 3). There were no differences between tibialis anterior muscle mass among the various treatment groups (Table 3).

Fat accumulation in muscle and liver

Oil Red O staining of liver and tibialis anterior muscle sections was used to quantify fat accumulation in all treatment groups. ROD treatment increased red stain in muscle tissue and appearance of lipid droplets in liver tissue compared to controls. RU486 was the only antagonist that promoted normalized lipid accumulation in both the liver and type IIa muscle fibers relative to controls animals (115.76±10.12 vs. 127.3±4.74, arbitrary units). The animals treated with the selective antagonists (C113176 and C108297) had similar ectopic lipid accumulation compared to ROD treated animals (144.52±3.17, 144.9±2.62, and 142.58±7.44 vs. 141.58±2.98, n=3-4).

11β-HSD1 content in visceral fat

At the tissue level, inactive GCs become activated by the action of the pre-receptor enzyme 11β-HSD1, which acts to convert inactive GCs into active GCs. Recent studies have shown that inhibition of 11β-HSD1 activity helps to reverse metabolic pathological conditions such as T2DM (393). ROD treatment resulted in ~ 4-fold increase in 11β-HSD1 content in epididymal fat compared to controls ($p<0.05$, Figure 5). RU486 normalized levels of 11β-HSD1 content in epididymal fat. C113176 and C108297 had similar levels of 11β-HSD1 compared to ROD animals that were elevated compared to controls ($p<0.05$). Animals treated with C113176 or C108297 had similar levels of 11β-HSD1 to the ROD treated group.

GSIS (Glucose stimulated insulin secretion)

Pancreatic islets were isolated from all animals and insulin secretion was stimulated by an exogenous glucose challenge. ROD treatment resulted in an elevation in GSIS in both low (2.8 mM) and high (16.7 mM) glucose media concentrations compared to controls ($p<0.05$, Figure 6). RU486 and C113176 normalized GSIS in low and high glucose media concentrations compared to controls. C108297 treatment resulted in similar levels as ROD treatment that had higher GSIS in high glucose media compared to control animals ($p<0.05$) with similar levels of GSIS compared to ROD treated islets.

Discussion

This study is the first to investigate the effectiveness of selective and non-selective GRII antagonists in a rodent model of ROD induced by GCs and HFD. We show that of the tested compounds, C113176 treatment is the more effective selective GRII antagonist as it attenuates glucose intolerance, reinstates β-cell function, and improves insulin sensitivity. The other selective antagonist tested in this study, C108297, also provides modest attenuation in hyperglycemia and peripheral insulin resistance and no changes to insulin response *in vivo* or β-cell function in this ROD model. By comparison, however, the non-selective antagonist RU486 demonstrated superior effectiveness in this animal model of hyperglucocorticoidemia/diabetes, completely normalizing all abnormal features of growth and metabolism. Nonetheless, the new selective antagonist C113176 may be of some therapeutic advantage for treatment of the

metabolic features of hyperglucocorticoidemia/diabetes since it does not bind to the progesterone receptor.

Elevated GCs induce a severe state of hypercatabolism that can lead to drastic metabolic complications, such as muscle wasting, low bone density and inhibited structural growth (135). GCs can also act in an anabolic fashion, promoting increased food intake and body fat deposition, especially in the abdominal region, thereby increasing an individual's risk for the development of diabetes (135). We have previously reported that ROD treatment decreases overall body mass (~ 50%) but increases visceral adiposity compared to control animals (328). In the present study, we show that RU486 treatment reverses body mass loss caused by ROD treatment, increasing body mass gain by ~ 20% compared to pre-surgery mass (Fig. 1A and B). Previous results have shown that RU486 and C108297 treatment lower body mass gain in C57BL/6J mice consuming a HFD and given access to 11% sucrose for 4 weeks (48). An obese phenotype is also alleviated with RU486 (271, 279, 394, 395) and C108297 (395) in other rodent and human models of disease. However, to our knowledge, C113176 administration in animals with ROD has never before been reported. We demonstrate in this study that C113176 antagonism restores pre-surgery body mass at day 8 of treatment and animals continue to maintain a healthy body mass until the termination of the study. In contrast, C108297 treatment promoted mass loss similar to that observed in untreated ROD animals, a finding that could be considered detrimental in this particular animal model of severe cachexia. In other studies, C108297 has been shown to decrease mass gain in C57BL/6J mice (48) as well as in rats treated with olanzapine, an anti-psychotic

medication associated with weight gain in rodents and humans (395). Body composition analysis was not reported in these studies to determine if the drug influenced lean or fat mass or both. Therefore, C113176 antagonism might be an appropriate treatment for body mass management in humans with Cushing's syndrome because C108297 did not prevent body mass loss.

RU486 has been used to treat patients with Cushing's syndrome (272). It is readily absorbed, has a half-life up to 48 hours, and has a greater binding affinity to GRII than GC agonists such as dexamethasone (3 to 4 times) and cortisol itself (18 times) (273-275). The potent blockade of the GRII with RU486 administration interrupts GC negative feedback to the HPA axis, which could have an effect on corticosterone levels. In our study, there were no differences in CORT AM levels between ROD and antagonist treated animals (Table 1). This finding is not surprising as our model of ROD administers exogenous GCs via CORT pellets at a level that already inhibits HPA axis negative feedback and reduces adrenal GC production (328). It can therefore be concluded that the results of the antagonists on whole-body metabolism are not due to differences in CORT levels as these were unchanged by the antagonists. It is known that increased levels of stress hormones not only promote hyperphagia (328) but also influence food choice decisions towards higher caloric foods (303). In this study, ROD treatment resulted in increased relative food intake compared to control animals and the GRII antagonist treated groups. Our study confirms that relative food intake is lower with the administration of GRII antagonists, as has been reported for RU486 treatment in rodents on a HFD (396) and in humans with Cushing's syndrome (271, 272). In addition, RU486

treatment in obese fa/fa rats with increased levels of circulating GCs, results in lower food intake (397) while no alterations in feeding are found in lean rats given the drug (398). Moreover, studies investigating the effects of selective GRII antagonists on weight gain show no differences in food intake in healthy rodents despite decreases in body mass gain (279). Taken together, these results suggest that GRII antagonism helps limit hyperphagia in Cushing's syndrome and in diabetic animals.

RU486 administration improves glycemic control and insulin sensitivity in rodents given HFD for 4 weeks (48) and lowers glycated hemoglobin levels in patients with Cushing's syndrome who often exhibit poor glycemic control (272). In our study, we show that RU486 administration resulted in normalized glycemic control, and that C113176 had a greater influence on attenuating glucose intolerance than the other selective GRII antagonist tested (C108297) (Figure 2A and B). Moreover, both RU486 and C113176 treatment resulted in higher AIRs to oral glucose challenge compared to the other treatment groups thereby suggesting that enhanced β-cell function occurs with GRII antagonism (Figure 2C). Animals treated with C108297 tended to have lower AIR compared to controls, suggesting poor β-cell sensitivity to exogenous glucose, similar to the effects seen in ROD animals. Treatment with RU486 also resulted in a significant increase in insulin AUC levels during the OGTT suggesting an elevated insulin response to exogenous glucose stimulation (Table 2). In accordance with these findings, we recently have shown that ROD treatment results in impaired islet glucose responsiveness *in vivo* and *ex vivo,* which likely exacerbates the poor glucose control caused by reduced insulin sensitivity (350). Importantly, this present study suggests that the non-selective

GRII antagonist RU486 reverses defective insulin responsiveness *in vivo*, which may help to explain the normal glucose control in these animals. In addition, β-cell function *in vivo* is improved with both RU486 and C113176 treatment but not with C108297 treatment (Figure 3C). There are very few studies to date that investigate the effects of RU486 on β-cell function *in vivo* and to the best of our knowledge, this study is the first to report on β-cell function *in vivo* with selective GRII antagonism. As such, it is possible to suggest that improvements to β-cell function *in vivo* are through exclusive inhibition of GRII as seen with C113176 administration. However, more investigations are required to fully understand the mechanisms of action with selective GRII antagonism.

Elevated GCs in rodents induce peripheral tissue abnormalities that affect liver and skeletal muscle insulin sensitivity/signalling, thereby promoting hyperglycemia (111, 339, 399). In our study, we show that RU486 normalizes whole body insulin sensitivity while C113176 and C108297 partially attenuated the condition (Figure 3A). The blockade of the GRII with RU486 helps to reduce peripheral insulin resistance in individuals with mild GC excess (400). Our study confirms these results, as insulin resistance was normalized with RU486 while attenuated with C113176 and C108297 administration (Figure 3B). Liver and skeletal muscle lipid accumulation is elevated in ROD treated animals, ultimately contributing to peripheral insulin resistance (328, 339). Interestingly, RU486 administration was able to lower both skeletal muscle and liver fat content, while no differences were measured between animals with ROD and animals treated with the selective GRII antagonists (Figure 4). Therefore, more studies are

required to investigate the mechanisms of action, especially with C113176 administration, on improving insulin resistance.

Patients with Cushing's syndrome have an increased risk of obesity, which heightens their risk (60-80%) of developing diabetes as the disease progresses (138). Recent research shows that administration of RU486 results in normal body mass gain in rodents and in healthy men (271, 394). In addition, selective GRII antagonists such as C112716 and C113083 have been shown to help reverse olanzapine-induced mass gain in rats. (279). In our study we found that none of the GRII antagonists normalized the visceral adiposity that is readily observable in ROD treated animals (Table 3). We propose that it is likely that GRII antagonism inhibits GC-induced lipolysis (110, 401) or off-target non-genomic effects that may indirectly increase GC tissue action (402), thereby promoting visceral adiposity. Moreover, increased 11β-HSD1 activity in adipose tissue has been linked to obese and/or insulin resistant individuals (403). Our ROD model demonstrates increased 11β-HSD1 content in visceral fat compared to controls. RU486 attenuates 11β-HSD1 content (Figure 5), contradicting the idea that an increase in GC activity results in more visceral adiposity as RU486 treated animals had similar visceral adiposity to the ROD treated animals. Therefore, we propose that the increase in visceral adiposity with RU486 is due to the anti-lipolytic effects of increased insulin levels. Insulin is an anabolic hormone that down-regulates non-genomic actions of GCs (lipolysis) (110, 404) thereby promoting increased adiposity. Together these data suggest that although GRII antagonism does not lower visceral adiposity it may decrease lipolytic

GC action in the adipose tissue of RU486 treated rats, in part indicating a lesser risk of developing adiposity-induced abnormalities.

Previously we have shown that ROD treatment results in increased islet 11β-HSD1 content as well as elevated GSIS in isolated islets (350). RU486 administration to insulin secreting cells *in vitro* reverses β-cell dysfunction through improvements in insulin biosynthesis, release and content (164) as well as β-cell [Ca2+]i response to glucose (165). Our study confirms these results as we show that RU486 and C113176 normalize GSIS compared to controls whereas C108297 has similar GSIS compared to ROD animals (Figure 6). This is the first study to report the effects of selective GRII antagonists on *ex vivo* islet GSIS. We observe that C113176 is an effective antagonist on GC action in the islet and it normalizes GSIS whereas C108297 does not demonstrate the same result. More studies are required *in vitro* to replicate and further investigate the mechanisms of C113176 action on GSIS.

It is evident that GCs play a major role in whole body physiology (151) and reducing their action can help eliminate some unwanted effects. Although RU486 binds to the GRII with high affinity (0.3 nM) it also binds with high affinity to the progesterone receptor, resulting in endometrial wall thickening causing early disruption to pregnancy in females (reviewed in, (267)). Therefore, selective GRII antagonists have a major advantage over non-selective antagonists and presently there is a significant effort underway to find replacements for non-selective GRII blockers (277). More experiments need to be completed before the best antagonist is identified but in our study we consistently see that one compound, C113176, attenuate diabetes symptoms. The

advantage of C113176 is that it binds to the GRII with excellent affinity (0.28 nM) and does not bind significantly to ER, AR, PR or MR (data obtained through personal communications with Corcept Therapeutics Inc.). It has been found to be more potent than C108297 in functional TAT (tyrosine amino transferase) *in vitro* assays that measure inhibition of dexamethasone induced activity in HepG2 cells and ratH4 cells (Corcept Therapeutics Inc.). For example, in HepG2 cells, the Ki values for C108297 and C113176 are 25 and 11 nM, and in rat H4 cells, the Ki values are 14 and 4 nM, respectively (Corcept Therapeutics Inc.). Compounds such as C108297 are described as having some beneficial effects in inhibiting GC action. However, C108297 does not completely reverse adverse GC effects in our ROD model. Perhaps, as previously described (278), this antagonist may actually work as a partial agonist, which could account for some of the results presented.

This study describes the various metabolic and morphologic outcomes of administering selective and non-selective GRII antagonists to our rodent model of ROD. We show that in comparison to RU486, the compound C113176 provides many therapeutic advantages over C108297 in ROD animals. C113176 helps to attenuate fasting hyperglycemia, insulin resistance and improves AIR, and pancreatic β-cell response. It may be a reasonable alternative medication to help patients suffering from Cushing's syndrome and other diseases associated with elevated GCs. Although C113176 did not completely normalize all complications of diabetes, it did provide clear benefits without any observable adverse effects. Thus, C113176 may be a good alternative to the non-selective GRII antagonist RU486.

Table 1. Corticosterone concentrations, absolute and relative food intake.

	Control		ROD		RU486		C113176		C108297	
	Day 7	**Day 14**	**Day 7**	**Day 14**	**Day 7**	**Day 14**	**Day 7**	**Day 14**	**Day 7**	**Day 14**
Corticosterone (ng/ml)	169±50^{a}	61±30^{a}	623±38^{b}	537±41^{b}	611±61^{b}	401±65^{b}	711±63^{bc}	637±58^{b}	442±61^{b}	344±60^{b}
	Day 10		**Day 10**		**Day 10**		**Day 10**		**Day 10**	
Food Intake (g)	20.9±0.6^{a}		24.0±1.2^{b*}		26.3±1.0^{b}		21.1±1.3^{a}		20.3±1.6^{a}	
Food Intake (kcal/g/BM)	0.23±0.4^{a}		0.46±0.02^{b}		0.40±0.01^{c}		0.40±0.02^{c}		0.40±0.03^{c}	

Note: BM= Body Mass. Different letters denote statistical significance, $p<0.05$, n=6-10. The * indicates that a significant difference was performed by a student's unpaired t-test. All values are mean ± SE.

Table 2. Fed and fasting glucose, insulin, insulin area under the curve (AUC) and non-esterified fatty acids (NEFAs) concentrations on day 12.

	Control	ROD	RU486	C113176	C108297
Fed Blood Glucose (mM)	6.6±0.2^{a}	20.6±1.4^{b}	9.5±1.3^{a}	20.7±1.3^{b}	23.6±2.3^{b}
Fasted Blood Glucose (mM)	4.8±0.2^{a}	21.0±0.6^{b}	6.2±0.1^{ac}	8.8±1.6^{c}	14.0±1.6^{d}
Fasted Insulin (ng/ml)	0.85±0.16^{a}	6.75±0.58^{b}	3.64±0.15^{c}	6.46±1.04^{b}	5.22±0.73^{b}
Insulin AUC	60.6±14.6^{a}	84.4±30.8^{ab}	174.0±37.6^{b}	95.0±49.9^{ab}	94.5±41.4^{ab}
Fasted NEFAs (mM)	0.45±0.03^{a}	1.08±0.07^{b}	0.49±0.05^{a}	1.10±0.15^{b}	1.06±0.12^{b}

Note: Insulin area under the curve (AUC) was measured relative to individual basal insulin concentrations. Different letters denote statistical significance, $p<0.05$, n=6-10. All values are means ± SE.

Table 3. Anthropometric data for epididymal fat pad, liver, heart, epitrochlearis, soleus and tibialis anterior mass (g/kg of body mass).

	Control	ROD	RU486	C113176	C108297
Epididymal Fat Pad (g/kg)	15.9±0.7^{a}	25.0±1.7^{b}	26.3±0.7^{b}	26.4±1.6^{b}	23.3±1.5^{b}
Liver (g/kg)	38.3±1.1^{a}	74.0±3.5^{b}	43.1±2.8^{a}	62.8±4.5^{b}	73.4±4.8^{b}
Heart (g/kg)	2.6±0.1^{a}	4.1±0.2^{b}	2.9±0.1^{a}	3.6±0.1^{c}	4.0±0.1^{bc}
Epitrochlearis (g/kg)	0.13±0.01^{a}	0.09±0.01^{b}	0.13±0.01^{a}	0.11±0.01^{ab}	0.14±0.02^{a}
Soleus (g/kg)	0.34±0.01^{a}	0.45±0.03^{b}	0.38±0.02^{ab}	0.41±0.02^{b}	0.44±0.02^{b}
Tibialis Anterior (g/kg)	1.61±0.05^{a}	1.51±0.08^{a}	1.54±0.04^{a}	1.88±0.06^{a}	1.55±0.07^{a}

Note: Different letters denote statistical significance, $p<0.05$, n=6-10. All values are means ± SE.

Figure Captions

Figure 1. C113176 treatment maintains body mass while RU486 increases body mass with ROD treatment. Animal body mass (g) were recorded every two days for 10 days as a measure of fold change from day 0, pellet surgery (A). Animal body mass on day 10 were measured as a percent change of body mass from day 0 (B). The dotted line (100%) represents no change in body mass from day 0. Arrow indicates that 2 days after pellet surgeries respective antagonists or vehicle were administered at 80 mg/kg/day to each treatment group. Bars that do not share similar letters denote statistical significance, $p<0.05$, one-way ANOVA using Tukey's post-hoc test. n=7-10. All values are means ± SE.

Figure 2. Glucose intolerance and acute insulin response (AIR) is improved with RU486 and C113176 treatment. Fasting (basal, 0 minutes) and stimulated blood glucose (mM) were measured at 5, 15, 30, 60, 90 and 120 minutes post oral glucose gavage using a handheld glucometer (A). Glucose area under the curve (AUC) was calculated based on fasting blood glucose of control animals (B). To measure insulin capacity acute insulin response (AIR) was measured by the difference in insulin levels between fasting insulin and 15 minutes post glucose gavage (C). Negative values represent a decrease in insulin response, indicating impairment in insulin secretion. Bars that do not share similar letters denote statistical significance, $p<0.05$, one-way ANOVA using Tukey's post-hoc. A student's unpaired t-test was performed between controls and ROD, C108297 and C113176 groups (C). n=7-10. All values are means ± SE.

Figure 3. Peripheral insulin sensitivity and β-cell function is enhanced with RU486 and C113176 administration. Fasting (basal, 0 minutes) and blood glucose levels (mM) were measured at 5, 10, 20 and 30 minutes post insulin i.p. injection using a handheld glucometer (A). HOMA-IR index was used to measure whole-body insulin resistance (B). HOMA-β index was used to measure pancreatic β-cell function (C). Bars that do not share similar letters denote statistical significance, $p<0.05$ one-way ANOVA using Tukey's post-hoc test. n=7-10. All values are means ± SE.

Figure 4. Fat accumulation is normalized with RU486 in skeletal muscle and liver cross sections. To determine fat content in skeletal muscle, tibialis anterior muscle was dissected and stained with a neutral lipid stain (Oil Red O) (A-E). Cross sections of liver were also stained with Oil Red O to measure lipid content (F-J).

Figure 5. 11β-HSD1 content in visceral fat is attenuated with RU486 treatment but not with C113176 or C108297 treatment. 11β-HSD1 content was measured in epididymal fat pads to represent visceral adipose tissue and expressed relative to α-tubulin content. Bars that do not share similar letters denote statistical significance, $p<0.05$ one-way ANOVA using Tukey's post-hoc test. n=6. All values are means ± SE.

Figure 6. Glucose stimulated insulin secretion (GSIS) was normalized with RU486 and C113176 treatment. GSIS in isolated islets was measured in low (2.8 mM) and high

(16.7 mM) glucose media for 1 hour incubations expressed as ng/ml/islet/hour. Bars that do not share similar letters denote statistical significance, $p<0.05$ one-way ANOVA using student's unpaired t-test. n=3-7. All values are means ± SE.

Figure 1.

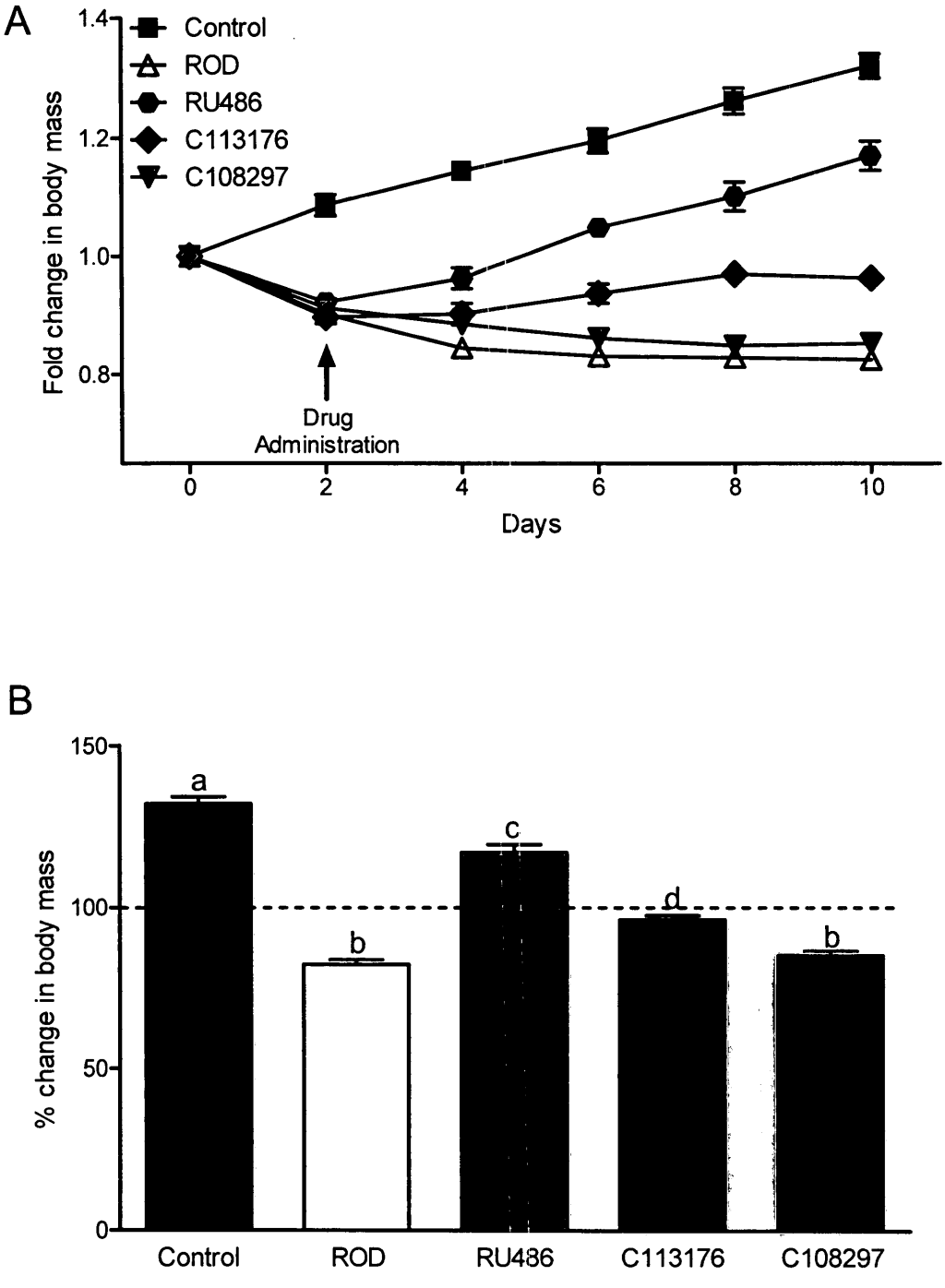
A
Control
ROD
RU486
C113176
C108297
Fold change in body mass
1.4
1.2
1.0
0.8
Drug
Administration
0
2
4
6
8
10
Days
B
% change in body mass
150
100
50
0
a
b
c
d
b
Control
ROD
RU486
C113176
C108297

Figure 2.

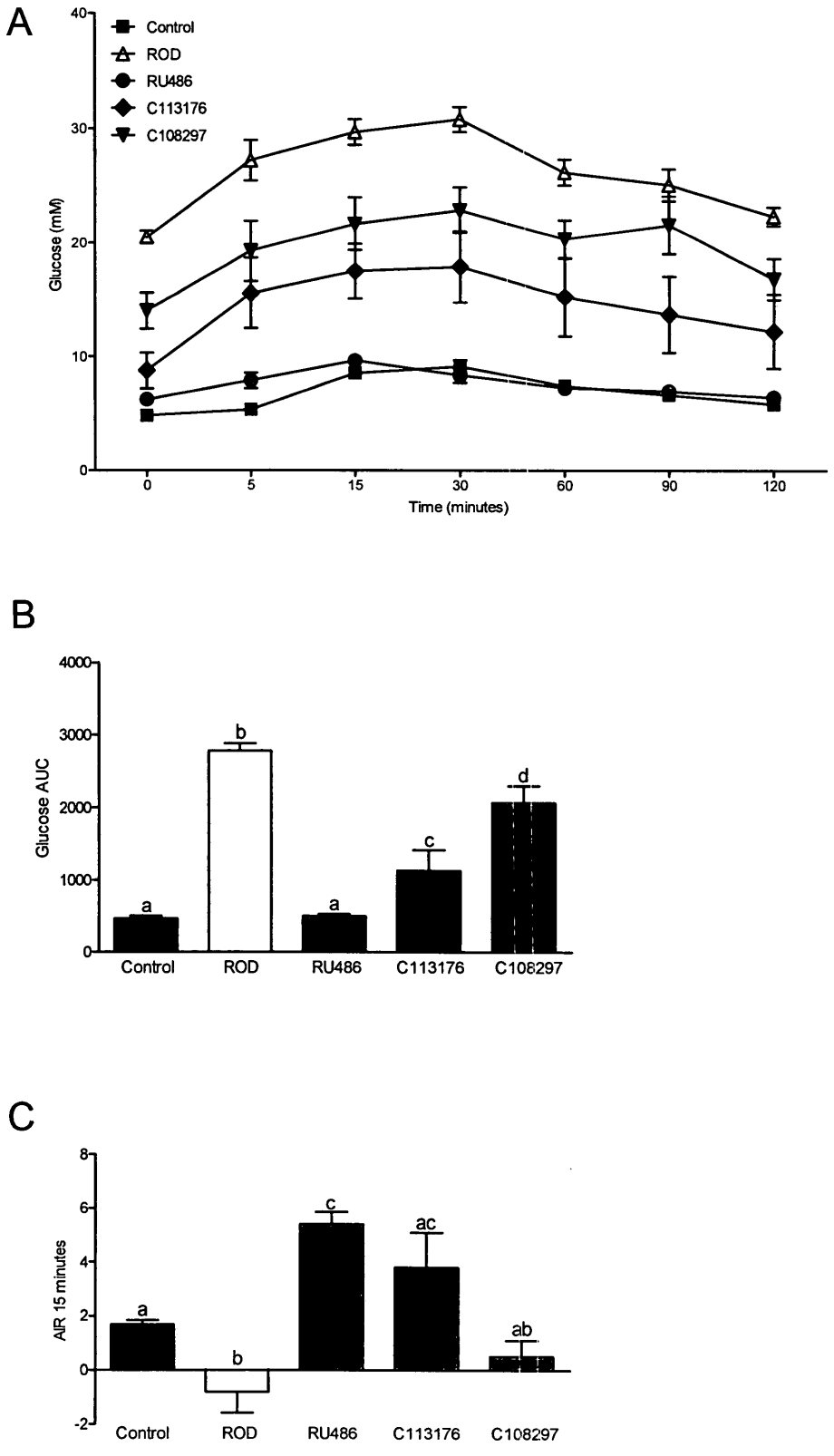
A
Control
ROD
RU486
C113176
C108297
Glucose (mM)
Time (minutes)
0
5
15
30
60
90
120
B
Glucose AUC
a
b
a
c
d
Control
ROD
RU486
C113176
C108297
C
AIR 15 minutes
a
b
c
ac
ab
Control
ROD
RU486
C113176
C108297

Figure 3.

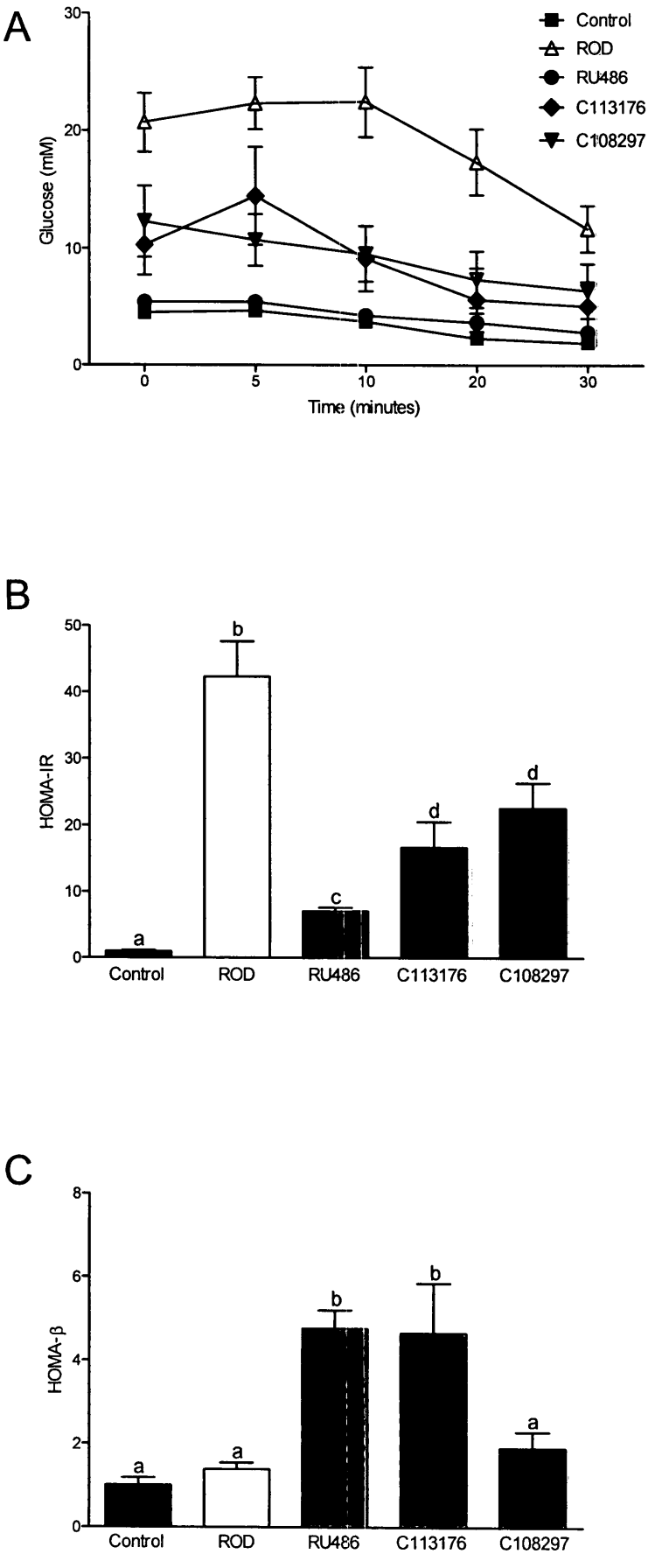
A
Control
ROD
RU486
C113176
C108297
Glucose (mM)
Time (minutes)
B
HOMA-IR
a
b
c
d
d
Control
ROD
RU486
C113176
C108297
C
HOMA-β
a
a
b
b
a
Control
ROD
RU486
C113176
C108297

Figure 4.

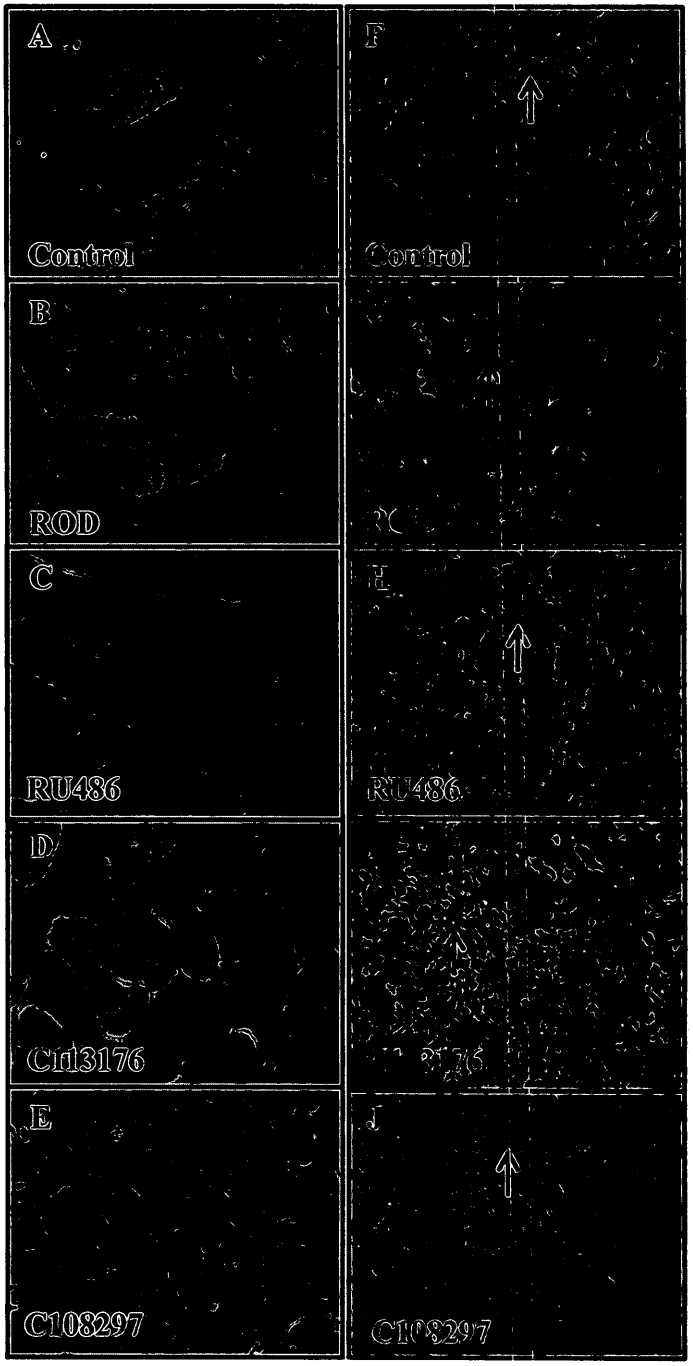
A
Control
F
Control
B
ROD
C
RU486
D
Ctrl3176
E
C108297
C108297

Figure 5.

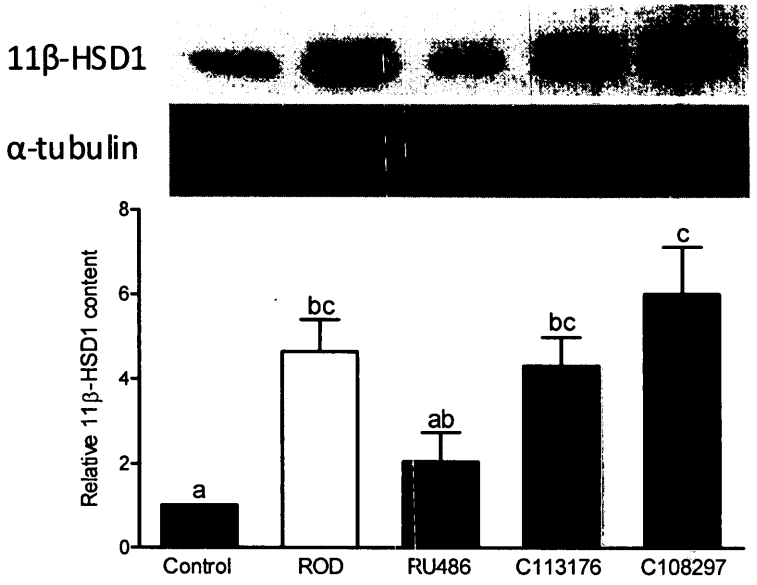

Figure 6.

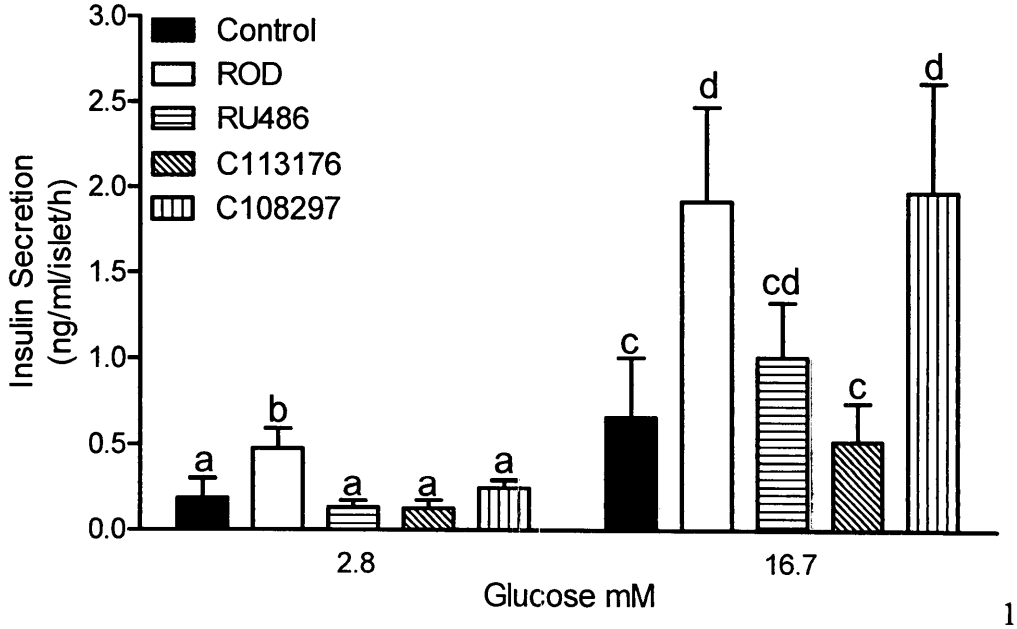

design an effective rodent model of diabetes that produced a similar metabolic profile to humans with T2DM. Using young healthy male Sprague-Dawley rats, we developed a model of elevated GCs brought on by slow release corticosterone (400 mg) and a HFD (60% of calories from fat) that induced rapid-onset diabetes (ROD) within 1-2 weeks from the start of the treatment. Through administration of exogenous GCs, we ameliorated GCs diurnal pattern and continuously elevated GCs to peak levels at all times. We demonstrated that ROD induced a plethora of symptoms that included decreased body mass gains, despite increased levels of food intake, lower glycolytic muscle mass, increased visceral adiposity, hepatic steatosis, muscle lipid deposition, hyperglycemia, hyperinsulinemia, dyslipidemia, and severe insulin resistance. We also showed that visceral and subcutaneous fat depots from GC treated animals expressed relatively more 11β-HSD1 mRNA expression than placebo animals, indicating increased adipose GC exposure, a mechanism contributing to whole-body impaired metabolic function. Interestingly, the ROD phenotype was not obtainable when elevated GCs and HFD were administered independently, and was only present when GCs and HFD were given simultaneously. Overall, manuscript #1 introduced a new cost effective and novel rodent model that paralleled similar symptoms experienced in individuals with T2DM. The study's results provided insight into the idea that elevated GCs and HFD act together to cause severe insulin resistance that overwhelms islet adaptation. Furthermore, the development of this rodent model of disease facilitates future investigations of various therapeutic approaches (i.e., pharmacological and exercise therapies) that act to help reduce or reverse ROD development. Therefore, future successful therapeutic

interventions may be appropriately applied to help protect or prevent T2DM development in individuals.

The findings from manuscript #1 demonstrated that elevated GCs and HFD synergistically imposed severe insulin resistance that overwhelmed islet function, leading to overt hyperglycemia. Therefore, the focus of manuscript #2 was to specifically investigate the role of elevated GCs and HFD on pancreatic islet function to understand mechanisms of impaired islet compensation. GCs are known to interfere with the signalling pathways of various insulin secretagogues and insulin gene synthesis; however, the exact mechanisms are still not clear (151). GCs administered *in vitro* to rodent islets induce major islet and β-cell dysfunction within a short period to time (1-6 hours), dose depending (3, 161). In contrast, acute (5 days) and prolonged exogenous GCs (>10 days) *in vivo*, in healthy rodents, with either dexamethasone or hydrocortisone (GC synthetic agonists) showed both unchanged and increased GSIS respectively (166, 335, 405). Interestingly, prolonged (>14 days) GC administration in healthy human subjects who were able to compensate for GC-induced insulin resistance in the short-term, induced impairments in insulin secretion (146, 156). Similarly, prolonged elevations in lipids impair insulin secretion, but results may be dependent on an individual's existing/established insulin sensitivity (140). We demonstrate in manuscript #2 that exogenous GCs and HFD reduces islet glucose responsiveness *in vivo*, despite increases in β-and α-cell areas and insulin secretion. Moreover, we showed that ROD treatment increased GC exposure directly in the islet, through elevated 11β-HSD1 content, which is known to alter insulin secretion (155). Further, we showed that elevated

GC levels, along with dyslipidemia induced lower phosphorylation of PKC content, which suggests a mechanism in which GCs may impair GSIS *in vivo*. We found that ROD treated islets had less insulin storage capacity as well as a lower fold change in GSIS, indicating abnormal islet adaptive mechanisms that cause islet glucose insensitivity. Taken together, manuscript #2 highlighted the effect of ROD on islet function demonstrating that severe insulin resistance induced impaired islet responsiveness, despite increased islet compensation i.e. islet proliferation and hyperinsulinemia. Overall these results demonstrated that elevated GCs and the addition of a HFD induce appropriate islet adaptation, causing overt hyperglycemia. These results suggest that GCs and HFD work synergistically, not independently to cause islet impairments. Therefore, these risk factors should continue to be studied in tandem to further our understanding of T2DM development.

Regular exercise such as voluntary wheel running is known to protect and prevent against the rise in insulin resistance and the metabolic syndrome (406). Exercise in early-life has been shown to improve β-cell function and growth (232). Exercise can reverse T2DM-like symptoms (255), and our laboratory has demonstrated that exercise training, either swimming or wheel running, helps to lower GC excess in ZDF rats and reverse pathological symptoms of T2DM, by improving glycemic control and β-cell function (63, 144, 150). There is little research that has investigated the role of exercise in compromised metabolic conditions, such as situations of elevated GCs. Therefore, the focus of manuscript #3 was to examine the effects of regular exercise on our model of ROD. We found that ROD animals that wheel ran for ~ 4 weeks had lowered glucose

intolerance, visceral adiposity, normalized glycolytic muscle loss, and muscle oxidative capacity. Furthermore, at the level of the pancreas, exercised ROD animals also displayed improved islet glucose responsiveness, β-cell function, and better insulin sensitivity *in vivo*, whereas *ex vivo* they had a normalized GSIS. These results are important, as they are one of the first to demonstrate that regular exercise can help to reverse detrimental effects of hypercortisolemia and dyslipidemia. In contrast to our hypothesis, we found no changes in body weight gain, whole-body insulin resistance or hepatic lipid accumulation with regular exercise and ROD, demonstrating that not all aspects of ROD were reversed or improved with regular exercise. These results show that more studies are necessary to further investigate the impact of exercise and ROD development. For example, a longer exercise protocol may be needed to observe complete prevention of ROD development, or it is possible that the level of GCs is too high for the exercise stimulus to overcome.

Another therapeutic approach to the ROD model was to investigate the effects of pharmacological intervention. Recently RU486, which is a known non-selective GRII antagonist, is used to treat hypercortisolemia. This type of pharmacological therapy reverses symptoms of hyperglycemia, visceral adiposity, depression, and muscle wasting in individuals suffering from hypercortisolemia or Cushing's syndrome, but due to its occupancy with other nuclear receptors, such as the progesterone receptor, it can induce undesirable side effects (276). Recently, the development of selective GRII antagonists has diminished unwanted side effects, but there is little research reported on them. Therefore, the aims of manuscript #4 were as follows; 1) to investigate the effect of GRII antagonists had on ROD development, 2) to determine if selective GRII antagonists, such

as C113176 and C108297, were more effective agents at reversing ROD development than non-selective antagonists, such as RU486. Impressively, RU486 treatment normalized the majority of ROD symptoms, such as body weight loss, impaired glucose tolerance, acute insulin response, insulin resistance, β-cell dysfunction, and hepatic and muscle lipid deposition. The other GRII antagonists did not completely reverse detrimental effects of ROD like RU486; however, C113176 was able to maintain pre-surgery body weight, attenuate hyperglycemia, insulin resistance, and improve acute insulin response, and β-cell function, whereas C108297 only partially improved glycemic control and insulin resistance. Therefore, RU486 was found to be the most effective agent at normalizing the detrimental effects of ROD, but selective GRII antagonists may still be an effective alternative to lowering and protecting against ROD development. Interestingly, no compound that was tested was able to reduce visceral adiposity with ROD treatment, but RU486 was able to lower GC excess, measured by 11β-HSD1 content in epididymal fat depots. In conclusion, lowering GC exposure at the level of the adipose tissue, or other peripheral tissues for that matter, may be an effective way to fully obtain complete glucose and metabolic control, even in states of obesity. Therefore, metabolic dysfunction may not necessarily develop with increased adiposity, but in combination with elevated GCs it can be very detrimental to the body.

Study Limitations

There are several limitations that are highlighted in each study's discussion; however, we have decided to further examine some additional potential limitations that

warrant discussion. Our rodent model of ROD does induce severe glucose intolerance, insulin resistance and insulin insensitivitiy, which are classic symptoms of an individual with T2DM. We have identified that ROD animals demonstrate a diabetogenic phenotype; however, one characteristic that is not a typical symptom of T2DM is the loss in body weight gain due to reduced muscle mass. Some may argue that this is a classic symptom of Cushing's syndrome; however, not all Cushing's syndrome patients have T2DM. The ROD animals do share many symptoms with T2DM individuals, but they could also be categorized as a model of Cushing's syndrome. In addition, the CORT pellet treatment was given to rats at a very young age (6 weeks). It is possible that the effect we are observing in our model may be due to the fact that these animals have decreases in growth hormone and normal body maturation that has an overall affect on body weight gain and muscle mass. Therefore, future studies should be carried out to investigate these hypotheses.

The use of voluntary wheel running as an exercise regime does not normalize all detrimental metabolic effects of ROD treatment. In fact, treadmill running may actually induce a sufficient amount of exercise intensity that may present better improvement to glucose intolerance in the ROD animals than volitional exercise. It is extremely difficult to identify the amount of exercise intensity during a volitional exercise protocol. In addition, there are many differences between animals and their desire to run freely within their cages. For example, some rats run more than others and it is very hard to reverse or encourage this behaviour in low activity rats. We found though our observational studies that rats that ran more had better glucose control than those who did not run at longer

distances. However, it is not possible to quantify the amount of exercise intensity of these rats unless video recordings were in place during exercise protocols. Therefore, we only can measure the distances run by the rats and draw conclusions from these data.

In manuscript #4 we did not utilize a dose response to determine our drug concentration administered to our ROD animals and instead we selected a dose that was previously published in the literature. Therefore, our conclusions in manuscript #4 identify that the selective GRII antagonists only had partial beneficial effects to our ROD model, but perhaps a dose response of the GRII may provide further insight into the true effects of these antagonists. For example, a higher dose of C113176 may conclude that this antagonist may provide more improvements to protect against ROD development than at the lower dose. Also, since our corticosterone pellet induced very high concentrations of corticosterone in the blood, that may not even be attainable in humans, the less potent antagonists such as C113176 and C108297 compared to RU486 may be 'out-competed' by the elevated GC levels, and therefore, appear to have lower efficacy. Therefore, our studies would benefit from studies investigating a dose response to GRII antagonists in ROD development.

Future Directions

There are several pathways that can be followed up with this research. It would be interesting to investigate the effect of prolonged treatment period. Our ROD model only lasts for a 2-week period, which can be considered an acute or short-term protocol. Therefore, it would be interesting to observe the effects of a four or six week treatment

period. Although this would probably require more technical manipulations to the original protocol because experiments that lasted for longer than 2 weeks during a dose response protocol had a lower amount of corticosterone levels by 4 and 6 weeks. It is possible that the pellets did not absorb as well as they did at the beginning of the study and this may need further examination before an understanding of the best way to keep corticosterone levels in the elevated state. In addition, to a prolonged ROD treatment protocol, it would also be interesting to administer pellets to rats that were older than 6 weeks of age. We are unsure whether our results are an effect of supraphysiological levels of corticosterone or if the rats are still very young when they receive the pellets and therefore it may exhibit more pronounced and detrimental phenotype.

It would be interesting to follow β-cell mass during this prolonged treatment period. We demonstrate that β-cell mass is increased with ROD treatment without any increase in apoptosis. Therefore, it would be interesting to investigate whether or not β-cell mass continues to increase with prolonged treatment or whether it starts to decline after a certain point due to elevations in GCs or chronic GC administration.

Another interesting follow-up study to the ROD model would be to observe the effects of replacing the HFD with a SD after a two-week treatment period. It is not known whether the animals would be able to recover from ROD and normalize glucose control or if they would remain in the same metabolic detrimental state due to permanent effects of the ROD treatment.

Although we observe beneifical effects of regular exercise, it is still unclear whether exercise intensity plays a role in reducing ROD development. Therefore, future studies that compare the effects of treadmill and volitional exercise would provide further insight into the role of exercise and ROD development. In addition, we observe beneficial effects of regular exercise and pharmacological intervention via GRII antagonists separately in the ROD model. Therefore, it would be interesting to examine the effects of the combined treatment of regular exercise and the administration of GRII antagonists together. We hypothesize that the combination of both therapeutic interventions would normalize ROD development and prevent glucose metabolism deteriotation.

Summary

Collectively, all of these studies show how elevations in GCs and HFD, when administered in combination, can induce metabolic dysfunction and that a therapeutic approach, such as exercise and pharmacological intervention, can help to attenuate some of these symptoms. This work demonstrates that exogenous GCs and HFD can induce severe levels of peripheral insulin resistance that overwhelms islet function, resulting in hyperglycemia. We also examined the detrimental effects of our treatment and how it adversely affects normal islet capacity in response to increased metabolic demand. Furthermore, this thesis demonstrated the positive metabolic effects of regular exercise on hypercortisolemia and dyslipidemia. Regular exercise decreased visceral adiposity, lowered glucose intolerance, and insulin insensitivity. In addition, RU486 treatment normalized glucose control better than regular exercise on ROD development, despite

having no changes in visceral adiposity. Moreover, we were the first to demonstrate that selective GRII antagonists showed some positive improvements to the metabolic profile of the ROD animals; however, were not as effective as RU486 treatment. Taken together, this dissertation displays the detrimental effects of elevated GCs and HFD in combination on whole-body physiology and islet function, and therapeutic strategies such as exercise and GRII antagonism are sufficient to prevent or even reverse development of ROD.

Lastly, it is extremely important to continue our studies of the effects of GC therapy on glucose metabolism. There are several investigations that are just emerging in the litature that have identified an association between GC therapy use and poor glucose control. Therefore, it should be conveyed more clearly to patients and physicians that this type of treatment can greatly effect glucose and whole-body metabolism. An individual's diet and fat distrubition plays an important part in an individual's healthy metabolism and in combination with elevated administrated GCs can greatly impair glucose homeostasis therefore, patients should be closely monitored.

APPENDICES Chapter 7

A. Extended Methods

Immunohistochemistry Staining Protocol

Materials List

- Xylene
- 100, 95, 70% Ethanol
- H2O2- Z16763
- Methanol
- PBS
- Sodium citrate buffer
- Wax pen-mini pad pen
- Protein blocker
- Primary antibody
- Secondary antibody
- Avidin-Biotin (Vitamin B)
- DAB-Diaminobenzadene
- Microwave
- Hematoxylin
- Plastic trays- VWR-47751-792
- Normal Serum Block SIG-31172-50-Covance signet antibodies
- Nordic Ware #62104> $60.50
- Caspase 3-D175 Rabbit Ab
- Cell Signalling #96615
- Dako Cytomation #A0564
- Labeling Reagent-SIG 322 4295
- Pink Level 2 USA HRP-enzyme conjugated avidin Biotin confer
- Staining apparatus-71430-20-electron microscopy sciences
- Embedding cassettes-simport plastics
- WINLAB 20-Slide Racks> 71430-20 WINLAB 20-Slide Rack, Model LS-20 each 46.00
- WINLAB 20-Slide Rack Carriers>
- Protein Blocker- SIG 31172-50 Covance Signet antibodies-Normal Serum Block

1. De-waxing
    a. Slides must be at room temperature
    b. 3 successive xylene baths 5 min each
    c. In between baths dab rack on paper towel to loose paraffin
2. Rehydration
    a. 100% EtOH 2X 5 min each
    b. 95% EtOH 1X 3 min
    c. 70% EtOH 1X 3 min each
3. Wash Slides
    a. Wash PBS 1X 5 min.
4. Inhibition of Endogenous Peroxidase Activity (3% H202 in PBS)
    a. Make 3% hydrogen peroxide in PBS (5ml 30% hydrogen peroxide in 45ml MEOH). Make fresh daily.
    b. Incubate slides in solution for 30 min at room temperature.
    c. Wash well in running tap H_2O for 5min
5. Protein Blocking (Covance Signet SIG-31172-50; to help decrease nonspecific staining)
    a. Treat sections with Protein Blocker (Blue bottle) for 30 min in humid chamber.
6. Primary Antibody
    a. Shake off excess fluid (shake off protein blocker).
    b. Add 100-400 ul of primary antibody to each section. Negative controls are blocking solution only (in this case, PBS only) RECOMMENDED dilution for cleaved caspase-3 (cell signal #9661 is 1:200). Try 1.33 in 200ul.
    c. Incubation should overnight in the fridge.
8. Wash
    a. Wash in PBS 5X 3 min (moderate shaking).

VERY IMPORTANT STEP!

9. Secondary antibody (biotinylated)
    a. Add 100-400 ul of secondary antibody to each section.
    b. Incubate at room temperature for 30 min.

RECOMMENDED dilution for BIOTINYLATED ANTI-GUINEA PIG (VECTOR BA-1000) is 1:500.

10. Wash
    a. Remove secondary antibody by shaking/tapping your slides.
    b. Wash in PBS 4X 2 min. (moderate shaking).
11. Labelling

a. Add 100-400 ul (1 drop) of labeling reagent (Pink Level 2 USA-HRP (Ultrastreptavidin Horseradish peroxidase; Convance Signet SIG-32242-95)) to each section.
b. Incubate for 30 min at room temperature in humid chamber.

This step here makes the enzyme conjugated avidin-biotin complex for amplification of signal.

12. Wash
    a. Remove labeling reagent by shaking/tapping your slides.
    b. Wash in PBS 4X 2 min. (gentle shaking).

13. DAB (Diaminobenzaden Sigma-Aldrich D4293-50set; please wear gloves as this chemical is TOXIC and CARCINOGENIC)
    a. Prepare DAB by dissolving 1 pellet of DAB and 1 pellet of Urea Hydrogen peroxide in 5 mL of ddH2O. Vortex for 1 min.
    b. Add 100-400 ul of DAB for variable amounts of time (as soon as you see brown on the slides). Should be around 1-3min.

16. Wash
    a. Wash in running tap water (gentle!!).

DO NOT LET THE WATER HIT DIRECTLY ON THE SLIDES!

17. Counterstain with Hematoxylin
    a. Immerse in Mayer's Hematoxylin (Sigma-aldrich MHS1) for 5 sec
    b. Stop staining and wash in running tap water, 5-10 min.

18. Dehydrate Sections
    a. 95% ethanol (2 changes): 10 sec.
    b. 100% ethanol (2 changes): 10 sec.
    c. Xylene (2 changes): 10 sec.

19. Mount coverslips
    a. Remove slides from xylene on paper towel (Let drip little and do this in the fumehood unless you love the smell of xylene).
    b. Add Permount (two drops) adjacent to the sections.
    c. Lay down coverslip gently and try to get rid of any air bubbles.
    d. Use nail polish to seal the coverslip.
    e. Let dry.

Pancreas Profusion and Removal

Materials Checklist for Pancreas Profusion and Removal

- Forceps
- 30ml Syringe with 23g needle
- PE50 tubing (45° angle from one end)
- Scissors
- Hemostats
- Suture (with and without needle)
- EtOH
- Gauze/Tissue
- Ice
- Conicals (50ml)
- Water Bath at 37°C
- Ketamine/HEP-SA
- Insulin Needle

Solution List

All Solutions must be kept on ice

1. Collagenase (Sigma-C6885-1g)

- 4.5-5mg of collagenase (estimate depending on collagenase activity- Start with 4.6mg) per 20mL RPMI without FBS. Each rat needs about 15mL collagenase.

2. RPMI without FBS (Fetal Bovine Serum) (good for 2 weeks after preparation)

- RPMI1640-glutathione-glucose 500mL
- 10mM HEPES 1.19-1.2g
- 1% Penicillin 5mL
- Glucose (50% dextrose) 250mg (0.5mL)

3. RPMI with FBS (good for 2 weeks after preparation)

- RPM1640-glutathione-glucose 500mL
- 10mM HEPES 1.19-1.2g
- 1% Penicillin 5mL
- 7% FBS 37.5mL
- Glucose (50% dextrose) 250mg (0.5mL)

Directions for solutions 2 & 3:

- Mix all
- pH Solution (~7.4) with 10N NaOH
- Filter solution for in vitro culture

4. KREB's Buffer (500ml of H2O)

- 125mM NaCl- 3.6525g
- 4.7mM KCl- 0.1750g
- 1.2mM KH2PO4-0.0816g
- 5 mM NaHCO3- 0.210g
- 2.5 mM CaCl2- 0.1385g
- 2.4 mM MgSO4- 0.144g
- 10 mM Hepes- 1.19g
- 0.1 % BSA- 0.5g

5. Krebs + 10mM HEPES + Glucose + BSA= pH 7.4
   - KREBS + 10mM HEPES 500mL
   - Glucose (50% dextrose) 250mg (0.5mL)
   - BSA 500mg

   (98% electrophoresis Sigma A7906)

6. Insulin Extraction Media

   - 12mM in 70% ETOH
   - 0.18mol/L in 70% ETOH
   - 1.5ml in 98.5 ml of 70% ETOH

Procedure:

1. Rats are anesthetized
2. Abdominal fur is shaved off
3. Alcohol is used to sterilize the shaved area
4. The abdomen is cut open with scissors
5. The aorta is cut in the abdomen and the blood is removed by gauze or tissue
6. The duodenum end of the common bile duct (the other end being underneath the liver) is tied off
7. An incision is made into the common bile duct right below the bifurcation
8. PE50 tubing is inserted into the hole towards down and ~15mL of collagenase solution is injected into the pancreas within 2-2.5minutes
9. The pancreas is removed (entangle the duodenum, then the large intestine; do not cut off the spleen till you remove the whole pancreas).
10. The pancreas is put into 50mL ice cold conical (it is about 5-10mL)

Islet Isolation Method

1. The pancreas is incubated for 20minutes at 37°C with agitation (speed 5 shaking) in water bath
2. Fill to 40mL of RPMI with FBS followed by vigorous shaking for 10sec
3. The mixture is centrifuged at 1600rpm for 4 minutes at 4°C
4. The supernatant is discarded and 20mL of RMPI with FBS is added
5. The mixture is gently shaken to mix the pellet and filtered
6. The filtrate is collected into a new conical

7. The conical and the filter are washed with 20mL RMPI with FBS and the filtrate is put into the same new conical final volume 40mL
8. The mixture is centrifuged at 1200rpm for 4minutes at 4°C
9. The supernatant is discarded
10. 10mL of Histopaque-1077 is added to the pellet
11. The mixture is gently shaken or mixed with 10mL pipette to dissolve the pellet
12. 10mL RMPI without FBS is added gently to the tubing using 10mL pipette (add onto the side of the conical) so that 2 layers are seen
13. The mixture is centrifuged at 2700rpm for 23minutes at 4°C (this step may have to be repeated if there is a lot of crap in the islets)
14. The mixture is poured into a new conical and KREB's solution is added up to 45mL. (Do this step in the fume hood)
15. The mixture is centrifuged at 1400rpm for 3minutes at 4°C
16. The supernatant is discarded
17. The pellet is suspended in 10mL KREB's, pipette well and poured in culture dishes.
18. Another 10mL KREB's is added to the conical washed and back to the same culture dish.
19. The plates are then incubated for 1 hour at 37°C in incubator

For insulin secretion:

Solution: Different glucose concentrations for islet incubation and secretion

For every 0.5L of KREBS (WITHOUT Glucose) + 10mM HEPES, add 05.g BSA (A)
Then add glucose per 100mL of (A) as follows:

- 252mg glucose: 2.8mM (same as solution 4) (Glucose 180.16)
- 495.5mg glucose: 5.5mM
- 999.8mg glucose: 11.1mM
- 2.252g glucose: 25mM

Each rat will require 12 test tubes (triplicate of each concentration):

- To 3 tubes, add 1mL of 2.8mM
- To 3 tubes, add 1mL of 5.5mM
- To 3 tubes, add 1mL of 11.1mM
- To 3 tubes, add 1mL of 25mM-To 12 welled plates

1. ~10 islets of medium size are sucked up with a P70 pipette and added to each tube (or plate) of different glucose concentrations
2. The tubes are incubated in an incubator at 37°C 5% CO2 and 95% O2 for 2hours

3. Plates were removed from the incubator and placed in the fridge for 15minutes to stop insulin secretion and 500ul of media was collected and put into -20°C freezer until further analysis.
4. An additional 10 islets x3 were isolated from same animal and were extracted in (12mM HCL in 70% ETOH) overnight and then spun down in microcentrifuge for 10min at 7.0 rpm. Supernatant was collected and then put into the -20°C freezer.

Leftover islets→ Collected for Western Analysis

1. Collect islets in Eppendorf tubes
2. Spin at 7000rpm for 30sec to get islet pellets
3. Discard supernatant
4. Add 1mL PBS
5. Spin and discard ALL LIQUID
6. Snap freeze with liquid nitrogen and store at -80°C

Islet Isolations Protocol

After islets have been isolated and re-suspended into KREB'S Buffer keep on ice

1. Pick up islets using a syringe needle or pipette and a dissecting microscope
2. Transfer islets with a little acinar and debris as possible to petri dish (1000cm^2) with KREB's buffer
3. Once all islets have been isolated then discard original petri dish and pick islets again and place into 35mm dish with 2ml of KREB's buffer
4. Once all islets have been transferred then remove supernatant (not all of it, do not want to dry islets out)
5. Wash with 1ml of RPMI with FBS and glucose buffer
6. Remove supernatant
7. Wash 1 ml of RPMI with FBS and glucose buffer
8. Add a final 2 ml of RPMI with FBS and glucose buffer and let islets rest in incubator over night

Glucose Stimulated Insulin Secretion (GSIS)

1. Remove 35mm plate from incubator and examine islets
2. Remove RPMI buffer and wash 2 x with KREB-Low glucose (LG)
3. Incubate islets in low glucose for 30minutes
4. Remove supernatant and incubate ~10 islets for 1 hour in LG (1ml) in 12 well plate
5. Remove 500ul of supernatant from each well of the plate and add to eppendorf tube. Spin tube for 1,200 rpm for 5minutes and transfer to new tube and freeze -20 until further analysis

6. Wash each well x 2 with KREB-HG and add 1ml KREB-HG and leave plate in incubator for 1 hour
7. Remove 500ul of supernatant and spin for 1,200rpm for 5 minutes and transfer to new eppendorf tube and transfer to a new tube and freeze at -20 until further analysis
8. Wash remaining islets with PBS in dish x 2
9. Remove most of supernatant and add lysis ethanol buffer (1ml). Pick up islets in each well and transfer to eppendorf tube.
10. Sonicate sample for 15seconds x 2 and spin at 12,000 rpm x 5 minutes at 4°C.
11. Transfer sample to new eppendorf tube and put into freezer until further analysis

Note: If you require more time after islet isolation until GSIS experiments then replace ~1ml of RPMI each day to avoid contamination

If isolating islets for protein concentrations then do not spin down at a high speed. Only 1,200rpm for 5 minutes and then wash in PBS.

NEFA Protocol (96 Well Microplate)

1. Prep materials: All samples (diluted if necessary) approx 100ml distilled water, NEFA standard solution, colour Reagent A and B mixed and ready to use.
2. Make the standards:
• Place 5 µL of DW in the top left well.
• Run the standard solutions in triplicates, at 2.5 µL, 5 µL and 10 µL
3. Pipette 5 µL of samples (in duplicates) into the remaining wells
4. Pipette 200 µL of colour reagent A to every well
• Mix well (approximately 30 seconds) and then incubate at 37 ^{0}C for 5 minutes
5. Measure the absorbance of each well at 550 nm
• Referred to as absorb 1. This serves as a baseline reading to compare the second absorbance reading (taken later)
6. Pipette 100 µL of colour reagent B to every well
• Mix well and then incubate at 37 ^{0}C for 5 minutes
7. Measure the absorbance of each well (550 nm)
• Referred to as absorb 2

Example:

	1	2	3	4
A	Blank	10 µL	Sp 4	
B	2.5 µL	10 µL	Sp 4	
C	2.5 µL	Sp 1	Etc…	
D	2.5 µL	Sp 1		
E	5 µL	Sp 2		
F	5 µL	Sp 2		
G	5 µL	Sp 3		
H	10 µL	Sp 3		

Excel Work

Note: In order to transfer the data from (insert computer program name here) into excel, select File – Export. Excel should come up, then select plates (tab on sub menu, top left of spreadsheet area) and click on the name of your plate, default M550.

Making the standard curve

1. Calculate the final absorbance: Absorb 2 – Absorb 1 for each well.

2. Subtract all final absorbance from the final absorbance of the blank (well 1) to obtain an adjusted absorbance

3. Take an average of the adjusted final absorbance for each concentration and plot the data on a graph (absorbance vs concentration). Obtain a regression equation ($r2 > 0.98$)

4. Calculate the calculated concentration by plugging in the standard absorbance into the regression equation and solving for x.

Calculating the sample concentrations

1. Calculate the final and adjusted absorbance for each sample and take an average (same procedure as with the standards)

2. Calculate the concentration (in mEq/L) by plugging in the absorbance values into the regression equation (as y) and solving for x.

3. To obtain the concentration in mmol/L, divide the concentration in mEq/L by the 5 μL standard concentration.

ORO Staining Protocol

(Modified from Koopman et al. 2001)

Preparation

1. Glass jars (enough for side samples, and x2 for staining, then place in freezer day of)
2. Beakers – 2x ddH_2O, 2x ORO, 1 fixation
3. ORO stock
4. Formaldehyde fixation
5. Put ORO stock in 37°C water bath

ORO stock solution

500mg ORO

100ml 60% triethyl-phosphate (or 40ml ddH_2O + 60ml 100% triethyl-phosphate)

Mix while on heat

Staining

1. Mix ORO solution 12ml stock ORO + 8ml ddH_2O (x4 for ~18 slides, always a 3:2 ratio)
2. Stir while on low heat
3. Double filter ORO solution in 37°C incubator with circular filter paper

Formaldehyde fixation

3ml 37% formaldehyde + 27ml ddH_2O

1. Determine slides to be used, serial (every other, use ones in between for fiber typing), with fiber type that worked.
2. Place slides in glass jars while in freezer.
3. Bring the jars with slides out of freezer and allow to defrost together.
5. Pour formaldehyde solution into jar (pour on the side and not directly into the slides), formaldehyde fixation for 60 minutes.
6. Prepare a beaker of ddH_2O.
7. When formaldehyde fixation is complete, wash slides in ddH_2O with 3 dips into the beaker.
8. Dab dry and place in empty jar.
9. Pour filtered ORO into the side of the jar, stain for 30min.
10. Prepare a beaker of ddH_2O.
11. When ORO stain is complete, wash the slides in ddH_2O by dipping three times into beaker.
12. Dab and allow slides to dry (standing up to prevent drops settling on section).
13. Place a drop of crystal mount (small white bottle) on slide, no bubbles, and allow it to run over section – allow drying standing up.

Muscle Fiber Type Staining

(modified from Ogilvie & Feeback. Stain Technology, 65:231-241, 1990)

Solutions

1. Toluidine Blue Stain (0.1% solution) – stock
   - 0.250 g Toluidine Blue
   - 250 ml ddH2O
2. CaCl Rinse (1% solution) – fresh every time
   - 4 g CaCl Dihydrate
   - 400 ml ddH2O
3. Tris Rinse – fresh every time
   - 270 ml ddH2O
   - 4.356 g Trisma Base [Tris (hydroxymethyl) Aminomethane]
   - 0.936 g CaCl Dihydrate

   pH to 7.8 with HCl – prior to adjustment pH is ~10.53

   top volume to 360 ml with ddH2O

4. Incubation Medium – fresh every time
   - 120 ml ddH2O
   - 0.632 g Glycine
   - 0.672 g CaCl2 Anhydrous
   - 0.608 NaCl
   - 3.04 ml of 0.1 g/ml NaOH (add about 2 pellets, add last)

   pH should be ~10.67 – pH to 9.4 with HCl…use concentrated and step down to diluted HCl if necessary – better to leave pH ~9.60 because adding ATP lowers pH

   top up volume to 160 ml with ddH2O

   add 0.32 of ATP just before use; readjust pH to 9.40 with HCl or NaOH (1/2=0.16g).

5. Pre-Incubation Medium – fresh every time
   - 120 ml ddH2O
   - 0.748 Potassium Acetate
   - 0.416 g CaCl2 Dihydrate

   pH prior to adjustment should be ~7.69 – lower to 4.45 with Glacial Acetic Acid – take ~half of the solution and then lower the pH of the other half to approximately 4.30 – 4.32 *** these pH's work well with mouse muscle,

however the original article develops this technique on human muscle and suggests a pH of 4.50 for pre-incubation.

Protocol

1. run slides in duplicate/triplicate; one set in each pre-incubation medium. Incubate for 4 min
2. 3 Tris rinses at 2 min each. Add ATP to incubation medium and correct pH during these rinses
3. incubatin medium for 25 min in the 37oC water bath
4. 3 CaCl rinses (pour in, swish-swish pour out, don't want the slides sitting in Ca for too long)
5. prepare beakers of Toluidine Blue, 2x ddH2O, 95% ethanol, 100% ethanol and glass jars of citri-solv.
6. stain slides for 15-20 seconds in Toluidine Blue solution (dip slide into beaker of stain).
7. rinse slides in ddH2O to remove excess TB solution (~5 seconds/dips).
8. dehydrate sections with 5 dips ni 95% ethanol; 5 dips in 100% ethanol.
9. clear the slides in 2 changes of citri-sol for 5 min each
10. allow slides to dry; mount cover slips with permount (no bubbles, place a drop beside section and push over with cover slip).

Important Notes

Make solutions accurately – pH and concentrations are critical. Success is not guranteed but sloppy solutions

Succinate Dehydrogenase (SDH) Stain

Protocol modified from: http://neuromuscular.wustl.edu/pathol/histol/sdh.htm, http://www.nottingham.ac.uk/pathology/protocols/sdh.html

Solutions

1. Phosphate buffer (100mM, pH 7.6)
   -Solution A (1.36g KH2PO4/100ml): 12ml
   -Solution B (1.42g Na2HPO4/100ml): 88ml

2. Nitroblue tetrazolium (NBT) stock – freeze into 2ml aliquots
   -Phosphate buffer: 100ml
   -KCN [SIGMA 207810]: 6.5mg (CAS 151-50-8)
   -EDTA: 185mg
   -Nitroblue tetrazolium [SIGMA N6876]: 100mg

3. Succinate stock (500mM sodium succinate) – ideally, make fresh
   -sodium succinate [SIGMA S2378]: 2.7g
   -ddH2O: 20ml

4. Incubation medium – mix just before use, keep out of strong light
   -NBT stock: 2ml
   -Succinate stock: 0.2ml
   -Phenazine methosulphate [SIGMA P9625]: 0.7mg (one small crystal)

Sections

Fresh or pre-cut frozen sections, 8-10μm thick

Incubation Protocol

1. Incubation time varies by species/tissue
   -rat TA/soleus @ room temp ~ 5min (less than mouse).
   -mouse TA/gastrocnemius @ room temp ~ 10 min
2. Use a pipette to cover section with incubation medium, and immediately cover.
3. Incubate then remove some liquid with pipette, rest will be removed with wash.
4. Rinse 3 times in ddH2O
5. Dehydrate 70%, 80%, 100% ethanol (~ 10s each)
6. Clear in xylene ~ 2min
7. Allow samples to air dry, permount and apply coverslip.

Result

Sites of mitochondrial SDH activity have blue/purple precipitate

B. Extended Results

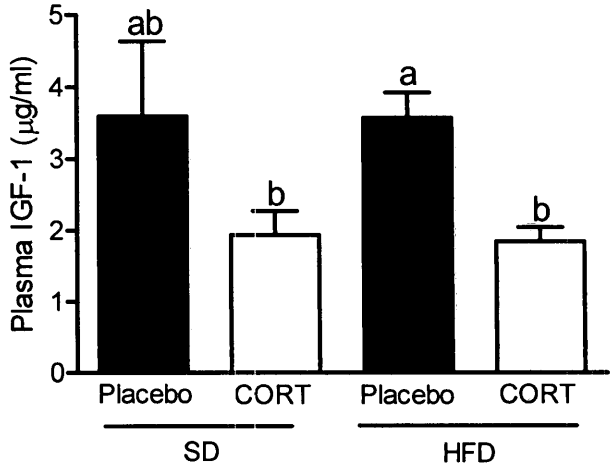

Figure1. Plasma insulin-like growth hormone-1 (IGF-1) measured in placebo- and corticosterone-treated rats with and without HFD. Both CORT-treated rat groups had lower IGF-1 levels compared to placebo-HFD animals and tended to have lower levels compared to placebo-SD animals. Lower IGF-1 levels indicate retarded growth or cell proliferation. Different letters denote statistical significance between groups. A student's unpaired t-test was performed to determine statistical significant with a criterion of $p<0.05$. N=3 for each group. Values are means ± SE.

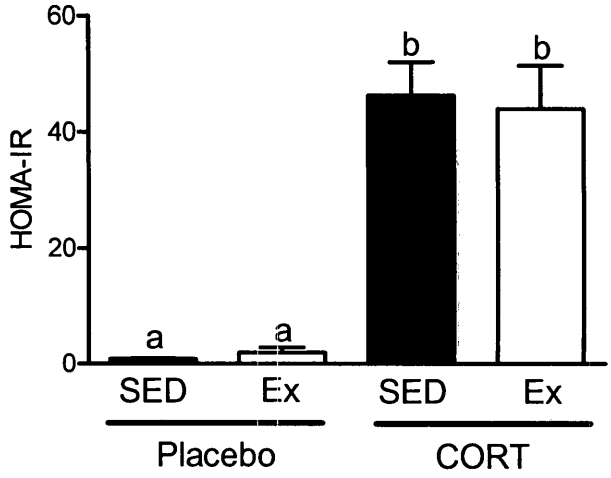

Figure2. Peripheral insulin resistance measured by HOMA-IR index in sedentary placebo-HFD and ROD animals, as well as in exercised placebo-HFD and ROD animals. Insulin resistance increased by ~ 40-fold in CORT-SED (ROD) and CORT-EX (exercise) animals compared to placebo-SED and EX animals ($p<0.001$). No differences were found between CORT-SED and EX animals indicating that 4 weeks of volitional wheel running were not sufficient to improve peripheral insulin action ($p>0.05$). Different

letters denote statistical significance between groups. A two-way ANOVA test was performed to determine statistical significant using Tukey's post-hoc criterion. N=6-10 for each group. Values are means ± SE.

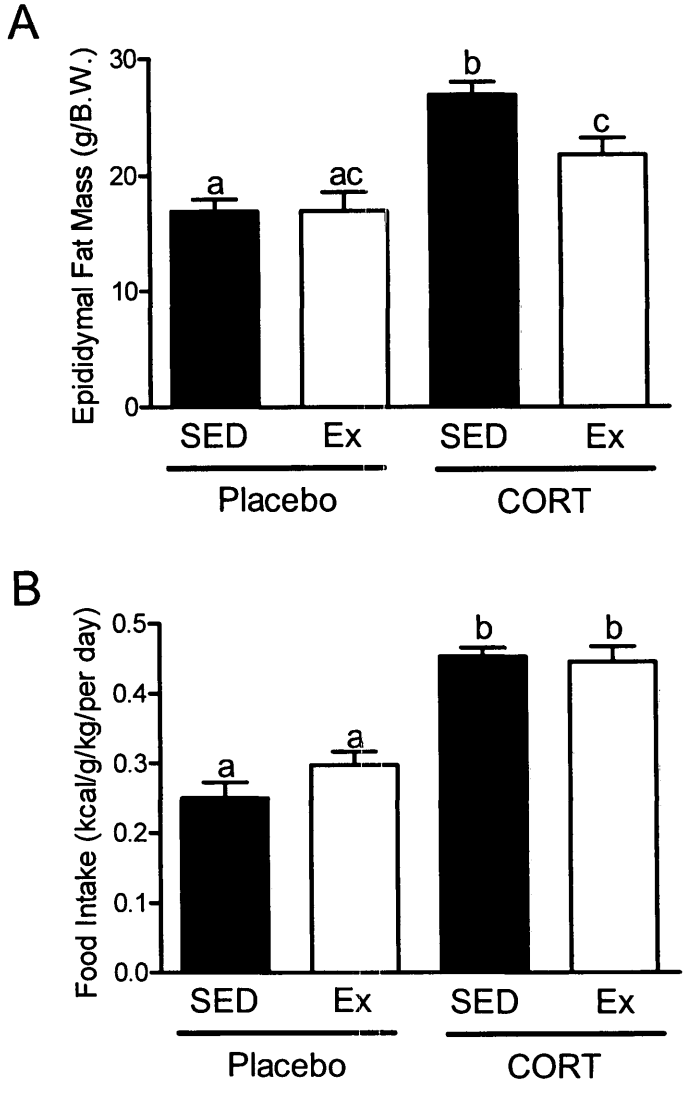

Figure3. Visceral adiposity measured by epididymal fat depots (A) and averaged food intake (B) after 10 days of ROD treatment in placebo and CORT-treated animals with and without exercise. Voluntary exercise lowered visceral adiposity in CORT-treated animals, while CORT-SED treatment increased visceral adiposity compared to placebo-treated animals ($p<0.05$). Food intake was increased with CORT-treated animals, regardless of exercise or not, compared to placebo-treated animals ($p<0.05$). Different letters denote statistical significance between groups. A two-way ANOVA test was performed to determine statistical significant using Tukey's post-hoc criterion. N=6-10 for each group. Values are means ± SE.

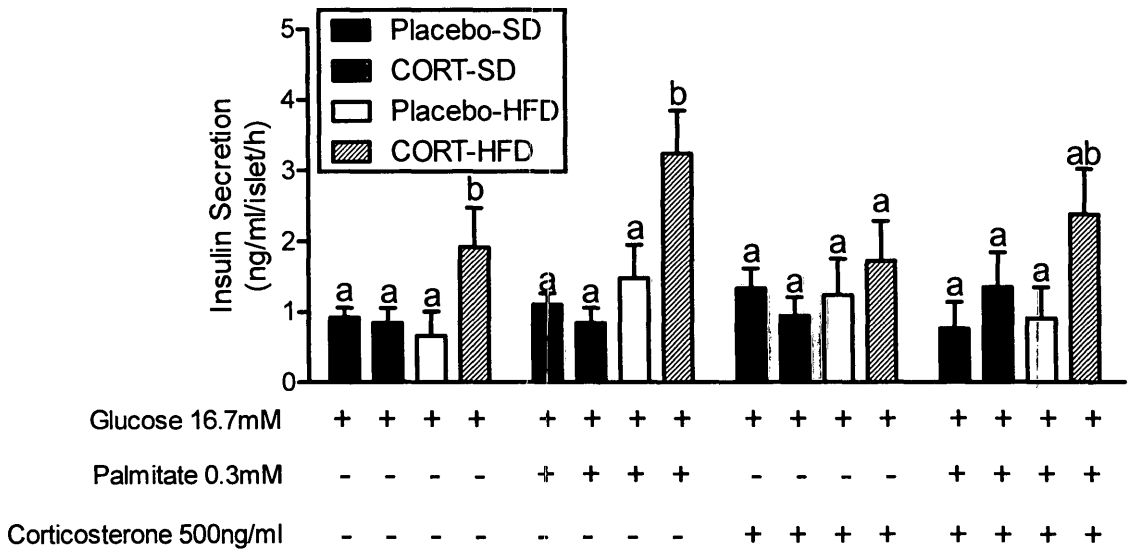

Figure4. Absolute glucose stimulated insulin secretion (GSIS, ng/ml/islet/hour) with palmitate, and corticosterone in isolated islets from placebo-SD, -HFD, CORT-SD and –HFD animals. High glucose media (16.7 mM) increased GSIS in CORT-HFD islets compared to all other treatment groups ($p<0.05$). Similarly, palmitate (0.3 mM) augmented GSIS in CORT-HFD islets compared to all other treatment groups ($p<0.05$). No differences were found between treatment groups when corticosterone (500 ng/ml) was added to the media ($p>0.05$). However, CORT-HFD islets had lower GSIS when corticosterone was added to the media compared to when palmitate was in the media ($p<0.05$). No differences were found when corticosterone and palmitate were added to the media ($p>0.05$). Different letters denote statistical significance between groups. A two-way ANOVA test was performed to determine statistical significant using Tukey's post-hoc criterion. N=5-6 for each group. Values are means ± SE.

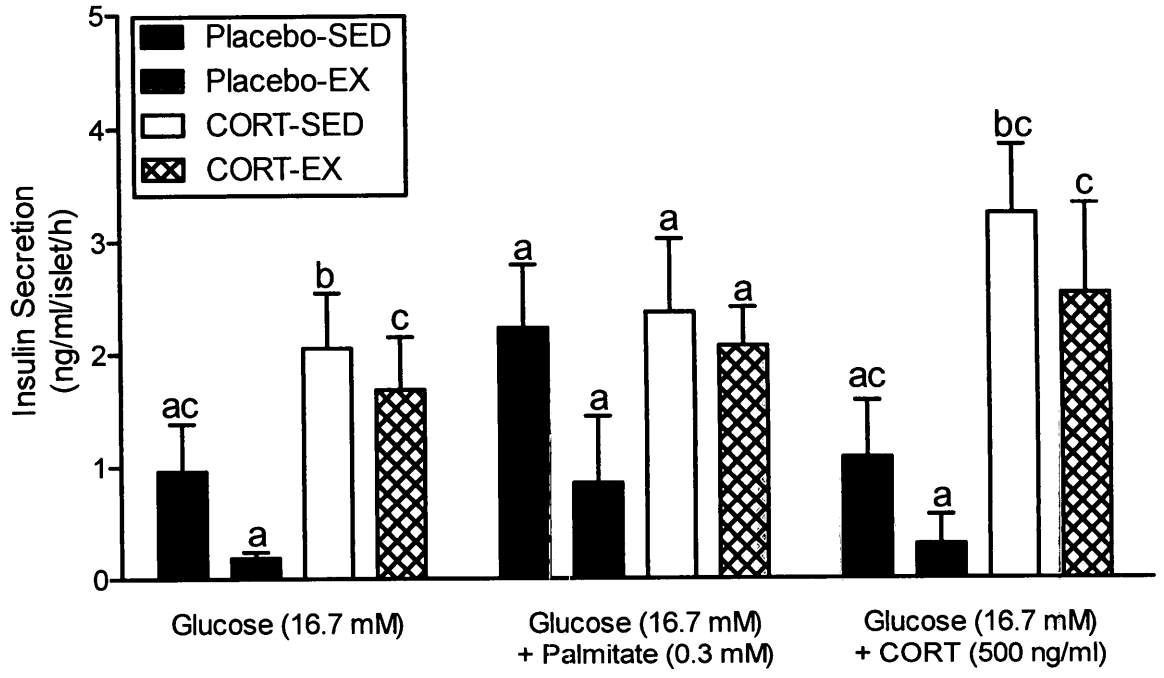

Figure5. Absolute glucose stimulated insulin secretion (GSIS, ng/ml/islet/hour) with palmitate, and corticosterone in isolated islets from placebo-SED, -EX, CORT-SED and –EX animals. High glucose media (16.7 mM) increased GSIS in CORT-SED and -EX islets compared to placebo-SED and -EX ($p<0.05$). Palmitate (0.3 mM) in the media showed no differences in GSIS between treatment groups ($p>0.05$) whereas corticosterone (500 ng/ml) added to the media increased GSIS in CORT-SED and –EX islets ($p<0.05$). Different letters denote statistical significance between groups. A two-way ANOVA test was performed to determine statistical significant using Tukey's post-hoc criterion. N=3-5 for each group. Values are means ± SE.

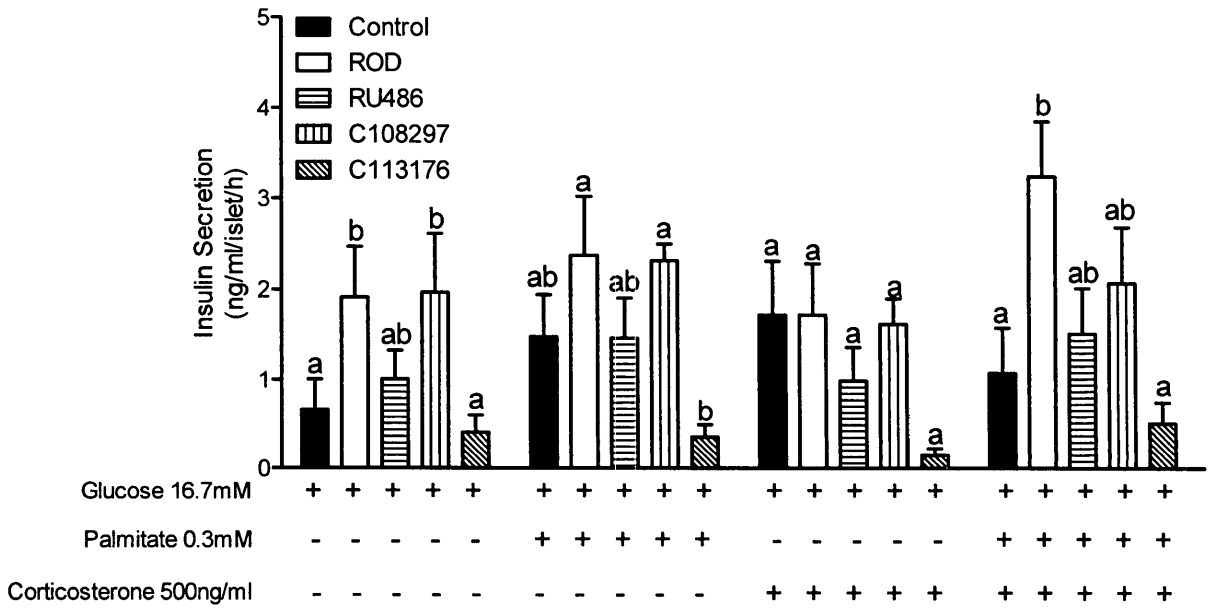

Figure6. Absolute glucose stimulated insulin secretion (GSIS, ng/ml/islet/hour) with palmitate, and corticosterone in isolated islets from placebo-HFD (control), ROD, ROD+RU486, ROD+C108297, ROD+C113176-treated animals. High glucose media (16.7 mM) increased GSIS in ROD and C108297 islets ($p>0.05$), but no differences were found between RU486 and C113176 islets compared to control islet ($p<0.05$). Palmitate (0.3 mM) in the media showed no differences in GSIS between treatment groups ($p>0.05$) except in C113176 treated islets that had the lowest GSIS compared to all treatment groups. Corticosterone (500 ng/ml) added to the media showed no differences in GSIS in between any treatment groups ($p>0.05$). ROD treatment increased GSIS when both palmitate and corticosterone were added to the media ($p<0.05$), but no differences were found between the other treatment groups ($p>0.05$). Therefore, these results suggest that ROD and C108297 treatment impair glucose sensitivity, GSIS was elevated with these two treatments, but RU486 and C113176 normalize GSIS. Different letters denote statistical significance between groups. A one-way ANOVA test was performed to determine statistical significant using Tukey's post-hoc criterion. N=5 for each group. Values are means ± SE.

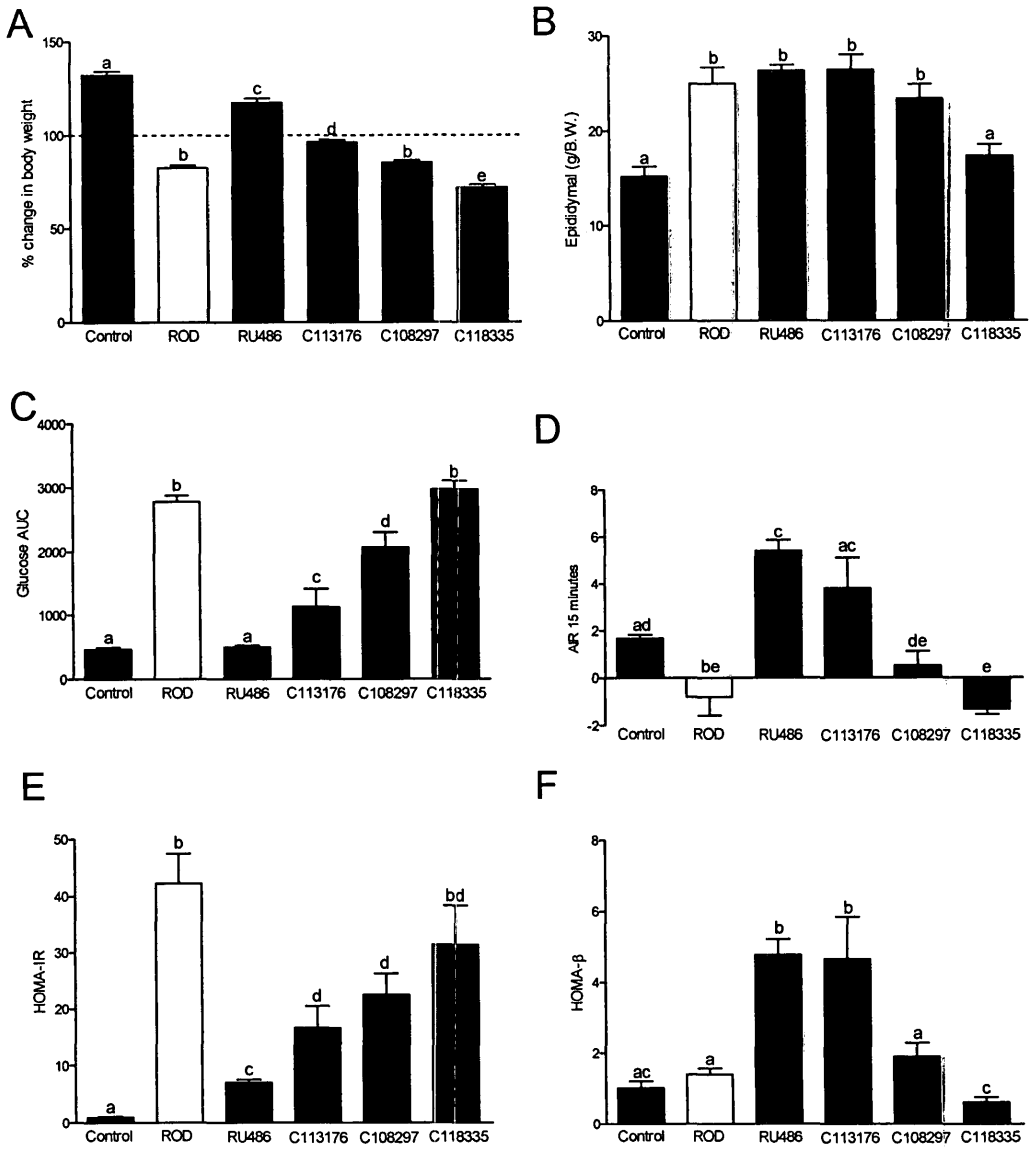

Figure7. Additional data to manuscript #4 that investigated the effect of the selective GRII antagonist, C118335 (80 mg/kg/day) in ROD animals on body weight (A), visceral adiposity (B), glucose tolerance (C), acute insulin response (AIR) (D), insulin resistance (E) and β-cell function (F). Body weight gain was significantly decreased (~30%) with C118335 treatment at 10 day of ROD treatment compared to all other treatment groups ($p<0.05$). Visceral adiposity was normalized with C118335 treatment, whereas it was elevated with all other antagonists compared to controls ($p<0.05$). Glucose intolerance, as measured by glucose under the curve (AUC) was increased with C118335 administration compared to controls ($p<0.05$) and was similar to ROD treated animals. AIR was lowered with C118335 similar to levels of ROD and C108297 treatment compared to controls ($p<0.05$). Peripheral insulin resistance, as measured by HOMA-IR index was elevated with C118335 treatment compared to

controls ($p<0.05$) and similar to ROD and C108297 treatment. β-cell function as measured by HOMA-β index was lower in C118335 treated animals compared to all other treatment groups ($p<0.05$). Overall, these results indicate that C118335 treatment did not improve ROD development, although it did decrease visceral adiposity. Different letters denote statistical significance between groups. A one-way ANOVA test was performed to determine statistical significant using Tukey's post-hoc criterion. N=6-10 for each group. Values are means ± SE.

Table 1. Adrenal, absolute soleus and plantaris muscle mass (mg/kg of body mass).

	Placebo		CORT	
	SD	HFD	SD	HFD
Adrenal	0.09±0.004	0.10±0.01	0.04±0.007*	0.04±0.004*
Soleus	0.14±0.01	0.18±0.01*	0.12±0.01*	0.13±0.01*
Plantaris	0.31±0.01	0.30±0.02	0.21±0.02*	0.17±0.02*

Note: The * indicates significance from placebo-SD.

C. Additional Contributions

The following papers were published during the completion of this dissertation:

A) First Authorships:

1. **Beaudry, J.L.** and Riddell, M.C. Effects of Glucocorticoids and Exercise on Pancreatic β Cell Function and Diabetes Development. *Diabetes Metab Res Rev.* 2012 Oct;28(7):560-73. doi: 10.1002/dmrr.2310.
2. **Beaudry, J.L.,** D'souza, A., and Riddell, M.C. Physical activity and stress: Peripheral physiological adaptations. Chapter 23. Section 6: Psychological Stress. (In: *Routledge Handbook of Physical Activity and Mental Health*, Editor: Mark Hamer).
3. **Beaudry, J.L.,** and Riddell, M.C. Stress and Pancreatic β Cell Function: Role of Glucocortoids, Exercise and Glucolipotoxicity. In: *Beta Cells: Functions, Pathology and Research*, Editor: Sarah E. Gallagher © 2010 Nova Science Publishers, Inc., ISBN: 978-1-61761-212-1.

B) Second Authorships:

1. Pereira, S., Yu, W.Q., Frigolet, M.E., **Beaudry, J.L.,** Shpilberg, Y., Park, E., Dirlea, C., Nyomba, B.L., Riddell, M.C., Fantus, I.G., Giacca, A. Effectiveness of sodium salicylate in preventing fat-induced hepatic insulin resistance depends on duration of plasma free fatty acid elevation. J Endocrinol. 2013 Mar 15;217(1):31-43. doi: 10.1530/JOE-12-0214.
2. Shikatani, E., Trifonova, A., Krylova, A., Szigiato, A., **Beaudry, J.,** Riddell, M.C., and Haas, T.L. Inhibition of proliferation, migration and proteolysis contribute to corticosterone mediated inhibition of angiogenesis. PLoS One. 2012. 7(10):e46625. doi: 10.1371/journal.pone.0046625. Epub 2012 Oct 2.
3. D'souza, A., **Beaudry, J.L.,** Szigiato, A., Trumble, S., Snook, L., Bonen, A., Giacca, A., and Riddell, M.C. Consumption of a High Fat Diet Rapidly Exacerbates the Development of Fatty Liver Disease that Occurs with Chronically Elevated Glucocorticoids. Am J Physiol Gastrointest Liver Physiol. 2012 Apr 15;302(8):G850-63.

References

1. **Sherwin R, Jastreboff AM** 2012 Year in diabetes 2012: The diabetes tsunami. J Clin Endocrinol Metab 97:4293-4301

2. **Rafacho A, Marroqui L, Taboga SR, Abrantes JL, Silveira LR, Boschero AC, Carneiro EM, Bosqueiro JR, Nadal A, Quesada I** 2010 Glucocorticoids in vivo induce both insulin hypersecretion and enhanced glucose sensitivity of stimulus-secretion coupling in isolated rat islets. Endocrinology 151:85-95

3. **Lambillotte C, Gilon P, Henquin JC** 1997 Direct glucocorticoid inhibition of insulin secretion. An in vitro study of dexamethasone effects in mouse islets. J Clin Invest 99:414-423

4. **Kim A, Miller K, Jo J, Kilimnik G, Wojcik P, Hara M** 2009 Islet architecture: A comparative study. Islets 1:129-136

5. **Gromada J, Franklin I, Wollheim CB** 2007 Alpha-cells of the endocrine pancreas: 35 years of research but the enigma remains. Endocr Rev 28:84-116

6. **Cabrera O, Berman DM, Kenyon NS, Ricordi C, Berggren PO, Caicedo A** 2006 The unique cytoarchitecture of human pancreatic islets has implications for islet cell function. Proc Natl Acad Sci U S A 103:2334-2339

7. **Weir GC, Bonner-Weir S** 2013 Islet beta cell mass in diabetes and how it relates to function, birth, and death. Ann N Y Acad Sci 1281:92-105

8. **Weir GC, Bonner-Weir S** 2004 Five stages of evolving beta-cell dysfunction during progression to diabetes. Diabetes 53 Suppl 3:S16-21

9. **Grodsky GM, Batts AA, Bennett LL, Vcella C, McWilliams NB, Smith DF** 1963 Effects of Carbohydrates on Secretion of Insulin from Isolated Rat Pancreas. Am J Physiol 205:638-644

10. **English PJ, Coughlin SR, Hayden K, Malik IA, Wilding JP** 2003 Plasma adiponectin increases postprandially in obese, but not in lean, subjects. Obes Res 11:839-844

11. **Grodsky GM, Curry D, Landahl H, Bennett L** 1969 Further studies on the dynamic aspects of insulin release in vitro with evidence for a two-compartmental storage system. Acta Diabetol Lat 6 Suppl 1:554-578

12. **Seino S, Shibasaki T, Minami K** 2011 Dynamics of insulin secretion and the clinical implications for obesity and diabetes. J Clin Invest 121:2118-2125

13. **Kahn SE** 2001 Clinical review 135: The importance of beta-cell failure in the development and progression of type 2 diabetes. J Clin Endocrinol Metab 86:4047-4058

14. **Jensen MV, Joseph JW, Ronnebaum SM, Burgess SC, Sherry AD, Newgard CB** 2008 Metabolic cycling in control of glucose-stimulated insulin secretion. Am J Physiol Endocrinol Metab 295:E1287-97

15. **Beaudry JL, Riddell MC** 2012 Effects of glucocorticoids and exercise on pancreatic beta-cell function and diabetes development. Diabetes Metab Res Rev 28:560-573

16. **Dunning BE, Gerich JE** 2007 The role of alpha-cell dysregulation in fasting and postprandial hyperglycemia in type 2 diabetes and therapeutic implications. Endocr Rev 28:253-283

17. **Gaisano HY, Macdonald PE, Vranic M** 2012 Glucagon secretion and signaling in the development of diabetes. Front Physiol 3:349

18. **Barg S** 2003 Mechanisms of exocytosis in insulin-secreting B-cells and glucagon-secreting A-cells. Pharmacol Toxicol 92:3-13

19. **Gaisano HY, Leung YM** 2008 Pancreatic islet alpha cell commands itself: secrete more glucagon! Cell Metab 7:474-475

20. **Bogan JS** 2012 Regulation of glucose transporter translocation in health and diabetes. Annu Rev Biochem 81:507-532

21. **Sasaki K, Cripe TP, Koch SR, Andreone TL, Petersen DD, Beale EG, Granner DK** 1984 Multihormonal regulation of phosphoenolpyruvate carboxykinase gene transcription. The dominant role of insulin. J Biol Chem 259:15242-15251

22. **Wang Y, Nakagawa Y, Liu L, Wang W, Ren X, Anghel A, Lutfy K, Friedman TC, Liu Y** 2011 Tissue-specific dysregulation of hexose-6-phosphate dehydrogenase and glucose-6-phosphate transporter production in db/db mice as a model of type 2 diabetes. Diabetologia 54:440-450

23. **Tsatsoulis A, Mantzaris MD, Bellou S, Andrikoula M** 2013 Insulin resistance: an adaptive mechanism becomes maladaptive in the current environment - an evolutionary perspective. Metabolism 62:622-633

24. **Topp BG, Atkinson LL, Finegood DT** 2007 Dynamics of insulin sensitivity, -cell function, and -cell mass during the development of diabetes in fa/fa rats. Am J Physiol Endocrinol Metab 293:E1730-5

25. **Shanik MH, Xu Y, Skrha J, Dankner R, Zick Y, Roth J** 2008 Insulin resistance and hyperinsulinemia: is hyperinsulinemia the cart or the horse? Diabetes Care 31 Suppl 2:S262-8

26. **Emerging Risk Factors Collaboration, Sarwar N, Gao P, Seshasai SR, Gobin R, Kaptoge S, Di Angelantonio E, Ingelsson E, Lawlor DA, Selvin E, Stampfer M, Stehouwer CD, Lewington S, Pennells L, Thompson A, Sattar N, White IR, Ray KK, Danesh J** 2010 Diabetes mellitus, fasting blood glucose concentration, and risk of vascular disease: a collaborative meta-analysis of 102 prospective studies. Lancet 375:2215-2222

27. **Gaede P, Lund-Andersen H, Parving HH, Pedersen O** 2008 Effect of a multifactorial intervention on mortality in type 2 diabetes. N Engl J Med 358:580-591

28. **Burr JF, Rowan CP, Jamnik VK, Riddell MC** 2010 The role of physical activity in type 2 diabetes prevention: physiological and practical perspectives. Phys Sportsmed 38:72-82

29. **Bonner-Weir S** 2001 Beta-Cell Turnover: its Assessment and Implications. Diabetes 50 Suppl 1:S20-4

30. **Butler AE, Janson J, Soeller WC, Butler PC** 2003 Increased beta-cell apoptosis prevents adaptive increase in beta-cell mass in mouse model of type 2 diabetes: evidence for role of islet amyloid formation rather than direct action of amyloid. Diabetes 52:2304-2314

31. **Sachdeva MM, Stoffers DA** 2009 Minireview: Meeting the demand for insulin: molecular mechanisms of adaptive postnatal beta-cell mass expansion. Mol Endocrinol 23:747-758

32. **Karam JH, Grodsky GM, Forsham PH** 1963 Excessive insulin response to glucose in obese subjects as measured by immunochemical assay. Diabetes 12:197-204

33. **Mitrakou A, Kelley D, Mokan M, Veneman T, Pangburn T, Reilly J, Gerich J** 1992 Role of reduced suppression of glucose production and diminished early insulin release in impaired glucose tolerance. N Engl J Med 326:22-29

34. **Perreault L, Bergman BC, Hunerdosse DM, Playdon MC, Eckel RH** 2009 Inflexibility in Intramuscular Triglyceride Fractional Synthesis Distinguishes Prediabetes From Obesity in Humans. Obesity (Silver Spring)

35. **Porte D,Jr** 1996 Normal physiology and phenotypic characterization of beta-cell function in subjects at risk for non-insulin-dependent diabetes mellitus. Diabet Med 13:S25-32

36. **Polonsky KS** 2000 Dynamics of insulin secretion in obesity and diabetes. Int J Obes Relat Metab Disord 24 Suppl 2:S29-31

37. **Vinik A** 2007 Advancing therapy in type 2 diabetes mellitus with early, comprehensive progression from oral agents to insulin therapy. Clin Ther 29 Spec No:1236-1253

38. **Butler AE, Janson J, Bonner-Weir S, Ritzel R, Rizza RA, Butler PC** 2003 Beta-cell deficit and increased beta-cell apoptosis in humans with type 2 diabetes. Diabetes 52:102-110

39. **Marchetti P, Bugliani M, Boggi U, Masini M, Marselli L** 2012 The pancreatic beta cells in human type 2 diabetes. Adv Exp Med Biol 771:288-309

40. **Finegood DT, McArthur MD, Kojwang D, Thomas MJ, Topp BG, Leonard T, Buckingham RE** 2001 Beta-cell mass dynamics in Zucker diabetic fatty rats. Rosiglitazone prevents the rise in net cell death. Diabetes 50:1021-1029

41. **Rahier J, Guiot Y, Goebbels RM, Sempoux C, Henquin JC** 2008 Pancreatic beta-cell mass in European subjects with type 2 diabetes. Diabetes Obes Metab 10 Suppl 4:32-42

42. **Hanley SC, Austin E, Assouline-Thomas B, Kapeluto J, Blaichman J, Moosavi M, Petropavlovskaia M, Rosenberg L** 2010 {beta}-Cell mass dynamics and islet cell plasticity in human type 2 diabetes. Endocrinology 151:1462-1472

43. **Rahier J, Goebbels RM, Henquin JC** 1983 Cellular composition of the human diabetic pancreas. Diabetologia 24:366-371

44. **French SA, Story M, Jeffery RW** 2001 Environmental influences on eating and physical activity. Annu Rev Public Health 22:309-335

45. **Sampey BP, Vanhoose AM, Winfield HM, Freemerman AJ, Muehlbauer MJ, Fueger PT, Newgard CB, Makowski L** 2011 Cafeteria diet is a robust model of human metabolic syndrome with liver and adipose inflammation: comparison to high-fat diet. Obesity (Silver Spring) 19:1109-1117

46. **Davidson EP, Coppey LJ, Calcutt NA, Oltman CL, Yorek MA** 2010 Diet-induced obesity in Sprague-Dawley rats causes microvascular and neural dysfunction. Diabetes Metab Res Rev 26:306-318

47. **Shortreed KE, Krause MP, Huang JH, Dhanani D, Moradi J, Ceddia RB, Hawke TJ** 2009 Muscle-specific adaptations, impaired oxidative capacity and maintenance of contractile function characterize diet-induced obese mouse skeletal muscle. PLoS One 4:e7293

48. **Asagami T, Belanoff JK, Azuma J, Blasey CM, Clark RD, Tsao PS** 2011 Selective Glucocorticoid Receptor (GR-II) Antagonist Reduces Body Weight Gain in Mice. J Nutr Metab 2011:235389

49. **Fraulob JC, Ogg-Diamantino R, Fernandes-Santos C, Aguila MB, Mandarim-de-Lacerda CA** 2010 A Mouse Model of Metabolic Syndrome: Insulin Resistance, Fatty Liver and Non-Alcoholic Fatty Pancreas Disease (NAFPD) in C57BL/6 Mice Fed a High Fat Diet. J Clin Biochem Nutr 46:212-223

50. **Buettner R, Scholmerich J, Bollheimer LC** 2007 High-fat diets: modeling the metabolic disorders of human obesity in rodents. Obesity (Silver Spring) 15:798-808

51. **Muntzel MS, Al-Naimi OA, Barclay A, Ajasin D** 2012 Cafeteria diet increases fat mass and chronically elevates lumbar sympathetic nerve activity in rats. Hypertension 60:1498-1502

52. **Pranprawit A, Wolber FM, Heyes JA, Molan AL, Kruger MC** 2013 Short-term and long-term effects of excessive consumption of saturated fats and/or sucrose on metabolic variables in Sprague Dawley rats: a pilot study. J Sci Food Agric

53. **Ginter E, Simko V** 2012 Type 2 diabetes mellitus, pandemic in 21st century. Adv Exp Med Biol 771:42-50

54. **Johnson AM, Olefsky JM** 2013 The origins and drivers of insulin resistance. Cell 152:673-684

55. **Eckel RH, Kahn SE, Ferrannini E, Goldfine AB, Nathan DM, Schwartz MW, Smith RJ, Smith SR** 2011 Obesity and type 2 diabetes: what can be unified and what needs to be individualized? J Clin Endocrinol Metab 96:1654-1663

56. **Chrousos GP** 2009 Stress and disorders of the stress system. Nat Rev Endocrinol 5:374-381

57. **Seligman ME, Beagley G** 1975 Learned helplessness in the rat. J Comp Physiol Psychol 88:534-541

58. **Rosmond R** 2005 Role of stress in the pathogenesis of the metabolic syndrome. Psychoneuroendocrinology 30:1-10

59. **De Kloet ER, Vreugdenhil E, Oitzl MS, Joels M** 1998 Brain corticosteroid receptor balance in health and disease. Endocr Rev 19:269-301

60. **Habib KE, Gold PW, Chrousos GP** 2001 Neuroendocrinology of stress. Endocrinol Metab Clin North Am 30:695-728; vii-viii

61. **Miller DB, O'Callaghan JP** 2002 Neuroendocrine aspects of the response to stress. Metabolism 51:5-10

62. **Seckl JR, Morton NM, Chapman KE, Walker BR** 2004 Glucocorticoids and 11beta-hydroxysteroid dehydrogenase in adipose tissue. Recent Prog Horm Res 59:359-393

63. **Campbell JE, Kiraly MA, Atkinson DJ, D'souza AM, Vranic M, Riddell MC** 2010 Regular exercise prevents the development of hyperglucocorticoidemia via adaptations in the brain and adrenal glands in male Zucker diabetic fatty rats. Am J Physiol Regul Integr Comp Physiol 299:R168-76

64. **Luger A, Deuster PA, Kyle SB, Gallucci WT, Montgomery LC, Gold PW, Loriaux DL, Chrousos GP** 1987 Acute hypothalamic-pituitary-adrenal responses to the stress of treadmill exercise. Physiologic adaptations to physical training. N Engl J Med 316:1309-1315

65. **Chrousos GP** 1998 Ultradian, circadian, and stress-related hypothalamic-pituitary-adrenal axis activity--a dynamic digital-to-analog modulation. Endocrinology 139:437-440

66. **Weitzman ED, Fukushima D, Nogeire C, Roffwarg H, Gallagher TF, Hellman L** 1971 Twenty-four hour pattern of the episodic secretion of cortisol in normal subjects. J Clin Endocrinol Metab 33:14-22

67. **Windle RJ, Wood SA, Shanks N, Lightman SL, Ingram CD** 1998 Ultradian rhythm of basal corticosterone release in the female rat: dynamic interaction with the response to acute stress. Endocrinology 139:443-450

68. **Chrousos GP** 1995 The hypothalamic-pituitary-adrenal axis and immune-mediated inflammation. N Engl J Med 332:1351-1362

69. **Aguilera G** 1994 Regulation of pituitary ACTH secretion during chronic stress. Front Neuroendocrinol 15:321-350

70. **Whitnall MH** 1988 Distributions of pro-vasopressin expressing and pro-vasopressin deficient CRH neurons in the paraventricular hypothalamic nucleus of colchicine-treated normal and adrenalectomized rats. J Comp Neurol 275:13-28

71. **Bartanusz V, Jezova D, Bertini LT, Tilders FJ, Aubry JM, Kiss JZ** 1993 Stress-induced increase in vasopressin and corticotropin-releasing factor expression in hypophysiotrophic paraventricular neurons. Endocrinology 132:895-902

72. **Antoni FA** 1993 Vasopressinergic control of pituitary adrenocorticotropin secretion comes of age. Front Neuroendocrinol 14:76-122

73. **Rivier C, Rivier J, Mormede P, Vale W** 1984 Studies of the nature of the interaction between vasopressin and corticotropin-releasing factor on adrenocorticotropin release in the rat. Endocrinology 115:882-886

74. **Abou-Samra AB, Harwood JP, Catt KJ, Aguilera G** 1987 Mechanisms of action of CRF and other regulators of ACTH release in pituitary corticotrophs. Ann N Y Acad Sci 512:67-84

75. **Gallo-Payet N, Cote M, Chorvatova A, Guillon G, Payet MD** 1999 Cyclic AMP-independent effects of ACTH on glomerulosa cells of the rat adrenal cortex. J Steroid Biochem Mol Biol 69:335-342

76. **Simpson ER, Waterman MR** 1988 Regulation of the synthesis of steroidogenic enzymes in adrenal cortical cells by ACTH. Annu Rev Physiol 50:427-440

77. **Andrews RC, Walker BR** 1999 Glucocorticoids and insulin resistance: old hormones, new targets. Clin Sci (Lond) 96:513-523

78. **Reul JM, de Kloet ER** 1985 Two receptor systems for corticosterone in rat brain: microdistribution and differential occupation. Endocrinology 117:2505-2511

79. **De Kloet R, Wallach G, McEwen BS** 1975 Differences in corticosterone and dexamethasone binding to rat brain and pituitary. Endocrinology 96:598-609

80. **Reul JM, van den Bosch FR, de Kloet ER** 1987 Differential response of type I and type II corticosteroid receptors to changes in plasma steroid level and circadian rhythmicity. Neuroendocrinology 45:407-412

81. **de Kloet ER, Joels M, Holsboer F** 2005 Stress and the brain: from adaptation to disease. Nat Rev Neurosci 6:463-475

82. **Itoi K, Mouri T, Takahashi K, Murakami O, Imai Y, Sasaki S, Yoshinaga K, Sasano N** 1987 Suppression by glucocorticoid of the immunoreactivity of corticotropin-releasing factor and vasopressin in the paraventricular nucleus of rat hypothalamus. Neurosci Lett 73:231-236

83. **Tasker JG, Di S, Malcher-Lopes R** 2006 Minireview: rapid glucocorticoid signaling via membrane-associated receptors. Endocrinology 147:5549-5556

84. **Clark BJ, Wells J, King SR, Stocco DM** 1994 The purification, cloning, and expression of a novel luteinizing hormone-induced mitochondrial protein in MA-10 mouse Leydig tumor cells. Characterization of the steroidogenic acute regulatory protein (StAR). J Biol Chem 269:28314-28322

85. **Keeney DS, Jenkins CM, Waterman MR** 1995 Developmentally regulated expression of adrenal 17 alpha-hydroxylase cytochrome P450 in the mouse embryo. Endocrinology 136:4872-4879

86. **Morita H, Isomura Y, Mune T, Daido H, Takami R, Yamakita N, Ishizuka T, Takeda N, Yasuda K, Gomez-Sanchez CE** 2004 Plasma cortisol and cortisone concentrations in normal subjects and patients with adrenocortical disorders. Metabolism 53:89-94

87. **Mune T, Morita H, Suzuki T, Takahashi Y, Isomura Y, Tanahashi T, Daido H, Yamakita N, Deguchi T, Sasano H, White PC, Yasuda K** 2003 Role of local 11 beta-hydroxysteroid dehydrogenase type 2 expression in determining the phenotype of adrenal adenomas. J Clin Endocrinol Metab 88:864-870

88. **Lewis JG, Bagley CJ, Elder PA, Bachmann AW, Torpy DJ** 2005 Plasma free cortisol fraction reflects levels of functioning corticosteroid-binding globulin. Clin Chim Acta 359:189-194

89. **Torpy DJ, Ho JT** 2007 Corticosteroid-binding globulin gene polymorphisms: clinical implications and links to idiopathic chronic fatigue disorders. Clin Endocrinol (Oxf) 67:161-167

90. **Ho JT, Al-Musalhi H, Chapman MJ, Quach T, Thomas PD, Bagley CJ, Lewis JG, Torpy DJ** 2006 Septic shock and sepsis: a comparison of total and free plasma cortisol levels. J Clin Endocrinol Metab 91:105-114

91. **Kanter ED, Wilkinson CW, Radant AD, Petrie EC, Dobie DJ, McFall ME, Peskind ER, Raskind MA** 2001 Glucocorticoid feedback sensitivity and adrenocortical responsiveness in posttraumatic stress disorder. Biol Psychiatry 50:238-245

92. **Tsigos C, Kyrou I, Chrousos GP, Papanicolaou DA** 1998 Prolonged suppression of corticosteroid-binding globulin by recombinant human interleukin-6 in man. J Clin Endocrinol Metab 83:3379

93. **Bernier J, Jobin N, Emptoz-Bonneton A, Pugeat MM, Garrel DR** 1998 Decreased corticosteroid-binding globulin in burn patients: relationship with interleukin-6 and fat in nutritional support. Crit Care Med 26:452-460

94. **Di Luigi L, Sgro P, Baldari C, Gallotta MC, Emerenziani GP, Crescioli C, Bianchini S, Romanelli F, Lenzi A, Guidetti L** 2012 The phosphodiesterases type 5 inhibitor tadalafil reduces the activation of the hypothalamus-pituitary-adrenal axis in men during cycle ergometric exercise. Am J Physiol Endocrinol Metab 302:E972-8

95. **Manco M, Fernandez-Real JM, Valera-Mora ME, Dechaud H, Nanni G, Tondolo V, Calvani M, Castagneto M, Pugeat M, Mingrone G** 2007 Massive weight loss decreases corticosteroid-binding globulin levels and increases free cortisol in healthy obese patients: an adaptive phenomenon? Diabetes Care 30:1494-1500

96. **Ousova O, Guyonnet-Duperat V, Iannuccelli N, Bidanel JP, Milan D, Genet C, Llamas B, Yerle M, Gellin J, Chardon P, Emptoz-Bonneton A, Pugeat M, Mormede P, Moisan MP** 2004 Corticosteroid binding globulin: a new target for cortisol-driven obesity. Mol Endocrinol 18:1687-1696

97. **Mendel CM** 1989 The free hormone hypothesis: a physiologically based mathematical model. Endocr Rev 10:232-274

98. **Bamberger CM, Schulte HM, Chrousos GP** 1996 Molecular determinants of glucocorticoid receptor function and tissue sensitivity to glucocorticoids. Endocr Rev 17:245-261

99. **Lu NZ, Cidlowski JA** 2004 The origin and functions of multiple human glucocorticoid receptor isoforms. Ann N Y Acad Sci 1024:102-123

100. **Cole TJ, Blendy JA, Monaghan AP, Krieglstein K, Schmid W, Aguzzi A, Fantuzzi G, Hummler E, Unsicker K, Schutz G** 1995 Targeted disruption of the glucocorticoid receptor gene blocks adrenergic chromaffin cell development and severely retards lung maturation. Genes Dev 9:1608-1621

101. **Oakley RH, Sar M, Cidlowski JA** 1996 The human glucocorticoid receptor beta isoform. Expression, biochemical properties, and putative function. J Biol Chem 271:9550-9559

102. **Lewis-Tuffin LJ, Cidlowski JA** 2006 The physiology of human glucocorticoid receptor beta (hGRbeta) and glucocorticoid resistance. Ann N Y Acad Sci 1069:1-9

103. **Oakley RH, Jewell CM, Yudt MR, Bofetiado DM, Cidlowski JA** 1999 The dominant negative activity of the human glucocorticoid receptor beta isoform. Specificity and mechanisms of action. J Biol Chem 274:27857-27866

104. **Stahn C, Buttgereit F** 2008 Genomic and nongenomic effects of glucocorticoids. Nat Clin Pract Rheumatol 4:525-533

105. **Cooper MS, Stewart PM** 2009 11Beta-hydroxysteroid dehydrogenase type 1 and its role in the hypothalamus-pituitary-adrenal axis, metabolic syndrome, and inflammation. J Clin Endocrinol Metab 94:4645-4654

106. **Masuzaki H, Paterson J, Shinyama H, Morton NM, Mullins JJ, Seckl JR, Flier JS** 2001 A transgenic model of visceral obesity and the metabolic syndrome. Science 294:2166-2170

107. **Tomlinson JW, Walker EA, Bujalska IJ, Draper N, Lavery GG, Cooper MS, Hewison M, Stewart PM** 2004 11beta-Hydroxysteroid Dehydrogenase Type 1: a Tissue-Specific Regulator of Glucocorticoid Response. Endocr Rev 25:831-866

108. **Morton NM, Seckl JR** 2008 11beta-Hydroxysteroid Dehydrogenase Type 1 and Obesity. Front Horm Res 36:146-164

109. **Seckl JR** 2004 11beta-Hydroxysteroid Dehydrogenases: Changing Glucocorticoid Action. Curr Opin Pharmacol 4:597-602

110. **Peckett AJ, Wright DC, Riddell MC** 2011 The effects of glucocorticoids on adipose tissue lipid metabolism. Metabolism 60:1500-1510

111. **Friedman JE, Yun JS, Patel YM, McGrane MM, Hanson RW** 1993 Glucocorticoids regulate the induction of phosphoenolpyruvate carboxykinase (GTP) gene transcription during diabetes. J Biol Chem 268:12952-12957

112. **Kuo T, Harris CA, Wang JC** 2013 Metabolic functions of glucocorticoid receptor in skeletal muscle. Mol Cell Endocrinol

113. **Follenius M, Brandenberger G, Hietter B** 1982 Diurnal cortisol peaks and their relationships to meals. J Clin Endocrinol Metab 55:757-761

114. **Rosmond R, Holm G, Bjorntorp P** 2000 Food-induced cortisol secretion in relation to anthropometric, metabolic and haemodynamic variables in men. Int J Obes Relat Metab Disord 24:416-422

115. **Wang J, Dourmashkin JT, Yun R, Leibowitz SF** 1999 Rapid changes in hypothalamic neuropeptide Y produced by carbohydrate-rich meals that enhance corticosterone and glucose levels. Brain Res 848:124-136

116. **la Fleur SE, Akana SF, Manalo SL, Dallman MF** 2004 Interaction between corticosterone and insulin in obesity: regulation of lard intake and fat stores. Endocrinology 145:2174-2185

117. **la Fleur SE** 2006 The effects of glucocorticoids on feeding behavior in rats. Physiol Behav 89:110-114

118. **Rutters F, Nieuwenhuizen AG, Lemmens SG, Born JM, Westerterp-Plantenga MS** 2009 Hyperactivity of the HPA axis is related to dietary restraint in normal weight women. Physiol Behav 96:315-319

119. **Oliver G, Wardle J** 1999 Perceived effects of stress on food choice. Physiol Behav 66:511-515

120. **Wallis DJ, Hetherington MM** 2009 Emotions and eating. Self-reported and experimentally induced changes in food intake under stress. Appetite 52:355-362

121. **Dallman MF** 2010 Stress-induced obesity and the emotional nervous system. Trends Endocrinol Metab 21:159-165

122. **Torres SJ, Nowson CA** 2007 Relationship between stress, eating behavior, and obesity. Nutrition 23:887-894

123. **Brunner EJ, Chandola T, Marmot MG** 2007 Prospective effect of job strain on general and central obesity in the Whitehall II Study. Am J Epidemiol 165:828-837

124. **Dallman MF, Warne JP, Foster MT, Pecoraro NC** 2007 Glucocorticoids and insulin both modulate caloric intake through actions on the brain. J Physiol 583:431-436

125. **Zellner DA, Loaiza S, Gonzalez Z, Pita J, Morales J, Pecora D, Wolf A** 2006 Food selection changes under stress. Physiol Behav 87:789-793

126. **Pecoraro N, Reyes F, Gomez F, Bhargava A, Dallman MF** 2004 Chronic stress promotes palatable feeding, which reduces signs of stress: feedforward and feedback effects of chronic stress. Endocrinology 145:3754-3762

127. **Krahn DD, Gosnell BA, Majchrzak MJ** 1990 The anorectic effects of CRH and restraint stress decrease with repeated exposures. Biol Psychiatry 27:1094-1102

128. **Harris BN, Perea-Rodriguez JP, Saltzman W** 2011 Acute effects of corticosterone injection on paternal behavior in California mouse (Peromyscus californicus) fathers. Horm Behav 60:666-675

129. **van Jaarsveld CH, Fidler JA, Steptoe A, Boniface D, Wardle J** 2009 Perceived stress and weight gain in adolescence: a longitudinal analysis. Obesity (Silver Spring) 17:2155-2161

130. **Spencer SJ, Tilbrook A** 2011 The glucocorticoid contribution to obesity. Stress 14:233-246

131. **Bujalska IJ, Kumar S, Hewison M, Stewart PM** 1999 Differentiation of adipose stromal cells: the roles of glucocorticoids and 11beta-hydroxysteroid dehydrogenase. Endocrinology 140:3188-3196

132. **Rebuffe-Scrive M, Krotkiewski M, Elfverson J, Bjorntorp P** 1988 Muscle and adipose tissue morphology and metabolism in Cushing's syndrome. J Clin Endocrinol Metab 67:1122-1128

133. **Rebuffe-Scrive M, Walsh UA, McEwen B, Rodin J** 1992 Effect of chronic stress and exogenous glucocorticoids on regional fat distribution and metabolism. Physiol Behav 52:583-590

134. **Cizza G, Nieman LK, Doppman JL, Passaro MD, Czerwiec FS, Chrousos GP, Cutler GB,Jr** 1996 Factitious Cushing syndrome. J Clin Endocrinol Metab 81:3573-3577

135. **Shibli-Rahhal A, Van Beek M, Schlechte JA** 2006 Cushing's syndrome. Clin Dermatol 24:260-265

136. **Leibowitz G, Tsur A, Chayen SD, Salameh M, Raz I, Cerasi E, Gross DJ** 1996 Pre-clinical Cushing's syndrome: an unexpected frequent cause of poor glycaemic control in obese diabetic patients. Clin Endocrinol (Oxf) 44:717-722

137. **Simard M** 2004 The biochemical investigation of Cushing syndrome. Neurosurg Focus 16:E4

138. **Simmons LR, Molyneaux L, Yue DK, Chua EL** 2012 Steroid-induced diabetes: is it just unmasking of type 2 diabetes? ISRN Endocrinol 2012:910905

139. **Unger RH, Grundy S** 1985 Hyperglycaemia as an inducer as well as a consequence of impaired islet cell function and insulin resistance: implications for the management of diabetes. Diabetologia 28:119-121

140. **Giacca A, Xiao C, Oprescu AI, Carpentier AC, Lewis GF** 2011 Lipid-induced pancreatic beta-cell dysfunction: focus on in vivo studies. Am J Physiol Endocrinol Metab 300:E255-62

141. **Poitout V, Amyot J, Semache M, Zarrouki B, Hagman D, Fontes G** 2010 Glucolipotoxicity of the pancreatic beta cell. Biochim Biophys Acta 1801:289-298

142. **Reynolds RM** 2010 Corticosteroid-mediated programming and the pathogenesis of obesity and diabetes. J Steroid Biochem Mol Biol 122:3-9

143. **Rose AJ, Vegiopoulos A, Herzig S** 2010 Role of glucocorticoids and the glucocorticoid receptor in metabolism: insights from genetic manipulations. J Steroid Biochem Mol Biol 122:10-20

144. **Kiraly MA, Bates HE, Kaniuk NA, Yue JT, Brumell JH, Matthews SG, Riddell MC, Vranic M** 2008 Swim training prevents hyperglycemia in ZDF rats: mechanisms involved in the partial maintenance of beta-cell function. Am J Physiol Endocrinol Metab 294:E271-83

145. **Lansang MC, Hustak LK** 2011 Glucocorticoid-induced diabetes and adrenal suppression: How to detect and manage them. Cleve Clin J Med 78:748-756

146. **Hoes JN, van der Goes MC, van Raalte DH, van der Zijl NJ, den Uyl D, Lems WF, Lafeber FP, Jacobs JW, Welsing PM, Diamant M, Bijlsma JW** 2011 Glucose tolerance, insulin sensitivity and beta-cell function in patients with rheumatoid arthritis treated with or without low-to-medium dose glucocorticoids. Ann Rheum Dis 70:1887-1894

147. **Conn JW, Louis LH, Wheeler CE** 1948 Production of temporary diabetes mellitus in man with pituitary adrenocorticotropic hormone; relation to uric acid metabolism. J Lab Clin Med 33:651-661

148. **Pickavance L, Widdowson PS, King P, Ishii S, Tanaka H, Williams G** 1998 The development of overt diabetes in young Zucker Diabetic Fatty (ZDF) rats and the effects of chronic MCC-555 treatment. Br J Pharmacol 125:767-770

149. **Shiota M, Printz RL** 2012 Diabetes in Zucker diabetic fatty rat. Methods Mol Biol 933:103-123

150. **Delghingaro-Augusto V, Decary S, Peyot ML, Latour MG, Lamontagne J, Paradis-Isler N, Lacharite-Lemieux M, Akakpo H, Birot O, Nolan CJ, Prentki M, Bergeron R** 2012 Voluntary running exercise prevents beta-cell failure in susceptible islets of the Zucker diabetic fatty rat. Am J Physiol Endocrinol Metab 302:E254-64

151. **van Raalte DH, Ouwens DM, Diamant M** 2009 Novel insights into glucocorticoid-mediated diabetogenic effects: towards expansion of therapeutic options? Eur J Clin Invest 39:81-93

152. **Rafacho A, Giozzet VA, Boschero AC, Bosqueiro JR** 2008 Functional alterations in endocrine pancreas of rats with different degrees of dexamethasone-induced insulin resistance. Pancreas 36:284-293

153. **Rafacho A, Cestari TM, Taboga SR, Boschero AC, Bosqueiro JR** 2009 High doses of dexamethasone induce increased beta-cell proliferation in pancreatic rat islets. Am J Physiol Endocrinol Metab 296:E681-9

154. **Rafacho A, Ribeiro DL, Boschero AC, Taboga SR, Bosqueiro JR** 2008 Increased pancreatic islet mass is accompanied by activation of the insulin receptor substrate-2/serine-threonine kinase pathway and augmented cyclin D2 protein levels in insulin-resistant rats. Int J Exp Pathol 89:264-275

155. **Hult M, Ortsater H, Schuster G, Graedler F, Beckers J, Adamski J, Ploner A, Jornvall H, Bergsten P, Oppermann U** 2009 Short-term glucocorticoid treatment increases insulin secretion in islets derived from lean mice through multiple pathways and mechanisms. Mol Cell Endocrinol 301:109-116

156. **van Raalte DH, Nofrate V, Bunck MC, van Iersel T, Elassaiss Schaap J, Nassander UK, Heine RJ, Mari A, Dokter WH, Diamant M** 2010 Acute and 2-week exposure to prednisolone impair different aspects of beta-cell function in healthy men. Eur J Endocrinol 162:729-735

157. **Dessein PH, Joffe BI** 2006 Insulin resistance and impaired beta cell function in rheumatoid arthritis. Arthritis Rheum 54:2765-2775

158. **Hansen KB, Vilsboll T, Bagger JI, Holst JJ, Knop FK** 2010 Reduced glucose tolerance and insulin resistance induced by steroid treatment, relative physical inactivity, and high-calorie diet impairs the incretin effect in healthy subjects. J Clin Endocrinol Metab 95:3309-3317

159. **Delaunay F, Khan A, Cintra A, Davani B, Ling ZC, Andersson A, Ostenson CG, Gustafsson J, Efendic S, Okret S** 1997 Pancreatic beta cells are important targets for the diabetogenic effects of glucocorticoids. J Clin Invest 100:2094-2098

160. **Davani B, Portwood N, Bryzgalova G, Reimer MK, Heiden T, Ostenson CG, Okret S, Ahren B, Efendic S, Khan A** 2004 Aged transgenic mice with increased glucocorticoid sensitivity in pancreatic beta-cells develop diabetes. Diabetes 53 Suppl 1:S51-9

161. **Jeong IK, Oh SH, Kim BJ, Chung JH, Min YK, Lee MS, Lee MK, Kim KW** 2001 The effects of dexamethasone on insulin release and biosynthesis are dependent on the dose and duration of treatment. Diabetes Res Clin Pract 51:163-171

162. **Ullrich S, Berchtold S, Ranta F, Seebohm G, Henke G, Lupescu A, Mack AF, Chao CM, Su J, Nitschke R, Alexander D, Friedrich B, Wulff P, Kuhl D, Lang F** 2005 Serum- and glucocorticoid-inducible kinase 1 (SGK1) mediates glucocorticoid-induced inhibition of insulin secretion. Diabetes 54:1090-1099

163. **Ullrich S, Zhang Y, Avram D, Ranta F, Kuhl D, Haring HU, Lang F** 2007 Dexamethasone increases Na+/K+ ATPase activity in insulin secreting cells through SGK1. Biochem Biophys Res Commun 352:662-667

164. **Linssen MM, van Raalte DH, Toonen EJ, Alkema W, van der Zon GC, Dokter WH, Diamant M, Guigas B, Ouwens DM** 2011 Prednisolone-induced beta cell dysfunction is associated with impaired endoplasmic reticulum homeostasis in INS-1E cells. Cell Signal 23:1708-1715

165. **Koizumi M, Yada T** 2008 Sub-chronic stimulation of glucocorticoid receptor impairs and mineralocorticoid receptor protects cytosolic Ca2+ responses to glucose in pancreatic beta-cells. J Endocrinol 197:221-229

166. **Ogawa A, Johnson JH, Ohneda M, McAllister CT, Inman L, Alam T, Unger RH** 1992 Roles of insulin resistance and beta-cell dysfunction in dexamethasone-induced diabetes. J Clin Invest 90:497-504

167. **Karlsson S, Ostlund B, Myrsen-Axcrona U, Sundler F, Ahren B** 2001 Beta cell adaptation to dexamethasone-induced insulin resistance in rats involves increased glucose responsiveness but not glucose effectiveness. Pancreas 22:148-156

168. **Ling ZC, Khan A, Delauny F, Davani B, Ostenson CG, Gustafsson JA, Okret S, Landau BR, Efendic S** 1998 Increased glucocorticoid sensitivity in islet beta-cells: effects on glucose 6-phosphatase, glucose cycling and insulin release. Diabetologia 41:634-639

169. **Wintergerst KA, Foster MB, Sullivan JE, Woods CR** 2012 Association of hyperglycemia, glucocorticoids, and insulin use with morbidity and mortality in the pediatric intensive care unit. J Diabetes Sci Technol 6:5-14

170. **Jensen DH, Aaboe K, Henriksen JE, Volund A, Holst JJ, Madsbad S, Krarup T** 2012 Steroid-induced insulin resistance and impaired glucose tolerance are both associated with a progressive decline of incretin effect in first-degree relatives of patients with type 2 diabetes. Diabetologia 55:1406-1416

171. **Knop FK, Vilsboll T, Madsbad S, Holst JJ, Krarup T** 2007 Inappropriate suppression of glucagon during OGTT but not during isoglycaemic i.v. glucose infusion contributes to the reduced incretin effect in type 2 diabetes mellitus. Diabetologia 50:797-805

172. **Deng S, Vatamaniuk M, Huang X, Doliba N, Lian MM, Frank A, Velidedeoglu E, Desai NM, Koeberlein B, Wolf B, Barker CF, Naji A, Matschinsky FM, Markmann JF** 2004 Structural and functional abnormalities in the islets isolated from type 2 diabetic subjects. Diabetes 53:624-632

173. **Davani B, Khan A, Hult M, Martensson E, Okret S, Efendic S, Jornvall H, Oppermann UC** 2000 Type 1 11beta -hydroxysteroid dehydrogenase mediates glucocorticoid activation and insulin release in pancreatic islets. J Biol Chem 275:34841-34844

174. **Duplomb L, Lee Y, Wang MY, Park BH, Takaishi K, Agarwal AK, Unger RH** 2004 Increased expression and activity of 11beta-HSD-1 in diabetic islets and prevention with troglitazone. Biochem Biophys Res Commun 313:594-599

175. **Turban S, Liu X, Ramage L, Webster SP, Walker BR, Dunbar DR, Mullins JJ, Seckl JR, Morton NM** 2012 Optimal elevation of beta-cell 11beta-hydroxysteroid dehydrogenase type 1 is a compensatory mechanism that prevents high-fat diet-induced beta-cell failure. Diabetes 61:642-652

176. **Ortsater H, Alberts P, Warpman U, Engblom LO, Abrahmsen L, Bergsten P** 2005 Regulation of 11beta-hydroxysteroid dehydrogenase type 1 and glucose-stimulated insulin secretion in pancreatic islets of Langerhans. Diabetes Metab Res Rev 21:359-366

177. **Unger RH, Clark GO, Scherer PE, Orci L** 2010 Lipid homeostasis, lipotoxicity and the metabolic syndrome. Biochim Biophys Acta 1801:209-214

178. **Oprescu AI, Bikopoulos G, Naassan A, Allister EM, Tang C, Park E, Uchino H, Lewis GF, Fantus IG, Rozakis-Adcock M, Wheeler MB, Giacca A** 2007 Free fatty acid-induced reduction in glucose-stimulated insulin secretion: evidence for a role of oxidative stress in vitro and in vivo. Diabetes 56:2927-2937

179. **Zhang X, Bao Y, Ke L, Yu Y** 2010 Elevated circulating free fatty acids levels causing pancreatic islet cell dysfunction through oxidative stress. J Endocrinol Invest 33:388-394

180. **Kelpe CL, Moore PC, Parazzoli SD, Wicksteed B, Rhodes CJ, Poitout V** 2003 Palmitate inhibition of insulin gene expression is mediated at the transcriptional level via ceramide synthesis. J Biol Chem 278:30015-30021

181. **Prentki M, Corkey BE** 1996 Are the beta-cell signaling molecules malonyl-CoA and cystolic long-chain acyl-CoA implicated in multiple tissue defects of obesity and NIDDM? Diabetes 45:273-283

182. **Prentki M, Joly E, El-Assaad W, Roduit R** 2002 Malonyl-CoA signaling, lipid partitioning, and glucolipotoxicity: role in beta-cell adaptation and failure in the etiology of diabetes. Diabetes 51 Suppl 3:S405-13

183. **Shimabukuro M, Zhou YT, Levi M, Unger RH** 1998 Fatty acid-induced beta cell apoptosis: a link between obesity and diabetes. Proc Natl Acad Sci U S A 95:2498-2502

184. **Mathias S, Pena LA, Kolesnick RN** 1998 Signal transduction of stress via ceramide. Biochem J 335 (Pt 3):465-480

185. **Solinas G, Naugler W, Galimi F, Lee MS, Karin M** 2006 Saturated fatty acids inhibit induction of insulin gene transcription by JNK-mediated phosphorylation of insulin-receptor substrates. Proc Natl Acad Sci U S A 103:16454-16459

186. **Carlsson C, Borg LA, Welsh N** 1999 Sodium palmitate induces partial mitochondrial uncoupling and reactive oxygen species in rat pancreatic islets in vitro. Endocrinology 140:3422-3428

187. **Syed I, Jayaram B, Subasinghe W, Kowluru A** 2010 Tiam1/Rac1 signaling pathway mediates palmitate-induced, ceramide-sensitive generation of superoxides and lipid peroxides and the loss of mitochondrial membrane potential in pancreatic beta-cells. Biochem Pharmacol 80:874-883

188. **Lenzen S, Drinkgern J, Tiedge M** 1996 Low antioxidant enzyme gene expression in pancreatic islets compared with various other mouse tissues. Free Radic Biol Med 20:463-466

189. **Maechler P, Wollheim CB** 1999 Mitochondrial glutamate acts as a messenger in glucose-induced insulin exocytosis. Nature 402:685-689

190. **Eizirik DL, Cardozo AK, Cnop M** 2008 The role for endoplasmic reticulum stress in diabetes mellitus. Endocr Rev 29:42-61

191. **Holness MJ, Smith ND, Greenwood GK, Sugden MC** 2005 Interactive influences of peroxisome proliferator-activated receptor alpha activation and glucocorticoids on pancreatic beta cell compensation in insulin resistance induced by dietary saturated fat in the rat. Diabetologia 48:2062-2068

192. **Gremlich S, Roduit R, Thorens B** 1997 Dexamethasone induces posttranslational degradation of GLUT2 and inhibition of insulin secretion in isolated pancreatic beta cells. Comparison with the effects of fatty acids. J Biol Chem 272:3216-3222

193. **Moraska A, Deak T, Spencer RL, Roth D, Fleshner M** 2000 Treadmill running produces both positive and negative physiological adaptations in Sprague-Dawley rats. Am J Physiol Regul Integr Comp Physiol 279:R1321-9

194. **Balon TW, Zorzano A, Treadway JL, Goodman MN, Ruderman NB** 1990 Effect of insulin on protein synthesis and degradation in skeletal muscle after exercise. Am J Physiol 258:E92-7

195. **Linderman JK, Whittall JB, Gosselink KL, Wang TJ, Mukku VR, Booth FW, Grindeland RE** 1995 Stimulation of myofibrillar protein synthesis in hindlimb suspended rats by resistance exercise and growth hormone. Life Sci 57:755-762

196. **Kriegsfeld LJ, Silver R** 2006 The regulation of neuroendocrine function: Timing is everything. Horm Behav 49:557-574

197. **Fediuc S, Campbell JE, Riddell MC** 2006 Effect of voluntary wheel running on circadian corticosterone release and on HPA axis responsiveness to restraint stress in Sprague-Dawley rats. J Appl Physiol 100:1867-1875

198. **Kennedy GA, Hudson R, Armstrong SM** 1994 Circadian wheel running activity rhythms in two strains of domestic rabbit. Physiol Behav 55:385-389

199. **Freeman DA, Zucker I** 2000 Temperature-independence of circannual variations in circadian rhythms of golden-mantled ground squirrels. J Biol Rhythms 15:336-343

200. **Coutinho AE, Campbell JE, Fediuc S, Riddell MC** 2006 Effect of voluntary exercise on peripheral tissue glucocorticoid receptor content and the expression and activity of 11beta-HSD1 in the Syrian hamster. J Appl Physiol 100:1483-1488

201. **Lightfoot JT, Turner MJ, Daves M, Vordermark A, Kleeberger SR** 2004 Genetic influence on daily wheel running activity level. Physiol Genomics 19:270-276

202. **Coutinho AE, Fediuc S, Campbell JE, Riddell MC** 2006 Metabolic effects of voluntary wheel running in young and old Syrian golden hamsters. Physiol Behav 87:360-367

203. **Shyu BC, Andersson SA, Thoren P** 1984 Spontaneous running in wheels. A microprocessor assisted method for measuring physiological parameters during exercise in rodents. Acta Physiol Scand 121:103-109

204. **Iversen IH** 1993 Techniques for establishing schedules with wheel running as reinforcement in rats. J Exp Anal Behav 60:219-238

205. **Cook MD, Martin SA, Williams C, Whitlock K, Wallig MA, Pence BD, Woods JA** 2013 Forced treadmill exercise training exacerbates inflammation and causes mortality while voluntary wheel training is protective in a mouse model of colitis. Brain Behav Immun

206. **Duclos M, Corcuff JB, Rashedi M, Fougere V, Manier G** 1997 Trained versus untrained men: different immediate post-exercise responses of pituitary adrenal axis. A preliminary study. Eur J Appl Physiol Occup Physiol 75:343-350

207. **Tharp GD** 1975 The role of glucocorticoids in exercise. Med Sci Sports 7:6-11

208. **Viru M, Litvinova L, Smirnova T, Viru A** 1994 Glucocorticoids in metabolic control during exercise: glycogen metabolism. J Sports Med Phys Fitness 34:377-382

209. **Gollnick PD, Soule RG, Taylor AW, Williams C, Ianuzzo CD** 1970 Exercise-induced glycogenolysis and lipolysis in the rat: hormonal influence. Am J Physiol 219:729-733

210. **Duclos M, Gouarne C, Bonnemaison D** 2003 Acute and chronic effects of exercise on tissue sensitivity to glucocorticoids. J Appl Physiol 94:869-875

211. **Hawley JA, Lessard SJ** 2008 Exercise training-induced improvements in insulin action. Acta Physiol (Oxf) 192:127-135

212. **Duclos M, Guinot M, Le Bouc Y** 2007 Cortisol and GH: odd and controversial ideas. Appl Physiol Nutr Metab 32:895-903

213. **Kiraly MA, Bates HE, Yue JT, Goche-Montes D, Fediuc S, Park E, Matthews SG, Vranic M, Riddell MC** 2007 Attenuation of type 2 diabetes mellitus in the male Zucker diabetic fatty rat: the effects of stress and non-volitional exercise. Metabolism 56:732-744

214. **Dal-Zotto S, Marti O, Armario A** 2000 Influence of single or repeated experience of rats with forced swimming on behavioural and physiological responses to the stressor. Behav Brain Res 114:175-181

215. **Garcia A, Marti O, Valles A, Dal-Zotto S, Armario A** 2000 Recovery of the hypothalamic-pituitary-adrenal response to stress. Effect of stress intensity, stress duration and previous stress exposure. Neuroendocrinology 72:114-125

216. **Lee TH, Jang MH, Shin MC, Lim BV, Kim YP, Kim H, Choi HH, Lee KS, Kim EH, Kim CJ** 2003 Dependence of rat hippocampal c-Fos expression on intensity and duration of exercise. Life Sci 72:1421-1436

217. **Droste SK, Gesing A, Ulbricht S, Muller MB, Linthorst AC, Reul JM** 2003 Effects of long-term voluntary exercise on the mouse hypothalamic-pituitary-adrenocortical axis. Endocrinology 144:3012-3023

218. **Droste SK, Schweizer MC, Ulbricht S, Reul JM** 2006 Long-term voluntary exercise and the mouse hypothalamic-pituitary-adrenocortical axis: impact of concurrent treatment with the antidepressant drug tianeptine. J Neuroendocrinol 18:915-925

219. **Droste SK, Chandramohan Y, Hill LE, Linthorst AC, Reul JM** 2007 Voluntary exercise impacts on the rat hypothalamic-pituitary-adrenocortical axis mainly at the adrenal level. Neuroendocrinology 86:26-37

220. **Campbell JE, Rakhshani N, Fediuc S, Bruni S, Riddell MC** 2009 Voluntary wheel running initially increases adrenal sensitivity to adrenocorticotrophic hormone, which is attenuated with long-term training. J Appl Physiol 106:66-72

221. **Peijie C, Zicai D, Haowen X, Renbao X** 2004 Effects of chronic and acute training on glucocorticoid receptors concentrations in rats. Life Sci 75:1303-1311

222. **Galbo H, Hedeskov CJ, Capito K, Vinten J** 1981 The effect of physical training on insulin secretion of rat pancreatic islets. Acta Physiol Scand 111:75-79

223. **Oliveira CA, Paiva MF, Mota CA, Ribeiro C, Leme JA, Luciano E, Mello MA** 2010 Exercise at anaerobic threshold intensity and insulin secretion by isolated pancreatic islets of rats. Islets 2:240-246

224. **Zawalich W, Maturo S, Felig P** 1982 Influence of physical training on insulin release and glucose utilization by islet cells and liver glucokinase activity in the rat. Am J Physiol 243:E464-9

225. **Farrell PA, Caston AL, Rodd D, Engdahl J** 1992 Effect of training on insulin secretion from single pancreatic beta cells. Med Sci Sports Exerc 24:426-433

226. **Almeida FN, Proenca AR, Chimin P, Marcal AC, Bessa-Lima F, Carvalho CR** 2012 Physical exercise and pancreatic islets: acute and chronic actions on insulin secretion. Islets 4:296-301

227. **Dela F, Mikines KJ, Tronier B, Galbo H** 1990 Diminished arginine-stimulated insulin secretion in trained men. J Appl Physiol 69:261-267

228. **King DS, Staten MA, Kohrt WM, Dalsky GP, Elahi D, Holloszy JO** 1990 Insulin secretory capacity in endurance-trained and untrained young men. Am J Physiol 259:E155-61

229. **Kirwan JP, Kohrt WM, Wojta DM, Bourey RE, Holloszy JO** 1993 Endurance exercise training reduces glucose-stimulated insulin levels in 60- to 70-year-old men and women. J Gerontol 48:M84-90

230. **Zoppi CC, Calegari VC, Silveira LR, Carneiro EM, Boschero AC** 2011 Exercise training enhances rat pancreatic islets anaplerotic enzymes content despite reduced insulin secretion. Eur J Appl Physiol 111:2369-2374

231. **Calegari VC, Abrantes JL, Silveira LR, Paula FM, Costa JM,Jr, Rafacho A, Velloso LA, Carneiro EM, Bosqueiro JR, Boschero AC, Zoppi CC** 2011 Endurance Training Stimulates Growth and Survival Pathways and the Redox Balance in Rat Pancreatic Islets. J Appl Physiol

232. **Laker RC, Gallo LA, Wlodek ME, Siebel AL, Wadley GD, McConell GK** 2011 Short-term exercise training early in life restores deficits in pancreatic beta-cell mass associated with growth restriction in adult male rats. Am J Physiol Endocrinol Metab 301:E931-40

233. **Fluckey JD, Kraemer WJ, Farrell PA** 1995 Pancreatic islet insulin secretion is increased after resistance exercise in rats. J Appl Physiol 79:1100-1105

234. **Tsatsoulis A, Fountoulakis S** 2006 The protective role of exercise on stress system dysregulation and comorbidities. Ann N Y Acad Sci 1083:196-213

235. **Storlien LH, James DE, Burleigh KM, Chisholm DJ, Kraegen EW** 1986 Fat feeding causes widespread in vivo insulin resistance, decreased energy expenditure, and obesity in rats. Am J Physiol 251:E576-83

236. **Flier SN, Kulkarni RN, Kahn CR** 2001 Evidence for a circulating islet cell growth factor in insulin-resistant states. Proc Natl Acad Sci U S A 98:7475-7480

237. **Sone H, Kagawa Y** 2005 Pancreatic beta cell senescence contributes to the pathogenesis of type 2 diabetes in high-fat diet-induced diabetic mice. Diabetologia 48:58-67

238. **Park S, Hong SM, Lee JE, Sung SR** 2007 Exercise improves glucose homeostasis that has been impaired by a high-fat diet by potentiating pancreatic beta-cell function and mass through IRS2 in diabetic rats. J Appl Physiol 103:1764-1771

239. **Opal SM, DePalo VA** 2000 Anti-inflammatory cytokines. Chest 117:1162-1172

240. **Pradhan AD, Manson JE, Rifai N, Buring JE, Ridker PM** 2001 C-reactive protein, interleukin 6, and risk of developing type 2 diabetes mellitus. JAMA 286:327-334

241. **Martin-Cordero L, Garcia JJ, Hinchado MD, Ortega E** 2011 The interleukin-6 and noradrenaline mediated inflammation-stress feedback mechanism is dysregulated in metabolic syndrome: effect of exercise. Cardiovasc Diabetol 10:42

242. **Slentz CA, Tanner CJ, Bateman LA, Durheim MT, Huffman KM, Houmard JA, Kraus WE** 2009 Effects of exercise training intensity on pancreatic beta-cell function. Diabetes Care 32:1807-1811

243. **Pold R, Jensen LS, Jessen N, Buhl ES, Schmitz O, Flyvbjerg A, Fujii N, Goodyear LJ, Gotfredsen CF, Brand CL, Lund S** 2005 Long-term AICAR administration and exercise prevents diabetes in ZDF rats. Diabetes 54:928-934

244. **Eriksson KF, Lindgarde F** 1991 Prevention of type 2 (non-insulin-dependent) diabetes mellitus by diet and physical exercise. The 6-year Malmo feasibility study. Diabetologia 34:891-898

245. **Orozco LJ, Buchleitner AM, Gimenez-Perez G, Roque I Figuls M, Richter B, Mauricio D** 2008 Exercise or exercise and diet for preventing type 2 diabetes mellitus. Cochrane Database Syst Rev (3):CD003054. doi:CD003054

246. **Duclos M, Corcuff JB, Pehourcq F, Tabarin A** 2001 Decreased pituitary sensitivity to glucocorticoids in endurance-trained men. Eur J Endocrinol 144:363-368

247. **Heath GW, Gavin JR,3rd, Hinderliter JM, Hagberg JM, Bloomfield SA, Holloszy JO** 1983 Effects of exercise and lack of exercise on glucose tolerance and insulin sensitivity. J Appl Physiol 55:512-517

248. **Knowler WC, Barrett-Connor E, Fowler SE, Hamman RF, Lachin JM, Walker EA, Nathan DM, Diabetes Prevention Program Research Group** 2002 Reduction in the incidence of type 2 diabetes with lifestyle intervention or metformin. N Engl J Med 346:393-403

249. **Nilsen V, Bakke PS, Gallefoss F** 2011 Effects of lifestyle intervention in persons at risk for type 2 diabetes mellitus - results from a randomised, controlled trial. BMC Public Health 11:893

250. **Christ CY, Hunt D, Hancock J, Garcia-Macedo R, Mandarino LJ, Ivy JL** 2002 Exercise training improves muscle insulin resistance but not insulin receptor signaling in obese Zucker rats. J Appl Physiol 92:736-744

251. **Etgen GJ,Jr, Brozinick JT,Jr, Kang HY, Ivy JL** 1993 Effects of exercise training on skeletal muscle glucose uptake and transport. Am J Physiol 264:C727-33

252. **Goodyear LJ, Hirshman MF, Valyou PM, Horton ES** 1992 Glucose transporter number, function, and subcellular distribution in rat skeletal muscle after exercise training. Diabetes 41:1091-1099

253. **Krotkiewski M, Lonnroth P, Mandroukas K, Wroblewski Z, Rebuffe-Scrive M, Holm G, Smith U, Bjorntorp P** 1985 The effects of physical training on insulin secretion and effectiveness and on glucose metabolism in obesity and type 2 (non-insulin-dependent) diabetes mellitus. Diabetologia 28:881-890

254. **Dela F, von Linstow ME, Mikines KJ, Galbo H** 2004 Physical training may enhance beta-cell function in type 2 diabetes. Am J Physiol Endocrinol Metab 287:E1024-31

255. **Bacchi E, Negri C, Zanolin ME, Milanese C, Faccioli N, Trombetta M, Zoppini G, Cevese A, Bonadonna RC, Schena F, Bonora E, Lanza M, Moghetti P** 2012 Metabolic effects of aerobic training and resistance training in type 2 diabetic subjects: a randomized controlled trial (the RAED2 study). Diabetes Care 35:676-682

256. **Richter EA, Mikines KJ, Galbo H, Kiens B** 1989 Effect of exercise on insulin action in human skeletal muscle. J Appl Physiol 66:876-885

257. **Kiraly MA, Campbell J, Park E, Bates HE, Yue JT, Rao V, Matthews SG, Bikopoulos G, Rozakis-Adcock M, Giacca A, Vranic M, Riddell MC** 2010 Exercise maintains euglycemia in association with decreased activation of c-Jun NH2-terminal kinase and serine phosphorylation of IRS-1 in the liver of ZDF rats. Am J Physiol Endocrinol Metab 298:E671-82

258. **Aguirre V, Uchida T, Yenush L, Davis R, White MF** 2000 The c-Jun NH(2)-terminal kinase promotes insulin resistance during association with insulin receptor substrate-1 and phosphorylation of Ser(307). J Biol Chem 275:9047-9054

259. **Burns N, Finucane FM, Hatunic M, Gilman M, Murphy M, Gasparro D, Mari A, Gastaldelli A, Nolan JJ** 2007 Early-onset type 2 diabetes in obese white subjects is characterised by a marked defect in beta cell insulin secretion, severe insulin resistance and a lack of response to aerobic exercise training. Diabetologia 50:1500-1508

260. **Cornil A, Decoster A, Copinschi G, Franckson JR** 1965 Effect of Muscular Exercise on the Plasma Level Cortisol in Man. Acta Endocrinol (Copenh) 48:163-168

261. **Cameron FJ, Warne GL** 1997 Familial Cushing's disease with severe weight loss occurring in late childhood. J Paediatr Child Health 33:74-77

262. **Pinheiro CH, Sousa Filho WM, Oliveira Neto J, Marinho Mde J, Motta Neto R, Smith MM, Silva CA** 2009 Exercise prevents cardiometabolic alterations induced by chronic use of glucocorticoids. Arq Bras Cardiol 93:400-8, 392-400

263. **Barel M, Perez OA, Giozzet VA, Rafacho A, Bosqueiro JR, do Amaral SL** 2010 Exercise training prevents hyperinsulinemia, muscular glycogen loss and muscle atrophy induced by dexamethasone treatment. Eur J Appl Physiol 108:999-1007

264. **Pauli JR, Gomes RJ, Luciano E** 2006 Hypothalamo-pituitary axis: effects of physical training in rats administered with dexamethasone. Rev Neurol 42:325-331

265. **Friedman TC, Mastorakos G, Newman TD, Mullen NM, Horton EG, Costello R, Papadopoulos NM, Chrousos GP** 1996 Carbohydrate and lipid metabolism in endogenous hypercortisolism: shared features with metabolic syndrome X and NIDDM. Endocr J 43:645-655

266. **Anagnostis P, Athyros VG, Tziomalos K, Karagiannis A, Mikhailidis DP** 2009 Clinical review: The pathogenetic role of cortisol in the metabolic syndrome: a hypothesis. J Clin Endocrinol Metab 94:2692-2701

267. **Johanssen S, Allolio B** 2007 Mifepristone (RU 486) in Cushing's syndrome. Eur J Endocrinol 157:561-569

268. **Belavic JM** 2013 Drug updates and approvals: 2012 in review. Nurse Pract 38:24-42; quiz 42-3

269. **Anonymous** 2012 Mifepristone (Korlym) for Cushing's syndrome. Med Lett Drugs Ther 54:46-47

270. **Bertagna X, Escourolle H, Pinquier JL, Coste J, Raux-Demay MC, Perles P, Silvestre L, Luton JP, Strauch G** 1994 Administration of RU 486 for 8 days in normal volunteers: antiglucocorticoid effect with no evidence of peripheral cortisol deprivation. J Clin Endocrinol Metab 78:375-380

271. **Gross C, Blasey CM, Roe RL, Allen K, Block TS, Belanoff JK** 2009 Mifepristone treatment of olanzapine-induced weight gain in healthy men. Adv Ther 26:959-969

272. **Fleseriu M, Biller BM, Findling JW, Molitch ME, Schteingart DE, Gross C, SEISMIC Study Investigators** 2012 Mifepristone, a glucocorticoid receptor antagonist, produces clinical and metabolic benefits in patients with Cushing's syndrome. J Clin Endocrinol Metab 97:2039-2049

273. **Bourgeois S, Pfahl M, Baulieu EE** 1984 DNA binding properties of glucocorticosteroid receptors bound to the steroid antagonist RU-486. EMBO J 3:751-755

274. **Heikinheimo O, Kontula K, Croxatto H, Spitz I, Luukkainen T, Lahteenmaki P** 1987 Plasma concentrations and receptor binding of RU 486 and its metabolites in humans. J Steroid Biochem 26:279-284

275. **Sartor O, Cutler GB,Jr** 1996 Mifepristone: treatment of Cushing's syndrome. Clin Obstet Gynecol 39:506-510

276. **Goldberg JR, Plescia MG, Anastasio GD** 1998 Mifepristone (RU 486): current knowledge and future prospects. Arch Fam Med 7:219-222

277. **Mohler ML, He Y, Wu Z, Hong SS, Miller DD** 2007 Non-steroidal glucocorticoid receptor antagonists: the race to replace RU-486 for anti-glucocorticoid therapy. Expert Opin Ther Pat 17:59-81

278. **Zalachoras I, Houtman R, Atucha E, Devos R, Tijssen AM, Hu P, Lockey PM, Datson NA, Belanoff JK, Lucassen PJ, Joels M, de Kloet ER, Roozendaal B, Hunt H, Meijer OC** 2013 Differential targeting of brain stress circuits with a selective glucocorticoid receptor modulator. Proc Natl Acad Sci U S A

279. **Belanoff JK, Blasey CM, Clark RD, Roe RL** 2011 Selective glucocorticoid receptor (type II) antagonists prevent weight gain caused by olanzapine in rats. Eur J Pharmacol 655:117-120

280. **Andrade C, Shaikh SA, Narayan L, Blasey C, Belanoff J** 2012 Administration of a selective glucocorticoid antagonist attenuates electroconvulsive shock-induced retrograde amnesia. J Neural Transm 119:337-344

281. **Hunt HJ, Ray NC, Hynd G, Sutton J, Sajad M, O'Connor E, Ahmed S, Lockey P, Daly S, Buckley G, Clark RD, Roe R, Blasey C, Belanoff J** 2012 Discovery of a novel non-steroidal GR antagonist with in vivo efficacy in the olanzapine-induced weight gain model in the rat. Bioorg Med Chem Lett 22:7376-7380

282. **Islam MS, Loots du T** 2009 Experimental rodent models of type 2 diabetes: a review. Methods Find Exp Clin Pharmacol 31:249-261

283. **Rolland V, Clement K, Dugail I, Guy-Grand B, Basdevant A, Froguel P, Lavau M** 1998 Leptin receptor gene in a large cohort of massively obese subjects: no indication of the fa/fa rat mutation. Detection of an intronic variant with no association with obesity. Obes Res 6:122-127

284. **Aleixandre de Artinano A, Miguel Castro M** 2009 Experimental rat models to study the metabolic syndrome. Br J Nutr 102:1246-1253

285. **Kennedy AJ, Ellacott KL, King VL, Hasty AH** 2010 Mouse models of the metabolic syndrome. Dis Model Mech 3:156-166

286. **Herder C, Karakas M, Koenig W** 2011 Biomarkers for the prediction of type 2 diabetes and cardiovascular disease. Clin Pharmacol Ther 90:52-66

287. **Clark JB, Palmer CJ, Shaw WN** 1983 The diabetic Zucker fatty rat. Proc Soc Exp Biol Med 173:68-75

288. **Chan O, Inouye K, Riddell MC, Vranic M, Matthews SG** 2003 Diabetes and the hypothalamo-pituitary-adrenal (HPA) axis. Minerva Endocrinol 28:87-102

289. **Matthews LC, Hanley NA** 2011 The stress of starvation: glucocorticoid restraint of beta cell development. Diabetologia 54:223-226

290. **Stewart PM** 1996 11 beta-Hydroxysteroid dehydrogenase: implications for clinical medicine. Clin Endocrinol (Oxf) 44:493-499

291. **Bujalska IJ, Draper N, Michailidou Z, Tomlinson JW, White PC, Chapman KE, Walker EA, Stewart PM** 2005 Hexose-6-phosphate dehydrogenase confers oxo-reductase activity upon 11 beta-hydroxysteroid dehydrogenase type 1. J Mol Endocrinol 34:675-684

292. **Tomiyama AJ, Dallman MF, Epel ES** 2011 Comfort food is comforting to those most stressed: Evidence of the chronic stress response network in high stress women. Psychoneuroendocrinology 36:1513-1519

293. **Gurwitz JH, Bohn RL, Glynn RJ, Monane M, Mogun H, Avorn J** 1994 Glucocorticoids and the risk for initiation of hypoglycemic therapy. Arch Intern Med 154:97-101

294. **Reed MJ, Meszaros K, Entes LJ, Claypool MD, Pinkett JG, Gadbois TM, Reaven GM** 2000 A new rat model of type 2 diabetes: the fat-fed, streptozotocin-treated rat. Metabolism 49:1390-1394

295. **Karatsoreos IN, Bhagat SM, Bowles NP, Weil ZM, Pfaff DW, McEwen BS** 2010 Endocrine and physiological changes in response to chronic corticosterone: a potential model of the metabolic syndrome in mouse. Endocrinology 151:2117-2127

296. **Gustavsson C, Soga T, Wahlstrom E, Vesterlund M, Azimi A, Norstedt G, Tollet-Egnell P** 2011 Sex-dependent hepatic transcripts and metabolites in the

development of glucose intolerance and insulin resistance in Zucker diabetic fatty rats. J Mol Endocrinol 47:129-143

297. **Meyer JS, Micco DJ, Stephenson BS, Krey LC, McEwen BS** 1979 Subcutaneous implantation method for chronic glucocorticoid replacement therapy. Physiol Behav 22:867-870

298. **Matthews DR, Hosker JP, Rudenski AS, Naylor BA, Treacher DF, Turner RC** 1985 Homeostasis model assessment: insulin resistance and beta-cell function from fasting plasma glucose and insulin concentrations in man. Diabetologia 28:412-419

299. **Koopman R, Schaart G, Hesselink MK** 2001 Optimisation of oil red O staining permits combination with immunofluorescence and automated quantification of lipids. Histochem Cell Biol 116:63-68

300. **Panthakalam S, Bhatnagar D, Klimiuk P** 2004 The prevalence and management of hyperglycaemia in patients with rheumatoid arthritis on corticosteroid therapy. Scott Med J 49:139-141

301. **Hans P, Vanthuyne A, Dewandre PY, Brichant JF, Bonhomme V** 2006 Blood glucose concentration profile after 10 mg dexamethasone in non-diabetic and type 2 diabetic patients undergoing abdominal surgery. Br J Anaesth 97:164-170

302. **Pasternak JJ, McGregor DG, Lanier WL** 2004 Effect of single-dose dexamethasone on blood glucose concentration in patients undergoing craniotomy. J Neurosurg Anesthesiol 16:122-125

303. **Dallman MF** 2003 Fast glucocorticoid feedback favors 'the munchies'. Trends Endocrinol Metab 14:394-396

304. **Dong H, Lin H, Jiao HC, Song ZG, Zhao JP, Jiang KJ** 2007 Altered development and protein metabolism in skeletal muscles of broiler chickens (Gallus gallus domesticus) by corticosterone. Comp Biochem Physiol A Mol Integr Physiol 147:189-195

305. **Falduto MT, Czerwinski SM, Hickson RC** 1990 Glucocorticoid-induced muscle atrophy prevention by exercise in fast-twitch fibers. J Appl Physiol 69:1058-1062

306. **Andersen H, Gjerstad MD, Jakobsen J** 2004 Atrophy of foot muscles: a measure of diabetic neuropathy. Diabetes Care 27:2382-2385

307. **Huang BK, Monu JU, Doumanian J** 2010 Diabetic myopathy: MRI patterns and current trends. AJR Am J Roentgenol 195:198-204

308. **LeBrasseur NK, Walsh K, Arany Z** 2011 Metabolic benefits of resistance training and fast glycolytic skeletal muscle. Am J Physiol Endocrinol Metab 300:E3-10

309. **Coleman DL, Hummel KP** 1973 The influence of genetic background on the expression of the obese (Ob) gene in the mouse. Diabetologia 9:287-293

310. **Coleman DL** 1978 Obese and diabetes: two mutant genes causing diabetes-obesity syndromes in mice. Diabetologia 14:141-148

311. **Gounarides JS, Korach-Andre M, Killary K, Argentieri G, Turner O, Laurent D** 2008 Effect of dexamethasone on glucose tolerance and fat metabolism in a diet-induced obesity mouse model. Endocrinology 149:758-766

312. **Bays HE, Gonzalez-Campoy JM, Bray GA, Kitabchi AE, Bergman DA, Schorr AB, Rodbard HW, Henry RR** 2008 Pathogenic potential of adipose tissue and metabolic consequences of adipocyte hypertrophy and increased visceral adiposity. Expert Rev Cardiovasc Ther 6:343-368

313. **Bray GA, Jablonski KA, Fujimoto WY, Barrett-Connor E, Haffner S, Hanson RL, Hill JO, Hubbard V, Kriska A, Stamm E, Pi-Sunyer FX, Diabetes Prevention Program Research Group** 2008 Relation of central adiposity and body mass index to the development of diabetes in the Diabetes Prevention Program. Am J Clin Nutr 87:1212-1218

314. **Unger RH** 2003 Minireview: weapons of lean body mass destruction: the role of ectopic lipids in the metabolic syndrome. Endocrinology 144:5159-5165

315. **Lara-Castro C, Garvey WT** 2008 Intracellular lipid accumulation in liver and muscle and the insulin resistance syndrome. Endocrinol Metab Clin North Am 37:841-856

316. **van der Zijl NJ, Goossens GH, Moors CC, van Raalte DH, Muskiet MH, Pouwels PJ, Blaak EE, Diamant M** 2011 Ectopic fat storage in the pancreas, liver, and abdominal fat depots: impact on beta-cell function in individuals with impaired glucose metabolism. J Clin Endocrinol Metab 96:459-467

317. **Samuel VT, Petersen KF, Shulman GI** 2010 Lipid-induced insulin resistance: unravelling the mechanism. Lancet 375:2267-2277

318. **Luijf YM, Hermanides J, Serlie MJ, Hoekstra JB, Soeters MR** 2011 The added value of oral glucose tolerance testing in pre-diabetes. Curr Diabetes Rev 7:56-60

319. **Pour OR, Dagogo-Jack S** 2011 Prediabetes as a therapeutic target. Clin Chem 57:215-220

320. **Kawano K, Hirashima T, Mori S, Saitoh Y, Kurosumi M, Natori T** 1992 Spontaneous long-term hyperglycemic rat with diabetic complications. Otsuka Long-Evans Tokushima Fatty (OLETF) strain. Diabetes 41:1422-1428

321. **Roy M, Collier B, Roy A** 1990 Hypothalamic-pituitary-adrenal axis dysregulation among diabetic outpatients. Psychiatry Res 31:31-37

322. **Gathercole LL, Stewart PM** 2010 Targeting the pre-receptor metabolism of cortisol as a novel therapy in obesity and diabetes. J Steroid Biochem Mol Biol 122:21-27

323. **Ceddia RB** 2005 Direct metabolic regulation in skeletal muscle and fat tissue by leptin: implications for glucose and fatty acids homeostasis. Int J Obes (Lond) 29:1175-1183

324. **Kumar V, Madhu SV, Singh G, Gambhir JK** 2010 Post-prandial hypertriglyceridemia in patients with type 2 diabetes mellitus with and without macrovascular disease. J Assoc Physicians India 58:603-607

325. **Rhen T, Cidlowski JA** 2005 Antiinflammatory action of glucocorticoids--new mechanisms for old drugs. N Engl J Med 353:1711-1723

326. **Clerc D, Wick H, Keller U** 1986 Acute cortisol excess results in unimpaired insulin action on lipolysis and branched chain amino acids, but not on glucose kinetics and C-peptide concentrations in man. Metabolism 35:404-410

327. **van Raalte DH, van Genugten RE, Linssen MM, Ouwens DM, Diamant M** 2011 Glucagon-like peptide-1 receptor agonist treatment prevents glucocorticoid-induced glucose intolerance and islet-cell dysfunction in humans. Diabetes Care 34:412-417

328. **Shpilberg Y, Beaudry JL, D'Souza A, Campbell JE, Peckett A, Riddell MC** 2012 A rodent model of rapid-onset diabetes induced by glucocorticoids and high-fat feeding. Dis Model Mech

329. **Bates HE, Kiraly MA, Yue JT, Goche Montes D, Elliott ME, Riddell MC, Matthews SG, Vranic M** 2007 Recurrent intermittent restraint delays fed and fasting hyperglycemia and improves glucose return to baseline levels during glucose tolerance tests in the Zucker diabetic fatty rat--role of food intake and corticosterone. Metabolism 56:1065-1075

330. **Tang C, Koulajian K, Schuiki I, Zhang L, Desai T, Ivovic A, Wang P, Robson-Doucette C, Wheeler MB, Minassian B, Volchuk A, Giacca A** 2012 Glucose-induced beta cell dysfunction in vivo in rats: link between oxidative stress and endoplasmic reticulum stress. Diabetologia 55:1366-1379

331. **Lacy PE, Kostianovsky M** 1967 Method for the isolation of intact islets of Langerhans from the rat pancreas. Diabetes 16:35-39

332. **Nguyen VN, Mirejovsky P, Mirejovsky T, Melinova L, Mandys V** 2000 Expression of cyclin D1, Ki-67 and PCNA in non-small cell lung cancer: prognostic significance and comparison with p53 and bcl-2. Acta Histochem 102:323-338

333. **Swali A, Walker EA, Lavery GG, Tomlinson JW, Stewart PM** 2008 11beta-Hydroxysteroid dehydrogenase type 1 regulates insulin and glucagon secretion in pancreatic islets. Diabetologia 51:2003-2011

334. **Clore JN, Thurby-Hay L** 2009 Glucocorticoid-induced hyperglycemia. Endocr Pract 15:469-474

335. **Rafacho A, Quallio S, Ribeiro DL, Taboga SR, Paula FM, Boschero AC, Bosqueiro JR** 2010 The adaptive compensations in endocrine pancreas from glucocorticoid-treated rats are reversible after the interruption of treatment. Acta Physiol (Oxf) 200:223-235

336. **Rafacho A, Abrantes JL, Ribeiro DL, Paula FM, Pinto ME, Boschero AC, Bosqueiro JR** 2011 Morphofunctional alterations in endocrine pancreas of short- and long-term dexamethasone-treated rats. Horm Metab Res 43:275-281

337. **McMahon M, Gerich J, Rizza R** 1988 Effects of glucocorticoids on carbohydrate metabolism. Diabetes Metab Rev 4:17-30

338. **Lottenberg AM, Afonso Mda S, Lavrador MS, Machado RM, Nakandakare ER** 2012 The role of dietary fatty acids in the pathology of metabolic syndrome. J Nutr Biochem 23:1027-1040

339. **D'souza AM, Beaudry JL, Szigiato AA, Trumble SJ, Snook LA, Bonen A, Giacca A, Riddell MC** 2012 Consumption of a high-fat diet rapidly exacerbates the development of fatty liver disease that occurs with chronically elevated glucocorticoids. Am J Physiol Gastrointest Liver Physiol 302:G850-63

340. **Park S, Kim da S, Kang S, Kwon DY** 2011 Ischemic hippocampal cell death induces glucose dysregulation by attenuating glucose-stimulated insulin secretion which is exacerbated by a high fat diet. Life Sci 88:766-773

341. **Nesher R, Anteby E, Yedovizky M, Warwar N, Kaiser N, Cerasi E** 2002 Beta-cell protein kinases and the dynamics of the insulin response to glucose. Diabetes 51 Suppl 1:S68-73

342. **Zawalich WS, Tesz GJ, Yamazaki H, Zawalich KC, Philbrick W** 2006 Dexamethasone suppresses phospholipase C activation and insulin secretion from isolated rat islets. Metabolism 55:35-42

343. **Piquer S, Casas S, Quesada I, Nadal A, Julia M, Novials A, Gomis R** 2009 Role of iduronate-2-sulfatase in glucose-stimulated insulin secretion by activation of exocytosis. Am J Physiol Endocrinol Metab 297:E793-801

344. **Warwar N, Efendic S, Ostenson CG, Haber EP, Cerasi E, Nesher R** 2006 Dynamics of glucose-induced localization of PKC isoenzymes in pancreatic beta-cells: diabetes-related changes in the GK rat. Diabetes 55:590-599

345. **Arkhammar P, Nilsson T, Welsh M, Welsh N, Berggren PO** 1989 Effects of protein kinase C activation on the regulation of the stimulus-secretion coupling in pancreatic beta-cells. Biochem J 264:207-215

346. **Yamazaki H, Zawalich KC, Zawalich WS** 2010 Physiologic implications of phosphoinositides and phospholipase C in the regulation of insulin secretion. J Nutr Sci Vitaminol (Tokyo) 56:1-8

347. **Rose T, Efendic S, Rupnik M** 2007 Ca2+-secretion coupling is impaired in diabetic Goto Kakizaki rats. J Gen Physiol 129:493-508

348. **Zhou YP, Grill VE** 1994 Long-term exposure of rat pancreatic islets to fatty acids inhibits glucose-induced insulin secretion and biosynthesis through a glucose fatty acid cycle. J Clin Invest 93:870-876

349. **Terauchi Y, Takamoto I, Kubota N, Matsui J, Suzuki R, Komeda K, Hara A, Toyoda Y, Miwa I, Aizawa S, Tsutsumi S, Tsubamoto Y, Hashimoto S, Eto K, Nakamura A, Noda M, Tobe K, Aburatani H, Nagai R, Kadowaki T** 2007 Glucokinase and IRS-2 are required for compensatory beta cell hyperplasia in response to high-fat diet-induced insulin resistance. J Clin Invest 117:246-257

350. **Beaudry JL, D'Souza A, Teich T, Tsushima R, Riddell MC** 2013 Exogenous glucocorticoids and a high-fat diet cause severe hyperglycemia and hyperinsulinemia and limit islet glucose responsiveness in young male Sprague-Dawley rats. Endocrinology

351. **Cameron OG, Kronfol Z, Greden JF, Carroll BJ** 1984 Hypothalamic-pituitary-adrenocortical activity in patients with diabetes mellitus. Arch Gen Psychiatry 41:1090-1095

352. **Chiodini I, Di Lembo S, Morelli V, Epaminonda P, Coletti F, Masserini B, Scillitani A, Arosio M, Adda G** 2006 Hypothalamic-pituitary-adrenal activity in type 2 diabetes mellitus: role of autonomic imbalance. Metabolism 55:1135-1140

353. **Hackney AC** 2006 Stress and the neuroendocrine system: the role of exercise as a stressor and modifier of stress. Expert Rev Endocrinol Metab 1:783-792

354. **LaMonte MJ, Blair SN** 2006 Physical activity, cardiorespiratory fitness, and adiposity: contributions to disease risk. Curr Opin Clin Nutr Metab Care 9:540-546

355. **Park E, Chan O, Li Q, Kiraly M, Matthews SG, Vranic M, Riddell MC** 2005 Changes in basal hypothalamo-pituitary-adrenal activity during exercise training are centrally mediated. Am J Physiol Regul Integr Comp Physiol 289:R1360-71

356. **Farrell PA, Garthwaite TL, Gustafson AB** 1983 Plasma adrenocorticotropin and cortisol responses to submaximal and exhaustive exercise. J Appl Physiol 55:1441-1444

357. **Few JD** 1974 Effect of exercise on the secretion and metabolism of cortisol in man. J Endocrinol 62:341-353

358. **Hill EE, Zack E, Battaglini C, Viru M, Viru A, Hackney AC** 2008 Exercise and circulating cortisol levels: the intensity threshold effect. J Endocrinol Invest 31:587-591

359. **Burr,J Rowan,C Jamnik,R Riddell,MC** In press November 2009 Physical Activity Targets Multi-Organ Dysfunction in Pre-diabetes to Prevent Diabetes.

360. **Nagatomo F, Fujino H, Kondo H, Kouzaki M, Gu N, Takeda I, Tsuda K, Ishihara A** 2012 The effects of running exercise on oxidative capacity and PGC-1alpha mRNA levels in the soleus muscle of rats with metabolic syndrome. J Physiol Sci 62:105-114

361. **Wallace TM, Levy JC, Matthews DR** 2004 Use and abuse of HOMA modeling. Diabetes Care 27:1487-1495

362. **Ogilvie RW, Feeback DL** 1990 A metachromatic dye-ATPase method for the simultaneous identification of skeletal muscle fiber types I, IIA, IIB and IIC. Stain Technol 65:231-241

363. **Hederstedt L, Rutberg L** 1981 Succinate dehydrogenase--a comparative review. Microbiol Rev 45:542-555

364. **Coderre L, Vallega GA, Pilch PF, Chipkin SR** 2007 Regulation of glycogen concentration and glycogen synthase activity in skeletal muscle of insulin-resistant rats. Arch Biochem Biophys 464:144-150

365. **Menezes LG, Sobreira C, Neder L, Rodrigues-Junior AL, Martinez JA** 2007 Creatine supplementation attenuates corticosteroid-induced muscle wasting and impairment of exercise performance in rats. J Appl Physiol 102:698-703

366. **Kaasik P, Umnova M, Pehme A, Alev K, Aru M, Selart A, Seene T** 2007 Ageing and dexamethasone associated sarcopenia: peculiarities of regeneration. J Steroid Biochem Mol Biol 105:85-90

367. **Yau SY, Lau BW, Zhang ED, Lee JC, Li A, Lee TM, Ching YP, Xu AM, So KF** 2012 Effects of voluntary running on plasma levels of neurotrophins, hippocampal cell proliferation and learning and memory in stressed rats. Neuroscience 222:289-301

368. **Patterson CM, Dunn-Meynell AA, Levin BE** 2008 Three weeks of early-onset exercise prolongs obesity resistance in DIO rats after exercise cessation. Am J Physiol Regul Integr Comp Physiol 294:R290-301

369. **Bi S, Scott KA, Hyun J, Ladenheim EE, Moran TH** 2005 Running wheel activity prevents hyperphagia and obesity in Otsuka long-evans Tokushima Fatty rats: role of hypothalamic signaling. Endocrinology 146:1676-1685

370. **Ahtikoski AM, Riso EM, Koskinen SO, Risteli J, Takala TE** 2004 Regulation of type IV collagen gene expression and degradation in fast and slow muscles during dexamethasone treatment and exercise. Pflugers Arch 448:123-130

371. **Chandola T, Brunner E, Marmot M** 2006 Chronic stress at work and the metabolic syndrome: prospective study. BMJ 332:521-525

372. **Bjorntorp P** 2001 Do stress reactions cause abdominal obesity and comorbidities? Obes Rev 2:73-86

373. **Stiegler P, Cunliffe A** 2006 The role of diet and exercise for the maintenance of fat-free mass and resting metabolic rate during weight loss. Sports Med 36:239-262

374. **Danielsen KK, Svendsen M, Maehlum S, Sundgot-Borgen J** 2013 Changes in body composition, cardiovascular disease risk factors, and eating behavior after an intensive lifestyle intervention with high volume of physical activity in severely obese subjects: a prospective clinical controlled trial. J Obes 2013:325464

375. **Gollisch KS, Brandauer J, Jessen N, Toyoda T, Nayer A, Hirshman MF, Goodyear LJ** 2009 Effects of exercise training on subcutaneous and visceral adipose tissue in normal- and high-fat diet-fed rats. Am J Physiol Endocrinol Metab 297:E495-504

376. **Gauthier MS, Couturier K, Charbonneau A, Lavoie JM** 2004 Effects of introducing physical training in the course of a 16-week high-fat diet regimen on hepatic steatosis, adipose tissue fat accumulation, and plasma lipid profile. Int J Obes Relat Metab Disord 28:1064-1071

377. **Park S, Jang JS, Jun DW, Hong SM** 2005 Exercise enhances insulin and leptin signaling in the cerebral cortex and hypothalamus during dexamethasone-induced stress in diabetic rats. Neuroendocrinology 82:282-293

378. **Roy RR, Gardiner PF, Simpson DR, Edgerton VR** 1983 Glucocorticoid-induced atrophy in different fibre types of selected rat jaw and hind-limb muscles. Arch Oral Biol 28:639-643

379. **Hasselgren PO** 1999 Glucocorticoids and muscle catabolism. Curr Opin Clin Nutr Metab Care 2:201-205

380. **Schakman O, Kalista S, Barbe C, Loumaye A, Thissen JP** 2013 Glucocorticoid-induced skeletal muscle atrophy. Int J Biochem Cell Biol

381. **Lewis MI, Monn SA, Sieck GC** 1992 Effect of corticosteroids on diaphragm fatigue, SDH activity, and muscle fiber size. J Appl Physiol 72:293-301

382. **Bates HE, Sirek AS, Kiraly MA, Yue JT, Goche Montes D, Matthews SG, Vranic M** 2008 Adaptation to mild, intermittent stress delays development of hyperglycemia in the Zucker diabetic Fatty rat independent of food intake: role of habituation of the hypothalamic-pituitary-adrenal axis. Endocrinology 149:2990-3001

383. **Tanner CJ, Koves TR, Cortright RL, Pories WJ, Kim YB, Kahn BB, Dohm GL, Houmard JA** 2002 Effect of short-term exercise training on insulin-stimulated PI 3-kinase activity in middle-aged men. Am J Physiol Endocrinol Metab 282:E147-53

384. **Tsuchiya M, Manabe Y, Yamada K, Furuichi Y, Hosaka M, Fujii NL** 2013 Chronic exercise enhances insulin secretion ability of pancreatic islets without change in insulin content in non-diabetic rats. Biochem Biophys Res Commun 430:676-682

385. **Funder JW** 1997 Glucocorticoid and mineralocorticoid receptors: biology and clinical relevance. Annu Rev Med 48:231-240

386. **Zhou J, Cidlowski JA** 2005 The human glucocorticoid receptor: one gene, multiple proteins and diverse responses. Steroids 70:407-417

387. **Kelly HW, Sternberg AL, Lescher R, Fuhlbrigge AL, Williams P, Zeiger RS, Raissy HH, Van Natta ML, Tonascia J, Strunk RC, CAMP Research Group** 2012 Effect of inhaled glucocorticoids in childhood on adult height. N Engl J Med 367:904-912

388. **Schacke H, Docke WD, Asadullah K** 2002 Mechanisms involved in the side effects of glucocorticoids. Pharmacol Ther 96:23-43

389. **Nielsen MF, Caumo A, Chandramouli V, Schumann WC, Cobelli C, Landau BR, Vilstrup H, Rizza RA, Schmitz O** 2004 Impaired basal glucose effectiveness but unaltered fasting glucose release and gluconeogenesis during short-term hypercortisolemia in healthy subjects. Am J Physiol Endocrinol Metab 286:E102-10

390. **Hoffman RP** 2008 Indices of insulin action calculated from fasting glucose and insulin reflect hepatic, not peripheral, insulin sensitivity in African-American and Caucasian adolescents. Pediatr Diabetes 9:57-61

391. **Campbell JE, Peckett AJ, D'souza AM, Hawke TJ, Riddell MC** 2011 Adipogenic and lipolytic effects of chronic glucocorticoid exposure. Am J Physiol Cell Physiol 300:C198-209

392. **Taskinen MR** 2003 Diabetic dyslipidaemia: from basic research to clinical practice. Diabetologia 46:733-749

393. **Chrousos GP** 2004 Is 11beta-hydroxysteroid dehydrogenase type 1 a good therapeutic target for blockade of glucocorticoid actions? Proc Natl Acad Sci U S A 101:6329-6330

394. **Beebe KL, Block T, Debattista C, Blasey C, Belanoff JK** 2006 The efficacy of mifepristone in the reduction and prevention of olanzapine-induced weight gain in rats. Behav Brain Res 171:225-229

395. **Belanoff JK, Blasey CM, Clark RD, Roe RL** 2010 Selective glucocorticoid receptor (type II) antagonist prevents and reverses olanzapine-induced weight gain. Diabetes Obes Metab 12:545-547

396. **Okada S, York DA, Bray GA** 1992 Mifepristone (RU 486), a blocker of type II glucocorticoid and progestin receptors, reverses a dietary form of obesity. Am J Physiol 262:R1106-10

397. **Langley SC, York DA** 1990 Effects of antiglucocorticoid RU 486 on development of obesity in obese fa/fa Zucker rats. Am J Physiol 259:R539-44

398. **Taylor AI, Frizzell N, McKillop AM, Flatt PR, Gault VA** 2009 Effect of RU486 on hepatic and adipocyte gene expression improves diabetes control in obesity-type 2 diabetes. Horm Metab Res 41:899-904

399. **Vander Kooi BT, Onuma H, Oeser JK, Svitek CA, Allen SR, Vander Kooi CW, Chazin WJ, O'Brien RM** 2005 The glucose-6-phosphatase catalytic subunit gene promoter contains both positive and negative glucocorticoid response elements. Mol Endocrinol 19:3001-3022

400. **Debono M, Chadarevian R, Eastell R, Ross RJ, Newell-Price J** 2013 Mifepristone reduces insulin resistance in patient volunteers with adrenal incidentalomas that secrete low levels of cortisol: a pilot study. PLoS One 8:e60984

401. **Haller J, Mikics E, Makara GB** 2008 The effects of non-genomic glucocorticoid mechanisms on bodily functions and the central neural system. A critical evaluation of findings. Front Neuroendocrinol 29:273-291

402. **Spiga F, Harrison LR, Wood SA, Atkinson HC, MacSweeney CP, Thomson F, Craighead M, Grassie M, Lightman SL** 2007 Effect of the glucocorticoid receptor antagonist Org 34850 on basal and stress-induced corticosterone secretion. J Neuroendocrinol 19:891-900

403. **Deschoolmeester J, Palming J, Persson T, Pereira MJ, Wallerstedt E, Brown H, Gill D, Renstrom F, Lundgren M, Svensson MK, Rees A, Eriksson JW** 2013 Differences between men and women in the regulation of adipose 11beta-HSD1 and in its association with adiposity and insulin resistance. Diabetes Obes Metab

404. **Dallman MF, la Fleur SE, Pecoraro NC, Gomez F, Houshyar H, Akana SF** 2004 Minireview: glucocorticoids--food intake, abdominal obesity, and wealthy nations in 2004. Endocrinology 145:2633-2638

405. **Wang ZL, Bennet WM, Wang RM, Ghatei MA, Bloom SR** 1994 Evidence of a paracrine role of neuropeptide-Y in the regulation of insulin release from pancreatic islets of normal and dexamethasone-treated rats. Endocrinology 135:200-206

406. **Haskell-Luevano C, Schaub JW, Andreasen A, Haskell KR, Moore MC, Koerper LM, Rouzaud F, Baker HV, Millard WJ, Walter G, Litherland SA, Xiang Z** 2009 Voluntary exercise prevents the obese and diabetic metabolic syndrome of the melanocortin-4 receptor knockout mouse. FASEB J 23:642-655